



MEDICAL UNIVERSITY
OF VIENNA

Elucidation of molecular mechanisms regulating insulin expression in pancreatic islet cells

Doctoral thesis at the Medical University of Vienna
for obtaining the academic degree

Doctor of Philosophy

Submitted by

Tamara Casteels, M.Res.

Supervisor:

Stefan Kubicek, PhD

CeMM Research Center for Molecular Medicine

of the Austrian Academy of Sciences

Lazarettgasse 14, AKH BT 25.3

1090 Vienna, Austria

Vienna, 08/2021

DECLARATION

The work presented in this doctoral thesis was performed at the Research Center for Molecular Medicine (CeMM) of the Austrian Academy of Sciences in Vienna, Austria unless otherwise stated below. Individual contributions are listed below in correspondence to Results Sections 2.1 and 2.2.

The results detailed in Section 2.1 have been previously reported in the following publication:

Casteels T, Zhang Y, Frogne T, Sturtzel C, Lardeau C-H, Sen I, Liu X, Hong S, Pauler FM, Penz T, Brandstetter M, Barbieux C, Berishvili E, Heuser T, Bock C, Riedel CG, Meyer D, Distel M, Hecksher-Sørensen J, Li J, Kubicek S (2021) An inhibitor-mediated beta cell dedifferentiation model reveals distinct roles for FoxO1 in glucagon repression and insulin maturation, *Molecular Metabolism*

<https://doi.org/10.1016/j.molmet.2021.101329>

TC, SK and JL designed the experiments and wrote the manuscript. **TC** and JL carried out all the murine cell line and human islet experiments. CHL performed the initial chemical screen. TF and JHS provided the cell lines. TP and CB performed the next generation sequencing. **TC**, FMP and JL analyzed the resulting RNA-seq datasets. Electron microscopy sample preparation and imaging was done by MB and TH at the Vienna BioCenter Electron Microscopy Facility. CB and EB isolated and prepared some of the human islet samples at the University of Geneva. CS and MD performed the zebrafish assays at the Children's Cancer Research Institute. Dauer formation assays were executed by IS and CGR at the University of Innsbruck. JL, XL, YZ and SH did all the in vivo and ex vivo experiments on murine islets at Fudan University. **TC** quantified all the immunofluorescence images. TH, CB, CGR, DM, MD, JHS, JL and SK supervised the work.

Section 2.2 corresponds to a manuscript submitted to a peer-reviewed journal for publication:

Casteels T, Bajew S, Reiniš J, Schuster M, Müller A, Wagner BK, Bock C and Kubicek S, SMNDC1 links chromatin remodeling and splicing to regulate pancreatic hormone expression (*submitted*).

TC and SK designed the study and wrote the manuscript. **TC** performed the wet-lab experiments. **TC**, MS and SB analyzed the RNA-seq data. JR analyzed the ATAC-seq data.

TC and **AM** analyzed the mass spectrometry data. **SK** and **BKW** performed the original RNAi screen at the Broad Institute in MA, USA. **CB**, **BKW** and **SK** supervised the work.

TABLE OF CONTENTS

Declaration	ii
Table of Contents	iv
List of Figures	vi
Abstract	vii
Zusammenfassung	ix
Publications Arising From This Thesis	xi
Abbreviations	xii
Acknowledgments	xv
1. Introduction	1
1.1 The endocrine pancreas: from embryo to adult	1
1.1.1 <i>Pancreas development and islet cell specification</i>	1
1.1.2 <i>Regulation of hormone expression in the mature pancreas</i>	5
1.1.3 <i>Insulin secretion in the mature beta cell</i>	10
1.2 Diabetes: physical and functional loss of the beta cell.....	12
1.2.1 <i>Beta cell loss behind Type I Diabetes and Maturity Onset Diabetes of the Young</i>	12
1.2.2 <i>Beta cell impairment during Type II Diabetes</i>	14
1.3 Beta Cell Regeneration	17
1.3.1 <i>Neogenesis</i>	17
1.3.2 <i>Replication</i>	20
1.3.3 <i>Transdifferentiation</i>	22
1.4 Aims	27
2. Results	28
2.1 An inhibitor-mediated beta cell dedifferentiation model reveals distinct roles for FoxO1 in glucagon repression and insulin maturation	28
2.2 SMNDC1 links chromatin remodeling and splicing to regulate pancreatic hormone expression.....	80

3. Discussion	143
3.1 General Discussion	143
3.2 Conclusion and Future Prospects	147
4. Materials and Methods	149
5. References	150
6. Curriculum Vitae	173

LIST OF FIGURES

Figure 1. Simplified overview of pancreatic differentiation	3
Figure 2. Immunofluorescence image of murine pancreas cross-section	4
Figure 3. Schematic representation of insulin and glucagon promoters.....	6
Figure 4. Model of three main pathways suggested for beta cell loss during T2D	15
Figure 5. Summary of various factors identified to induce beta cell regeneration	26
Figure 6. Overview of the two projects constituting this thesis and their main respective aim	27
Figure 7. Loperamide treatment leads to rapid decrease in phosphorylated AKT levels	145
Figure 8. Genome browser tracks for event MmuEX0003147	147
Figure 9. Summary of thesis work findings.....	148

ABSTRACT

Blood glucose homeostasis is predominantly regulated by the actions of two hormone-producing cells in the endocrine pancreas, specifically the insulin-secreting beta cells and the glucagon-secreting alpha cells. Under normal circumstances, beta cells sense mounting glucose concentrations and secrete insulin, while peripheral tissues, namely the liver and muscle, react to that insulin and clear glucose from the bloodstream. Peripheral tissue desensitization to insulin, known as insulin resistance, thus leads to chronic hyperglycemia, which results in beta cell dysfunction, dedifferentiation into progenitor cells and even transdifferentiation into alpha cells. This loss of beta cell identity and functionality represents the defining step in the pathogenesis of type 2 diabetes. Type 1 diabetes, on the other hand, is characterized by a complete physical loss of the functional beta cell pool secondary to autoimmune attack. Therefore, both disorders are characterized by severely diminished insulin secretion and disease-defining hyperglycemia, highlighting an important therapeutic need for beta cell regeneration strategies. A key step towards that goal is understanding the regulatory mechanisms controlling hormone expression in alpha and beta cells, both at the RNA and protein level. Multiple studies have shown that binding of distinct transcription factors to the insulin and glucagon promoters can trigger activation or repression of transcription, however, less is known about the chromatin factors and signaling molecules directing the expression and localization of said transcription factors.

In the first part of my thesis, I therefore aimed to identify processes that could counter the loss of insulin and gain of glucagon expression observed during beta cell dedifferentiation. Prior to this work, no cellular system existed to properly model beta cell dedifferentiation in vitro in a reproducible manner amenable to high-content screening. Hence, we characterized a dedifferentiation system in a beta cell line and utilized it to find inhibitors of said process. In this manner we identified the small molecule, loperamide, capable of reducing aberrant glucagon co-expression in both dedifferentiated beta cell lines, human islets and in vivo in diabetic murine islets. Mechanistically, loperamide promoted an increase in the activity of the transcription factor FoxO1 and its downstream targets, resulting in intracellular calcium mobilization, pH modulation and increased insulin biosynthesis and secretion.

In the second part of my thesis, I focused on identifying and counteracting mechanisms repressing insulin expression in alpha cells, with the overall goal of stimulating transdifferentiation. Using a genetic RNA interference screen, we identified the splicing factor, Survival Motor Neuron Domain Containing 1 (Smndc1), to repress insulin transcription in alpha cells. More specifically, loss of Smndc1 induced an increase in beta cell markers and

chromatin accessibility in alpha cells, including stabilization of the key beta cell transcription factor, Pdx1, and subsequent activation of insulin transcription. We thus successfully identified and characterized chemical and genetic factors able to respectively promote beta cell identity in diabetic settings and in non-beta cells.

ZUSAMMENFASSUNG

Der Blutzuckerspiegel wird in erster Linie durch zwei Zelltypen in den pankreatischen Langerhans-Inseln reguliert, und zwar durch die Insulin-sekretierenden Betazellen und die Glukagon-sekretierenden Alphazellen. Die Betazellen reagieren auf ansteigende Glukosekonzentration mit der Ausschüttung von Insulin, und dieses Hormon verursacht die Aufnahme von Glukose aus dem Blutkreislauf durch die peripheren Gewebe, insbesondere durch die Leber und Muskeln. Die Desensibilisierung des peripheren Gewebes gegenüber Insulin, die als Insulinresistenz bezeichnet wird, führt zu einer chronischen Hyperglykämie, die eine Dysfunktion der Betazellen, ihre Dedifferenzierung in Vorläuferzellen und sogar ihre Transdifferenzierung in Alphazellen zur Folge haben kann. Dieser Verlust der Betazellidentität und -funktionalität ist der entscheidende Schritt in der Pathogenese von Typ-2-Diabetes. Typ-1-Diabetes hingegen wird durch einen vollständigen physischen Verlust des funktionellen Betazellpools infolge eines Autoimmunangriffs verursacht. Beide Erkrankungen sind durch eine stark verminderte Insulinsekretion und eine krankheitsdefinierende Hyperglykämie gekennzeichnet, was den wichtigen therapeutischen Bedarf von Strategien zur Regeneration funktioneller Betazellen unterstreicht. Ein wichtiger Schritt auf dem Weg zu diesem Ziel ist das Verständnis der regulatorischen Mechanismen, die die Hormonexpression in Alpha- und Betazellen sowohl auf der Ebene der RNA also auch der Proteine kontrollieren. Frühere Studien haben gezeigt, dass die Bindung verschiedener Transkriptionsfaktoren an die jeweiligen Promotoren die Transcription des Insulin- bzw. Glukagongens aktivieren oder unterdrücken kann. Hingegen ist bis jetzt weniger über die Chromatinfaktoren und Signalmoleküle bekannt, die die Expression und Lokalisierung der genannten Transkriptionsfaktoren steuern.

Im ersten Teil meiner Dissertation wollte ich daher Prozesse identifizieren, die der Betazell-Dedifferenzierung, und insbesondere dem damit einhergehenden Verlust der Insulinexpression und der Induktion der Glukagonexpression, entgegenwirken. Vor dieser Arbeit gab es kein zelluläres System, mit dem die Betazell-Dedifferenzierung *in vitro* in reproduzierbarer Weise modelliert werden konnte. Daher entwickelten und charakterisierten wir ein System zur pharmakologischen Dedifferenzierung einer Betazelllinie und nutzten es, um Hemmstoffe für diesen Prozess zu finden. Auf diese Weise identifizierten wir die niedermolekulare Substanz Loperamid. Loperamid kann der Induktion der Glukagon-Expression sowohl in dedifferenzierten Betazelllinien als auch in menschlichen Langerhans-Inseln und *in vivo* in Betazellen in einem diabetischen Mausmodell reduzieren. Wir fanden heraus, dass dem Mechanismus von Loperamid eine Zunahme der Aktivität des Transkriptionsfaktors FoxO1 und seiner Targetgene zugrundeliegt, was zu einer

intrazellulären Kalziummobilisierung, einer pH-Modulation und einer erhöhten Insulinbiosynthese und -sekretion führt.

Im zweiten Teil meiner Arbeit konzentrierte ich mich auf die Identifizierung und Inhibition von Mechanismen, die die Insulinexpression in Alphazellen unterdrücken, mit dem übergeordneten Ziel, die Transdifferenzierung zu stimulieren. Durch einen genetischen RNA-Interferenz-Screens identifizierten wir den Spleißfaktor Survival Motor Neuron Domain Containing 1 (Smndc1), der die Insulin-Transkription in Alphazellen unterdrückt. Der Verlust von Smndc1 führte zu einem Anstieg der Beta-Zell-Marker und der Chromatin-Zugänglichkeit in Alpha-Zellen, einschließlich der Stabilisierung des wichtigen Beta-Zell-Transkriptionsfaktors Pdx1 und der anschließenden Aktivierung der Insulin-Transkription.

Im Rahmen dieser Arbeit habe ich erfolgreich chemische und genetische Faktoren identifiziert und charakterisiert, die die Betazellidentität in diabetischen und nicht-beta-Zellen induzieren können.

PUBLICATIONS ARISING FROM THIS THESIS

Section 2.1 of this thesis was published in the journal *Molecular Metabolism* in 2021.

Impact Factor 2020: 7.422

An inhibitor-mediated beta cell dedifferentiation model reveals distinct roles for FoxO1 in glucagon repression and insulin maturation

Casteels T, Zhang Y, Frogne T, Sturtzel C, Lardeau C-H, Sen I, Liu X, Hong S, Pauler FM, Penz T, Brandstetter M, Barbieux C, Berishvili E, Heuser T, Bock C, Riedel CG, Meyer D, Distel M, Hecksher-Sørensen J, Li J, Kubicek S

Molecular Metabolism 2021

PII: S2212-8778(21)00176-9

DOI: <https://doi.org/10.1016/j.molmet.2021.101329>

Reference: MOLMET 101329

Submitted: June 22, 2021

Accepted: August 20, 2021

Reprinted from (Casteels *et al*, 2021)

© 2021. This manuscript version is made available under the CC-BY-NC-ND 4.0 license
<https://creativecommons.org/licenses/by-nc-nd/4.0/>

ABBREVIATIONS

Adox	adenosine dialdehyde
ATAC	assay for transposase accessible chromatin
aTC1	murine alpha cell line alphaTC1
ATP	adenosine triphosphate
Atrx	alpha-thalassemia/mental retardation, X-linked
BAF	Brg1- or Brm-associated factors
bHLH	basic helix-loop-helix
bp	base pair
bTC3	murine beta cell line betaTC3
CaMKII	calcium/calmodulin-dependent protein kinase II
ChIP	chromatin immunoprecipitation
CHX	cycloheximide
CRISPR	clustered regularly interspaced short palindromic repeats
CS	Carnegie Stage
DiffAS	differentially spliced events
DISR	disrupted coding sequence
DMEM	Dulbecco's modified Eagle medium
DMSO	dimethyl sulfoxide
DNA	deoxyribonucleic acid
dPSI	change in percentage spliced in
DYRK1A	dual specificity tyrosine phosphorylation regulated kinase 1A
E	embryonic day
eGFP	enhanced green fluorescent protein
EGFR	epidermal growth factor receptor
ELISA	enzyme-linked immunosorbent assay
ER	endoplasmic reticulum
EV	empty vector
FACS	fluorescence-activated cell sorting
FDA	US food and drug administration
FoxO1	forkhead box protein O1
FoxOi	FoxO1 inhibitor AS1842856
FPKM	fragments per kilobase of transcript per million mapped reads
GAD65	glutamate decarboxylase 65-kilodalton isoform
Gck	glucokinase

GFP	green fluorescent protein
GLP-1	glucagon-like peptide-1
GO	gene ontology
GSIS	glucose-stimulated insulin secretion
GWAS	genome-wide association study
H3K27me3	tri-methylation of lysine 27 on histone H3
HLA	human leukocyte antigen
IF	immunofluorescence
IgG	immunoglobulin G
IPGTT	intraperitoneal glucose tolerance test
IP-MS	immunoprecipitation coupled to mass spectrometry
IV	intravenous
JNK	c-Jun N-terminal kinase
KD	knockdown
kDa	kilodalton
KEGG	Kyoto encyclopedia of genes and genomes
KRB	Krebs Ringer buffer
m ⁶ A	N ⁶ -methyladenosine
Mafa	MAF bZIP transcription factor A
MCC	Manders correlation coefficient
mM	millimolar
MODY	maturity onset diabetes of the young
mRNA	messenger ribonucleic acid
mTORC1	mechanistic target of rapamycin complex 1
Ngn3	neurogenin-3
nM	nanomolar
NMD	nonsense mediated decay
ORF	open reading frame
PCi	prohormone convertase inhibitor
Pdgfr	platelet-derived growth factor receptor
Pdx1	pancreatic and duodenal homeobox 1
PKCζ	protein kinase C zeta type
PMPs	pancreas-derived multipotent precursor
POC	percent of control
Ppy	pancreatic polypeptide
PROT	preserved coding sequence

ABBREVIATIONS

Ptf1a	pancreas transcription factor 1
rER	rough endoplasmic reticulum
RIP	rat insulin promoter
RIP	ribonucleic acid immunoprecipitation
RNA	ribonucleic acid
RNAi	ribonucleic acid interference
RNAseq	ribonucleic acid sequencing
RT-qPCR	reverse transcription quantitative real-time polymerase chain reaction
scRNAseq	single cell ribonucleic acid sequencing
Serca	sarco(endo)plasmic reticulum Ca ²⁺ -ATPase
Shh	Sonic hedgehog
shRNA	short hairpin ribonucleic acid
SMA	spinal muscular atrophy
Smn1	survival of motor neuron 1
Smndc1	survival motor neuron domain containing 1
STZ	streptozotocin
T1D	Type I Diabetes Mellitus
T2D	Type II Diabetes Mellitus
TGFb	transforming growth factor beta
TGN	<i>trans</i> -Golgi network
TSS	transcriptional start site
UPR	unfolded protein response
UTR	untranslated region
VGCC	voltage-gated calcium channel
μM	micromolar
3D	three dimensional

ACKNOWLEDGMENTS

Almost seven years have passed since I began my PhD. I was only 22 when I started and I would not be the person nor the scientist I am today if it weren't for the people who contributed and supported me, both personally and professionally, during this long journey. All the work detailed in this thesis is thanks to them. I would like to use this opportunity to single out some of the most important ones here below.

First and foremost, I would like to thank my supervisor Stefan Kubicek, for not only believing in me and offering me this opportunity 7 years ago, but for remaining a constant cheerleader and constructive mentor throughout this whole process. Stefan, I honestly can't thank you enough. You went out of your way to provide a wonderful place to work, always making time for regular meetings to exchange thoughts and ideas and spearheading unforgettable lab outings and retreats. Your open-door policy, openness to new ideas, and overall positive and supportive energy pushed me to explore and learn without restrictions, which is all anyone can ask for in a PhD.

Next there's all the Kubicek lab members, both past and present, you guys made coming into the lab every day barely feel like work. Thank you for all the laughs, bouldering sessions, terrace drinks and holiday snacks. A particular thank you goes out to the beta cell team for all the emotional and intellectual support every Thursday.

My two main collaborators, Jin and Simon, thank you for all the Skype meetings, scientific help and brainstorming sessions. Jin, you were also my mentor for the first year of my PhD and I will always be grateful to you for helping me find my footing and teaching me how to approach scientific problems practically and efficiently.

Thank you also to my PhD thesis committee: Christoph Bock, Tibor Harkany and Harry Heimberg for your thoughtful discussions and helpful feedback.

Last but certainly not least, I need to mention my family and friends. Ima, Aba and Lugi, it's only thanks to your support and belief that I am even here. Thank you for always being there to chat when I needed encouragement, for all the unforgettable trips around the world and for getting me to this point. Rob, I am so thankful that I got to go on this journey with you by my side, both in and out of the lab. You've been an amazing partner, always there to lean on when things got stressful and the first person to celebrate when I got good news. Sharing craft beer, burgers and bike rides with you is what got me through the finish line. I also want to

ACKNOWLEDGMENTS

acknowledge the people I started my PhD with, specifically my travel buddies Rico, Hatton and Andre. I feel so incredibly lucky to have met you all and to have shared all these experiences together. You brought life to my time in Vienna. One of the strongest motivators in finishing this PhD is to be reunited with you all again. Here's to many more adventures in the future.

Thank you all!

1. INTRODUCTION

1.1 The endocrine pancreas: from embryo to adult

The pancreas consists of two main functional compartments: exocrine and endocrine. The exocrine pancreas, made up of ductal and acinar cells, is responsible for the production and transport of digestive enzymes into the duodenum, whereas the endocrine pancreas, comprising the islets of Langerhans, secretes peptide hormones into the bloodstream to maintain glucose homeostasis. The mature endocrine compartment is highly vascularized and innervated and makes up 1-2% of the total pancreas (Larsen & Grapin-Botton, 2017). It consists of alpha-, beta-, delta- and PP cells, which interact together to maintain normoglycaemia through secretion of their respective hormones: glucagon, insulin, somatostatin and pancreatic polypeptide (Campbell & Newgard, 2021). During development, a fifth islet cell type is also present, the ghrelin-secreting epsilon-cell, but its numbers are greatly decreased postnatally (Heller *et al*, 2005). This next section will detail the tightly regulated process by which specific transcription factors control the development, maturation and maintenance of islet cell identity.

1.1.1 Pancreas development and islet cell specification

Pancreatic development is initiated at embryonic day (E) 8.5 in mice (Jørgensen *et al*, 2007) and Carnegie stage (CS) 12 in humans, ~29 days post-conception (Jennings *et al*, 2013), with the induction of pancreatic and duodenal homeobox 1 (*Pdx1*) expression in the posterior foregut endoderm. This is followed by pancreas-specific transcription factor 1a (*Ptf1a*) at E9.5. These two transcription factors are crucial for proper pancreatic organogenesis in both mice and humans, as protein-null mutations in either gene trigger pancreatic agenesis (Jonsson *et al*, 1994; Stoffers *et al*, 1997; Krapp *et al*, 1998; Sellick *et al*, 2004). However, pancreatic bud formation is still initiated in these mutants, suggesting there are still unknown factors preceding *Pdx1* expression (Bastidas-Ponce *et al*, 2017). Other cases of pancreatic agenesis have been described in humans and mice with *Gata4* and *Gata6* deficiencies (Allen *et al*, 2011; Decker *et al*, 2006; Xuan *et al*, 2012; Shaw-Smith *et al*, 2014). Expression of *Gata4* and *Gata6* transcription factors ensures pancreatic progenitor specification through repression of hedgehog signaling (Xuan & Sussel, 2016). Repression of hedgehog signaling is important for the proper spatial organization of the endocrine pancreas (Apelqvist *et al*, 1997). In effect, the expressions of sonic hedgehog (*Shh*) and *Pdx1* in the developing gut endoderm are mutually exclusive. Disrupting this profile through overexpression of *Shh* in the *Pdx1*⁺ pancreatic endoderm redirects it to an intestinal fate (Apelqvist *et al*, 1997). Activin and FGF signaling

are equally important in hedgehog signaling inhibition and subsequent pancreatic development (Hebrok *et al*, 1998). The transcription factor Sox9 promotes these FGF signals, in a positive feedback loop, with loss of Sox9 resulting in pancreas-to-liver cell fate redirection (Seymour *et al*, 2012). Moreover, inhibition of Shh in chick embryos results in pancreatic heterotopia in the stomach and duodenum (Kim & Melton, 1998), overall highlighting the importance of hedgehog signaling repression in pancreatic endocrine specification.

Around E11.5, several other transcription factors join Pdx1, Ptf1a, Sox9, Gata4 and Gata6 to specify multipotent pancreatic progenitors. These include Mnx1, Hnf1b and Nkx6.1 (Bastidas-Ponce *et al*, 2017). These multipotent pancreatic progenitors are then segregated into two domains: tip or trunk, based on their expression of *Ptf1a* or *Nkx6.1* and their levels of Notch signaling. The trunk domain, characterized by high Notch activity, high *Nkx6.1* expression and repressed *Ptf1a*, specifies an endocrine/duct fate, whereas the *Ptf1a* expressing tip domain drives the progenitors towards an acinar fate (Esni *et al*, 2004; Schaffer *et al*, 2010). Specification to the endocrine lineage requires the expression of *Ngn3*, the main endocrine progenitor marker. Lineage tracing experiments revealed all final endocrine cells arise from *Ngn3*-positive progenitors (Gu *et al*, 2002), while *Ngn3*-null mutations result in pancreata devoid of endocrine cells (Gradwohl *et al*, 2000), undeniably underscoring the importance of *Ngn3* in the generation of all endocrine cell types. The segregation between endocrine or ductal exocrine cell fate once again relies on thresholds of Notch signaling. Notch signaling induces Sox9 expression, which is responsible for instigating *Ngn3* expression in the bipotent trunk cells. However, maintained high Notch signaling also turns on *Hes1* expression, which represses *Ngn3* and specifies a Sox9/*Hes1*-positive ductal fate. Thus, to secure an endocrine fate, *Ngn3* itself inhibits Sox9 expression, rescuing it from Notch-dependent regulation and defining the ultimate *Ngn3*/*Pdx1*/*Nkx6.1*-positive endocrine precursor cell (Shih *et al*, 2012). This final specification occurs between E12.5-E15.5, in a step also known as “the secondary transition” (Pan & Wright, 2011). The peak in *Ngn3* expression at E15.5 then triggers the specification into the final endocrine cell types, defined by mono-hormonal expression of their respective glucose-responsive hormones (Figure 1). Interestingly, the *Ngn3*-positive precursor cell pool no longer represents a multipotent progenitor pool, but rather a committed unipotent pool, in which each *Ngn3*-positive cell will go on to differentiate into solely one cell type (Desgraz & Herrera, 2009).

This final differentiation depends on the tight interplay and expression of several transcription factors. Similar to the antagonistic actions of *Nkx6.1* and *Ptf1a* in acinar vs. endocrine cell specification, or *Hes1* vs. *Ngn3* in endocrine vs. ductal fate acquisition, there are two transcription factors that define early endocrine differentiation through mutual repression of

each other's expressions: *Arx* and *Pax4* (Collombat *et al*, 2003). High expression levels of *Arx* induce an alpha-/PP-cell fate (Collombat *et al*, 2007), whereas *Pax4* expression specifies a beta-/delta-cell lineage (Sosa-Pineda *et al*, 1997). Subsequent loss of *Pax4* and its downstream effector, *Mnx1*, induces a gain of *Hhex* expression and delta-cell differentiation (Pan *et al*, 2015; Zhang *et al*, 2014), whereas sustained *Pax4* and *Mnx1* along with *Pdx1* and *Nkx6.1* specifies a beta cell fate. In effect, the expression of the early players *Pdx1* and *Nkx6.1* starts to become almost exclusively restricted to beta cells. Both of them are indispensable for proper beta cell differentiation and function. Loss of *Nkx6.1* results in severely reduced beta cell mass, while *Pdx1* is essential for insulin expression (Bastidas-Ponce *et al*, 2017). The interplay between two additional transcription factors, *Nkx2-2* and *NeuroD1*, is equally important for specific endocrine cell specification. *Nkx2-2*, through either suppression or activation of *NeuroD1* levels, directs differentiation towards an alpha or beta cell fate, respectively (Mastracci *et al*, 2013). Complete loss of *Nkx2-2*, on the other hand, causes a substantial increase in ghrelin-secreting cells at the expense of beta, alpha and PP-cells, highlighting its importance in specifying multiple islet cell lineages (Prado *et al*, 2004).

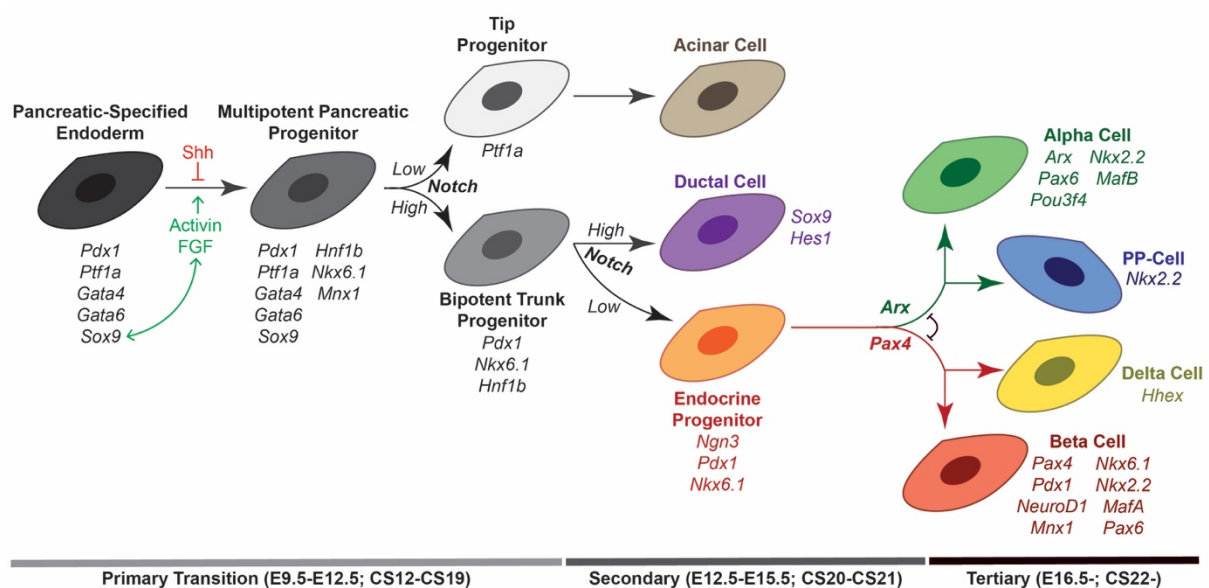


Figure 1. Simplified overview of pancreatic differentiation from pancreatic-specified endoderm to final mono-hormonal secreting cells, with defining transcription factors and signaling molecules highlighted.

Formation of the final islet architecture occurs in parallel to endocrine cell type specification. As the bipotent trunk cells in the epithelial cord are segregated into *Ngn3*-positive endocrine or *Ngn3*-negative ductal exocrine cells, the differentiating *Ngn3*-positive fraction begins to migrate away from the neighboring duct cells in cohesive bud-like clusters (Sharon *et al*, 2019). As new cells adopt *Ngn3* expression and begin differentiating, they are recruited to

these growing clusters, forming an endocrine peninsula separate from the epithelial cord. Hence, the final spatial position of a cell directly correlates with its temporal differentiation position. Temporally, alpha cells begin to appear a full 24 hours before insulin-positive cells, E13.5 vs. E14.5 (Johansson *et al*, 2007; Sharon *et al*, 2019). This explains why murine alpha cells are mostly found around the periphery of the mature islets, with beta cells constituting the core (Figure 2).

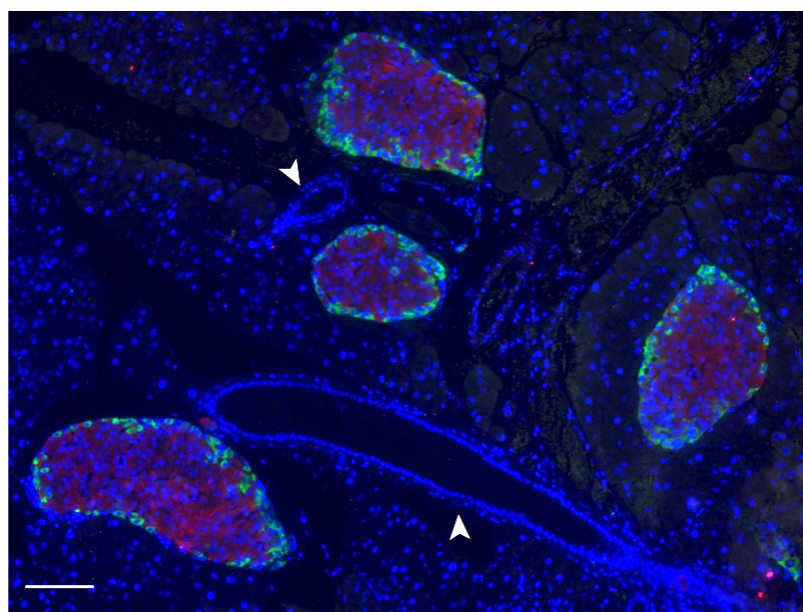


Figure 2. Immunofluorescence image of C57BL/6 murine pancreas cross-section taken on an inverted Leica microscope at 20X objective. Islets are labelled with glucagon (green – ab92517) and insulin (red – DAKO A0564) antibodies, highlighting the spatial organization of glucagon-positive alpha cells at the periphery and insulin-positive beta cells at the core of the islets. DAPI is used to visualize the nuclei of individual cells. White arrows point to pancreatic ducts. The proximity of the ducts to the individual islets reflects their initial progenitor co-localization and the subsequent branching off of the islets. Scale bar = 50µm.

Perinatal proliferation of the peninsular differentiated cells results in acquisition of the final spherical shape and migration from the pancreatic ducts in an EGFR and mTOR-dependent manner (Song *et al*, 2016; Miettinen *et al*, 2000; Sinagoga *et al*, 2017). Maintenance of this islet ultrastructure relies on intercellular communications between the distinct cell adhesion molecules on the individual cells, evident by the loss of peripheral alpha cell localization in N-CAM-depleted mice (Esni *et al*, 1999) or the complete failure to form proper islet-like structures in alpha-cell deficient *Pax6*-null mice (St-Onge *et al*, 1997). Moreover, re-localization of beta cells to the periphery of the islet through reaggregation results in rapid beta-to-alpha cell transdifferentiation, highlighting the critical correlation between final islet cell localization and

function (Spijker *et al*, 2013). The final islet composition is largely made up of beta cells, ~80% in rodents and ~65% in primates, due to the larger starting number of beta cell-committed unipotent Ngn3-positive precursor cells and the higher proliferation rate of beta cells around birth (Desgraz & Herrera, 2009; Arrojo e Drigo *et al*, 2015).

Our detailed understanding of beta cell development, from the transcription factor expression profiles to the signaling cues, has paved the way for the generation of pluripotent stem cell-derived beta cells. The first of these fully *in vitro* differentiation protocols yielding functional, glucose-sensing, insulin-secreting beta cells were reported in 2014 (Pagliuca *et al*, 2014; Rezanian *et al*, 2014). These protocols successfully specified an endocrine fate through continuous FGF supplementation, as well as timed treatments with activin and specific Shh antagonists (Pagliuca *et al*, 2014; Rezanian *et al*, 2014; Nostro *et al*, 2015). They further allowed for endocrine cell differentiation by chemically modulating *Ngn3* expression, and yielded monohormonal insulin-positive cells through sustained inhibition of TGF beta signaling. These protocols are consistently being updated to improve efficiency and functionality, with recent studies even achieving robust and dynamic insulin secretion by ceasing TGF beta inhibition post-specification and dissociating/reaggregating cell clusters (Velazco-Cruz *et al*, 2020). Hence, we now have the tools to generate large quantities of functional beta cells and to study and probe beta cell development *in vitro*.

1.1.2 Regulation of hormone expression in the mature pancreas

Once the final four mono-hormonal endocrine cells are specified, they begin a process of maturation, remodeling and replication during the last stages of development, E16.5 until birth, coined the “tertiary transition” (Dassaye *et al*, 2016). During this time, key transcription factors epigenetically mold the different cell types into their final functional identities. In the endocrine pancreas, this cellular identity is inherently tied to hormone expression. Hence, many studies have focused on understanding the transcription factors and downstream effectors involved in the maintenance of insulin expression. In humans, insulin is encoded by a single gene, *INS*. In rodents, a retrotransposon-mediated duplication of a partially processed insulin mRNA resulted in a two-gene system: the full length *Ins2*, comprising two introns, and the single intron *Ins1* (Melloul *et al*, 2002). *Ins2* is the main gene, orthologous to other species and necessary for full insulin expression, whereas *Ins1*-null mice exhibit no phenotype (Babaya *et al*, 2006). Future references to insulin, unless otherwise stated, will therefore refer to *INS* or *Ins2*.

The insulin promoter spans over 1000 base pairs, with the most important and evolutionarily conserved regulatory elements located within 400bp upstream of the transcriptional start site (TSS) (Figure 3). Specifically, the A3, C1 and E1 boxes are the most highly conserved within mammals and have the most detrimental effects on transcription when mutated (Hay & Docherty, 2006). A3, found -216bp from the TSS, contains a common TAAT motif which recruits homeodomain-containing proteins, most notably Pdx1 (Hay & Docherty, 2006; Melloul *et al*, 2002). C1, located 128bp upstream of the TSS, is the binding site for MafA, while E1, 104bp upstream of the TSS, recruits NeuroD1. Hence, Pdx1, MafA and NeuroD1 all have a direct impact on insulin expression.

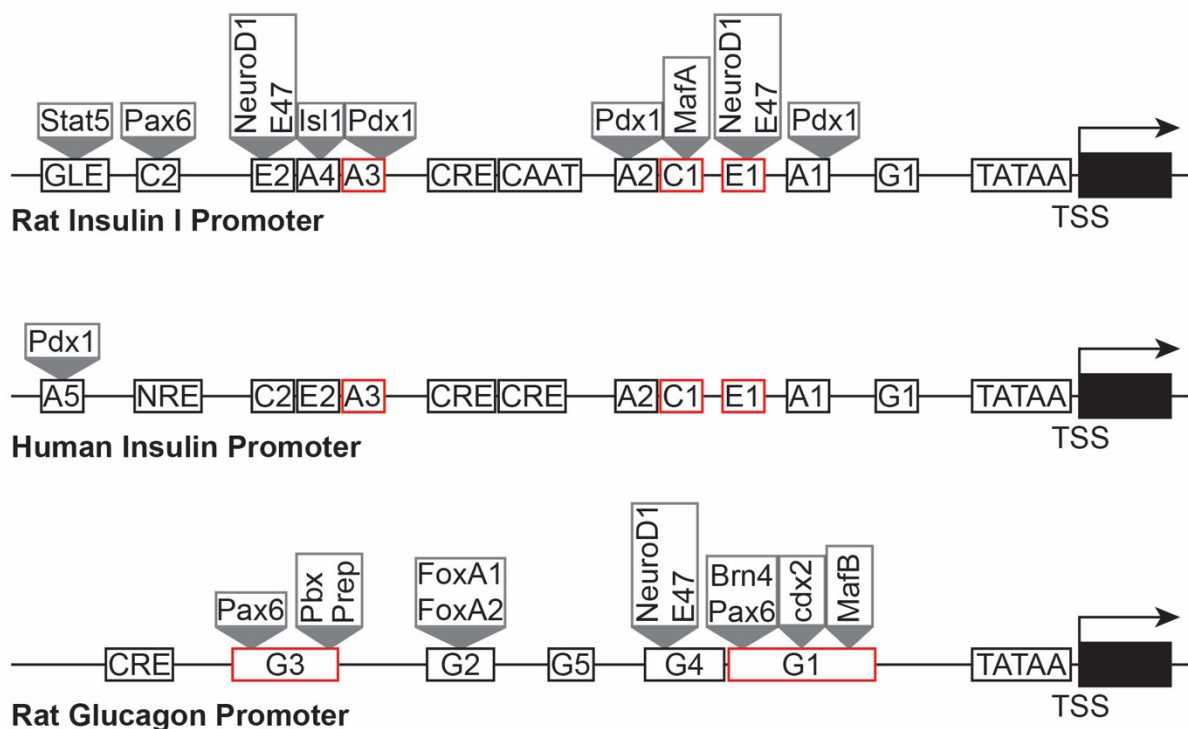


*Figure 3. Schematic representation of insulin and glucagon promoters. Red boxes highlight domains critical for transcription. Pax6 is essential for glucagon transcription while the combination of NeuroD1, Pdx1 and MafA are necessary to confer insulin expression. Importantly, the critical NeuroD1, Pdx1 and MafA binding sites on the insulin promoter are evolutionarily conserved between rodents and humans. Figure adapted from (Melloul *et al*, 2002; Gosmain *et al*, 2011; Wilson *et al*, 2003).*

Postnatal *Pdx1* deletion in beta cells corroborates its direct role in the promotion of insulin transcription (Ahlgren *et al*, 1998; Gao *et al*, 2014; Holland *et al*, 2002). Drastic decreases in insulin, *Nkx6.1*, *Iapp* and *Slc2a2* (Glut2) mRNA levels, as well as in glucose tolerance, are observed following *Pdx1* loss. Interestingly, *Pdx1* also maintains beta cell identity via continued repression of non-beta cell genes. *Pdx1* directly binds upstream of *MafB*'s TSS (-

942/-933bp site), maintaining inhibition of both *MafB* expression and downstream glucagon (Gao *et al*, 2014). This repression is not beta cell specific, as Pdx1 overexpression in mature alpha cells can equally suppress established glucagon expression (Yang *et al*, 2011). *Pdx1* itself is regulated at its evolutionarily conserved enhancer-like region located -2800 to -1600bp upstream of its transcriptional start site, known as Areas I-III (Fujitani, 2017). This region contains binding sites for important beta cell maturation genes, including Hnf1a, FoxA2, Pax6, MafA, MafB and Pdx1 itself, yielding a positive feedback loop of expression (Vanhoose *et al*, 2008; Fujitani, 2017). Homozygous deletion of this enhancer region results in decreased expression of Pdx1 and defective regulation of pancreatic endocrine marker genes downstream of the transcription factor (Fujitani *et al*, 2006).

RNA methylation, particularly N⁶-methyladenosine (m⁶A), has been shown to be essential for the expression of *Pdx1* and *MafA* mRNA and protein in beta cells (Wang *et al*, 2020b; De Jesus *et al*, 2019). In effect, m⁶A-modifications on *Pdx1* and *MafA* transcripts directly increase their stability and translation (Wang *et al*, 2020b; Regué *et al*, 2021), loss of which results in decreased insulin expression. What's more, hypomethylations are enriched in type 2 diabetic patients (De Jesus *et al*, 2019; Wang *et al*, 2020b), reaffirming the importance of these two transcription factors in the maintenance of beta cell identity through the extent of regulation involved in their expression.

MafA and MafB are alpha and beta cell transcription factors with a distinct expression pattern relative to all the other islet-specific regulators, in that their expression is mostly restricted to the final hormone producing cells, impacting maturation and function rather than differentiation (Hang & Stein, 2011). MafA is even more unique in this aspect, as its expression peaks relatively late during development and is restricted to mature beta cells (Matsuoka *et al*, 2004; Artner *et al*, 2010). In fact, no developmental phenotype is observed in *MafA*-null mice, but they do go on to develop hyperglycemia and diabetes due to decreased levels of insulin, Pdx1, MafA, Slc2a2 and glucose responsiveness in the mature beta cells (Zhang *et al*, 2005; Artner *et al*, 2010; Hang *et al*, 2014).

Contrastingly, MafB is expressed in both immature beta and alpha cells prior to detection of MafA, before later becoming restricted to mature alpha cells in mice (Hang & Stein, 2011). The dual function of MafB in specifying both alpha and beta cell character relies on the presence of Nkx6.1. Like MafA, Nkx6.1 is also restricted to beta cells during the secondary transition. *Nkx6.1* levels are regulated by both Pdx1 and Nkx2.2 through direct binding sites on its promoter (Watada *et al*, 2000). *Nkx6.1*-null mice exhibit loss of beta cell precursors and undetectable *MafA* expression, suggesting Nkx6.1 acts upstream of MafA and is vital for beta

cell specification (Sander *et al*, 2000; Matsuoka *et al*, 2004). Binding of MafB to the insulin promoter depends on the co-expression of Nkx6.1, hence insulin is only transcribed in immature beta cells, whereas the absence of Nkx6.1 and Pdx1 in immature alpha cells activates glucagon transcription through direct binding of MafB to the glucagon locus (Nishimura *et al*, 2006; Artner *et al*, 2006). Interestingly, beta cell development is not halted in *MafB*-null mice, only strongly delayed, suggesting MafA can compensate for its loss, while alpha cell numbers and function are significantly compromised (Kato *et al*, 2018; Artner *et al*, 2007; Conrad *et al*, 2016). The *MafB* locus is silenced in mature beta cells through Pdx1 binding, Dnmt3a-mediated methylation and deposition of repressive chromatin marks absent from neonatal beta cells (Cyphert *et al*, 2019; Gao *et al*, 2014). The switch from MafB to MafA upon maturation is vital for the acquisition of glucose responsiveness and overall function (Zhang *et al*, 2005; Artner *et al*, 2010). However, premature MafA signal acquisition fully impairs endocrine differentiation (He *et al*, 2014; Nishimura *et al*, 2009), while continued repression of MafB is necessary to maintain mature beta cell identity, underscoring how tightly transcription factor expressions are temporally regulated for proper endocrine specification.

While *MafA* and *MafB* expressions become mutually exclusive in rodents' mature islets, human beta cells continue to co-express both *MAFA* and *MAFB* postnatally (Dai *et al*, 2012). *MAFA* expression is still restricted to mature beta cells in humans, however its expression takes much longer to peak than in mice (Arda *et al*, 2016). *MAFB*'s role in adult human beta cells has not yet been fully established, although recent studies revealed that co-expression of both *MAFA* and *MAFB* is necessary for expression of genes involved in cell identity, glucose metabolism and insulin secretion (Shrestha *et al*, 2021; Scoville *et al*, 2015; Russell *et al*, 2020).

NeuroD1 and Pax6 are noteworthy transcription factors, as they are present in both mature alpha and beta cells, and bind to both the insulin and glucagon promoters, yet in a cell-type specific manner (Sander *et al*, 1997; Dumonteil *et al*, 1998). Pax6 directly controls the transcription of insulin, glucagon, *Pdx1*, *MafA*, *Nkx6.1*, *MafB* and *NeuroD1*, essential for the proper functioning of adult alpha and beta cells (Gosmain *et al*, 2011, 2012). Homozygous loss of *NeuroD1* results in impaired endocrine differentiation and perinatal onset of severe diabetes in both mice and humans (Naya *et al*, 1997; Romer *et al*, 2019), whereas overexpression of *NeuroD1* in *Pdx1*⁺ progenitors is sufficient to induce premature endocrine differentiation (Schwitzgebel *et al*, 2000). Furthermore, glucose-stimulated insulin secretion (GSIS), the main characteristic of functional beta cells, is strongly impeded in *NeuroD1*-deficient adult beta cells (Gu *et al*, 2010).

NeuroD1 is a member of the basic helix-loop-helix (bHLH) family of transcription factors and it forms a heterodimer with another bHLH transcription factor, E47, necessary for its binding to both the insulin and glucagon promoters (Yi *et al*, 2002; Naya *et al*, 1997; Dumonteil *et al*, 1998). Similarly, Pax6 also forms heterodimers with Cdx2 and MafB (Hussain & Habener, 1999; Andersen *et al*, 1999; Ritz-Laser *et al*, 1999; Gosmain *et al*, 2011). Ultimately, it's the presence of other cell type-specific transcription factors, e.g. Pdx1 or Brn4, that dictates their binding to either insulin or glucagon's promoters. In beta cells, the coactivator p300 brings Pdx1, NeuroD1/E47, Pax6 and MafA into contact with the transcription machinery to facilitate insulin transcription (Yi *et al*, 2002; Iype *et al*, 2005). In alpha cells, the same feat is accomplished upon binding of p300 to Brn4, Cdx2, MafB and Pax6 to enable glucagon transcription (Hussain & Habener, 1999; Gosmain *et al*, 2007). In beta cells, Nkx6.1, Pdx1 and Pax4 recognize and bind Pax6's G1 binding site (Figure 3), outcompeting it and maintaining a repressed glucagon state (Gosmain *et al*, 2011). Interestingly, a PPARgamma-RXR heterodimer was found to do the same (Krätzner *et al*, 2008), hinting at multiple layers of cell and context-specific control.

While transcription factors are at the crux of gene expression regulation, chromatin factors can regulate their localization, binding affinity and expression. The BAF chromatin remodeling complex, for instance, can directly bind the insulin locus and depending on its subunit composition, either promote or suppress transcription (McKenna *et al*, 2015). More specifically, its binding to the insulin gene enhancer region in beta cells was identified as a prerequisite for future Pdx1 binding (Spaeth *et al*, 2019). Methylation also plays an important role. The insulin enhancer region is uniquely hypomethylated in mature beta cells, while the *Arx* locus is maintained in a state of consistent methylation and repression (Kuroda *et al*, 2009; Neiman *et al*, 2017; Dhawan *et al*, 2011). Nkx2-2, together with Grg3 and Dnmt3a, constitute a large repressor complex in beta cells which binds the *Arx* promoter when hypermethylated and recruits HDAC1 to repress *Arx* transcription (Papizan *et al*, 2011). The methyl-binders MeCP2 and Prmt6 are also recruited to the *Arx* locus in beta cells, and they prevent the deposition of activating H3K4me3 marks that are deposited on the locus in alpha cells (Dhawan *et al*, 2011). Dnmt3a levels, directly regulated by mTORC1, are necessary not just for the maintenance of hypermethylation at the *Arx* promoter, but also at other beta cell disallowed gene loci with consequences on insulin secretion (Ni *et al*, 2017; Dhawan *et al*, 2015). Correspondingly, depletion of Nkx2-2 in adult beta cells also stimulates loss of monohormonal cellular identity and function (Gutiérrez *et al*, 2017). Nkx2-2's tinman (TN) domain is the binding site for Grg3. Loss of this interaction during development compromises beta cell maturation in the tertiary transition post E15.5, and triggers beta to alpha cell

transdifferentiation, highlighting the importance of Nkx2-2, Grg3 and methylation in the maintenance of beta cell identity through continuous *Arx* repression (Papizan *et al*, 2011).

Ultimately, an extensive amount of cross-regulation exists between all the islet transcription factors. For instance, Pax6 can bind and activate the promoters of *Pdx1* and *MafA*, while MafA directly drives *Pdx1* transcription, and Pdx1 regulates *MafA* expression (Gosmain *et al*, 2012). At the same time, all three transcription factors bind and positively regulate the insulin promoter, whereas antagonistic binding of Pdx1 vs. Pax6 can control glucagon transcription (Wilson *et al*, 2003; Melloul *et al*, 2002; Gosmain *et al*, 2011). Thus, an intricate network of control is maintained, allowing the different islet cells to share certain transcription factors yet maintain a unique identity and function.

1.1.3 Insulin secretion in the mature beta cell

Insulin secretory granule formation is observed in the tertiary transition from 12-14 weeks of development in humans (Moin & Butler, 2019). Secretory granules make up 10-20% of a total beta cell's volume, with up to 200,000 insulin molecules per granule and 10,000 granules per cell (Suckale & Solimena, 2010). Beta cells are finely attuned to the glucose levels in their environment on account of Glut1/Slc2a1 or Glut2/Slc2a2 glucose transporters on their membrane (Campbell & Newgard, 2021). Following uptake, glucose gets phosphorylated by glucokinase (Gck) and metabolized into ATP. The increase in ATP levels triggers the closing of ATP-sensitive potassium channels (Sur1/Kir6.2) in the beta cell membrane, depolarization of said membrane and consequent calcium influx through voltage-gated calcium channels (Cacna1c and Cacna1d). High intracellular calcium concentrations then stimulate secretion of a readily releasable pool of insulin granules primed near the plasma membrane. This is known as the "triggering pathway" which takes place within 10 minutes of glucose contact (Campbell & Newgard, 2021; Pagliuca & Melton, 2013). However, a second, slower and more sustained phase of insulin secretion is instigated after this, following several signaling cascades resulting in increased insulin transcription, translation, processing and secretion (Campbell & Newgard, 2021). Maintenance of all these steps is integral to beta cell functionality.

Effectively, high glucose concentrations regulate the insulin promoter itself. For instance, under basal conditions, *Isl1* interacts with NeuroD1 at the A3/A4 and E1 boxes (Figure 3). However, under high glucose challenge, *Isl1* is replaced with Pdx1 triggering an increase in insulin transcription (Wang *et al*, 2016a). This process is assisted by the glucose-induced splicing of *Isl1* by the RNA binding protein Rbm4 (Lin *et al*, 2013). In fact, several distinct RNA binding proteins can regulate insulin transcription and translation in a glucose-mediated

manner. The 3'UTR of the insulin transcript is important for its overall stability, with glucose-stimulated binding by Ptbp1 shown to increase overall stability and destabilization observed upon hnRNP K binding (Magro & Solimena, 2013). Consequently, high glucose conditions can extend insulin mRNA half-life from 29 to 77 hours (Lee & Gorospe, 2010). However, chronic hyperglycemia, as observed during diabetes, can decrease insulin mRNA levels due to accumulating ER stress, upregulation of the *Ptbp1*-targeting mir-133a and decreased *MafA* expression and binding to the insulin promoter (Poitout *et al*, 1996; Kataoka *et al*, 2002; Lipson *et al*, 2008; Fred *et al*, 2010). The insulin 5'UTR, on the other hand, is involved in its translation efficiency. Glucose-stimulated binding by Pabpc1 has been linked to increased insulin biosynthesis and Elavl4 to repression (Kulkarni *et al*, 2011; Lee *et al*, 2012). The RNA helicase Ddx1 has also been implicated in linking insulin mRNA to the translation machinery (Li *et al*, 2018b).

Once translated, the preproinsulin product enters the ER, where its signal peptide is cleaved, and proper folding of proinsulin is initiated. Proinsulin is then loaded into immature secretory granules along with 50-150 other proteins, although this number is contested due to difficulties in extracting purified granules (Suckale & Solimena, 2010). Nonetheless, proinsulin makes up over 50% of the total granule protein composition. Proinsulin consists of the final insulin protein and a C-peptide, which gets cleaved off with the help of two prohormone convertases: Pcsk1/3 and Pcsk2. These two enzymes are highly sensitive to pH and calcium levels, hence mature secretory granules maintain an acidic pH of 5.0-5.5 (Chen *et al*, 2018). Pcsk1/3 is the predominant enzyme within human beta cells (Ramzy *et al*, 2020), and its levels are directly modulated by Pax6, MafA and Ptbp1 binding (Wen *et al*, 2009; Wang *et al*, 2007; Knoch *et al*, 2004), whereas its translation, similarly to insulin, is also regulated by Ptbp1 binding. Zinc, transported through the granular membrane transporter Slc30a8, allows for insulin crystallization into its final insoluble, secrete-able hexameric form (Suckale & Solimena, 2010).

Pcsk1/3 and Pcsk2 also play an important role in the post-translational processing of proglucagon. Unlike insulin, the glucagon gene encodes for multiple protein products. The specific peptides formed rely on the prohormone convertase. Notably, Pcsk2 is necessary to yield the final glucagon hormone in alpha cells, whereas Pcsk1/3 is required for the generation of the incretin hormone Glp-1 in the proglucagon-expressing intestinal L-cells (Moede *et al*, 2020). Glp-1 and glucagon are both produced and secreted in a glucose-mediated manner. Conversely to glucagon, however, Glp-1 is secreted postprandially in elevated glucose conditions. They both signal to beta cells through Glp-1 and glucagon receptors and enhance glucose-stimulated insulin secretion in a Pdx1- and cAMP-dependent manner (Li *et al*, 2005; Svendsen *et al*, 2018; Moede *et al*, 2020). Loss of both receptors is detrimental to insulin

secretion, while increased paracrine Glp1 signaling, through overexpression of Pcsk1/3 in alpha cells, has been shown to drastically improve insulin secretion (Wideman *et al*, 2006; Svendsen *et al*, 2018). The heterogenous make-up of pancreatic islets is therefore essential for their proper functioning.

1.2 Diabetes: physical and functional loss of the beta cell

Insulin's identification and isolation in 1921 by Banting, Best, Macleod and Collip is arguably one of the greatest medical breakthroughs of the 20th century (Banting *et al*, 1922). This discovery, exactly 100 years ago, successfully converted diabetes from a terminal disease to a manageable disorder, saving countless lives. In non-diabetic individuals, blood glucose levels are hormonally regulated via the endocrine cells of the pancreatic islets of Langerhans (Campbell & Newgard, 2021). Beta cells secrete the peptide hormone insulin that signals the cellular uptake of glucose from the blood into secondary organs such as the liver or muscle. Loss of functional beta cells and insulin secretion thus result in deregulated glucose homeostasis and severe hyperglycemia, the main hallmarks of diabetes. The developmental and identity-defining programs described in the previous section are directly linked to the pathological processes driving disease onset and progression. The next sections will detail the differences between the main subcategories of diabetes and the transcription factors involved.

1.2.1 Beta cell loss behind Type I Diabetes and Maturity Onset Diabetes of the Young

Type I Diabetes (T1D) usually develops during childhood or adolescence due to T-cell mediated destruction of the pancreatic beta cells. Patients can be identified prior to symptomatic onset due to the presence of autoantibodies directed at beta-cell specific proteins. Common examples are autoantibodies against insulin itself, glutamate decarboxylase 2 (GAD65) responsible for GABA synthesis and Zinc transporter 8 (Slc30a8) found on the surface of insulin secretory granules (Katsarou *et al*, 2017; Ilonen *et al*, 2019). However not as common, Pdx1 autoantibodies have also been characterized (Li *et al*, 2010). It is a complex disease as it is influenced by both genetic and environmental factors (Ilonen *et al*, 2019). GWAS studies have identified several prominent risk factors, predominantly within the class II HLA region (Roep *et al*, 2021), however genetic predisposition does not necessarily correlate with disease onset in most individuals as observed in family and monozygotic twin studies (Redondo *et al*, 2008; Tuomilehto, 2013). The current increased incidence of childhood T1D diagnoses, especially among children moving from low- to high-

incidence countries, provides further evidence for the contribution of environmental factors (Ilonen *et al*, 2019). The triggers for the development of autoantibodies only in select individuals is not yet fully understood. Viral infections, gut microbiota, nutrition, most notably Vitamin D levels, and beta cell stress have all been proposed as potential contributors (Roep *et al*, 2021; Ilonen *et al*, 2019).

Beta cell function is indeed compromised in several T1D patients due to genetic mutations in key transcription factors. For instance, specific mutations in *MafA* have been identified in T1D patients and murine models linked with decreased *Ins2* thymic expression (Noso *et al*, 2010). *Pdx1* and *NeuroD1* insertions and mutations have also been identified in diabetic families, producing impaired p300 activator complex formation on the insulin promoter and consequent beta cell dysfunction (Yi *et al*, 2002). Hence, *MafA*, *Pdx1* and *NeuroD1* polymorphisms can increase susceptibility to T1D. More commonly, though, functional mutations in one of these genes will trigger a monogenetic form of diabetes known as Maturity Onset Diabetes of the Young (MODY). Patients with MODY do not present with autoantibodies but experience progressive beta cell functional decline. Commonly implicated genes include: *Hnf1a* and *Hnf4a* mutations associated with increased beta cell apoptosis and decreased proliferation (McDonald & Ellard, 2013), *NeuroD1* and *Pdx1* mutations affecting their transactivation domains and subsequent insulin promoter binding (Horikawa & Enya, 2019; Staffers *et al*, 1997), and *MafA* missense mutations impairing mRNA stability and glucose-stimulated insulin secretion (Iacovazzo *et al*, 2018).

As of yet no permanent cure exists for T1D, although several treatment options are available to help regulate glycaemia. In effect, the people affected rely on regular insulin injections, which although lifesaving, never reach perfect glycemic control, leaving patients at increased risks of micro- and macrovascular complications (Daneman, 2006; Pagliuca & Melton, 2013). Efforts to mitigate these complications have recently yielded promising technological solutions. One of these is closed-loop insulin systems, also known as artificial pancreases (Boughton & Hovorka, 2021). These systems aim to provide fully automated, all-in-one glucose-measuring and insulin injection capabilities that should limit human error and delayed detections. Existing clinical trial results are promising, with significant improvements to patients' time spent within their target glycemic range. Other groups are working on so-called 'smart insulins', forms of glucose-responsive insulin molecules that only adopt a functional confirmation upon glucose detection, to hopefully protect patients from life-threatening states of hypoglycemia (Chen *et al*, 2021; Mannerstedt *et al*, 2021). In severe cases, healthy donor islet transplantations are performed. However, aside from the common transplantation limitations of organ availability and dependence on immunosuppressants, this treatment does

not offer a long-term solution, with few patients maintaining glycemic control five years post-transplantation (Zinger & Leibowitz, 2014). Encapsulated, stem cell-derived beta cell implants directly address the limitations of islet availability and immune rejection. In 2016, a collaborative project between several groups in Boston developed a chemically modified alginate-based coating resistant to fibrosis (Vegas *et al*, 2016). Transplantation of stem cell-derived beta cells, encapsulated in this coating, into an immunocompetent, diabetic murine model attained long-term normoglycemia, free of immune cell infiltration. Genetically-engineering human pluripotent stem cell-derived beta cells to be HLA-deficient, i.e. hypoimmunogenic, prior to transplantation also prevented immune rejection (Parent *et al*, 2021), offering promising alternatives to classical transplantation.

Recent experiments using murine models of T1D have tested beta-cell driven approaches to mitigate or reverse disease pathogenesis. One group suggested maintenance of beta cells in an immature state prior to immune infiltration could protect them from immune attack, thanks to a decrease in autoantibody expression and antigen presentation (Lee *et al*, 2020). Another study discovered that a subset of beta cells in T1D islets undergoes stress-induced senescence and acquires a senescence-associated secretory phenotype which exacerbates disease progression (Thompson *et al*, 2019). Elimination of this subpopulation in a murine model of T1D arrested the immune destruction, rescued beta cell mass and prevented T1D. While incredibly exciting, whether these experiments in diabetic murine models can be directly translated to humans and how early these therapeutic strategies need to be implemented prior or within disease development have yet to be determined.

1.2.2 Beta cell impairment during Type II Diabetes

Type II Diabetes (T2D) is a much more prevalent disorder than T1D, accounting for more than 90% of diabetic cases, and presenting with a more complex etiology. Peripheral tissues, such as the liver, equally contribute to disease progression through insulin resistance and defective gluconeogenesis on top of beta cell dysfunction (Campbell & Newgard, 2021; Sun & Han, 2020). Unlike in T1D, loss of insulin secretion and beta cell mass in T2D is not purely the result of beta cell death. The chronic hyperglycemic environment beta cells are subjected to post-insulin resistance results in both stress-induced beta cell dysfunction and loss of beta cell identity either through regression to a more primitive state, characterized by loss of key beta cell transcription factor expression and gain of progenitor marks, otherwise known as 'dedifferentiation', or 'transdifferentiation' into other islet cell types (Figure 4)(Swisa *et al*, 2017b).

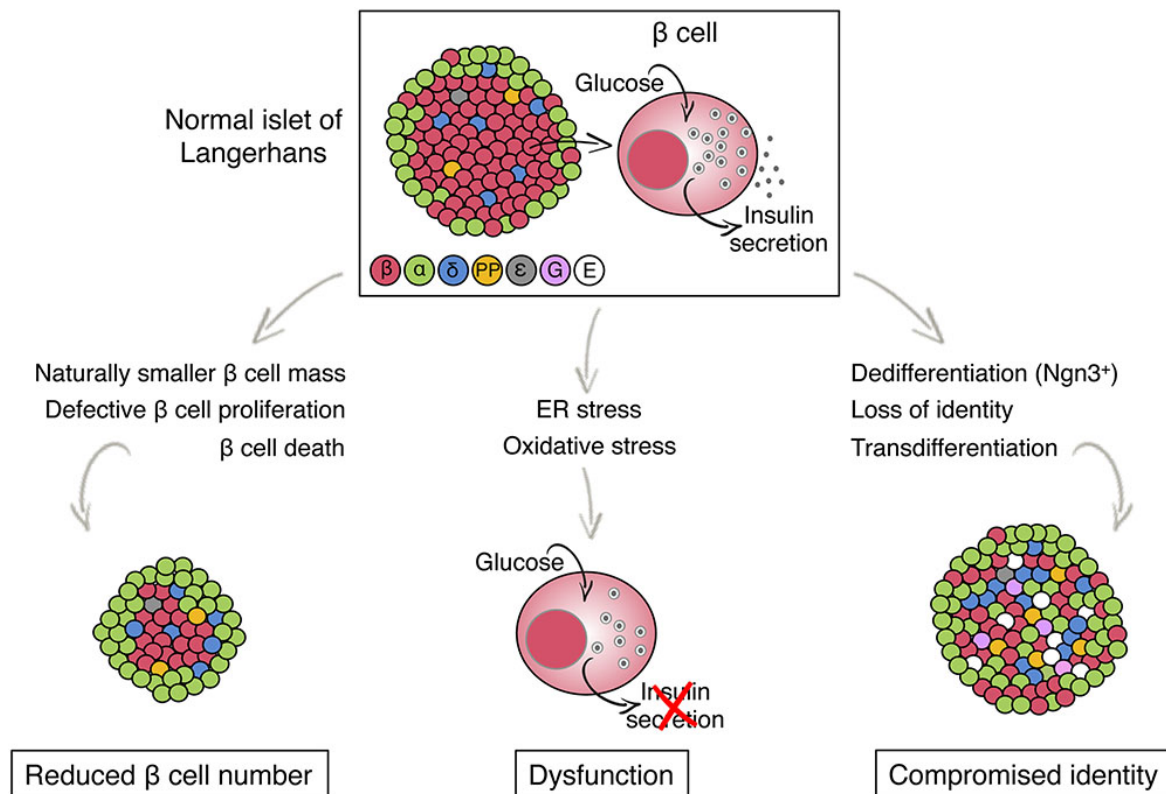


Figure 4. Model of three main pathways suggested for beta cell loss during T2D. Diagram from (Swisa *et al*, 2017b) licensed under CC BY 4.0.

Upon glucose exposure, beta cells increase insulin secretion to maintain normoglycemia. Impressively, insulin processing and production can be enhanced up to 20-fold in response to glucose, a process that strongly relies on the ER compartment (Meyerovich *et al*, 2016). When insulin demand is increased, more peptides transition through the ER and a greater number of misfolded proteins need to be addressed by the unfolded protein response (UPR), specifically the misfolding-prone proinsulin (Sun *et al*, 2015). Under normal conditions, the UPR proteins ATF6, PERK and IRE1a mediate ER stress by pausing translation and increasing autophagy to deal with the burden of unfolded proteins (Ghosh *et al*, 2019). During T2D and insulin resistance, however, beta cells become subjected to sustained hyperglycemia, otherwise known as “glucose toxicity”. Inability to cope with the mounting ER stress results in beta cell apoptosis as the cells switch from adaptive to terminal UPR, as is highlighted by increased TUNEL staining, accumulating levels of ER pro-apoptotic transcription factors, islet amyloid protein aggregates and other UPR apoptotic markers in diabetic islets (Ghosh *et al*, 2019; Meyerovich *et al*, 2016; Butler *et al*, 2003). Interestingly, it was recently discovered that SARS-CoV-2 can cause beta cell transdifferentiation and dedifferentiation through increased ER stress (Tang *et al*, 2021), highlighting the importance of proper ER functioning for beta cell identity.

At a certain level, chronic exposure to glucose also begins to exceed the glycolytic capacity of beta cells, resulting in the shunting of glucose and other glycolysis by-products to other pathways yielding augmented reactive oxygen species production (Robertson, 2004). Unfortunately, beta cells are ill-equipped to handle oxidative stress due to low expression levels of antioxidants, such as superoxide dismutase, resulting in sustained oxidative stress and beta cell dysfunction (Robertson *et al*, 2003; Kitamura & Ido Kitamura, 2007). Both oxidative and ER stress trigger the activation of the c-Jun N-terminal kinase (JNK), which in turn phosphorylates the predominantly cytoplasmic beta cell transcription factor FoxO1 (Kawamori *et al*, 2006). Phosphorylated FoxO1 translocates into the nucleus and becomes transcriptionally active upon deacetylation by Sirt1. It then directly binds to the promoters of the key transcription factors *MafA* and *NeuroD1*, increasing their expression and downstream insulin secretion (Kitamura *et al*, 2005; Talchai *et al*, 2012; Kim-Muller *et al*, 2016). A gain-of-function FoxO1 mutation in wild-type mice can recapitulate these increases in insulin secretion, *Pdx1* and *MafA* expressions (Kim-Muller *et al*, 2016), underlining that FoxO1 can protect beta cell identity during periods of metabolic stress. However, deacetylated FoxO1 is also more sensitive to ubiquitination and degradation, revealing a tightly regulated control mechanism (Kitamura *et al*, 2005). Consequently, diabetic islets from T2D patients with chronic hyperglycemia present with depleted FoxO1 and *MafA* levels, and loss of beta cell identity (Kitamura & Ido Kitamura, 2007; Talchai *et al*, 2012). More specifically, loss of FoxO1 results in increased expression of progenitor markers, namely *Ngn3*, and the emergence of alpha and delta cell markers such as glucagon and somatostatin, indicative of both dedifferentiation and transdifferentiation (Talchai *et al*, 2012; Cinti *et al*, 2016; Spijker *et al*, 2015; White *et al*, 2013). In fact, induction of oxidative stress on its own can mimic the loss of *Pdx1*, *MafA* and *Nkx6.1* transactivation observed in T2D patients (Guo *et al*, 2013). Particularly, the decreased expression of these critical beta cell genes also correlates with increased promoter hypermethylation in T2D donor islets (Davegårdh *et al*, 2018). Furthermore, hydroxyl radicals have been shown to interfere with *Pdx1* mRNA translation, compounding the disruption of insulin transcription and secretion (Robertson *et al*, 2003). Impressively, re-establishment of normoglycemia through acute insulin treatment in T2D patients has been shown to transiently improve beta cell function and revert beta cell dedifferentiation in murine models (Swisa *et al*, 2017b), results corroborated by antioxidant treatment (Del Guerra *et al*, 2005; Lupi *et al*, 2007; Guo *et al*, 2013), reinforcing the impact persistent glucose-toxicity induced stress has on beta cell identity. Whether or not there is a “point of no return”, however, has yet to be established.

Single cell transcriptomics has also opened up a whole new level of beta cell characterization in healthy vs. diabetic patients, with two studies discovering a global de-maturation process in T2D patient beta cells underscored by increased expression of juvenile genes, reflective of dedifferentiation (Wang *et al*, 2016c; Avrahami *et al*, 2020).

1.3 Beta Cell Regeneration

Loss of functional beta cells in diabetes recognizes a therapeutic need to replenish beta cell mass. This area of research was spearheaded by early studies uncovering substantial pancreas regeneration and the emergence of whole new islets following surgical resection of 90% of the pancreas (Bonner Weir *et al*, 1983). Since then, three main approaches to beta cell regeneration have been identified: (1) neogenesis, involving the differentiation of a stem or progenitor cell into a functional beta cell product, (2) replication of existing beta cells, and (3) transdifferentiation, characterized by the adoption of beta cell identity in a terminally differentiated non-beta cell (Aguayo-Mazzucato & Bonner-Weir, 2018). The next sections will delve in detail into our current knowledge and progress in these three areas.

1.3.1 Neogenesis

The presence of beta cell progenitors in adult pancreata is heavily debated. The widely accepted model of beta cell development relies on transient, high *Ngn3* expression in multipotent pancreatic progenitors during the secondary transition, driving them to adopt a post-mitotic endocrine precursor fate, as described in Section 1.1.1. However, it has recently been suggested that a population of transcriptionally active low *Ngn3*-expressing progenitors persists until late into development (Bechard *et al*, 2016). These progenitors can both self-renew or stimulate endocrine differentiation in a cell cycle dependent manner. Progenitor propagation relies on cell cycle dependent activation of cyclin-dependent kinases, which phosphorylate *Ngn3* and target it for proteasomal degradation (Azzarelli *et al*, 2017; Krentz *et al*, 2017). Interestingly, between E11.5 to E13.5 during development, the G1 phase in *Pdx1*-expressing progenitors is significantly lengthened, allowing for the accumulation of *Ngn3* and its downstream cell cycle inhibitor *Cdkn1a* (Krentz *et al*, 2017; Miyatsuka *et al*, 2011). The resultant cell cycle arrest stabilizes *Ngn3* and permits further induction of *Ngn3* transcriptional targets, e.g. *NeuroD1*, promoting cell cycle exit, commitment to an endocrine fate, loss of *Ngn3* expression and subsequent full endocrine cell differentiation (Azzarelli *et al*, 2017; Krentz *et al*, 2017; Miyatsuka *et al*, 2011). Hence, very specific thresholds of *Ngn3* expression are required throughout development to trigger endocrine differentiation or maintain a progenitor pool. The persistence of this progenitor pool in individuals postnatally is unclear

though. Low levels of Ngn3 have been detected in differentiated, adult, hormone-positive islet cells, maintaining a critical role in their overall function, but only a negligible hormone-negative population that could potentially represent progenitors was identified (Wang *et al*, 2009). Importantly, work from two other groups also identified this minimal Ngn3-expressing hormone-negative population lining the pancreatic ducts, and noticed that they could be activated upon pancreatic duct ligation (Xu *et al*, 2008; Van de Casteele *et al*, 2013), transcription factor misexpression (Al-Hasani *et al*, 2013; Courtney *et al*, 2013) or prolonged GABA treatment (Ben-Othman *et al*, 2017) to generate new beta cells. A fasting mimicking diet was also shown to expand the hormone-negative Ngn3-positive pool, yielding beta cell regeneration upon refeeding (Cheng *et al*, 2017). Excitingly, this cycle of fasting-refeeding could also rescue beta cells and insulin secretion in diabetic mice and human islets. Hence, conditions of stress or injury might be necessary to reignite *Ngn3* expression and differentiation capabilities in this hard to detect progenitor pool. Another theory is that this progenitor pool originates from dedifferentiated exocrine cells and therefore might only be formed under conditions of stress or injury (Gomez *et al*, 2015). This could all also explain why one group failed to detect beta cell neogenesis after postnatal day 5 (Xiao *et al*, 2013).

Interestingly, several groups also started looking within the Ngn3-expressing hormone-positive population in adult islets for signs of potential precursors. One study identified a neogenic niche near the islet periphery composed of “virgin beta cell” precursors (van der Meulen *et al*, 2017). These cells are enriched for MafB, Ngn3, with strong nuclear Nkx6.1 staining yet are MafA-negative, thus resembling perinatal immature beta cells prior to their MafB/MafA switch. They, however, do not have the proliferative capacity of perinatal beta cells, with turnover similar to mature beta cells (Lee *et al*, 2021) and they are functionally incompetent due to absent cell surface expression of the Glut2 (Slc2a2) glucose transporter (van der Meulen *et al*, 2017). They only constitute around 1.5% of all beta cells and are believed to represent an intermediary phase within alpha to beta cell transdifferentiation. A second group also identified an Ngn3/Pdx1/Nkx6.1/Pax6/Pax4/insulin-positive, Glut2-null, immature beta cell-like population in both human and murine islets, but with the capacity to give rise to multiple pancreatic and neural cell lineages (Seaberg *et al*, 2004; Smukler *et al*, 2011). Importantly, these cells also had the capacity to self-renew and maintain multipotency and were thus named pancreas-derived multipotent progenitors (PMPs) (Seaberg *et al*, 2004). PMPs could give rise to glucose-responsive, insulin-secreting beta cells *in vitro* (Seaberg *et al*, 2004) and ameliorate hyperglycemia in diabetic mice when transplanted *in vivo* (Smukler *et al*, 2011). Stress, hyperglycemia and ageing all stimulate proliferation and differentiation of this PMP population towards a mature beta cell fate (Razavi *et al*, 2015).

An additional endocrine progenitor was recently proposed, this time negative for both *Ngn3* and hormone expression (Wang *et al*, 2020a). The defining feature of these cells is their expression of the surface protein, Procr, shared among several other tissue resident stem cells. Procr⁺ cells represent approximately 1% of islet cells, with a distinct expression profile reminiscent of E14.5 *Ngn3*-positive endocrine precursors. Interestingly, they arise from *Ngn3*-positive endocrine precursors, yet subsequently lose *Ngn3* expression at some stage. They can self-renew and give rise to all islet endocrine lineages. Similarly to PMPs, they could also give rise to insulin-secreting mature beta cells *in vitro* and rescue hyperglycemia in diabetic mice upon *in vivo* transplantation.

It was recently discovered that this co-existence and balance between immature and mature beta cell populations within pancreatic islets is critical for proper functioning (Nasteska *et al*, 2021). Additional subpopulations of immature beta cells, detailed by multiple groups and characterized by decreased insulin granularity, secretion and key beta cell transcription factor expression, were actually found to respond faster to glucose and coordinate global secretion (Szabat *et al*, 2012; Bader *et al*, 2016; Johnston *et al*, 2016; Wills *et al*, 2016; Salem *et al*, 2019; Nasteska *et al*, 2021). One specific subpopulation, named “hubs” due to their high level of co-activity, is characterized by increased expression of glucose-sensing proteins, such as glucokinase, and increased mitochondrial activity (Johnston *et al*, 2016). Targeted ablation of these hub cells, both *in vitro* and *in vivo*, resulted in dampened glucose response by the remaining beta cells (Johnston *et al*, 2016; Salem *et al*, 2019). *Ftpt* gene expression further subdivided beta cells into immature, proliferative *Ftpt*-negative and mature, insulin-secreting *Ftpt*-positive subpopulations (Bader *et al*, 2016). Accordingly, *Ftpt*-knockout mice displayed impaired glucose-stimulated insulin secretion. Intriguingly, it was shown that calcium signaling can negatively regulate the expression of key beta cell genes, such that low *Pdx1* expression correlates with strongest calcium response to glucose (Nasteska *et al*, 2021). Work from the Grompe lab further subdivided human beta cells into 4 subcategories based on expression of ST8SIA1 and CD9 (Dorrell *et al*, 2016). The most abundant populations were negative for ST8SIA1, accounting for over 80% of beta cells, and enriched for proteins involved in insulin secretion and glucose sensing, e.g. GLUT2, and beta cell maturity, e.g. NEUROD1 and MAFB. Correspondingly, the cells negative for both ST8SIA1 and CD9 displayed the most robust glucose stimulated insulin secretion ratios. These results were corroborated by a second lab who characterized a non-proliferative population of beta cells with low ST8SIA1 and CD9 coupled with high PDX1 and insulin expressions (Wang *et al*, 2016b). Interestingly, these glucose responsive ST8SIA1-negative cells are decreased in the islets of T2D patients, potentially correlating with the loss of expression and function observed in diabetic islets. This

correlates with the preferential loss of hub and Fltp-positive cells under diabetic conditions (Johnston *et al*, 2016; Bader *et al*, 2016).

All in all, these studies uncovered widespread heterogeneity within the beta cell pool, including the key point that not all insulin-expressing cells represent mature beta cells, and provided multiple new populations of progenitor cells to manipulate for beta cell mass expansion. Furthermore, all stem cell differentiation protocols transition through a Ngn3-positive phase (Pagliuca *et al*, 2014; Rezanian *et al*, 2014; Nostro *et al*, 2015), meaning they could benefit from these Ngn3-pool expanding studies listed above to potentially increase efficiency.

1.3.2 Replication

The presence of ongoing beta cell replication in the adult pancreas has been convincingly documented using genetic labelling (Dor *et al*, 2004; Zhao *et al*, 2021), Ki67/BrdU staining (Georgia & Bhushan, 2004; Meier *et al*, 2008; Nir *et al*, 2007; Teta *et al*, 2007; Cox *et al*, 2016) and fluorescent dye-dilution (Brennand *et al*, 2007). It was noted that levels of beta cell mass expansion are highest during infancy, underscored by ~2.6% Ki67-positive beta cells, but that this becomes negligible at later time points (Meier *et al*, 2008; Teta *et al*, 2005). Mechanistically, beta cell ageing is accompanied by accumulating levels of the CDK4 inhibitor, p16^{INK4a} (Krishnamurthy *et al*, 2006). CDK4 and its binding partner, cyclin D2, are essential for postnatal beta cell replication, thus their progressive inhibition correlates with diminished proliferation (Rane *et al*, 1999; Georgia & Bhushan, 2004; Krishnamurthy *et al*, 2006). Bmi-1 and Ezh2, two Polycomb group proteins, which negatively regulate p16^{INK4A} expression through maintained H3K27 trimethylation on its locus, also see their expression decline in an age-dependent manner (Dhawan *et al*, 2009; Chen *et al*, 2009). Impressively, however, during moments of drastic beta cell ablation, they become re-induced, re-inhibiting p16^{INK4A} and consequently allowing for replenishment of beta cell mass. Increased insulin demand during pregnancy (Parsons *et al*, 1992; Teta *et al*, 2007), insulin resistance (Sachdeva & Stoffers, 2009) and obesity (Cox *et al*, 2016) equally results in enhanced beta cell replication. In fact, beta cell volume is more than doubled in obese mice and humans (Bock *et al*, 2003; Butler *et al*, 2003). Hence, stress and metabolic demand can alleviate ageing associated replicative senescence.

Ezh2 levels were found to be regulated by platelet-derived growth factor receptor (Pdgfr) signaling (Chen *et al*, 2011). Pdgfr and its ligands experience a similar expression pattern to Ezh2 and Bmi-1, including age-related depletion and rescue during chemically induced beta cell ablation. Importantly, overexpression of a constitutively active mutant form of Pdgfr could

rescue beta cell replication and glucose tolerance in aged mice. TGF beta signaling, on the other hand, was characterized as a potent inducer of p16^{INK4A} expression, through phosphorylation and nuclear translocation of Smad3, a member of a methyltransferase complex that deposits activating H3K4me3 marks on p16^{INK4A}'s locus (Dhawan *et al*, 2016). Treatment of aged murine and grafted human islets with characterized TGF beta inhibitors successfully repressed p16^{INK4A} and rescued beta cell proliferation. In fact, efforts to induce beta cell replication using small molecules is at the forefront of therapeutic diabetes research. Most impressively in 2015, by some coordinated luck, three independent laboratories identified three distinct small molecule inhibitors that all induced robust beta cell replication and targeted the same protein: dual-specificity tyrosine phosphorylation–regulated kinase 1A (DYRK1A) (Wang *et al*, 2015; Shen *et al*, 2015; Dirice *et al*, 2016). The increase in human beta cell proliferation was pronounced, with 3-6% EdU-positive cycling beta cells, not far from the levels observed during early postnatal life (Meier *et al*, 2008). Importantly, they could all rescue hyperglycemia when given to diabetic murine models (Wang *et al*, 2015; Shen *et al*, 2015; Dirice *et al*, 2016). DYRK1A is involved in the phosphorylation, nuclear export and inactivation of NFAT transcription factors. All three small molecule inhibitors triggered an increase in NFAT nuclear localization. NFAT signaling is necessary for proper transcription of insulin, *Pdx1*, *MafA* and *NeuroD1*, as well as key cell cycle gene expressions, such as cyclin D2 and *Cdk4*, critical for beta cell replication (Heit *et al*, 2006). In fact, overexpression of cyclin D2 on its own was found to be sufficient to trigger beta cell replication, even in aged mice (Tschen *et al*, 2017). Hyperglycemic or hyperinsulinemic local environments induce cyclin D2 expression and downstream beta cell replication in a GLP-1, EGFR, mTOR and PKC ζ -dependent manner (Balcazar *et al*, 2009; Lakshmi pathi *et al*, 2016; Xie *et al*, 2014; Song *et al*, 2016). Hence, GLP-1 agonists, such as Exendin-4, have been widely used to stimulate beta cell replication (Stoffers, 2000; Xie *et al*, 2014; Fusco *et al*, 2017) along with increasing insulin secretion. Since 2005 they have been in regular use in the clinic as a diabetes treatment (Prasad-Reddy & Isaacs, 2015), highlighting the translational capacity of beta cell replication research.

Still, the debate over the contributions of beta cell neogenesis vs. beta cell replication to the postnatal pancreas remains heated. While convincing evidence for the presence of resident beta cell progenitors exists in the adult pancreas, as detailed in the previous section, many groups still argue that beta cell self-renewal is the unique source of postnatal beta cell mass expansion. Firstly, an initial, seminal paper detailing beta cell pulse-chase labelling experiments, with a rat insulin promoter driving expression of a tamoxifen-inducible Cre recombinase, revealed that all new beta cells arose from lineage-labeled ones, concluding, quite controversially, that self-replication is the sole form of mass expansion in the adult

pancreas (Dor *et al*, 2004). These data were later replicated and reinforced in contexts of stress and diabetes by multiple labs (Nir *et al*, 2007; Teta *et al*, 2007; Zhao *et al*, 2021). However, as previously mentioned, several populations of insulin-positive progenitors have been identified in adult islets (Seaberg *et al*, 2004; Smukler *et al*, 2011; van der Meulen *et al*, 2017) that (1) contribute to the mature beta cell pool and (2) would be labelled by a rat insulin promoter driven cassette. Not to mention that the low beta cell labelling efficiency (~30%) (Dor *et al*, 2004) might not have been sufficient to detect minimally abundant neogenesis events. Secondly, there is the observation that human beta cell mass expansion correlates with increased beta cell numbers per islet, i.e. larger islets, and not increased islet number (Meier *et al*, 2008), yet this argument does not hold up either, as several labs have highlighted the heterogeneity within the beta cell pool, with examples of peripheral “virgin” beta cells and Fltp-negative cells contributing to their intra-islet mature beta cell pool (van der Meulen *et al*, 2017; Bader *et al*, 2016). Lastly, one group correlated the absence of increased Ngn3 signal upon recovery from beta cell ablation as an indicator of absent progenitor proliferation (Nir *et al*, 2007), which we now know is not a necessity due to contributions by Ngn3-negative Procr-expressing progenitors (Wang *et al*, 2020a). Hence, it is most likely that beta cell neogenesis contributes to the beta cell pool in addition to beta cell replication.

1.3.3 Transdifferentiation

Reprogramming of terminally differentiated cells and the ideas of continued cellular plasticity and reversible differentiation were first reported back in 1962, when nuclei from adult frog intestinal cells were transplanted into oocytes and gave rise to all tissues (Gurdon, 1962). Several decades later, seminal work by Yamanaka uncovered the cocktail of four transcription factors necessary for this reinduction of pluripotency in somatic cells (Takahashi & Yamanaka, 2006). Transcription factors therefore represent the keys to cellular identity. Due to the unipotency of Ngn3-positive pancreatic precursors, forced expression of different transcription factors pre-specification can easily redirect differentiation. For example, *Pax4* (Collombat *et al*, 2009) and *Pdx1* overexpression (Yang *et al*, 2011) or loss of *Arx* (Collombat *et al*, 2003; Courtney *et al*, 2013; Wilcox *et al*, 2013) at this stage redirects alpha cells towards a beta cell fate. Conversely, overexpression of *Arx* increases alpha cell differentiation at the expense of beta and delta cells (Collombat *et al*, 2007).

In fact, fully differentiated pancreatic alpha and beta cells have also been shown to exhibit a high degree of plasticity, specifically in contexts of stress and genetic manipulation. Concomitant activating H3K4me3 and repressive H3K27me3 lysine methylation marks in so-called bivalent chromatin domains are a key characteristic of stem cell epigenomes during

development (Li *et al*, 2018a). This marks genes as primed for both activation and repression, an important hallmark of stemness. Hence, it was remarkable to find that a large number of key alpha and beta cells genes, particularly *Irx1*, *Arx*, *MafA* and *Pdx1*, share this bivalency (Bramswig *et al*, 2013). What's more, the insulin promoter was found to be hypomethylated in both alpha and beta cells, with differential methylation only found at the enhancer level (Neiman *et al*, 2017), while many more open chromatin regions were detected in alpha cells compared to beta cells (Ackermann *et al*, 2016). Overall, this suggests that alpha cells are predisposed to plasticity, not unlike pluripotent cells. Consequently, it was hypothesized that the use of histone methyltransferase inhibitors would have a potent effect on the transcriptional landscape of alpha cells. Use of the unspecific histone methyltransferase inhibitor, adenosine dialdehyde (Adox), triggered a global decrease in H3K27me3 and initiated nuclear expression of *Pdx1* and co-expression of insulin in glucagon positive cells (Bramswig *et al*, 2013). Similarly, the small molecule BRD7552 induced an increase in H3K4me3 and decrease in H3K27me3 marks on the *Pdx1* promoter, which immediately increased *Pdx1* expression in a murine alpha cell line and human islets (Yuan *et al*, 2013). Additionally, the histone lysine methyltransferase inhibitor, chaetocin, was shown to potently decrease *Arx* and *Brn4* expressions, while inducing *Ins2*, *Pax4*, *Gck* and *Nkx6.1* transcription within 24h in alpha cells (Kubicek *et al*, 2012). Overall, these experiments reinforce the finding that alpha cells are epigenetically "poised" for cellular conversion.

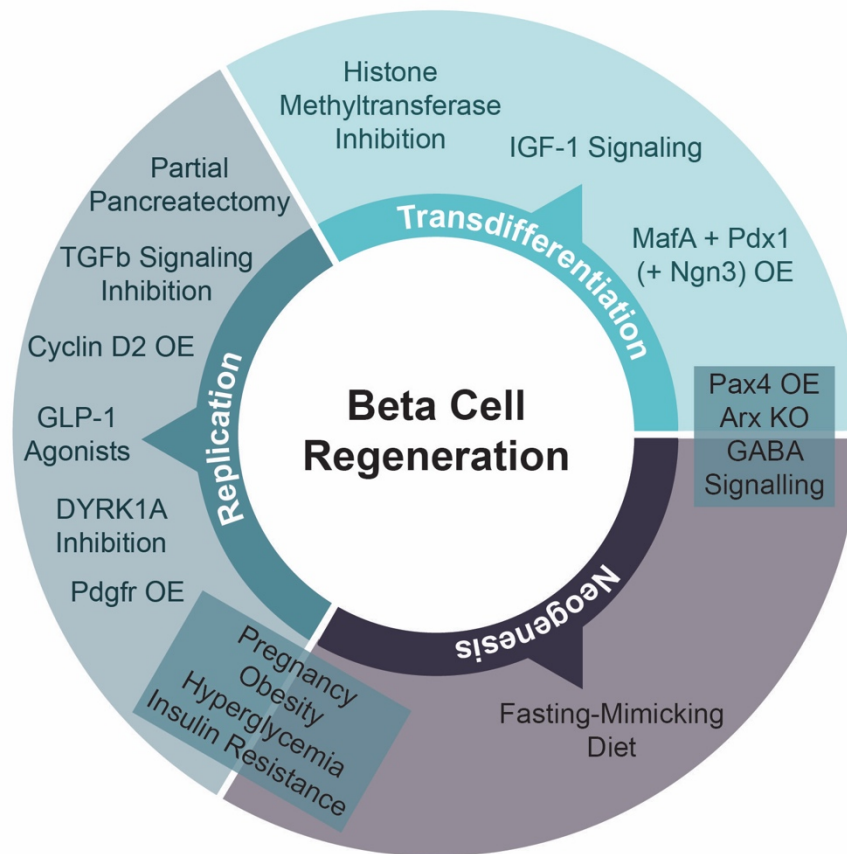
Interestingly, the influence of different transcription factors changes during development. For instance, *Pdx1* overexpression in endocrine progenitors can cause a dramatic loss of glucagon, *Brn4* and *Arx* expression and trigger a complete shift from alpha to beta cell character, whereas *Pdx1* overexpression in committed alpha cells cannot (Yang *et al*, 2011). It turns out that at that point, overexpression of *MafA* in combination with *Pdx1* is required to fully commit mature alpha cells to a beta cell fate in both mice and humans (Matsuoka *et al*, 2017; Xiao *et al*, 2018; Furuyama *et al*, 2019). The resultant beta cells are also fully functional and capable of restoring normoglycemia in T1D mouse models (Xiao *et al*, 2018; Furuyama *et al*, 2019). *MafA* on its own can only activate limited insulin transcription in a murine alpha cell line, highlighting the importance of *Pdx1* and *MafA* co-expression (Matsuoka *et al*, 2004). The importance of both *Pdx1* and *MafA* in the stimulation of beta cell identity is further highlighted in multiple studies that successfully switch non-endocrine cell types to a beta cell fate by overexpressing *Pdx1* and *MafA* alongside *Ngn3* (Ariyachet *et al*, 2016; Banga *et al*, 2012; Chen *et al*, 2014; Hickey *et al*, 2013; Luo *et al*, 2014; Yamada *et al*, 2015; Zhou *et al*, 2008). As *Ngn3* is required for the development of the four hormone-secreting cells that comprise the mature endocrine pancreas, its overexpression likely helps direct cells to a general endocrine state, prior to the more defined beta cell fate specified by *MafA* and *Pdx1*

(Gradwohl *et al*, 2000). In accordance with Yamanka's pluripotency factors, *Ngn3*, *Pdx1* and *MafA* thus represent the specific cocktail of transcription factors needed to unlock an insulin-secreting beta-like fate. Interestingly, *Ngn3* and *MafA* overexpression in the absence of *Pdx1* triggers the transdifferentiation of acinar cells to glucagon-expressing alpha cells (Li *et al*, 2014). On the other hand, overexpression of *Pdx1* alone, reprograms acinar cells into all endocrine cells except for alpha cells (Miyazaki *et al*, 2016), overall reinforcing *Pdx1*'s role in the repression of alpha cell identity and importance in specification to the beta cell lineage.

The alpha cell lineage is heavily reliant on the expression of *Arx*. In fact, loss of *Arx* is sufficient to drive alpha to beta cell transdifferentiation in adult alpha cells (Courtney *et al*, 2013; Spijker *et al*, 2013; Chakravarthy *et al*, 2017). Likewise, overexpression of *Arx*'s antagonist *Pax4* equally causes adult glucagon-positive alpha cells to lose *Arx* expression and adopt a functional beta-like cell identity (Al-Hasani *et al*, 2013). Conversely, increasing *Arx* expression in adult beta cells, either through forced overexpression (Collombat *et al*, 2007) or hypomethylation of *Arx*'s promoter by *Dnmt1* depletion (Dhawan *et al*, 2011), induces a switch to alpha cell identity. Screens for inhibitors of *Arx* in adult alpha cells identified the anti-malarial drugs, artemisinins, to induce the nuclear ejection of *Arx*, in a GABA signaling-mediated manner, and the consequent stimulation of insulin expression and secretion (Li *et al*, 2017). Simultaneously, it was found that GABA supplementation, on its own, could downregulate *Arx* expression in adult alpha cells, triggering their shift towards a *Pax4*-positive beta cell identity (Ben-Othman *et al*, 2017). The transdifferentiated cells were further capable of restoring beta cell mass and euglycemia following chemically induced diabetes. GABA, normally co-secreted with insulin by beta cells, signals the inhibition of glucagon secretion in alpha cells via their surface GABA_A receptors (Rorsman *et al*, 1989). Therefore, it has been postulated that autocrine glucagon signaling plays a role in propagating the loss of alpha cell identity (Li *et al*, 2017). The proposed link between glucagon and alpha cell identity is not a new one, with previous work in glucagon receptor knockout mice correlating remarkable increases in plasma glucagon with alpha cell hyperplasia and increased expressions of both *Arx* and glucagon (Parker *et al*, 2002; Gelling *et al*, 2003; Sørensen *et al*, 2006). Interestingly, glucagon gene knockdown strongly diminished alpha to beta cell transdifferentiation in a zebrafish model (Ye *et al*, 2015). This was rescued by exogenous glucagon or Glp-1 agonist Exendin-4 treatment, reaffirming the notion that glucagon gene product signaling contributes to the destabilization of alpha cell identity. On the other hand, insulin signaling was shown to negatively affect alpha to beta cell fate switch, as treatment with *Igfbp1*, which is directly inhibited by insulin signaling, or embryonic insulin knockdown both triggered ectopic *Pdx1* expression, loss of alpha cell identity and consequent alpha to beta cell transdifferentiation in murine, human and zebrafish islets (Lu *et al*, 2016; Ye *et al*, 2016). It therefore appears a delicate balance between insulin

and glucagon levels is necessary to unlock alpha cell plasticity. This could explain why near-total beta cell ablation, and concomitant loss of insulin signaling, can drive alpha cells towards a beta cell fate in both murine and zebrafish models, independent of genetic perturbation (Thorel *et al*, 2010; Chung *et al*, 2010; Ye *et al*, 2015). More specifically, pioneering work from the Herrera lab revealed that upon diphtheria toxin-induced murine beta cell ablation, alpha cells convert to beta cells via an insulin and glucagon bihormonal cell phase (Thorel *et al*, 2010), results later reproduced in zebrafish (Ye *et al*, 2015) and in toxic glucose analog-driven beta cell ablation in combination with pancreatic duct ligation (Chung *et al*, 2010). Interestingly, the same diphtheria toxin beta cell ablation model in prepubescent mice sees replenishment of the beta cell mass from a delta cell origin (Chera *et al*, 2014). Juvenile delta cells maintain the ability to downregulate FoxO1, dedifferentiate, proliferate and restore beta cells following loss, an ability lost with age and replaced with proliferation-independent alpha to beta cell direct conversion.

In summary, depending on the stressor imposed on the pancreas, be it physical damage through pancreatic duct ligation, metabolic demand during obesity or pregnancy, transcription factor misexpression, or chemically and genetically induced beta cell destruction, as well as the developmental timing, the beta cell pool can be restored through beta cell replication or non-beta cell origins either via progenitor neogenesis or transdifferentiation (Figure 5). Importantly, this adaptation to stress is maintained throughout life, but it can be exacerbated following long-term insulin resistance and establishment of T2D.



ALL: Pancreatic Duct Ligation and Beta Cell Ablation (in combination or individually)

Figure 5. Summary of various factors identified to induce beta cell regeneration.

1.4 Aims

The aims of this thesis were to understand insulin transcriptional and translational regulation, as well as downstream protein biosynthesis, in diabetic beta cells and healthy alpha cells, i.e. respective models of diminished or repressed insulin expression. More specifically, we wanted to reverse the loss of beta cell identity and insulin expression observed in T2D islets post-FoxO1 depletion, and identify and characterize new epigenetic factors mediating insulin silencing in wild-type, healthy alpha cells. Therefore, we performed (1) a high-content small molecule screen to uncover chemical inhibitors of beta cell dedifferentiation and (2) an RNA interference screen to isolate factors whose loss elicits an increase in insulin expression in alpha cells and promotes their transdifferentiation to beta cells. Elucidating and characterizing novel targets and pathways permitting the reversal of beta cell dedifferentiation or stimulation of alpha cell transdifferentiation ties into the strong therapeutic need of replenishing functional beta cell mass in diabetic patients and provides us with valuable information regarding the regulation and rescue of insulin expression, beta cell identity and functionality.

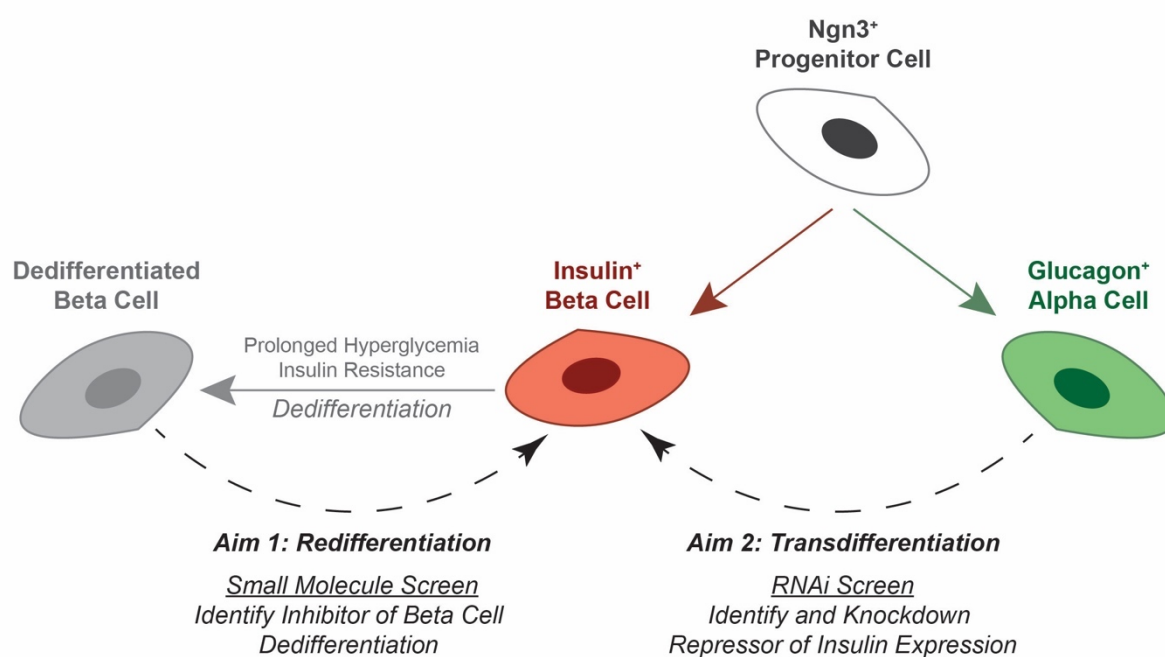


Figure 6. Overview of the two projects constituting this thesis and their main respective aim: re-establishing insulin expression in dedifferentiated beta cells through chemical inhibition and inducing it in alpha cells via targeted genetic knockdowns.

2. RESULTS

2.1 An inhibitor-mediated beta cell dedifferentiation model reveals distinct roles for FoxO1 in glucagon repression and insulin maturation

Diabetic beta cells experience dedifferentiation and loss of insulin secretion upon prolonged exposure to hyperglycemia and insulin resistance. In order to study diabetic beta cells in detail and understand how to reverse their loss of insulin secretion, we established and characterized a cellular model system that successfully mimics FoxO1-mediated diabetic beta cell dedifferentiation *in vitro*. Performing a high content screen with this cellular model system identified the FDA-approved anti-diarrheal drug loperamide as a potent inducer of insulin biosynthesis. Through calcium mobilization, pH modulation and increased FoxO1 expression and nuclear import, loperamide promotes increased proinsulin trafficking, secretory granule maturation and insulin secretion. Importantly, loperamide could increase beta cell transcription factor expression and insulin secretion in diabetic human islets and ameliorate hyperglycemia in a diabetic murine model. Impressively, loperamide also decreased bihormonal insulin/glucagon-positive cells, characteristic of dedifferentiation, in favor of increased monohormonal insulin-positive cells both *ex vivo* in human islets and *in vivo* in a diabetic murine model.

Molecular Metabolism 2021

PII: S2212-8778(21)00176-9

DOI: <https://doi.org/10.1016/j.molmet.2021.101329>

Reference: MOLMET 101329

Submitted: June 22, 2021

Accepted: August 20, 2021

Reprinted from (Casteels *et al*, 2021)

© 2021. This manuscript version is made available under the CC-BY-NC-ND 4.0 license <https://creativecommons.org/licenses/by-nc-nd/4.0/>

An inhibitor-mediated beta cell dedifferentiation model reveals distinct roles for FoxO1 in glucagon repression and insulin maturation

Tamara Casteels¹, Yufeng Zhang², Thomas Frogne³, Caterina Sturtzel⁴, Charles-Hugues Lardeau¹, Ilke Sen^{5,6}, Xiaocheng Liu⁷, Shangyu Hong², Florian M. Pauler¹, Thomas Penz¹, Marlene Brandstetter⁸, Charlotte Barbieux⁹, Ekaterine Berishvili⁹, Thomas Heuser⁸, Christoph Bock¹, Christian G. Riedel^{5,6}, Dirk Meyer¹⁰, Martin Distel⁴, Jacob Hecksher-Sørensen³, Jin Li^{1,2,*} and Stefan Kubicek^{1,*}

¹CeMM Research Center for Molecular Medicine of the Austrian Academy of Sciences. Lazarettgasse 14, A-1090 Vienna, Austria

²State Key Laboratory of Genetic Engineering and School of Life Sciences, Fudan University, Collaborative Innovation Center for Genetics and Development, Shanghai, 200438, China

³Novo Nordisk A/S, Novo Nordisk Park, DK-2760 Måløv, Denmark

⁴Zebrafish Group, Children's Cancer Research Institute, Vienna, Austria

⁵Integrated Cardio Metabolic Center, Karolinska Institutet, Novum, Blickagången 6, SE-141 57 Huddinge, Sweden

⁶Department of Biosciences and Nutrition, Karolinska Institutet, Blickagången 16, SE-141 52 Huddinge, Sweden

⁷Department of Obstetrics and Gynecology, Obstetrics and Gynecology Hospital of Fudan University, Shanghai 20011, China

⁸Electron Microscopy Facility, Vienna BioCenter Core Facilities GmbH, Vienna, Austria

⁹Cell Isolation and Transplantation Center, Department of Surgery, Geneva University Hospitals and University of Geneva, Geneva, Switzerland

¹⁰Institute of Molecular Biology, Leopold-Franzens-University Innsbruck, Technikerstr. 25, 6020 Innsbruck, Austria

*To whom correspondence should be addressed

Email, Phone: skubicek@cemm.oeaw.ac.at, +43-1/40160-70036 or li_jin_lifescience@fudan.edu.cn, +86-21-31246503

Running Title: Inhibition of beta cell dedifferentiation

Key words: Diabetes/Beta Cell Dedifferentiation/FoxO1 inhibitor/Loperamide

Abstract

Objective: Loss of FoxO1 signaling in response to metabolic stress contributes to the etiology of type II diabetes, causing the dedifferentiation of pancreatic beta cells to a cell type reminiscent of endocrine progenitors. Lack of methods to easily model this process *in vitro*, however, have hindered progress into identification of key downstream targets and potential inhibitors. We therefore aimed to establish such an *in vitro* cellular dedifferentiation model and apply it to identify novel agents involved in the maintenance of beta cell identity.

Methods: The murine beta cell line, Min6, was used for primary experiments and high content screening. Screens encompassed a library of small molecule drugs representing the chemical and target space of all FDA-approved small molecules with an automated immunofluorescence read-out. Validation experiments were performed in a murine alpha cell line as well as in primary murine and human diabetic islets. Developmental effects were studied in zebrafish and *C. elegans* models, while diabetic db/db mouse models were used to elucidate global glucose metabolism outcomes.

Results: We show that short-term pharmacological FoxO1 inhibition can model beta cell dedifferentiation by downregulating beta-cell specific transcription factors, resulting in the aberrant expression of progenitor genes and the alpha cell marker glucagon. From a high content screen, we identified loperamide as a small molecule that can prevent FoxO inhibitor-induced glucagon expression and further stimulate insulin protein processing and secretion by altering calcium levels, intracellular pH and FoxO1 localization.

Conclusions: Our study provides novel models, molecular targets and drug candidates for studying and preventing beta cell dedifferentiation.

Introduction

In type II diabetes initial peripheral insulin resistance often progresses to insulin deficiency caused by beta cell dedifferentiation and apoptosis. A key regulator of beta cell dedifferentiation is the transcription factor Forkhead box protein O1 (FoxO1). Prolonged and severe hyperglycemia results in the loss of FoxO1 expression and concomitant beta cell failure[1,2]. The dedifferentiation of beta cells via inhibition of FoxO family proteins is not yet fully understood, but it has been linked with decreased metabolic flexibility[3]. Introduction of a metabolic stressor to beta cells lacking FoxO1 triggers a loss of function and a subsequent increase in the pancreatic endocrine progenitor marker Neurogenin3 (Ngn3). Additionally, a subset of the dedifferentiated beta cells begin expressing the alpha cell marker glucagon, supporting the multi-lineage potential of these progenitors[4]. Notably, dedifferentiated beta cells have been identified in human islets from diabetic donors[5].

Identifying mechanisms to inhibit or reverse beta cell dedifferentiation represent key goals in current type II diabetes research. Robust models to study this process *in vitro* have yet to be established[6]. Existing efforts to identify compounds that improve beta cell health have focused on differentiation models with knockouts of type II diabetes GWAS susceptibility genes DKAL1, KCNQ1, or KCNJ11[7] or on FGF2-mediated beta cell dedifferentiation[8]. Here, our aim was to establish an *in vitro* model for FoxO1-dependent beta cell dedifferentiation that was highly reproducible, did not rely on precious materials and was amenable for high-content screening.

We hypothesized that pharmacological FoxO1 inhibition in beta cell lines could provide an *in vitro* model system for the beta cell dedifferentiation process observed in mice following genetic knock-out of the transcription factor FoxO1[4]. Here we show that pharmacological inhibition of FoxO1 in beta cell lines mimics many aspects of *in vivo* dedifferentiation. Subsequently, using a high content screening assay, we identify the small molecule loperamide to reverse aspects of this FoxO1 inhibition in beta cells. We show that it modulates calcium signaling, intracellular pH, secretory granule maturation and FoxO1 expression in pancreatic islet cells and causes corresponding physiological effects *in vivo*.

Results

A cellular model for beta cell dedifferentiation

To establish a screenable model system for inhibitors of beta cell dedifferentiation, we treated the murine beta cell line Min6 with the selective small molecule FoxO1 inhibitor AS1842856

(FoxOi)[9] for 48 hours (Fig. 1A). We observed a ~3-fold reduction in insulin mRNA, accompanied by an upregulation of the pancreatic progenitor marker Ngn3 and a strong induction of the alpha cell marker glucagon (Fig. 1B and SFig. 1A), with comparable changes at the protein level (Fig. 1C, SFig. 1B and C). On a population level, most cells showed reduced insulin levels and in approximately a quarter of cells glucagon was strongly increased (Fig. 1D, SFig. 1D). In these cells, glucagon staining was granular and partially overlapped with the remaining insulin staining (Fig. 1E). Washout of the inhibitor for 48h successfully reestablished insulin protein levels, however the glucagon positive subpopulation remained stable and converted to a double-positive phenotype (SFig. 1E). It is possible that later time points post-washout might reveal a complete reversibility of the phenotype. Overexpression of a constitutively active form of FoxO1 significantly decreased the fraction of FoxOi-induced glucagon positive cells (SFig. 1F-H). Importantly, FoxOi caused gene expression changes comparable to the existing triple FoxO knockout mouse model[10], both in terms of FoxO1 target genes (Fig. 1F) and genome-wide (SFig. 1I). Beta cell specific genes were downregulated, whereas progenitor (i.e. Sox9, Myc, Hes1) and alpha cell markers (i.e. Gcg, Mafb) were enriched (Fig. 1F and G). This correlates with depleted Pdx1, Nkx6-1, MafA and Mafk mRNA levels observed in diabetic human islets[11] and inactivation of these transcription factors after simulation of a diabetic milieu[11]. These results support the hypothesis that chemical inhibition of FoxO1 in this beta cell line is able to phenocopy the genetic depletion of FoxO in mice and generally mimic beta cell dedifferentiation.

A high content screen identifies inhibitors of beta cell dedifferentiation

We next wanted to test the suitability of our cellular system for the identification of small molecule dedifferentiation inhibitors. To do so, we used an immunofluorescence assay for glucagon and insulin on an automated microscope. The cells were treated with FoxOi for 48h in combination with a library of 283 representative, clinically-approved drugs covering the diversity of clinically used compounds with regards to chemical structure and molecular targets[12]. We found that a subset of these compounds caused an increase in insulin staining and a reduction in glucagon intensity compared to FoxOi treatment alone (Fig. 2A and SFig. 2A). Among them, loperamide treatment was the most effective at antagonizing the actions of FoxOi without affecting cell numbers (Fig. 2A and B, SFig. 2A and B). When we analyzed gene expression changes caused by loperamide, we observed that the compound decreased glucagon mRNA levels regardless of FoxOi treatment (Fig. 2C and SFig. 2C). Globally, loperamide countered FoxOi mediated transcriptional effects on transcription factors important for beta cell development (Fig. 2D), genes linked to beta cell metabolic inflexibility and dysfunction[3,10] (SFig. 2D), and insulin secretion (Fig. 2D and SFig. 2E). Interestingly, loperamide treatment had no effect on insulin mRNA levels (Fig. 2E and SFig. 3A), yet resulted

in a strong upregulation of intracellular insulin protein levels (Fig. 2F and SFig. 3B-E). Enhanced insulin biosynthesis (i.e. translation, processing) or hindered secretion could account for such changes. Glucose-stimulated insulin secretion assays, however, revealed an increase in secreted insulin following loperamide treatment in both low and high glucose conditions (Fig. 2G and SFig. 3F), able to fully counter the decrease induced by FoxOi. The most striking difference was noted when we compared the ratio of mature insulin to precursor proinsulin protein levels (SFig. 3C and D). 48-hour loperamide treatment induced a 6-fold increase compared to controls, suggesting a strong stimulation of proinsulin processing (Fig. 2H). Combined, these initial results propose a role for loperamide in the reinforcement of beta cell character and function.

Loperamide increases FoxO1 expression and nuclear localization promoting changes in calcium signaling

Loperamide is a mu-opioid receptor agonist[13] which has been used for the treatment of diarrhea since the 1970s (FDA application No. 017694). In contrast to other opioid receptor agonists, loperamide does not have effects on the central nervous system. To test if activation of mu-opioid receptors could inhibit beta cell dedifferentiation and phenocopy loperamide's actions, we used a novel mu-opioid receptor agonist, herkinorin, in combination with FoxOi[14,15]. Like loperamide, herkinorin prevented the decrease of insulin levels following FoxO inhibition. However, herkinorin did not inhibit the upregulation of glucagon in Min6 cells (SFig. 4A). To further investigate on- vs. off-target effects of loperamide, the opioid receptor antagonist naltrexone was used in combination with loperamide. While naltrexone did not prevent the loperamide-mediated decrease in glucagon or increase in insulin levels, the beta cell master regulatory transcription factor Pdx1 was repressed (SFig. 4B and C). In summary, loperamide's effects on dedifferentiation cannot fully be explained by the activation of mu-opioid receptors, supported by their noticeably low expression level in Min6 cells (SFig. 4D).

Based on FoxOi's published role as a selective FoxO1 inhibitor [9], we tested whether loperamide treatment had any effect on the expression levels or activity of FoxO1. Remarkably, we observed an increase in FoxO1 mRNA and protein levels (Fig. 3A and B, SFig 5A and B). Moreover, loperamide was able to completely rescue FoxOi's suppression of FoxO1 transcription (SFig. 5A). Further experiments by subcellular fractionation of Min6 cells treated with loperamide uncovered that the increase in FoxO1 protein is mostly restricted to the nucleus (Fig. 3B and C), indicating that loperamide induces an increase in active nuclear FoxO1 protein. This increase occurs within hours and is maintained when loperamide is co-treated with FoxOi (Fig. 3B, SFig. 5C and D). Immunofluorescence experiments highlight a positive cellular correlation between nuclear FoxO1 and insulin expression levels upon

loperamide treatment, with higher levels of both evident in approximately one third of cells compared to control (Fig. 3B).

To determine whether the increase in nuclear FoxO1 also corresponded with an increase in genomic binding and activity, we compared our loperamide RNAseq dataset to published global FoxO1 ChIPseq results from murine islets[16]. A core positive enrichment was observed between genes bound by FoxO1 and upregulated with loperamide (SFig. 5E). Within those genes, a 26-fold enrichment in high voltage-gated calcium channels (VGCC) was identified (GO: 0061577) (Fig. 3D, SFig. 5F and G). Notably on the list were $Ca_v1.2$ (Cacna1c) and $Ca_v1.3$ (Cacna1d), the two major L-type calcium channel isoforms necessary for insulin secretion [17,18]. Interestingly, FoxOi treatment appears to globally downregulate genes related to calcium channel activity (SFig. 5H). Their loss is an early marker of beta cell dysfunction, but loperamide appears capable of rescuing their levels independently of FoxOi (Fig. 3D). In effect, previous studies on loperamide have suggested it increases free intracellular calcium levels (Harper et al, 1997; He et al, 2003). Coupled with this knowledge, we utilized the Fura-2 and Fluo-4 calcium stains to confirm a strong increase in intracellular calcium levels with loperamide (Fig. 3E and F).

Increased intracellular calcium is able to trigger FoxO1 nuclear translocation in a CamKII-dependent pathway in hepatocytes [19]. We observe an accumulation of active, phosphorylated CamKII in Min6 cells within hours of loperamide exposure, sustained during prolonged treatment (Fig. 3G, SFig. 5I). Treatment with KN-93, a CamKII inhibitor, significantly halted loperamide's increase in insulin protein and FoxO1 nuclear localization (Fig. 3H, SFig. 6A-D), supporting a role for the kinase downstream of loperamide and reinforcing a key role for calcium in beta cell maintenance.

Loperamide counters FoxOi-mediated changes in pH

It is widely accepted that regulation of intracellular pH and Ca^{2+} concentration play vital roles in pancreatic hormone processing and secretion[20,21]. Calcium and pH levels facilitate and dictate every stage of insulin's biosynthesis process. Starting from proper proinsulin folding in the neutral rER, to proinsulin processing in the acidic and Ca^{2+} -rich secretory granules. More specifically, the primary insulin processing enzymes, PCSK1/3 and PCSK2, require a minimum of 1 mM Ca^{2+} and an acidic pH of 5.0-5.5 to properly exert their function[22]. Furthermore, the final secreted hormone has an important autocrine function in regulating future transcription and secretion[23,24]. Perturbations to this delicate feedback loop via aberrant intracellular pH and Ca^{2+} changes could explain FoxOi's role in effecting beta cell dysfunction and loperamide's counteraction.

Consequently, we observed an increase in the majority of vacuolar ATPase subunits upon FoxO inhibition (SFig. 7A). This was accompanied by a global and glucagon granule specific increase in intracellular acidification (SFig. 7B-D). Treatment with loperamide reduced this FoxOi-induced intracellular acidification (SFig. 7B and C). Interestingly, another hit compound from our screen (SFig. 2A), chloroquine, is known to increase lysosomal pH[25]. We show that chloroquine treatment phenocopies many aspects of loperamide's effects in the FoxOi-mediated beta cell dedifferentiation model (SFig. 8), reaffirming the role pH plays in hormone processing.

Loperamide alters the ER proteome, rescuing FoxOi-induced arrest of insulin granule maturation and promotes autophagy

Analysis of our gene expression datasets for other deregulated pathways found a large subset of ER proteins involved in protein processing and transport to be downregulated following treatment of Min6 cells with loperamide (Fig. 4A and B). Notably, the most significantly decreased genes all corresponded to protein disulfide isomerases (i.e. P4hb, Pdia3, Pdia4 and Pdia6) (Fig. 4A, SFig 9A). While necessary for the proper folding of proinsulin, knockdown of P4hb induces faster export, maturation and secretion of newly synthesized proinsulin with an increased insulin to proinsulin ratio [26], highly reminiscent of loperamide's phenotype (Fig. 2F-H) and a possible explanation for the increased proinsulin turnover. Interestingly, loperamide also upregulated both ER calcium ATPases, Serca2 and Serca3 (Fig. 4A, SFig. 9B-D), with increases in Serca2 protein and mRNA observed as early as 3 hours post-loperamide treatment (Fig. 4C and SFig. 9B). Serca2's locus is bound by FoxO1 in multiple tissues [16,27,28], suggesting its upregulation is downstream of FoxO1's translocation. To understand SERCA's role in loperamide's phenotype, we treated our beta cell line with the SERCA inhibitor, thapsigargin. Thapsigargin induced a significant decrease in proinsulin and SERCA protein levels already within 2 hours (SFig. 9E and F). 24-hour thapsigargin treatment further decreased both pro- and mature insulin protein levels (Fig. 4D, SFig. 9G and H). Interestingly, while co-treatment of loperamide with thapsigargin incited a decrease in the total levels of proinsulin and insulin, the ratio of insulin to proinsulin remained significantly increased (Fig. 4E, SFig. 9I). This suggests that while proinsulin generation and export require ER calcium stores, loperamide's role in granule maturation does not. Disruption of the *trans*-Golgi network (TGN), the site of secretory granule packaging and proinsulin processing initiation, perfectly mirrored this result (SFig. 10A-C). Contrastingly, prolonged loss of prohormone convertase activity depleted all insulin stores and countered loperamide's glucagon decrease (SFig. 10D).

The importance of a processable proinsulin pool for loperamide's action was further strengthened upon co-inhibiting translation and prohormone convertase activity. While translation inhibition predictably diminished proinsulin levels, downregulation of mature insulin protein was only observed following prohormone convertase co-inhibition (Fig. 4F). This reinforces the notion that while active translation is necessary to maintain the proinsulin pool, loperamide sustains mature insulin levels via a different mechanism, i.e. enhanced processing within secretory granules, which relies heavily on prohormone convertases.

In line with increased export and proinsulin processing, analysis of FoxOi and loperamide treated Min6 cells revealed a discrepancy in the localization of insulin/proinsulin. Upon FoxOi treatment, insulin/proinsulin stains are highly colocalized and restricted to regions in the nuclear periphery, whereas loperamide induces an increase in granules near the membrane (Fig. 3B, SFig. 10E).

Ultrastructural studies reinforce previous findings, revealing an overall decrease in insulin secretory granules with FoxOi, a phenotype prevented upon loperamide addition (Fig. 4G and SFig. 11). Interestingly, an abundance of smaller (80-120nm) granules with an electron-lucent core is evident, specifically in DMSO and FoxOi treated Min6 cells (Fig. 4G-I and SFig. 11; green arrows). These most likely represent very early stage or stalled secretory granules[29]. Strikingly, loperamide treatment, regardless of FoxOi, minimized the number of these small nascent granules in favor of an observable increase in larger (200-300nm) mature insulin granules with a concomitant increase in (autophago-)lysosomes (Fig. 4G-I and SFig. 10F and 11; blue and red arrows). This is corroborated by loperamide's transcriptional enrichment of genes involved in autophagosome maturation (SFig. 10G and H). To further validate these observations, we tested whether loperamide promotes autophagy by blotting for the autophagosome marker LC3B. On its own, loperamide induces a mild increase in LC3B-II and decrease in LC3B-I levels (Fig. 4J). Co-treatment with Bafilomycin A1 (BafA1), a potent inhibitor of autophagolysosomal fusion, revealed no synergistic increase in LC3B-II levels, indicative of loperamide stimulating autophagic flux (Fig. 4K). Active autophagy is essential for the maintenance of functional healthy beta cells and optimal insulin content [30–32]. Hence, it appears loperamide stimulates both the maturation of insulin granules, while equally regulating their concentration by promoting healthy lysosomal recycling.

Many of these pathways are conserved in the different endocrine cell types, and we therefore tested drug effects in the alpha cell line aTC1 (SFig. 12). We observed that also in alpha cells loperamide represses glucagon and increases FoxO1 and Serca2 levels.

Loperamide counters FoxO inhibition in multiple model systems

FoxO proteins are known to promote dauer formation in *C. elegans*[33] (Fig. 5A). Therefore, we used it as a model organism to test the effects of FoxOi and loperamide. Interestingly, the chemical inhibition of FoxO decreased the dauer formation rate (Fig. 5B, left), as expected from loss of FoxO, while loperamide increased it (Fig. 5B, right). These results support the conclusion that loperamide's effects on FoxO proteins are conserved in different organisms.

We next tested the compounds in a zebrafish model. Interestingly, loperamide was able to rescue a FoxOi-induced developmental defect in the zebrafish (Fig. 5C), underscoring its ability to counteract FoxOi's global effects. To observe the effects of loperamide during islet development, we utilized zebrafish larvae carrying double reporters: Gcg-GFP and Ins-mCherry. High concentrations of loperamide resulted in increased alpha and beta cell numbers (Fig. 5D, SFig. 13A and B).

Next, we treated intact human islets from healthy donors with loperamide for 48h to test the compound's effects on mature, *ex vivo*, human alpha and beta cells. Compared to the control population, loperamide treatment decreased the number of alpha cells and increased beta cell and double positive cell numbers (Fig. 5E). Loperamide treatment also dramatically decreased glucagon transcription, however without a significant effect on insulin transcription (Fig. 5F), consistent with previous findings. Contrastingly, analysis on human islets from diabetic donors treated with loperamide revealed an increase in insulin mRNA and protein levels (Fig. 5G, SFig. 13C). This was accompanied by a decrease in glucagon and increase in PDX1, SERCA2, SERCA3, CACNA1C, CACNA1D and FOXO1 expressions (SFig. 13D). At the transcriptome-wide level, loperamide treatment led to a general suppressive effect on alpha cell specific genes (SFig. 13E). Loperamide also appeared to rescue the glucose responsiveness of these diabetic islets, sparking a significant increase in insulin secretion upon high glucose treatment (Fig. 5H). We further validated these results in a diabetic murine model, with similar increases in insulin mRNA, protein and secretion observed upon loperamide treatment (Fig. 5I, SFig 13F and G). Overall, these results strengthen the notion that loperamide has a positive influence on beta cell identity and function also in relevant models of diabetic islets.

Loperamide decreases fasting blood glucose and double positive islet cells in diabetic mice

At present, no studies have focused on the long-term effects of loperamide treatment on glucose metabolism in a diabetic setting. Thus, we set out to study its systemic effects by treating 8-week-old *db/db* mice on a chow diet with loperamide or vehicle (a mix of DMSO,

PEG300, Tween-80 and PBS at a 1:4:0.5:4.5 ratio) for 4 weeks. Loperamide treatment triggered a striking decrease in fasting blood glucose levels with no change in overall body weight (Fig. 6A and B). The vehicle-treated mice had a high average fasting blood glucose concentration of 304.5 mg/dL characteristic of a diabetic mouse model. The loperamide-treated group, on the other hand, had an average fasting concentration of 156.4 mg/dL, almost half that of the control-treated mice, and well below the 250 mg/dL threshold generally used to stratify diabetic mice [34]. Furthermore, following a 20-minute IP glucose tolerance test (IPGTT), blood glucose concentrations remained lower in the loperamide-treated mice (Fig. 6A). Interestingly, serum insulin concentrations post-IPGTT were also significantly decreased with loperamide (Fig. 6C). Based on the observed decrease in blood glucose levels, one would expect a concomitant increase in circulating insulin. These results, therefore, suggest that loperamide treatment likely accelerates glucose clearance, indicative of improved insulin sensitivity. Conversely, glucagon serum levels remain unchanged relative to control (Fig. 6D). These changes were specific to diabetic mice, as no significant effects were observed in wild-type treated animals (SFig. 14A-C).

Next, we wanted to identify whether long-term loperamide treatment had any islet-specific effects. Islet immunofluorescence analysis in the control mice revealed a large number of insulin/glucagon double positive cells (Fig. 6E and F), accounting for 10% of total islet volume, characteristic of diabetic islets [35,36]. Strikingly, this number was significantly reduced in the loperamide-treated animals (Fig. 6F). Thresholded Manders correlation coefficient (MCC) colocalization quantifications reiterated these results, with decreased colocalization observed in both the insulin and glucagon channels (Fig. 6G and H). This effect was especially pronounced in the insulin channel, underscoring that loperamide treatment dramatically increased the percent of mono-hormonal insulin-positive cells (Fig. 6G). Comparisons of total islet volume occupied by insulin or glucagon signal reinforced these findings, highlighting a decrease in glucagon area from 18% to just over 10% of total with loperamide, with no change to insulin (Fig. 6I and J). Hence, it would appear loperamide specifically represses the emergence of glucagon expression in insulin-positive cells. The high Aldh1a3 expression observed in the control mice is a further characteristic of dedifferentiated beta cells [10], also strikingly reduced by loperamide treatment (Fig. 6K and L). Mechanistically, we also detected a noticeable increase in FoxO1 protein levels upon loperamide treatment (SFig. 14D and E), in line with observations in Min6 cells (Fig. 3A and B) and in diabetic human islets (SFig. 13D). FoxO1 deficiency is another known driver and marker of beta cell dedifferentiation [4]. Thus, loperamide's ability to enhance FoxO1 expression and minimize Aldh1a3 levels and double positive cell numbers suggest loperamide's reinforcement of beta cell character is conserved *in vivo*, and for the first time show that long-term loperamide treatment has globally positive

effects on glucose metabolism.

Discussion

Beta cell failure as a result of sustained insulin resistance is the key driver in the pathogenesis of type II diabetes. Beta cell death, dysfunction and dedifferentiation have been proposed as the main sources of this failure[6]. Interfering with this process might prevent, or at least delay, the progression of diabetes and therefore underscores an important therapeutic target.

Physical evidence supporting the presence of beta cell dedifferentiation include increased numbers of hormone-negative cells[5,37], double positive cells[35,36] and degranulated beta cells[38] in islets from type II diabetic patients. The molecular basis for this loss of beta cell identity remains to be fully elucidated. Several proposed mechanisms exist in addition to loss of FoxO1 signaling, such as decreased PRC2-mediated progenitor gene silencing[39], oxidative-stress mediated upregulation of microRNAs targeting beta cell transcription factors[40–43], and hypoxia induced adaptive UPR inactivation[21].

We developed an *in vitro* cell system that allowed us to specifically study and understand the molecular mechanisms underlying FoxO1-mediated beta cell dysfunction. In our cellular system, beta cell dedifferentiation can be robustly induced by a two-day treatment with a small molecule FoxO inhibitor. This phenotype is not restricted to the cell line model, as we have recently shown that the compound also induces beta cell dedifferentiation in primary human and murine pancreatic islets[44]. With this cellular beta cell dedifferentiation model, we uncovered that increased intracellular acidification is a critical step in beta cell dedifferentiation. By performing a high-content chemical screen, we identified the approved drug loperamide to counteract the observed dedifferentiation by neutralizing intracellular pH, mobilizing intracellular calcium ions, enhancing insulin processing and elevating FoxO1 expression and activity (Figure 7).

More specifically, loperamide triggers a calcium and CamKII-dependent nuclear shift of FoxO1 with a concomitant increase in the expression of over 1000 of its target genes. An important fraction of these genes are involved in calcium ion mobilization into the cytoplasm and the ER. The most notable of these: SERCA2, CACNA1C and CACNA1D are reduced in the islets of diabetic mice and humans [17], highlighting their importance in beta cell maintenance. Loperamide's increase in SERCA2, coupled with its decrease in protein disulfide isomerases, most likely provides the heightened pool of exported proinsulin near the membrane. In effect, glucose uptake triggers an increase in insulin processing, mature granule numbers and

secretion by invoking an initial increase in ER calcium levels [45], highlighting a parallel between glucose and loperamide. Secretion relies on heightened local concentrations of calcium, ten times higher than the cytoplasmic average. These are observed near clusters of $Ca_v1.2$, $Ca_v1.3$ and actively secreted insulin granules [18,20]. This clustering is disrupted in type II diabetic islets, indicative of their stunted secretion. Loperamide successfully counters this by increasing secretion and the expressions of $Ca_v1.2$ and $Ca_v1.3$ in diabetic islets.

Loperamide equally neutralizes intracellular pH which is known to further affect calcium signaling and secretion[46]. Acidification of secretory vesicles is an important event required for the posttranslational processing of proinsulin to the mature hormone[47]. In effect, loss of the $\alpha 3$ isoform of V-ATPase, which is highly expressed in alpha and beta cells, results in reduced insulin and glucagon secretion[48]. Typically, effects of increasing granule pH on impaired prohormone convertase activity are studied. Since prohormone convertases have a relatively tight pH optimum in the range of pH 5-5.5, the lowered pH we observe following FoxO inhibition might also be responsible for impaired hormone processing and secretion. Finally, since glucose controls V-ATPase activity, which in turn is required for PKA signaling[49], it is clear that intracellular pH, calcium and glucose signaling are all tightly interwoven and that all three are affected by FoxOi and loperamide.

Limited literature exists regarding loperamide's *in vivo* effects on glucose metabolism. Encouragingly, a few studies observed that IV-injected loperamide dramatically decreased serum glucose concentrations in streptozotocin (STZ)-induced diabetic rats within three days[50–52]. Interestingly, this decrease was only observed in STZ-induced and obese Zucker rats [53] but not in non-diabetic Wistar rats, suggesting it may functionally ameliorate organs affected in diabetes such as islets, liver or muscle. Consistently, patent US20050234100 specifically attributes loperamide's effects to the improvement of insulin sensitivity in fructose-induced insulin resistant rats. Unfortunately, all of these represented short-term treatments, from minutes to three days. Consequently, ours is the first study to focus on the long-term effects of loperamide on glucose metabolism. Excitingly, we could show that the decrease in blood glucose concentrations is maintained after 4-week treatment, as well as the potential increase in insulin sensitivity. In effect, our observations that: (1) long-term *in vivo* loperamide treatment decreases double positive islet cell numbers and Aldh1a3 levels in diabetic mice and (2) *ex vivo* loperamide treatment increases insulin secretion and expression in diabetic islets, are the first to support the hypothesis that loperamide exerts its effects on glucose metabolism directly via the islets. However, the decrease in serum insulin levels post-loperamide coupled to the unchanged serum glucagon concentrations suggest the effect is more complex and likely relies on multiple tissues.

In summary, we established a novel screenable cellular assay to model beta cell dedifferentiation, amenable to transcriptional studies and high-throughput screening. With this model we identified the small molecule loperamide, which successfully increases mature insulin protein levels and secretion in various models of beta cell failure. These results should help accelerate our understanding of the mechanisms underlying beta cell dedifferentiation and aid in the development of future therapies for beta cell failure in diabetes.

Materials and Methods

Reagents

Antibodies used in this project are directed against Insulin (Agilent Dako IR00261-2 and Abcam ab7842 (Fig. 4F)), Glucagon (Abcam ab92517), Histone H2B (Cell Signaling Technology 2934), beta Actin (Abcam ab8227), alpha Tubulin (Abcam ab7291), FoxO1 (Cell Signaling Technology 2880P), Aldh1a3 (Novus Biologicals NBP2–15339), p-CamKII (Cell Signaling Technology 12716T), CamKII (Santa Cruz Biotechnology sc-13141) and LC3B (Novus Biologicals NB100-2220). The FoxO inhibitor AS1842856 and Proprotein Convertase inhibitor (US1537076) were obtained from Calbiochem. Herkinorin (ab120147) and Naltrexone (ab120075) were ordered from Abcam. Golgicide A (HY-100540) was acquired from MedChemExpress. Thapsigargin (BML-PE180-0001) came from Enzo Life Sciences. Chloroquine (C6628), loperamide (L4762), cycloheximide (01810), KN-93 (K1385) and primers were obtained from Sigma. All the fluorescently labeled secondary antibodies were purchased from Thermo Fischer Scientific.

Cell culture

Min6 and alpha-TC1 cell lines were obtained from ATCC. Min6 cells were grown in high-glucose DMEM supplemented with 15% Tet System Approved FBS (Biowest S181T), 71 μ M 2-mercaptoethanol, 50 U/mL penicillin and 50 μ g/mL streptomycin. The mouse pancreatic cell line alpha-TC1 was grown in low-glucose DMEM medium supplemented with 10% FBS, 50 U/ml penicillin and 50 μ g/ml streptomycin.

Human Islets

Donor Information

	Gender	Age (years)	BMI	HbA1c	Source	Figure
1	Female	42	27.7	-	ECIT; <i>University of Geneva</i>	5F
2	Female	57	28.0	5.5%	IIDP; <i>Southern California Islet Cell Resource Center</i>	5F
3	Female	56	26.6	-	IIDP; <i>The Scharp-Lacy Research Institute</i>	5F
4	Female	62	29.8	5.5%	IIDP;	5E-F

					<i>Southern California Islet Cell Resource Center</i>	
5	Male	47	28.0	8.2%	IIDP; <i>University of Wisconsin</i>	5G-H and SFig. 13E
6	Female	62	28.5	7.6%	IIDP; <i>Southern California Islet Cell Resource Center</i>	5G-H and SFig. 13C-D

Human islets were obtained through the Integrated Islet Distribution Program (IIDP; NIH Grant # 2UC4DK098085) and the European Consortium on Islet Transplantation (ECIT): Islets for Basic Research Program from approved brain-dead organ donors (JDRF awards 31-2012-783 and 1-RSC-2014-100-I-X). All studies were approved by the Ethics Committee of the Medical University of Vienna (EK-Nr. 1228/2015). No material or information for this study was procured from living individuals. Human islets were cultured in CMRL medium (Life technology) supplemented with 10% FBS, 2 mM glutamine, 100 U/mL penicillin, and 100 µg/mL streptomycin. Intact islets were treated with different drugs for two days. Half of the intact islets were collected for RT-qPCR or RNAseq. The other half of the islets were incubated in Accutase (Life technology) at 37 °C for 20 min, neutralized by CMRL medium, seeded to a 384 well plate and utilized for immunofluorescence assays.

High-content screening

Compounds (10mM in 25 nL) were transferred to 384-well plates (Corning 3712) from DMSO stock plates using acoustic transfer (Labcyte Inc.). Min6 cells (3000 cells per well) incubated with 10µM FoxO inhibitor were plated in 50 µl media on top of the compounds. Two days after treatment, cells were fixed in 3.7% formaldehyde for ten minutes at room temperature. Following PBS washing, cells were fixed with cold pure methanol in -20°C for 10 minutes, permeabilized by 1% Triton X-100 in PBS for 30 minutes and blocked by 3% BSA in PBS for 30 minutes. Twenty microliters of primary anti-Insulin antibody and anti-Glucagon antibody, both diluted in 1:2000 in 1.5% BSA, was added per well and incubated in 4 °C overnight. After washing with PBS twice, 20µl fluorescence labeled secondary antibody diluted 1:1000 and 10µg/mL Hoechst 3342 in PBS was added per well and incubated for 1 h. After two washes with PBS, plates were stored in 4 °C in the dark until analysis.

Images were taken by an automated microscope (Perkin Elmer) using a 20X objective. Images were exposed for 10 ms in Hoechst channel and 400 ms in Alexa Fluor 488 and 546 channels. Images were analyzed by Harmony software. Nuclei were identified by Harmony Method C and cytoplasm was defined based on the nuclei (Harmony Method C). In total, 283 compounds were screened from the CLOUD library, CeMM's collection of clinical approved drugs with unique structures. Hits were selected based on the intensity of Insulin in the Alexa Fluor 548 channel, intensity of glucagon in the Alexa Fluor 488 channel, amount of DNA and cell numbers in the Hoechst channel. Cells whose Hoechst intensity was lower than 1000 were treated as dead cells and removed from the screening. All the other immunofluorescence assays were done and analyzed in the same way unless otherwise specified.

RNA-sequencing

Cells were lysed and RNA isolated using the RNeasy Mini Kit (Qiagen) according to the manufacturer's protocol. The libraries for RNA-seq for 24h induction in Min6 cells were prepared with Ribo-zero Kit and Scriptseq v2 Kit obtained from Epicenter by following the manual from the provider. For the rest of the RNA-seq libraries the amount of total RNA was quantified using Qubit 2.0 Fluorometric Quantitation system (Life Technologies) and the RNA integrity number (RIN) was determined using Experion Automated Electrophoresis System (Bio-Rad). RNA-seq libraries were prepared with TruSeq Stranded mRNA LT sample preparation kit (Illumina) using Sciclone and Zephyr liquid handling robotics (PerkinElmer). Library amount was quantified using Qubit 2.0 Fluorometric Quantitation system (Life Technologies) and the size distribution was assessed using Experion Automated Electrophoresis System (Bio-Rad). For sequencing libraries were pooled and sequenced on Illumina HiSeq 2000 using 50 bp single-read. Reads were aligned with tophat (v2.0.4) with the --no-novel-juncs --no-novel-indels options[54]. Gene expression was calculated as Fragments Per Kb per Millions of reads (FPKM) using FPKM_count.py from RSeQC package[55] and the NCBI RNA reference sequences collection (RefSeq) downloaded from UCSC[56]. The enrichment calculation was done by Gene Set Enrichment Analysis[57]. The basal expressions of genes in alpha and beta cells were taken from microarray data in literature[58,59].

RT-qPCR

After the RNA was isolated with the RNeasy Mini Kit (Qiagen), it was reverse transcribed with random primers using the High Capacity cDNA Reverse Transcription Kit (Applied Biosystems). Quantitative PCR was performed with Power SYBR Green PCR Master Mix (Applied Biosystems) on LightCycler 480 qPCR machine (Roche). All the results were analyzed using the delta-delta-Ct method, normalized to beta-actin and representative of 3

biological replicates and 2 technical replicates. Primer sequences used are the same as previously published ones[60,61] except for mouse Ngn3 (F: 5'TCCGAAGCAGAAGTGGGTGACT; R: 5'CGGCTTCTTCGCTGTTTGCTGA), mouse FoxO1 (F: 5'GGGTGATTTTCCGCTCTTGC; R: 5'GGGTGATTTTCCGCTCTTGC) and mouse MafA (F: 5'TTCAGCAAGGAGGAGGTCAT; R: 5'CCGCCAACTTCTCGTATTTC).

Western blotting

Whole cell extracts were generated by lysing cells in Triton lysis buffer containing 150 mM sodium chloride, 1mM EDTA, 1.0% Triton X-100 and 50 mM Tris, pH 7.4 supplemented with Protease Inhibitor Cocktail (Roche). 20 µg whole-cell lysates were loaded onto an SDS–polyacrylamide gel and then transferred by electrophoresis to a nitrocellulose membrane (GE Healthcare Life Science). All the blots were incubated with corresponding primary antibodies diluted 1:1000 in 5% milk at 4 °C overnight and in HRP-labeled secondary antibodies diluted 1:20000 for 1h at RT. The signals were detected using ECL Prime Western Blotting Detection Reagent (Amersham).

Intracellular insulin and proinsulin content measurements

Min6 cells were pretreated with FoxOi and loperamide for 48 hours. Cell pellets were lysed using Triton lysis buffer and intracellular insulin and proinsulin levels were measured using an Insulin ELISA (Alpco 80-INSMS-E01) or Proinsulin ELISA (Merodia 10-1232-01). All results are representative of 3 biological replicates and 2 technical replicates.

Insulin secretion assay in mouse beta cell line and murine islets

Min6 cells were pretreated with FoxOi and loperamide for 48 hours. Cells were incubated in low glucose (0.3 g/L glucose) KRB buffer for one hour followed by high glucose (3 g/L glucose) KRB buffer for another hour. Supernatants after both the low and high glucose challenges were collected to measure insulin content using a Mouse Insulin ELISA (Alpco 80-INSMS-E01). All results are representative of 3 biological replicates and 2 technical replicates.

Islets from db/db mice (GemPharmatech, Nanjing) were purified and cultured in high-glucose DMEM supplemented with 10% FBS (Gibco), 50 U/mL penicillin and 50 µg/mL streptomycin. The islets were pretreated with loperamide for 48 hours. Islets were incubated in low glucose (0.3 g/L glucose) KRB buffer for one hour followed by high glucose (3 g/L glucose) KRB buffer for another hour. Supernatants after both the low and high glucose challenges were collected. The islets were also collected after high glucose challenges and lysed with Triton lysis buffer for intracellular insulin content measurement. To measure insulin content, a Mouse Ultrasensitive Insulin ELISA kit was used (Alpco 80-INSMSU-E01).

Intracellular pH measurement

To measure the intracellular pH change in Min6 cells, they were pretreated with FoxOi with or without chloroquine/loperamide for two days. The measurement was performed using pHrodo® Red AM Intracellular pH Indicator (Life technologies) following the manufacturer's guidelines. The images were taken by an automated microscope (Operetta - Perkin Elmer) using a 20X objective and the relative intensity was quantified using the Harmony software. All results are representative of 3 biological replicates.

Calcium staining

The calcium staining was done in live Min6 cells with a Fura-2 kit (F-1201, Life technologies). Min6 cells were seeded and pretreated with loperamide for 18h before the assay. The staining was performed according to the manufacturer's guidelines. Min6 cells were also stained with 2µM Fluo-4 AM (ab241082, Abcam) in KRB buffer supplemented with 0.1% Pluronic® F127 and 2mM probenecid for 30 minutes at 37°C, followed by 30min at RT prior to 2h loperamide treatment at 37°C. All results are representative of 3 biological replicates.

Electron Microscopy

Min6 cells were grown on Aclar® fluoropolymer discs (Aclar® 33C, 199µm thickness; EMS, Hatfield, USA) after sterilizing and pre-soaking the discs in media. After a 48h treatment with either DMSO, FoxOi, Loperamide or the combination of FoxOi and Loperamide, the cells reached a confluency of about 80-90%. The discs were immersed in EM-grade glutaraldehyde (Agar Scientific, Essex, UK) diluted to 2.5% in 0.1M cacodylate buffer pH 7.4 and fixed for 1h at RT. After rinsing in 0.1M cacodylate buffer, post-fixation was done in 0.5% osmium tetroxide (prepared from crystals; EMS, Hatfield, USA) diluted in 0.1M cacodylate buffer for 1h on ice, followed by further washing steps. Samples were dehydrated in a graded series of acetones: 40%, 60%, 80%, 95% and 2x 100% for 5min each, done on ice. Infiltration with epoxy resin (Agar 100; Agar Scientific, Essex, UK) was done in mixtures of acetone and resin in the following ratios: 2:1, 1:1 and 1:2 for 30min each at RT, followed by 1h in pure, freshly thawed resin. Polymerization took place at 60°C for 48h. Ultra-thin sections with a nominal thickness of 70nm were cut on a Leica UCT ultramicrotome (Leica Microsystems, Vienna, Austria) and picked up on 100mesh Cu/Pd grids (Agar Scientific, Essex, UK), previously coated with a formvar support film. For enhanced contrast, the sections were post-stained with 2% aqueous uranyl acetate pH 4 (Merck, Darmstadt, Germany) and Reynold's lead citrate. Inspection of the grids was done in a FEI Morgagni 268D TEM (Thermo Fisher, Eindhoven, The Netherlands), operated at 80kV. Examination regions on the sections were selected randomly.

Digital images were acquired using an 11 megapixel Morada CCD camera from Olympus-SIS (Muenster, Germany). Granule measurement analysis was performed using Fiji/ImageJ.

Dauer formation

C. elegans strain CB1370 carrying the *daf-2(e1370)* allele (hypomorphic allele of the insulin/IGF-like receptor that makes animals prone to form Dauer larvae) was seeded by egg-lay onto plates containing FoxO1 or loperamide at concentrations of 0, 5, 10, or 50 μ M. For testing the effect of FoxO1 inhibitor on the suppression of dauer formation, worms were then grown at 23°C. For testing the effect of loperamide on the promotion of Dauer formation, worms were grown at 22°C. Animals were evaluated after 7 days by scoring their survival after a 30 min treatment with 1% (w/v) SDS.

Zebrafish larvae assay

Larvae of intercross Gcg:GFP and ins:NTR-mcherry fish were treated 26hpf (fertilization) with loperamide; on day 5 they were sorted for potentially double positive larvae (stereo microscope), embedded into agarose and pictures were taken on the confocal at 25x. With these pictures 3D models of the islets were established and the GFP positive cells and mCherry positive cells were counted by a 3D imaging tool.

Mouse models

All the animal experiments were performed in the SPF level animal facility of Fudan University School of Life Science, according to procedures approved by the experimental animal ethics committee of Fudan University School of Life Sciences. The 8-week old db/db mice or wild-type C57 B6/J mice (GemPharmatech, Nanjing) were maintained under a 12 h light/12 h dark cycle at constant temperature (23°C) with free access to chow diet and water. Loperamide (MedChemExpress, China) was freshly prepared daily as DMSO: PEG300: Tween 80: Saline in a ratio of 1:4:0.5:4.5. The mice were treated with vehicle or loperamide at 1 mg/kg via intraperitoneal injection daily. The mice were fasted overnight and IPGTT was performed by injecting 1g/kg glucose in PBS. After 4-week treatment, the mice were sacrificed in a CO₂ chamber and the pancreata were collected into a 4% PFA solution for fixation. Immunofluorescence was performed as previously described[61]. Colocalization quantifications were performed using the ImageJ plugin “Colocalization Threshold”. Quantifications were done on individual islets isolated within each image using a specified Region of Interest. Signal thresholds were determined using the Costes method. The resultant thresholded Manders correlation coefficients were then used. Total volume was determined based on total pixel number per islet, consequent percent volume colocalized references the number of pixels positive for both the red and green channels above the set threshold as a

fraction of the total islet pixels, whereas the percent insulin and glucagon values correspond to pixels positive for the red or green channel respectively. Mean FoxO1 and Aldh1a3 intensities per cell were calculated using CellProfiler, with Hoechst and insulin counterstains used to specify nuclei, cytoplasm and beta cells.

Statistical methods

All the p-values were calculated by Student's t-test, unless otherwise specified.

Conflict of interest

The authors declare that they have no conflict of interest.

Author contributions

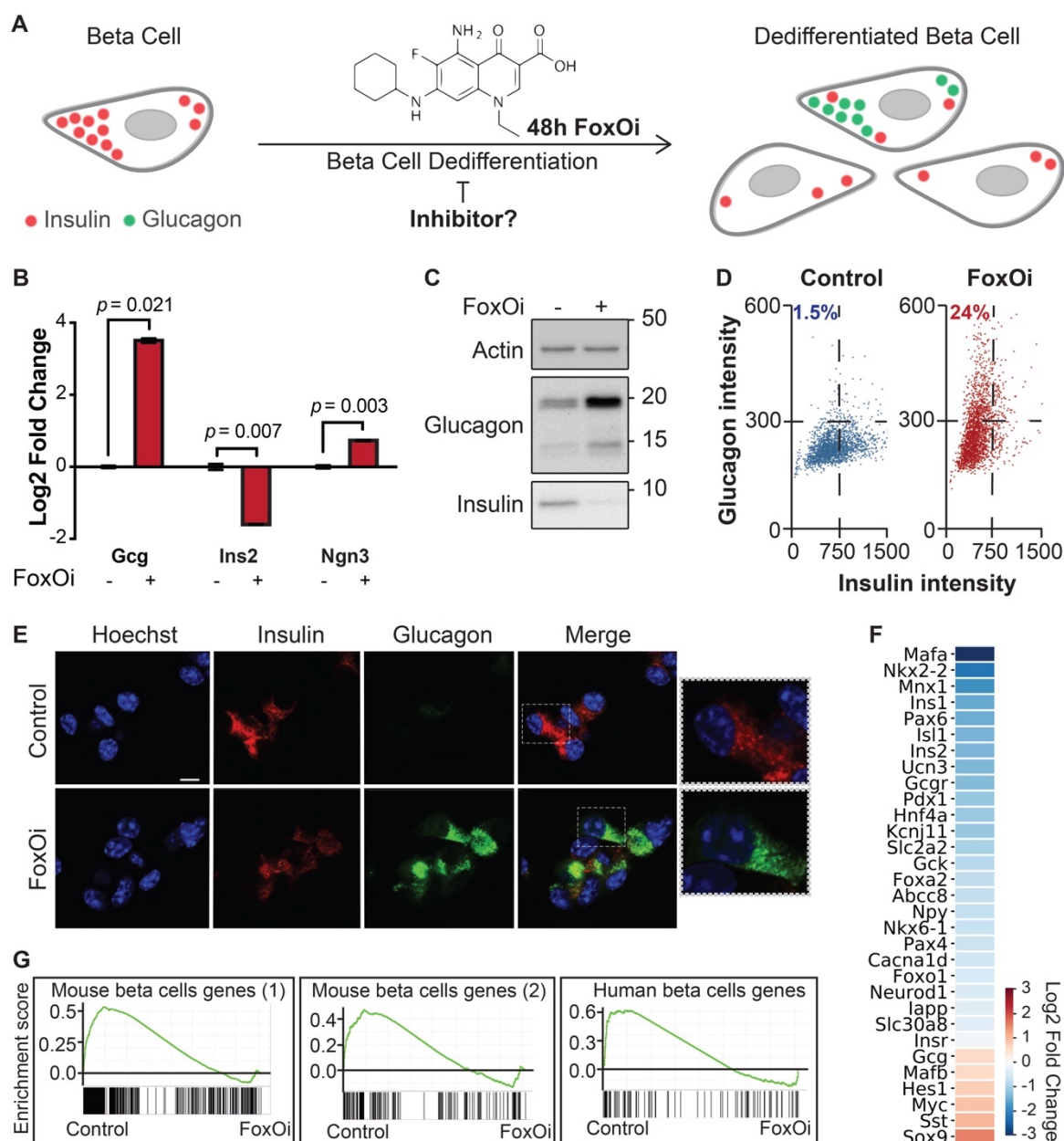
Conception and design: SK and JL. Cell line provision: TF and JH. Next generation sequencing: TP and CB. RNA-seq analysis: FP, TC and JL. Electron microscopy sample preparation and imaging: MB and TH. Human islet preparations: CB and EB. Zebrafish assays: CT and MD. Dauer formation assay: CR and IS. Mouse experiments: JL, XL, YZ and SH. Performing experiments: TC, JL, CHL, XL, YZ and SH. Manuscript writing: TC, JL and SK with input from all co-authors.

Acknowledgements

The drug library was designed by Freya Klepsch and Patrick Markt from the PLACEBO team. Next generation sequencing was performed by the Biomedical Sequencing Facility at CeMM. Electron microscopy was performed by the Electron Microscopy Facility at the Vienna BioCenter Core Facilities (VBCF), member of the Vienna BioCenter (VBC), Austria. Robert Pazdzior from the Kubicek lab assisted in the development of the CellProfiler image analysis pipelines. This work was supported by JDRF grants 3-SRA-2015-20-Q-R and 17-2011-258. Research in the Kubicek lab is supported by the Austrian Federal Ministry of Science, Research and Economy, the National Foundation for Research, Technology, and Development, and the Marie Curie Career Integration Grant EPICAL.

Funding

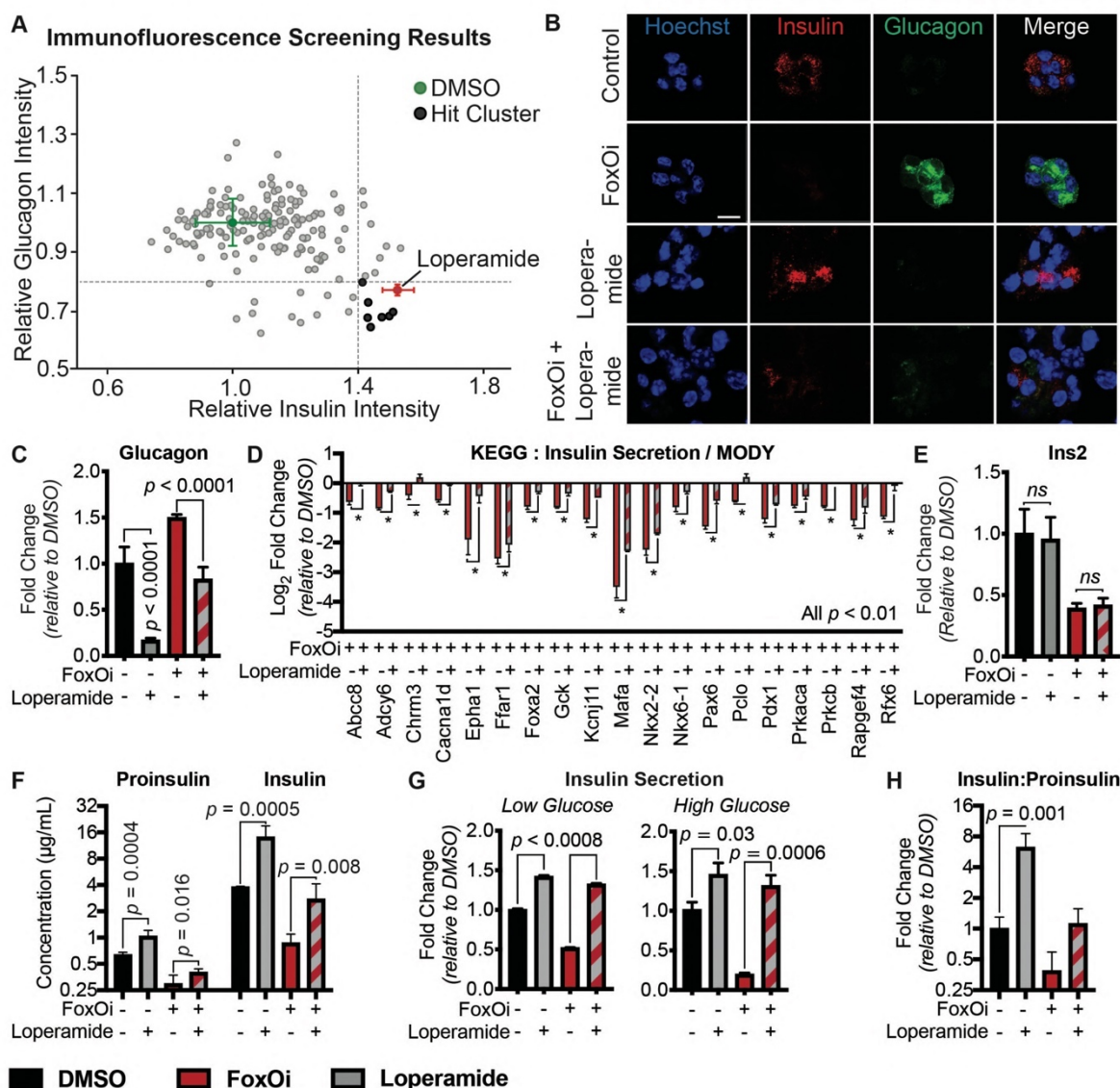
This work was funded by JDRF grants 3-SRA-2015-20-Q-R and 17-2011-258 (Generation of beta cells from alternative pancreatic subtypes). Human islets were provided through the JDRF awards 31-2012-783 and 1-RSC-2014-100-I-X (ECIT: Islet for Research program). Li lab is funded by MOST 2018YFA0801300, 2020YFA0803600, SKLGE-2118 and NSFC 32071138.



Casteels et al. Figure 1: Cellular model for FoxO mediated beta cell dedifferentiation

A. Schematic overview of our cellular model for FoxO mediated beta cell dedifferentiation, with potential to screen for inhibitors. **B.** Transcription of *Ins2*, *Gcg* and *Ngn3* in Min6 cells after two-day FoxO inhibitor (FoxOi, 1 μ M unless otherwise stated) treatment, as measured by qPCR. **C.** Western blot of glucagon and insulin protein expression in Min6 cells following two-day FoxO inhibitor treatment. **D.** Measurement of insulin and glucagon intensity in Min6 cells treated with FoxO inhibitor at the single cell level, as quantified by immunofluorescence. **E.** Representative images of Min6 cells stained for insulin and glucagon after two-day treatment. Scale bars = 10 μ m. **F.** RNAseq transcriptional expression changes in pancreatic endocrine factors after 2-day FoxOi treatment versus control DMSO treatment in Min6 cells. All RNAseq results are representative of 3 biological replicates (n=3). **G.** Gene Set Enrichment Analysis

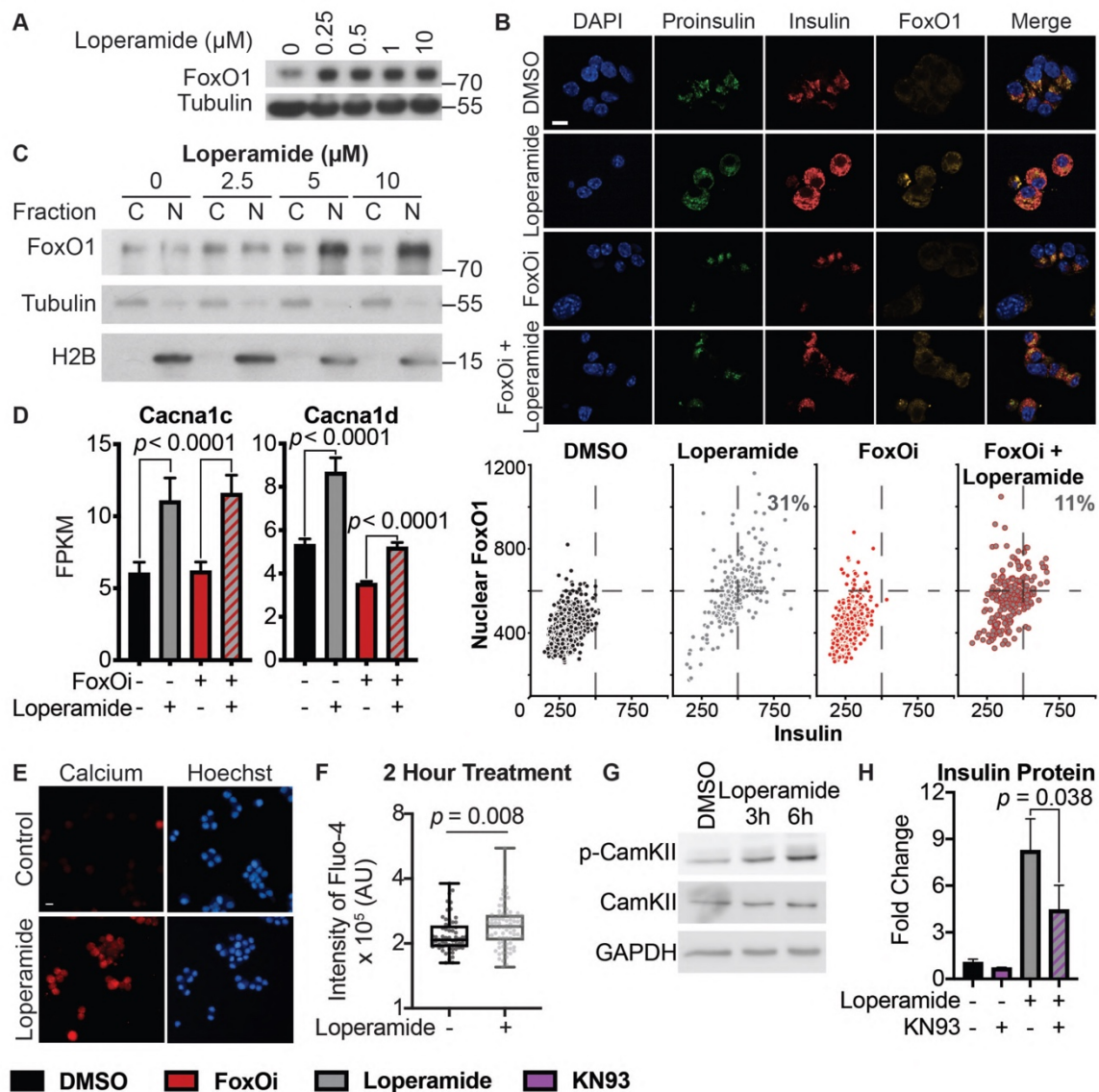
(GSEA) showing downregulation of mouse (left)[58,59] and human (right)[61] beta cell specific genes with FoxO inhibitor treatment.



Casteels et al. Figure 2: High content screen identifies loperamide to counter aspects of FoxOi-mediated beta cell dedifferentiation

A. Overview of the small molecule screening results. All the results were normalized to the DMSO control. Each dot represents the mean value of three replicates. Results whose standard deviations were more than 20% of the mean values were removed. Compounds that decreased mean cell numbers by more than 20% were considered cytotoxic and were also removed. Hit Cluster = all compounds that yielded a greater than 1.5-fold increase in insulin intensity. **B.** Representative images of Min6 cells treated with/without FoxO inhibitor in combination with loperamide (5µM unless otherwise stated). Scale bar = 10 µm. **C.** Loperamide suppresses FoxOi-induced glucagon transcription in Min6 cells, as measured by RNAseq with Fragments per Kilobase of transcript per Million mapped reads (FPKM). **D.**

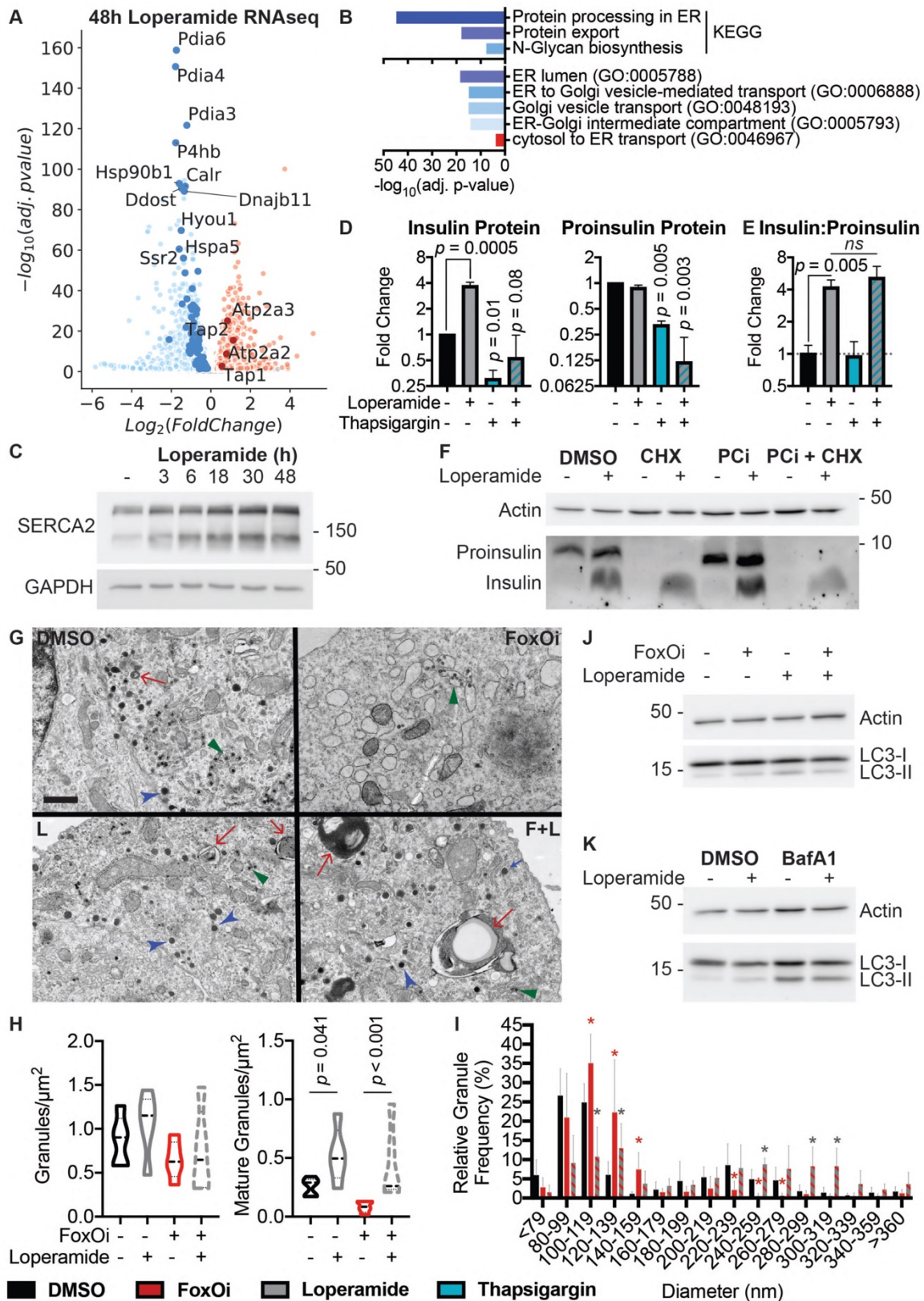
Rescue of the expression of genes involved in insulin secretion with loperamide in Min6 cells treated with FoxOi for 48h, as measured by RNAseq. **E.** Loperamide does not affect insulin mRNA levels, as measured by RNAseq. **F.** Intracellular insulin and proinsulin protein concentrations in Min6 cells following 48h FoxOi/loperamide treatment, as measured by ELISA. **G.** Insulin secretion from Min6 cells in low (0.3 g/L) and high (3 g/L) glucose medium pretreated with FoxOi and loperamide for 48h. **H.** Insulin to proinsulin total protein ratio following 48h FoxOi/loperamide treatment, relative to DMSO control, measured by ELISA.



Casteels et al. Figure 3: Loperamide increases FoxO1 expression and nuclear localization promoting changes in calcium signalling

A. Western blot showing an increase of FoxO1 protein with loperamide treatment in Min6 cells. **B.** Top: Representative immunofluorescence images of Min6 cells treated with loperamide and FoxOi for 48h. Scale bar = 10 μ m. Bottom: Quantification of insulin and nuclear FoxO1 intensities at the single cell level. **C.** Western blot of FoxO1 protein expression in the cytoplasm

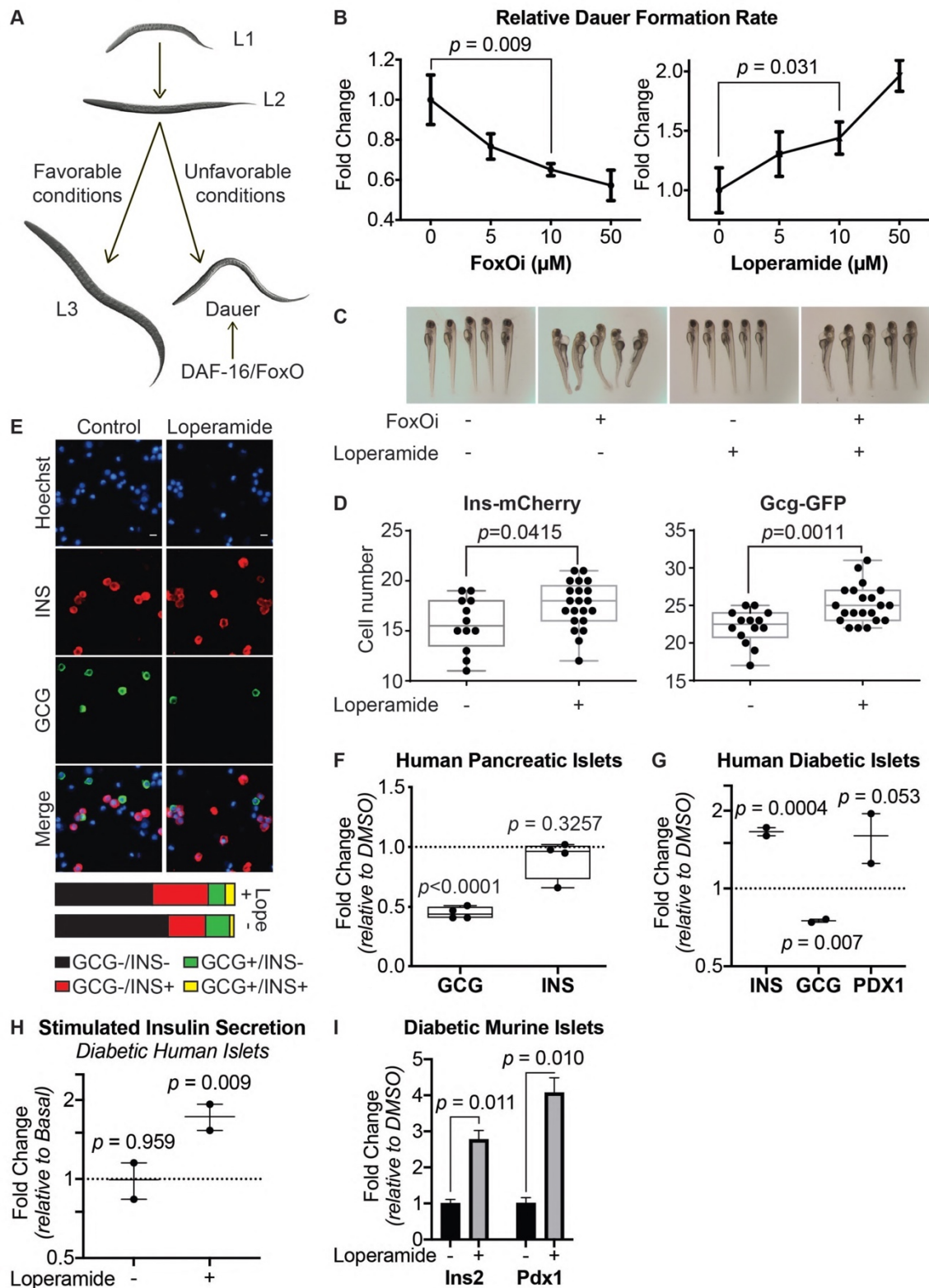
vs. nucleus of Min6 cells following different doses of loperamide treatment. **D.** mRNA levels of L-type voltage-gated calcium channels *Cacna1c* and *Cacna1d* in Min6 cells upon 48h loperamide and FoxOi treatment, as measured by RNAseq. **E.** Fura-2 staining in Min6 cells pre-treated with loperamide for 18h. **F.** Quantification of Fluo-4 staining at the single cell level in Min6 cells treated with loperamide for 2h. **G.** Western blot highlighting increase in p-CamKII relative to total CamKII protein levels in Min6 cells when treated with loperamide for the stated hours. **H.** Total mature insulin protein levels in Min6 cells treated with loperamide and 1 μ M KN-93 for 24h.



Casteels et al. Figure 4: Loperamide alters ER proteome, rescuing FoxO1-induced arrest in insulin granule maturation and promotes autophagy

A. Volcano plot of gene expression changes upon 48h loperamide treatment, as measured by RNAseq. **B.** Overview of top enrichment terms for genes both significantly altered by

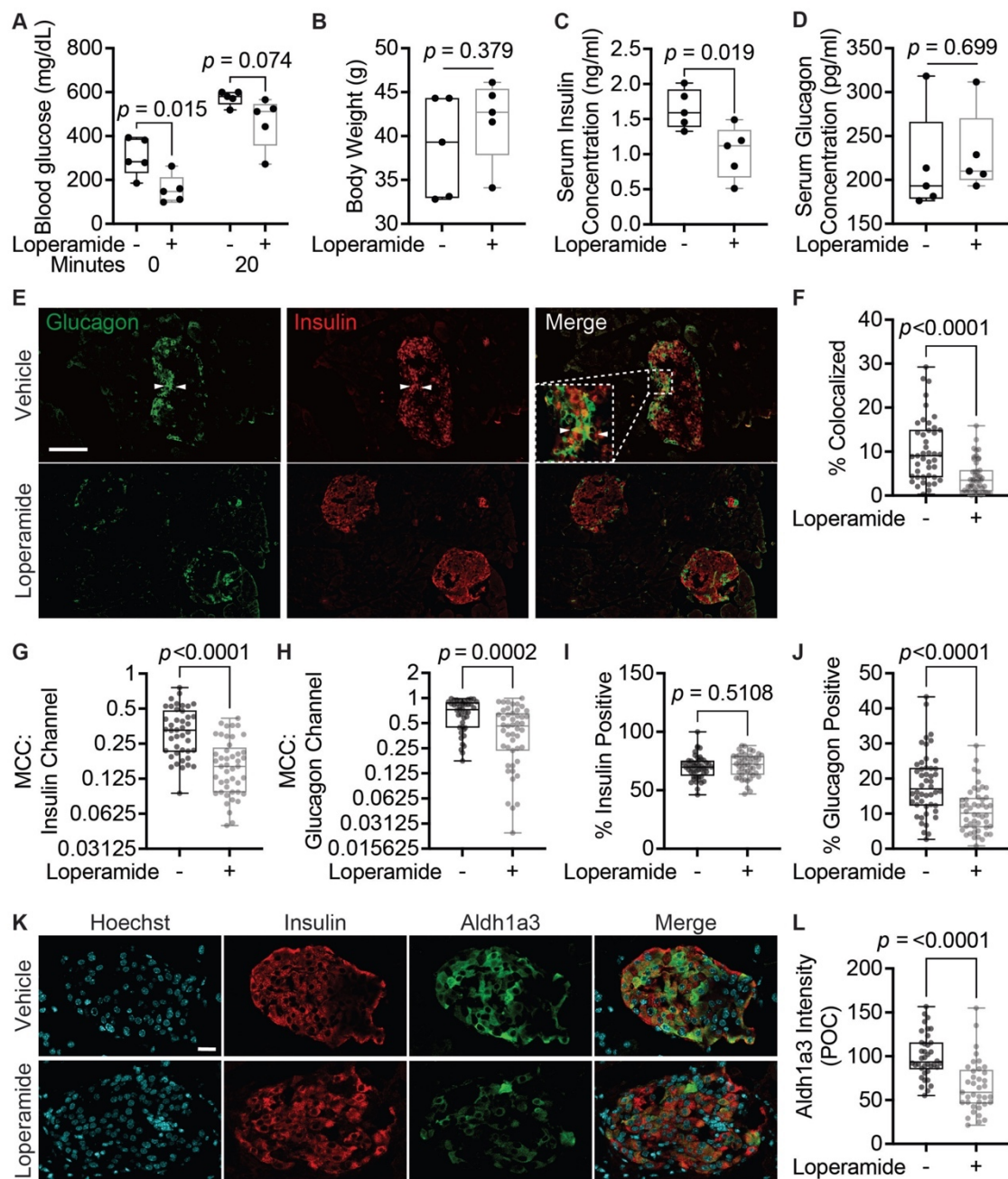
loperamide relative to control and significantly rescued when co-treated with FoxOi relative to FoxOi. Volcano plot highlights top KEGG term (protein processing in ER) in blue and GO:0046967 in red. **C.** Western blot showing increase in SERCA2 protein upon loperamide treatment in Min6 cells. **D.** Total intracellular insulin and proinsulin protein levels in Min6 cells treated with loperamide and 100nM thapsigargin for 24h, as quantified by ELISA. **E.** Ratio of mature insulin to proinsulin protein. **F.** Western blot of proinsulin and insulin protein levels following 48h treatment of Min6 cells with loperamide +/- 200µg/mL cycloheximide (CHX) or 10µM prohormone convertase inhibitor (PCi) for the final 24h. **G.** Representative electron microscopy images of Min6 cells treated with FoxOi or loperamide. L = Loperamide; F+L = FoxOi + Loperamide. Green arrows pointing to immature secretory granules. Red arrows highlighting (autophago-)lysosomes. Blue arrows indicate mature insulin secretory granules. Scale bar = 1µm. **H.** Quantification of insulin granule density in electron microscopy images. Total number of granules per µm² (right) and number of mature (>160µm in diameter) granules per µm². N = 5 cells per treatment condition. **I.** Histogram of insulin granule size distribution upon FoxOi/loperamide treatment. DMSO = black; FoxOi = red; FoxOi + Loperamide = red/gray stripes. N = 5 cells per treatment condition. **J.** Levels of LC3B in Min6 cells treated with FoxOi and loperamide for 48h. **K.** Levels of LC3B in Min6 cells treated with loperamide for 48h +/- 200nM Bafilomycin A1 for the final 2h.



Casteels et al. Figure 5: Loperamide counters FoxO inhibition in different model systems

A. Overview of *C. elegans* development in favorable or unfavorable environmental conditions.
B. Effects of FoxOi and loperamide treatment on the FOXO-dependent developmental process of Dauer formation in *C. elegans*. Eggs of CB1370 animals were hedged and grown

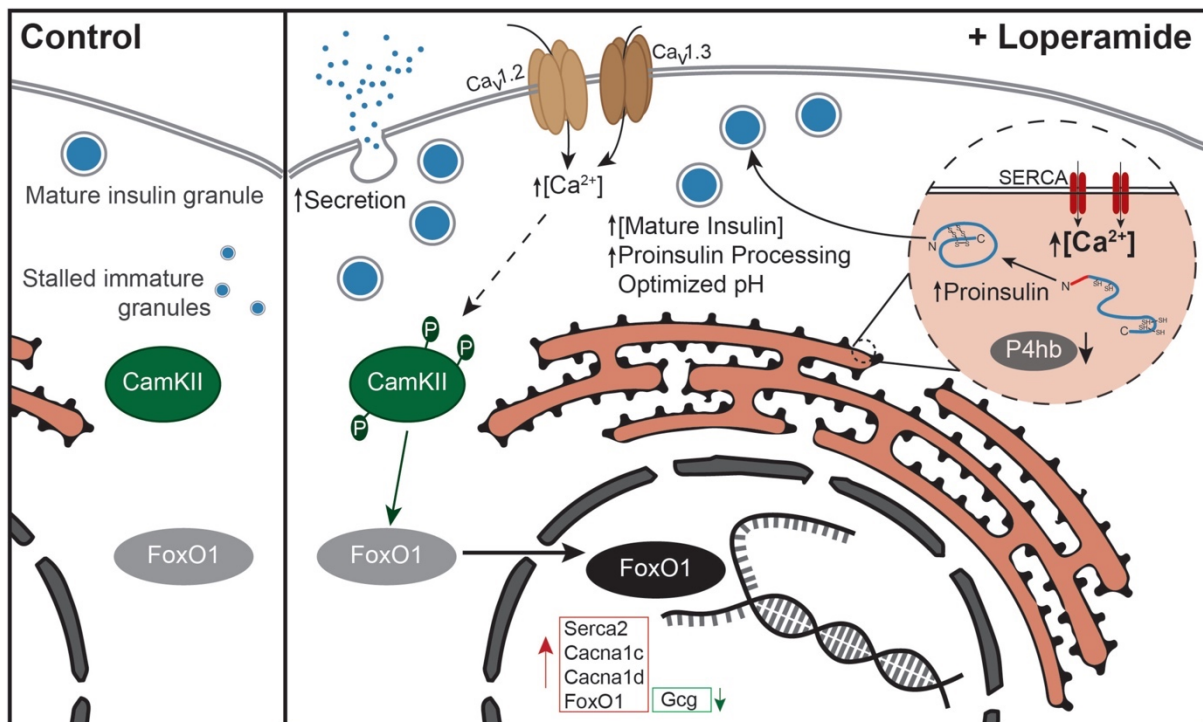
at 23°C (left panel) or 22°C (right panel) in the presence of FoxOi or loperamide at the indicated concentrations. In the absence of compounds (0 μ M), the fraction of animals forming Dauers was 20.2% (left panel) and 3.2% (right panel). Compound-induced fold changes of this fraction are shown. N=3; 100 animals per condition and replicate. **C.** Representative images of developmental defects in zebrafish larvae following 48h FoxOi treatment, and rescue with loperamide. **D.** Quantification of insulin or glucagon positive cells following loperamide treatment in zebrafish larvae. N_{control}=12; N_{loperamide}=21. **E.** Representative images of pancreatic human islets stained for insulin and glucagon. Scale bars = 10 μ m. On the right: summary of the population distribution change in the human islets. **F.** Measurement of INS and GCG transcription in human islets treated with loperamide by RT-qPCR. All the data points are normalized to DMSO control, n=4. **G.** Transcription of GCG, INS and PDX1 in pancreatic islets from human diabetic donors treated for 48h with Loperamide, as measured by RT-qPCR, n=2. **H.** Glucose stimulated insulin secretion assay on diabetic human islets pre-treated with loperamide for 48h, n=2. Basal = 0.3g/L glucose; Stimulated = 3g/L glucose. **I.** Relative insulin and Pdx1 mRNA levels in islets from db/db mice pre-treated with loperamide for 48h.



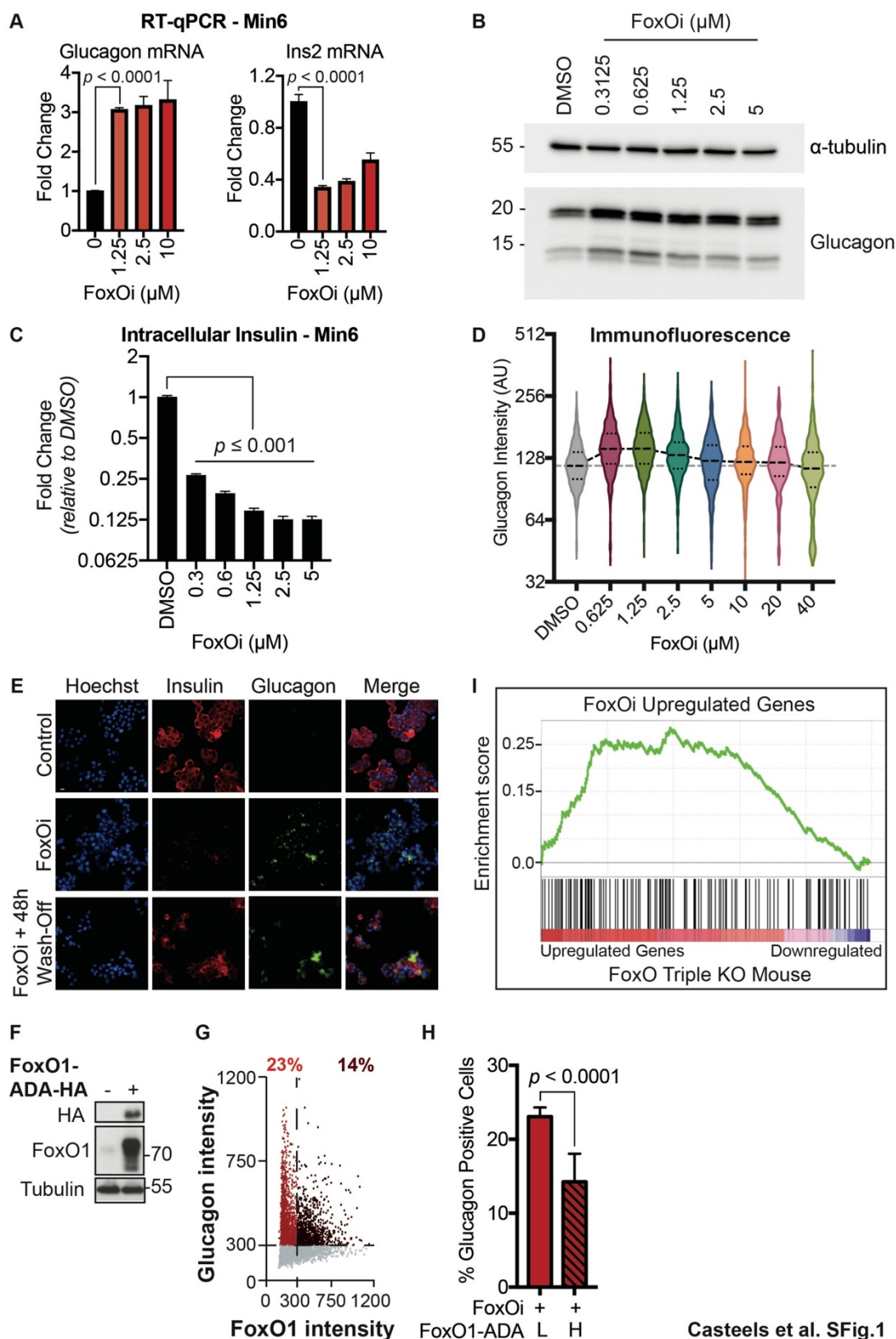
Casteels et al. Figure 6: Loperamide has positive systemic and islet-specific *in vivo* effects in diabetic mice

A. Serum glucose concentrations after overnight fast (0 min) and 20 minutes after IP injection with 1g/kg glucose (20 min). N=5 mice/treatment. **B.** Body weight measured after 4-week treatment. **C.** Serum insulin concentration measured by ELISA. **D.** Serum glucagon concentration measured by ELISA. **E.** Representative immunofluorescence panel of pancreas sections stained with insulin and glucagon antibodies. White arrows point to insulin/glucagon double positive cells. Scale bar = 100 μ m. **F-J.** Quantifications of immunofluorescence images. N=45 islets/treatment from 5 different mice/treatment. **F.** Percent of total islet pixel number

representing colocalized red/green channel pixels. **G-H.** Thresholded Manders correlation coefficients for the insulin (red) channel or glucagon (green) channel per islet. **I-J.** Percent of total islet volume occupied by the insulin (red) channel or glucagon (green) channel pixels. **K.** Representative immunofluorescence panel of db/db mouse pancreas sections 4-weeks post loperamide treatment, stained for insulin and Aldh1a3. Scale bar = 20µm. **L.** Quantification of immunofluorescence images. Cytoplasmic Aldh1a3 intensity was only calculated within insulin-positive cells. POC = percent of control. N=38 islets/treatment from 5 different mice/treatment.



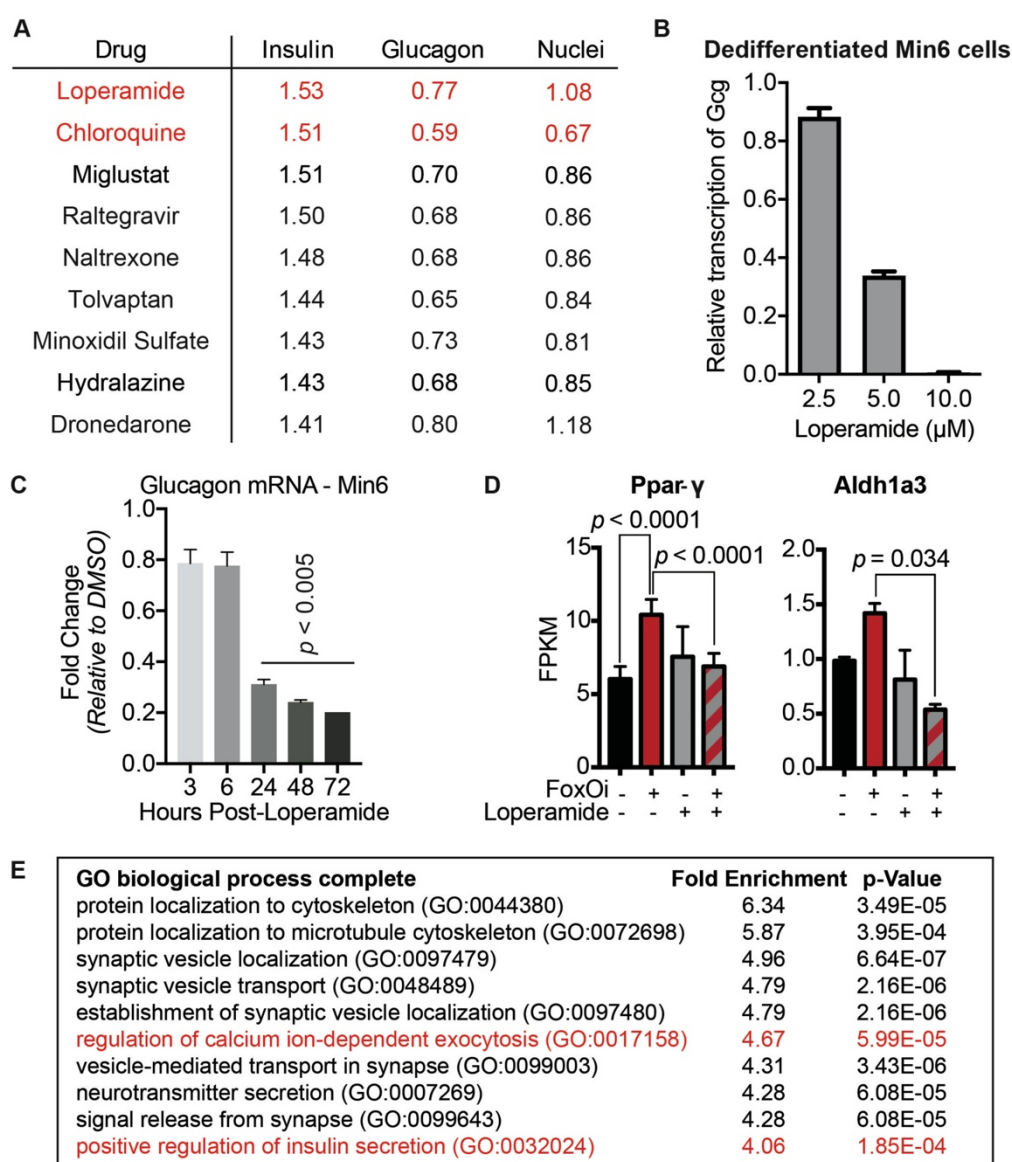
Casteels et al. Figure 7: Overview of loperamide's effects in beta cells



A. Relative mRNA levels of glucagon and insulin following 48h incubation with increasing doses of FoxOi, as measured by RT-qPCR. **B.** Western blot highlighting the increase in glucagon protein levels after 48h incubation with increasing concentrations of FoxOi. **C.**

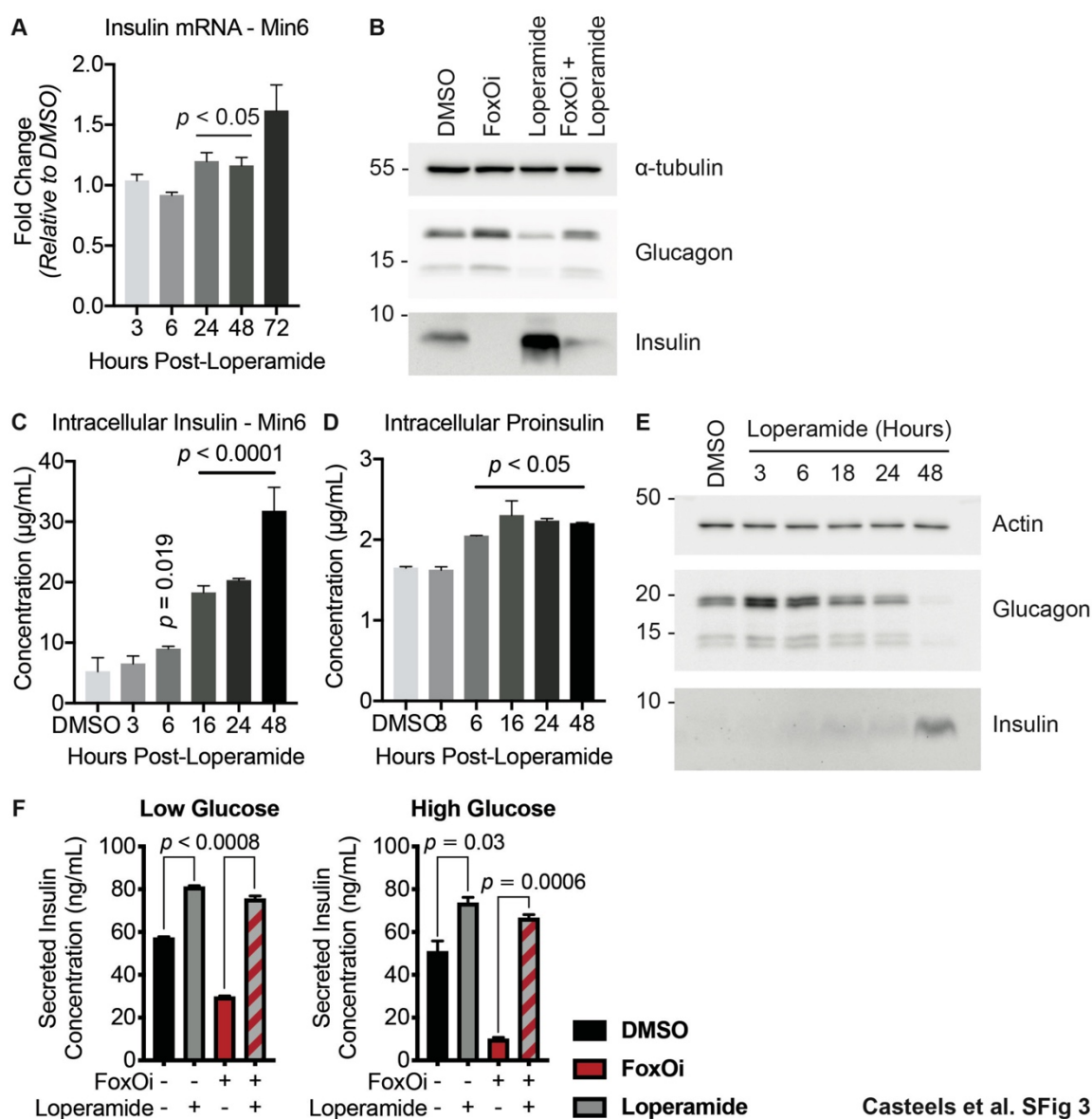
RESULTS

Intracellular insulin protein concentrations in Min6 cells following 48h FoxOi treatment, at different concentrations, as measured by ELISA. **D.** Measurement of glucagon immunofluorescence intensity in single Min6 cells treated with increasing concentrations of FoxOi for 48h. **E.** Representative images of Min6 cells stained for insulin and glucagon after 48h FoxOi treatment followed by 48h washing off of the compound. Scale bars = 10 μ m. **F.** Western blot showing the overexpression of FoxO1. **G.** Glucagon-positive cell fractions in Min6 cells treated with FoxO inhibitor, with and without overexpression of FoxO1 constitutively active construct, as measured by immunofluorescence. **H.** Quantification of SFig. 1G. L = low levels of FoxO1-ADA; H = high levels of FoxO1-ADA **I.** GSEA showing general co-upregulation of similar genes in both FoxOi treated Min6 cells and the FoxO triple knockout mouse[10].



Casteels et al. SFig 2

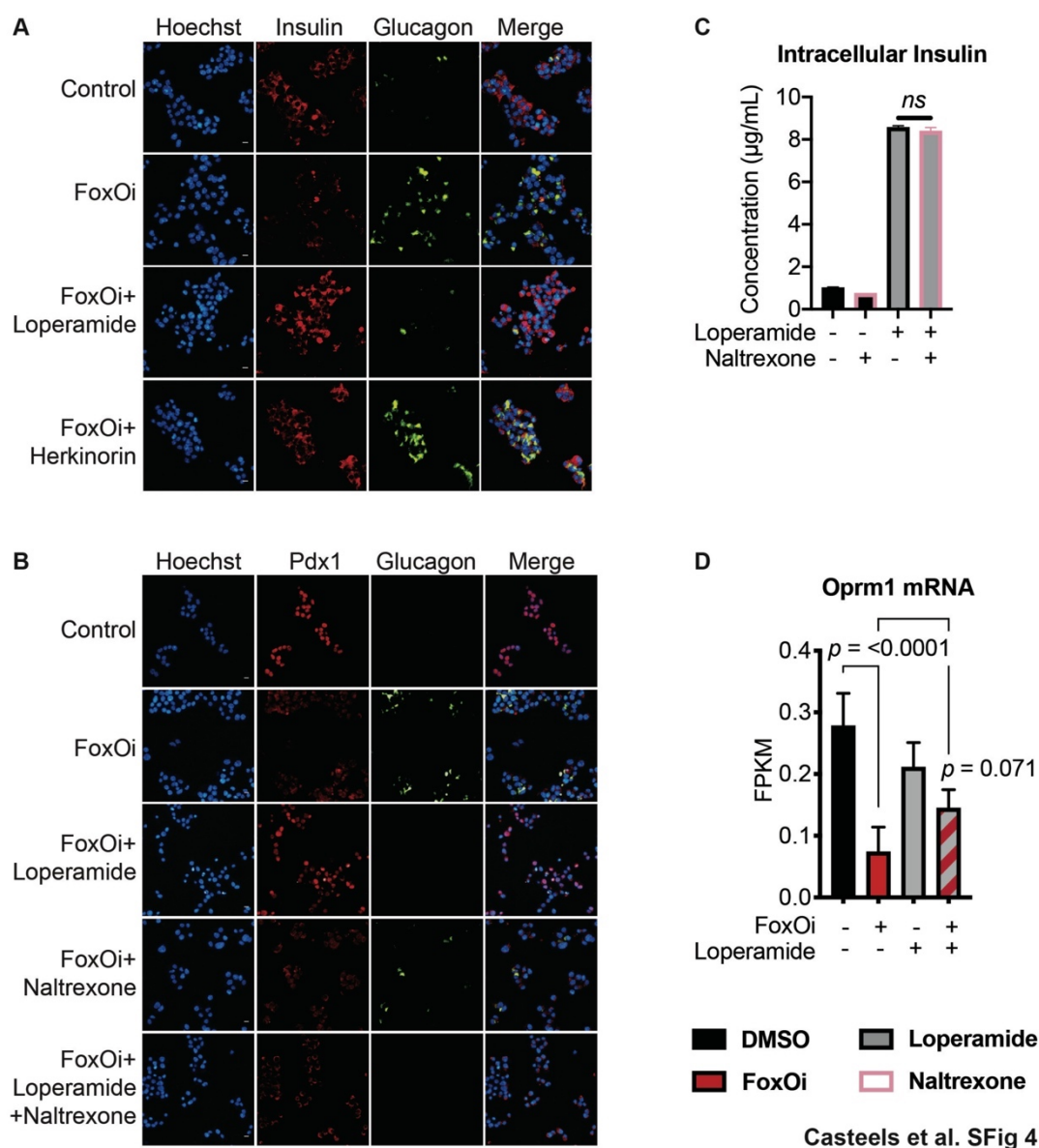
A. List of top candidate compounds from immunofluorescence screen with their respective fold changes for insulin and glucagon expression, and for the number of DAPI-positive nuclei, as measured via immunofluorescence intensity. **B.** Loperamide dose response suppression of glucagon transcription in Min6 cells treated with FoxO inhibitor. **C.** Glucagon mRNA levels in Min6 cells following loperamide time course, as measured by RT-qPCR. **D.** Ppar-gamma and Aldh1a3 transcription in Min6 cells treated with FoxOi/loperamide for 48h, measured by RNAseq. **E.** Gene ontology enrichment terms for RNAseq dataset of genes significantly downregulated by FoxOi and significantly rescued by loperamide after 48h treatment in Min6 cells.



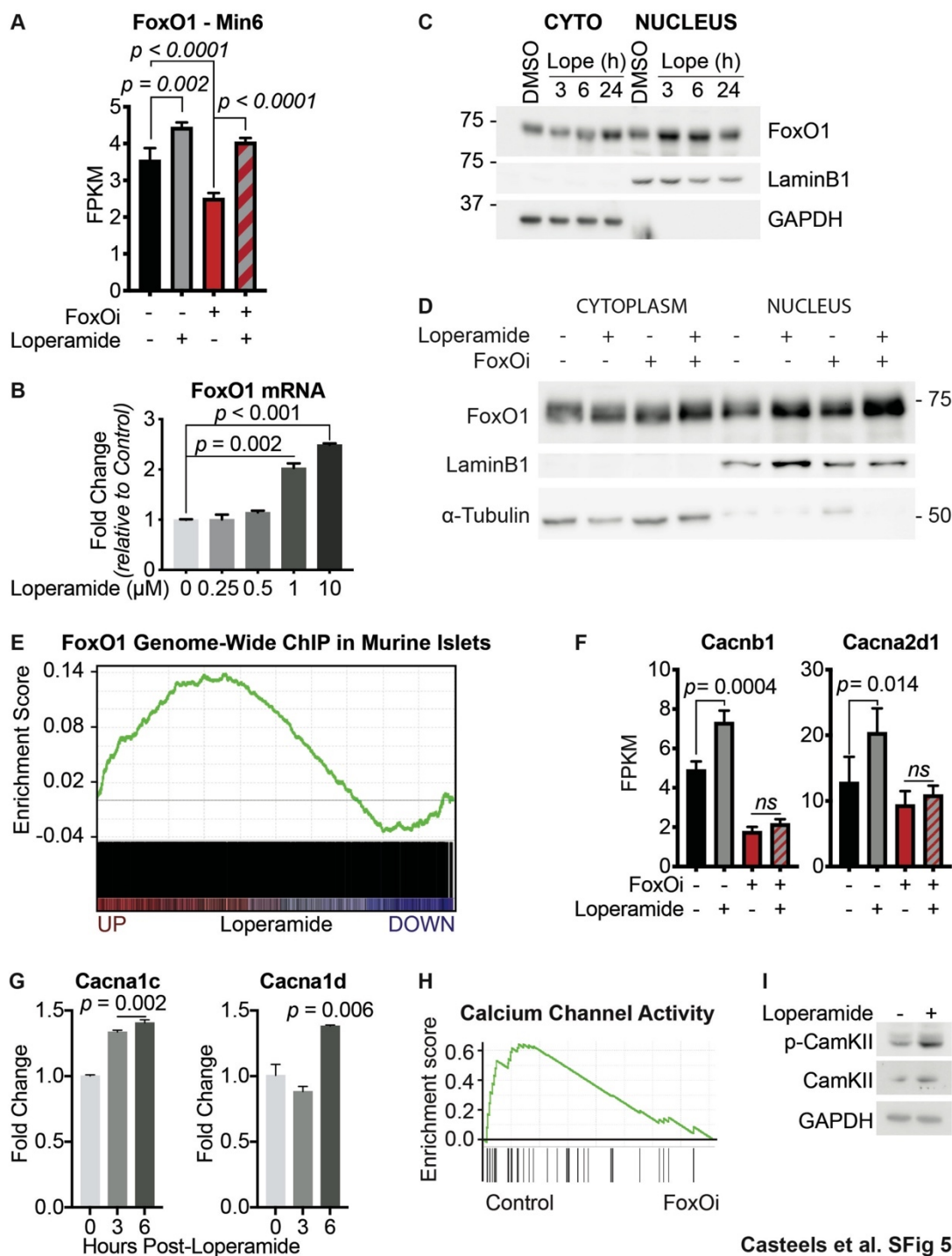
Casteels et al. SFig 3

A. Insulin mRNA levels in Min6 cells following loperamide time course, as measured by RT-qPCR. **B.** Western blot highlighting the increase in insulin and decrease in glucagon protein levels after 48h incubation with loperamide and the rescue of glucagon and insulin protein

upon combination treatment with FoxOi and loperamide. **C-D.** Intracellular insulin and proinsulin protein levels in Min6 cells following loperamide time course, as measured by ELISA. **E.** Simultaneous decrease in glucagon and increase in insulin protein levels with increasing loperamide treatment time in Min6 cells. **F.** Insulin secretion from Min6 cells in low (0.3 g/L) and high (3 g/L) glucose medium pretreated with FoxOi and loperamide for 48h.



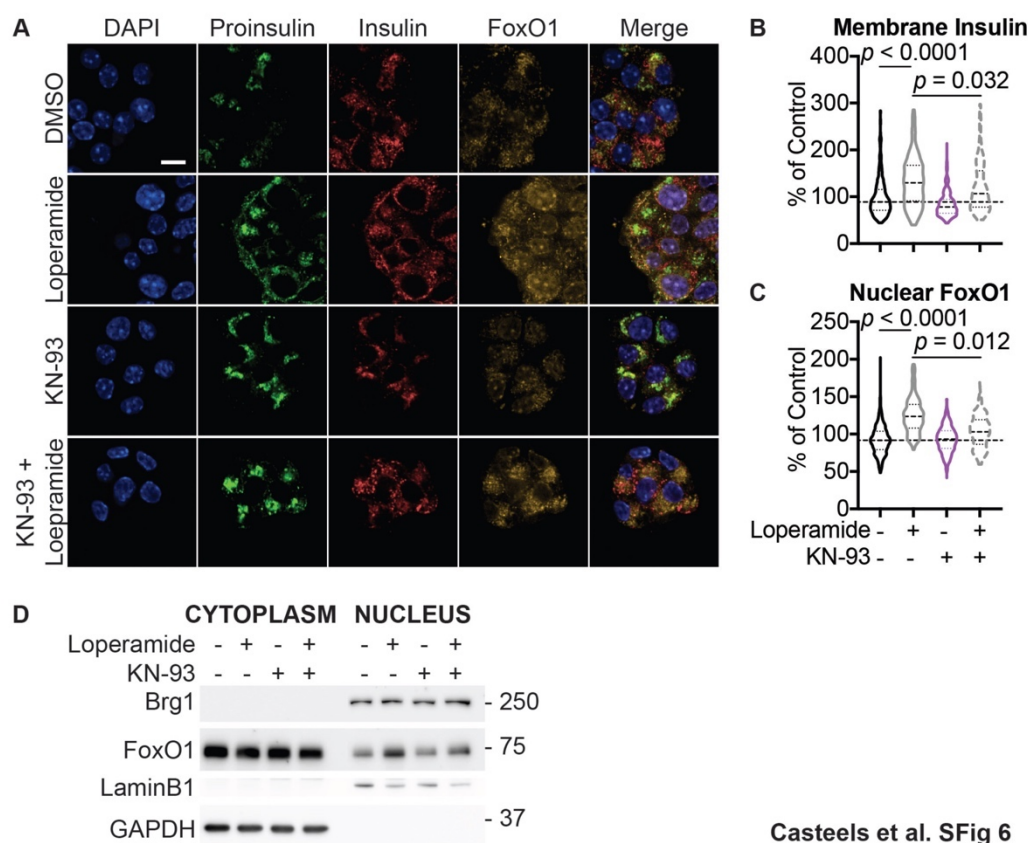
A. Representative images of Min6 cells stained for insulin and glucagon. Herkinorin was used at 15 μ M for two days. Scale bars 10 μ m. **B.** Representative images of Min6 cells stained for Pdx1 and glucagon. Naltrexone was used at 20 μ M for two days. Scale bars 10 μ m. **C.** Intracellular insulin protein levels in Min6 cells following 48h loperamide and naltrexone treatment, as measured by ELISA. **D.** Oprm1 gene expression in Min6 cells, as measured by RNAseq.



Casteels et al. SFig 5

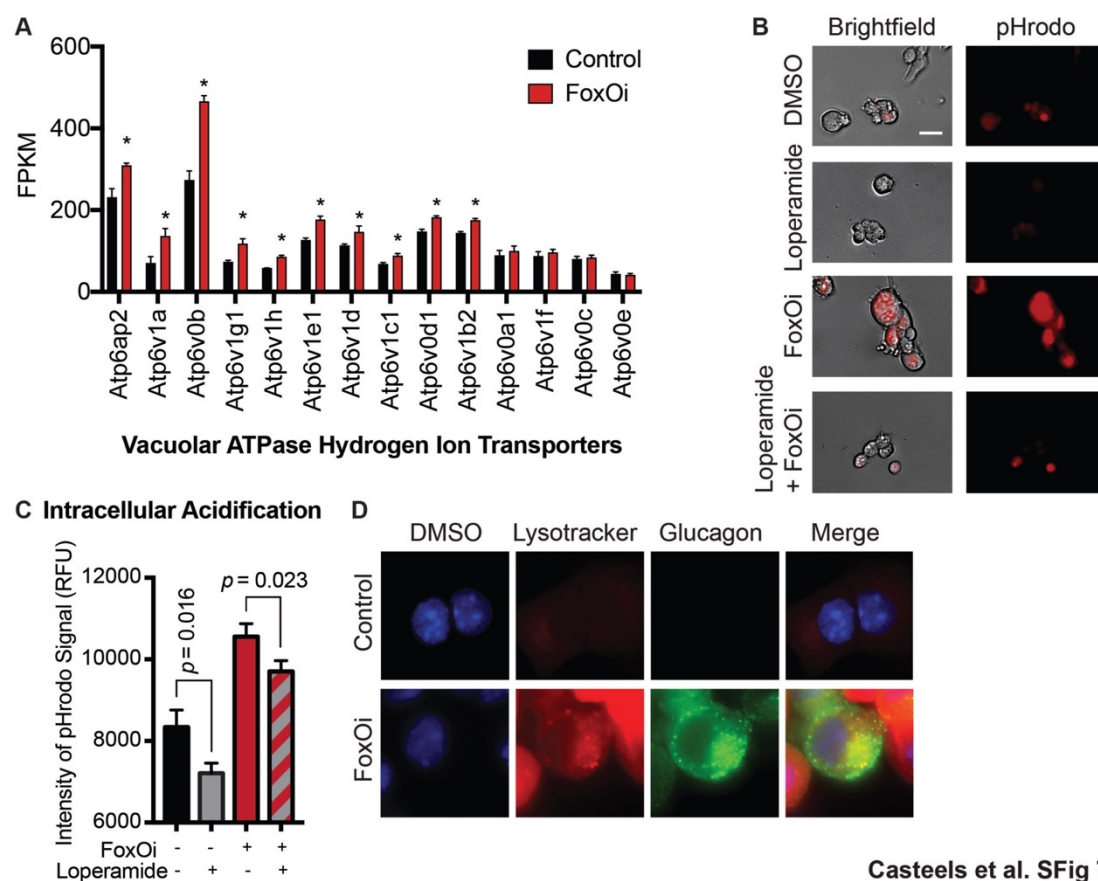
A. FoxO1 transcription in Min6 cells following 48h FoxOi/loperamide treatment, measured via RNAseq. **B.** FoxO1 transcription at different concentrations of loperamide in Min6 cells, measured via RT-qPCR. **C.** Western blot of FoxO1 protein expression in the cytoplasm vs. nucleus of Min6 cells following treatment with loperamide for the indicated hours. **D.** Western blot of FoxO1 protein expression in the cytoplasm vs. nucleus of Min6 cells following 48h loperamide and FoxOi treatments. **E.** GSEA showing general enrichment of FoxO1 genomic

binding sites [16] in loperamide-upregulated genes. FWER p-value = 0.001. **F.** mRNA levels of *Cacnb1* and *Cacna2d1* in Min6 cells upon 48h loperamide and FoxOi treatment, as measured by RNAseq. **G.** RT-qPCR time course of *Cacna1c* and *Cacna1d* expressions upon loperamide treatment. **H.** GSEA results for genes involved in calcium channel activity in DMSO vs. FoxOi-treated Min6 cells. **I.** Western blot of p-CamKII increase after 48h loperamide treatment in Min6 cells.

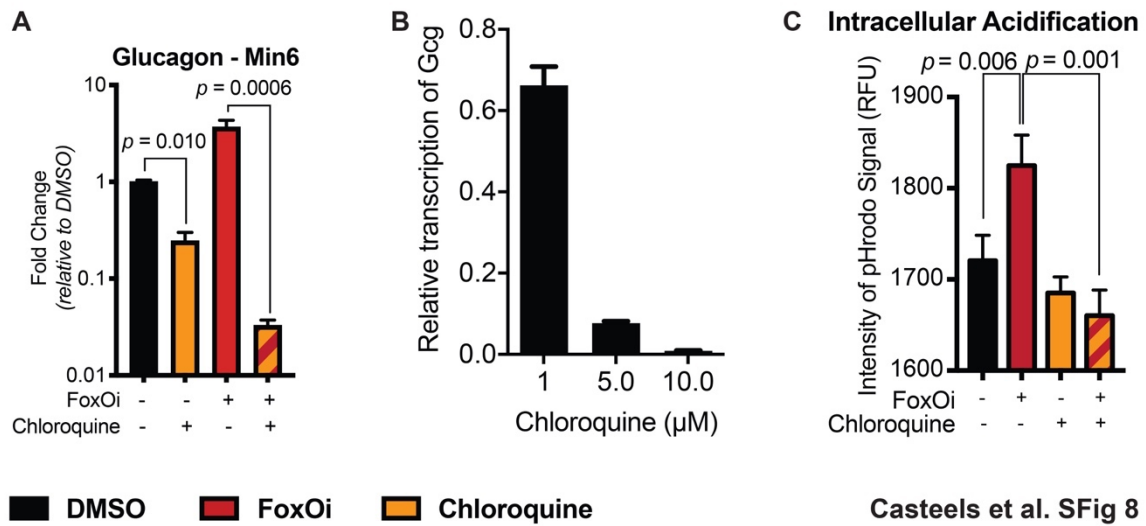


Casteels et al. SFig 6

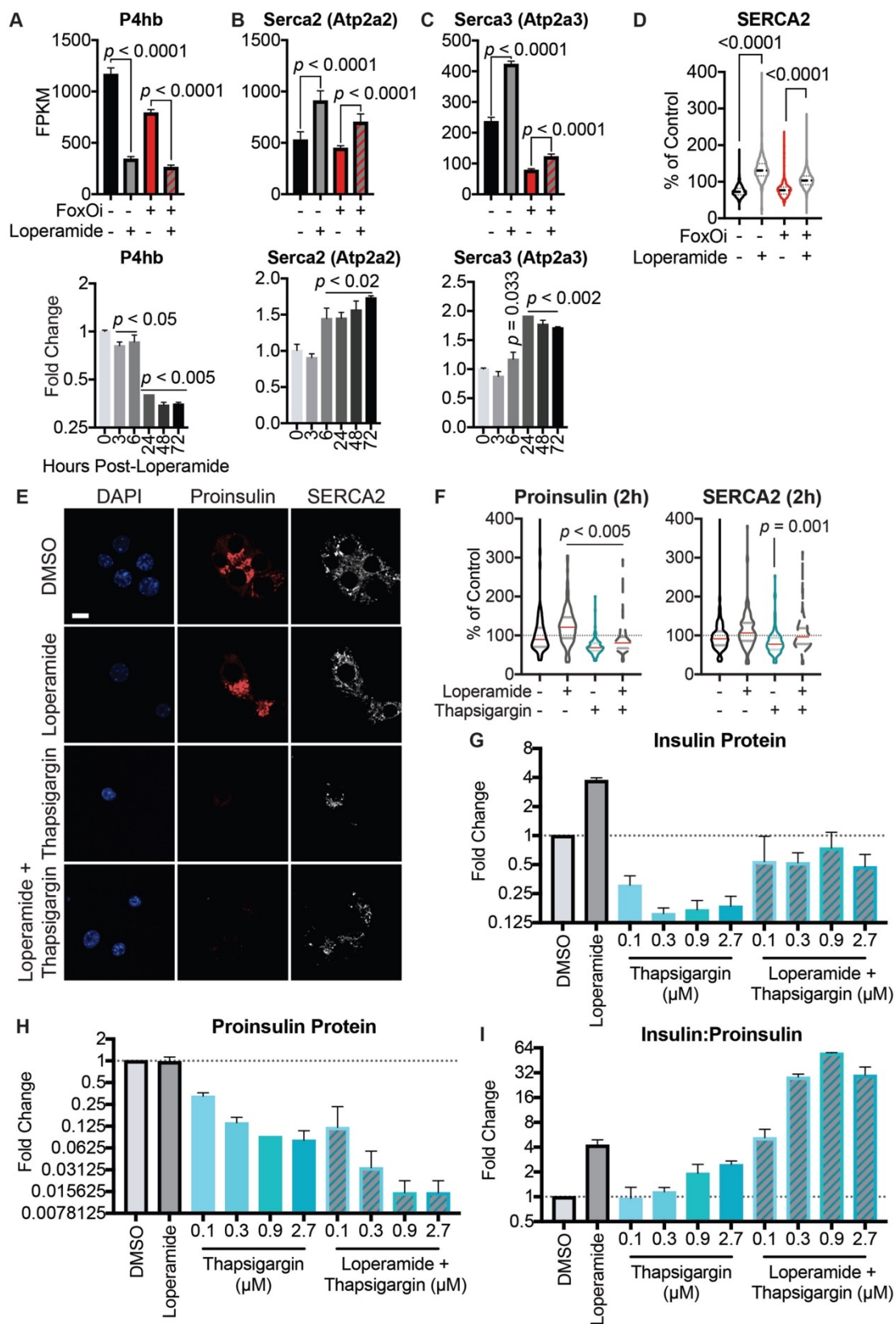
A. Immunofluorescence panel of Min6 cells treated with loperamide and 1 μ M KN-93 for 48h. Scale bar = 10 μ m. **B-C.** Quantification of immunofluorescence signal intensities of: **(B)** insulin at plasma membrane and **(C)** FoxO1 in the nucleus. Plasma membrane and nucleus defined using Harmony 4 (PerkinElmer) software. **D.** Western blot of fractionated Min6 cells pretreated with loperamide and 1 μ M KN-93 for 24h, highlighting KN-93's prevention of loperamide-induced FoxO1 nuclear translocation.



A. FoxO inhibitor treatment upregulates the transcription of lysosomal hydrogen ion transporters in Min6 cells, as measured by RNA-seq. **B-C** Intracellular pH indicator shows increased intracellular acidification after two days of FoxO inhibitor treatment in Min6 cells. **B.** Representative images of pHrodo live imaging in Min6 cells. Scale bars = 10 μ m. **C.** Quantification of pHrodo live staining signal intensity in Min6 cells pretreated with loperamide/FoxOi for 48h. **D.** Representative images of lysotracker staining in Min6 cells. Scale bars = 10 μ m.

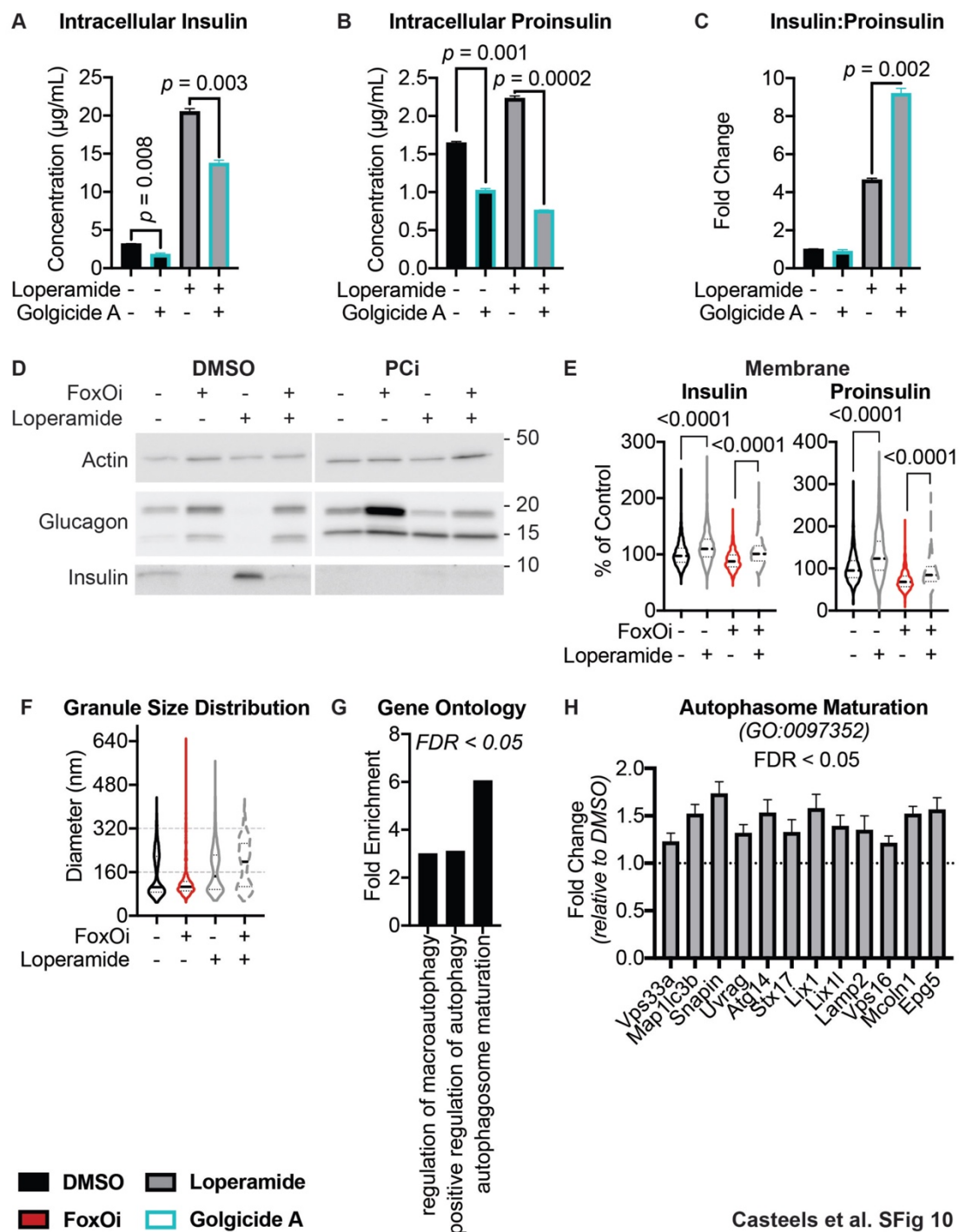


A. Chloroquine inhibits FoxOi-induced glucagon transcription in Min6 cells, as measured by RT-qPCR. **B.** Chloroquine dose response on glucagon transcription in Min6 cells treated with FoxO inhibitor (i.e. dedifferentiated Min6 cells). **C.** Quantification of pHrodo live staining signal intensity in Min6 cells pretreated with chloroquine/FoxOi for 48h.



A-C. Top: RNAseq expression levels after 48h treatment; Bottom: RT-qPCR time course of mRNA levels for **A.** P4hb. **B.** Atp2a2. **C.** Atp2a3. **D.** Quantification of SERCA2

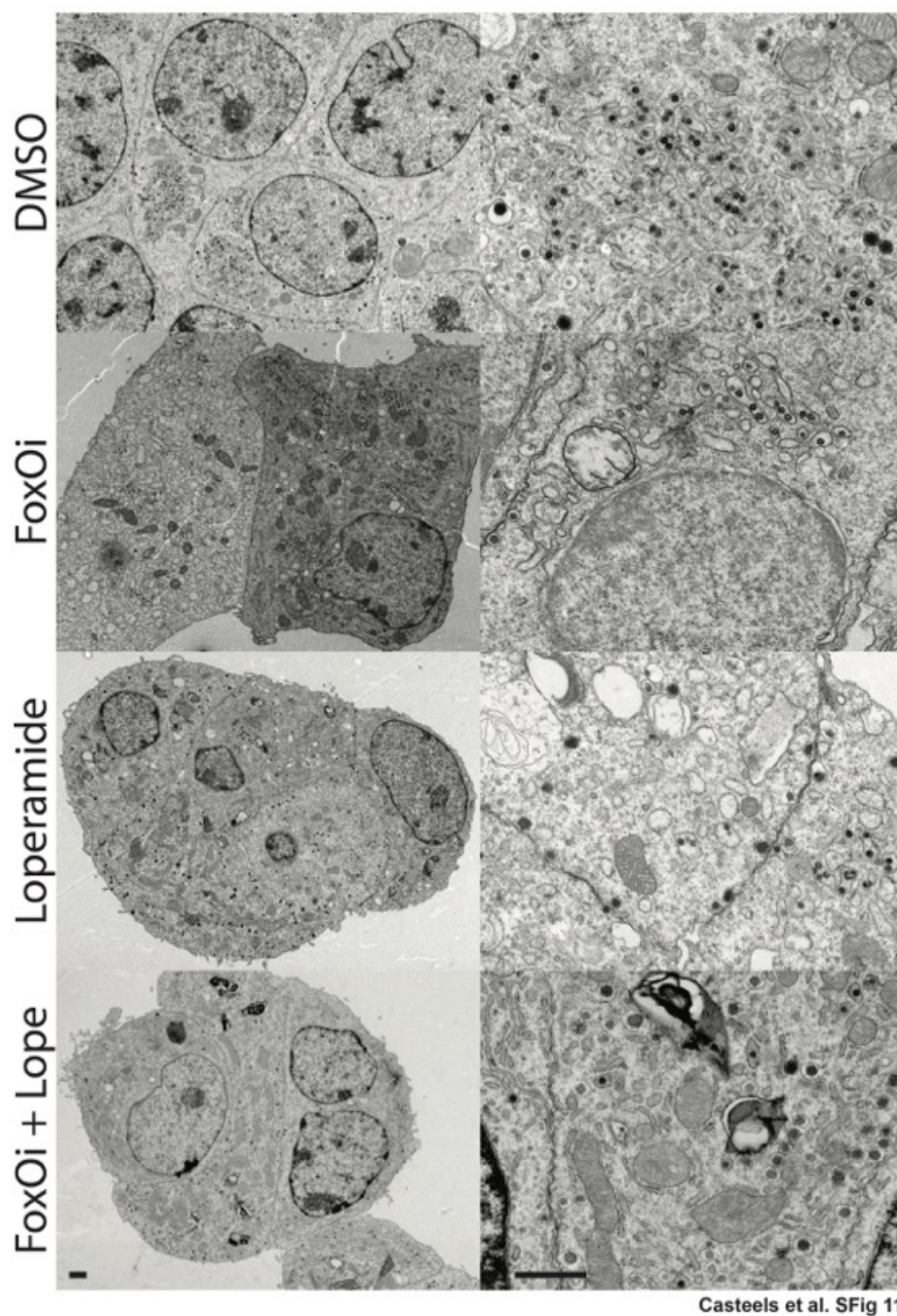
immunofluorescence intensity in Min6 cells treated with loperamide and FoxOi for 48h. **E.** Representative immunofluorescence images of Min6 cells treated with loperamide and thapsigargin for 2 hours. Scale bar = 10 μ m. **F.** Quantification of proinsulin and SERCA2 immunofluorescence intensity in Min6 cells treated with loperamide and thapsigargin for 2 hours. **G-H.** Protein levels of mature insulin or proinsulin in Min6 cells after 24h treatment with varying concentrations of thapsigargin +/- loperamide, as measured by ELISA. **I.** Ratio of insulin to proinsulin protein levels.



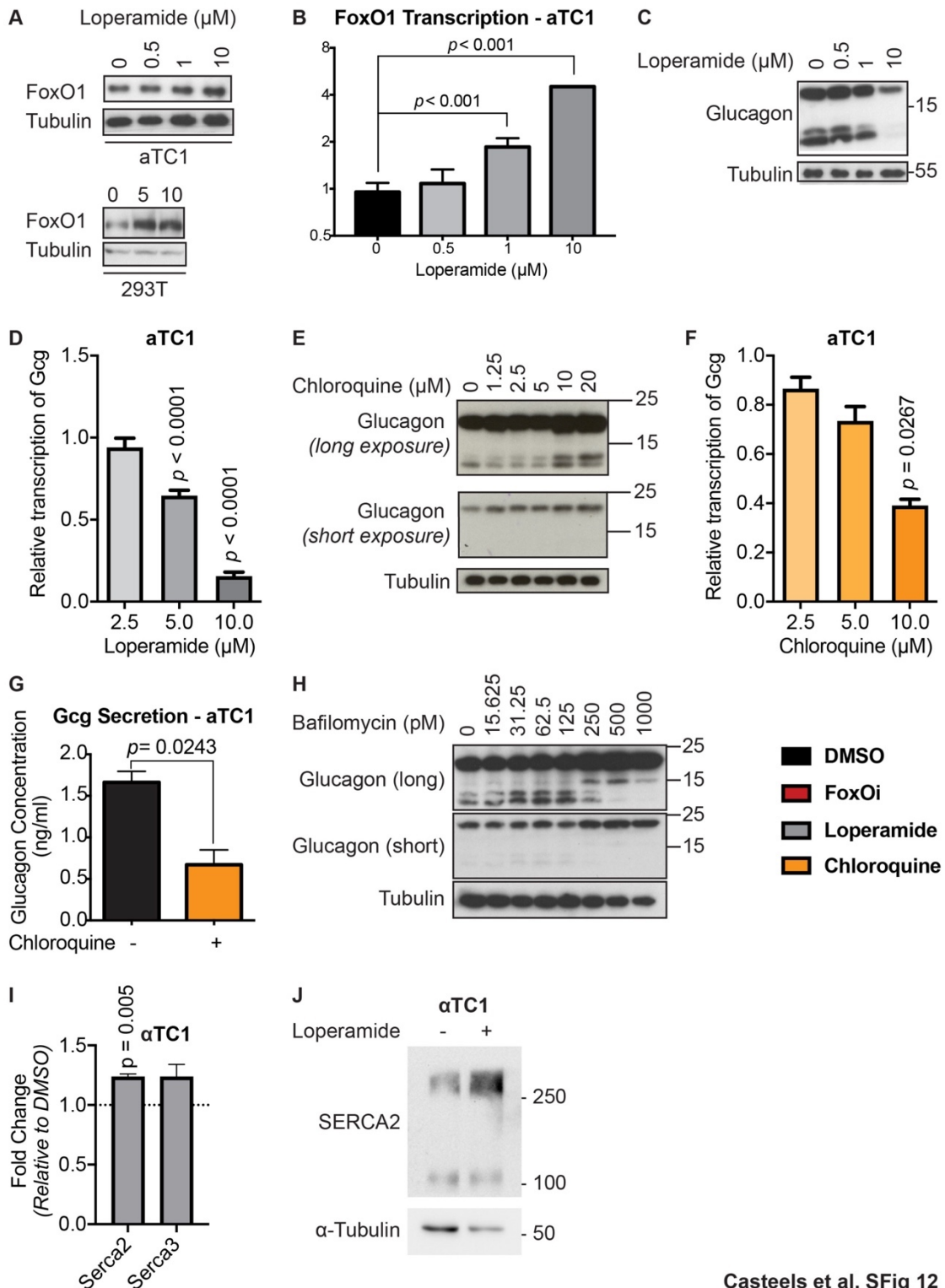
Casteels et al. SFig 10

A-B. Intracellular insulin and proinsulin protein levels after 30h loperamide treatment +/- 10µM Golgicide A for the final 6h, as measured by ELISA. **C.** Ratio of insulin to proinsulin protein levels. **D.** Western blot for glucagon and insulin protein levels in Min6 cells after 48h FoxOi/loperamide/PCi treatment. **E.** Quantification of insulin and proinsulin immunofluorescence intensities at the cell plasma membrane after 48h loperamide and FoxOi treatment. Plasma membrane defined using Harmony 4 (PerkinElmer) software. **F.**

Quantification of insulin granule size distribution from electron microscopy images. N = 5 cells per treatment condition. **G.** Gene ontology enrichment terms for RNAseq dataset of genes significantly upregulated by loperamide after 48h treatment in Min6 cells. **H.** Significantly upregulated genes involved in autophagosome maturation following 48 loperamide treatment in Min6 cells.



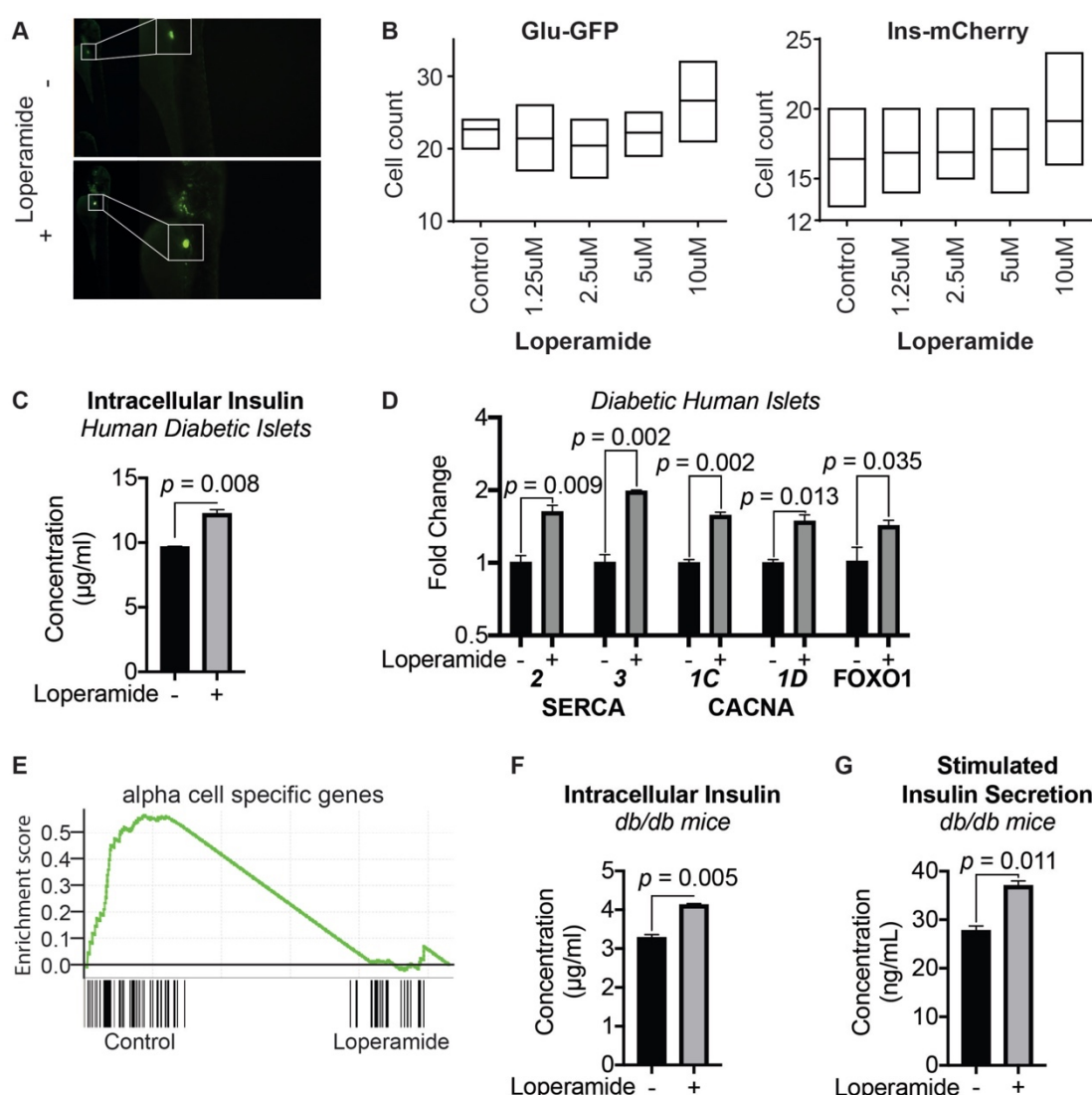
Additional representative electron microscopy images of Min6 cells at two different magnifications. Scale bar = 1 μ M.



Casteels et al. SFig 12

A-D. Effects of loperamide treatment on FoxO1 and glucagon levels in alpha cells. **A.** Western blot showing an increase of FoxO1 protein with loperamide treatment in alpha and HEK cells. **B.** FoxO1 transcription at different concentrations of loperamide in alpha cells, measured via RT-qPCR. **C.** Western blot showing decrease of glucagon protein with different concentrations of loperamide in alpha cells. **D.** Suppression of glucagon transcription by increasing doses of

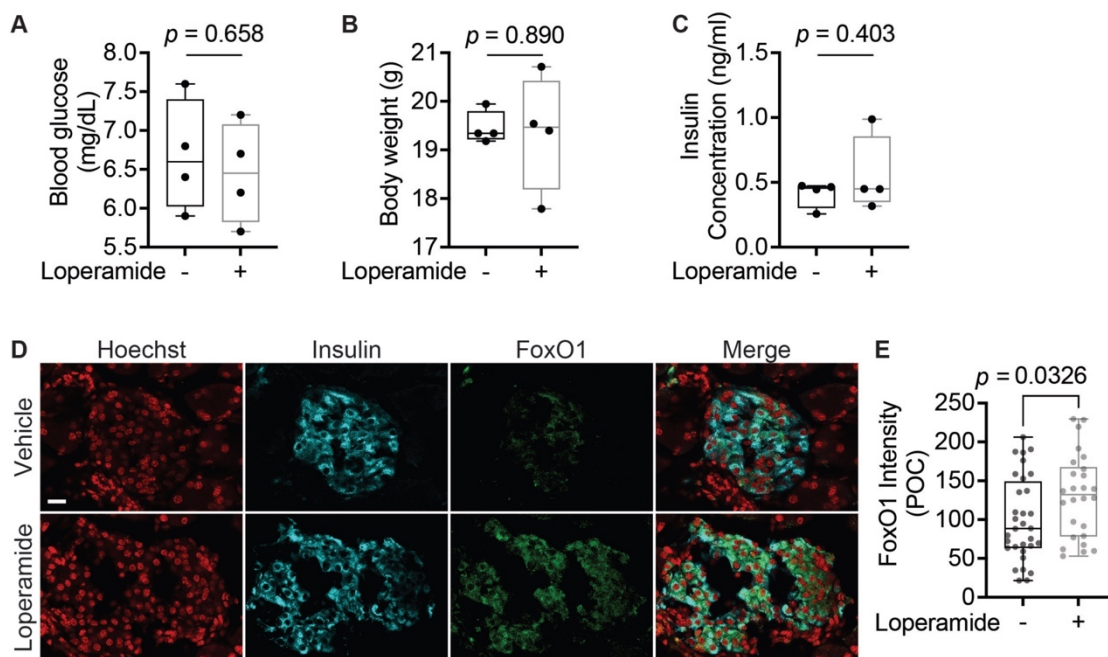
loperamide in alpha cells. **E-G.** Effects of chloroquine treatment on glucagon in alpha cells. **E.** Western blot showing changes to glucagon protein expression in alpha cells following 24h chloroquine treatment. **F.** Chloroquine suppresses glucagon transcription in alpha cells in a dose dependent manner. **G.** Glucagon secretion from alpha cells in low glucose medium pretreated with chloroquine (5 μ M) for 24h, concentration measured by ELISA. **H.** Western blot of glucagon gene protein products in alpha cells treated with different doses of bafilomycin (V-ATPase inhibitor) overnight. **I.** Increase in Atp2a2 and Atp2a3 mRNA levels in alpha cells after 24h loperamide treatment. **J.** Western blot highlighting increase in SERCA2 protein in alpha cells after 24h loperamide treatment.



Casteels et al. SFig 13

A. Representative images of insulin positive cells in zebrafish larvae. **B.** Quantification of insulin or glucagon positive cells following different doses of loperamide treatment in zebrafish

larvae. N=8-10. **C.** Intracellular insulin protein in diabetic human islets pre-treated with loperamide for 48h, as measured by ELISA. **D.** RT-qPCR mRNA levels of CACNA1C, CACNA1D, FOXO1, ATP2A2 and ATP2A3 in diabetic human islets pre-treated with loperamide for 48h. **E.** GSEA results show a downregulation of alpha cell specific genes in loperamide-treated diabetic human islets vs. DMSO. **F.** Intracellular insulin protein in db/db murine islets pre-treated with loperamide for 48h. **G.** Concentration of secreted insulin from db/db murine islets following 48h loperamide pre-treatment.



Casteels et al. SFig. 14

A-C. Results of 4-week loperamide treatment in wild-type non-diabetic mice. N=4 mice/treatment. **A.** Serum glucose concentrations after overnight fast. **B.** Body weight. **C.** Serum insulin concentration measured by ELISA. **D.** Representative immunofluorescence panel of db/db mouse pancreas sections 4-weeks post loperamide treatment, stained for insulin and FoxO1. Scale bar = 20 μ m. **E.** Quantification of immunofluorescence images. FoxO1 intensity was only calculated within insulin-positive cells. POC = percent of control. N_{DMSO} = 32 islets and N_{Loperamide} = 26 islets from 5 different mice each.

References

- [1] Gupta, D., Leahy, A.A., Monga, N., Peshavaria, M., Jetton, T.L., Leahy, J.L., 2013. Peroxisome proliferator-activated receptor γ (PPAR γ) and its target genes are downstream effectors of FoxO1 protein in islet β -cells: mechanism of β -cell compensation and failure. *The Journal of Biological Chemistry* 288(35): 25440–9, Doi: 10.1074/jbc.M113.486852.
- [2] Kluth, O., Mirhashemi, F., Scherneck, S., Kaiser, D., Kluge, R., Neschen, S., et al., 2011. Dissociation of lipotoxicity and glucotoxicity in a mouse model of obesity associated diabetes: role of forkhead box O1 (FOXO1) in glucose-induced beta cell failure. *Diabetologia* 54(3): 605–16, Doi: 10.1007/s00125-010-1973-8.
- [3] Kim-Muller, J.Y., Zhao, S., Srivastava, S., Mugabo, Y., Noh, H.-L., Kim, Y.R., et al., 2014. Metabolic inflexibility impairs insulin secretion and results in MODY-like diabetes in triple FoxO-deficient mice. *Cell Metabolism* 20(4): 593–602, Doi: 10.1016/j.cmet.2014.08.012.
- [4] Talchai, C., Xuan, S., Lin, H. V., Sussel, L., Accili, D., 2012. Pancreatic β cell dedifferentiation as a mechanism of diabetic β cell failure. *Cell* 150(6): 1223–34, Doi: 10.1016/j.cell.2012.07.029.
- [5] Cinti, F., Bouchi, R., Kim-Muller, J.Y., Ohmura, Y., Sandoval, P.R., Masini, M., et al., 2016. Evidence of β -Cell Dedifferentiation in Human Type 2 Diabetes. *The Journal of Clinical Endocrinology and Metabolism* 101(3): 1044–54, Doi: 10.1210/jc.2015-2860.
- [6] Efrat, S., 2019. Beta-Cell Dedifferentiation in Type 2 Diabetes: Concise Review. *Stem Cells* 37(10): 1267–72, Doi: 10.1002/stem.3059.
- [7] Zeng, H., Guo, M., Zhou, T., Tan, L., Chong, C.N., Zhang, T., et al., 2016. An Isogenic Human ESC Platform for Functional Evaluation of Genome-wide-Association-Study-Identified Diabetes Genes and Drug Discovery. *Cell Stem Cell* 19(3): 326–40, Doi: 10.1016/j.stem.2016.07.002.
- [8] Diedisheim, M., Oshima, M., Albagli, O., Huldt, C.W., Ahlstedt, I., Clausen, M., et al., 2018. Modeling human pancreatic beta cell dedifferentiation. *Mol Metab* 10(2212-8778 (Electronic)): 74–86, Doi: 10.1016/j.molmet.2018.02.002.
- [9] Nagashima, T., Shigematsu, N., Maruki, R., Urano, Y., Tanaka, H., Shimaya, A., et al., 2010. Discovery of novel forkhead box O1 inhibitors for treating type 2 diabetes: improvement of fasting glycemia in diabetic db/db mice. *Molecular Pharmacology* 78(5): 961–70, Doi: 10.1124/mol.110.065714.
- [10] Kim-Muller, J.Y., Fan, J., Kim, Y.J., Lee, S.A., Ishida, E., Blaner, W.S., et al., 2016. Aldehyde dehydrogenase 1a3 defines a subset of failing pancreatic beta cells in diabetic mice. *Nat Commun* 7: 12631, Doi: 10.1038/ncomms12631.

- [11] Guo, S., Dai, C., Guo, M., Taylor, B., Harmon, J.S., Sander, M., et al., 2013. Inactivation of specific beta cell transcription factors in type 2 diabetes. *J Clin Invest* 123(8): 3305–16, Doi: 10.1172/jci65390.
- [12] Licciardello, M.P., Ringler, A., Markt, P., Klepsch, F., Lardeau, C.H., Sdelci, S., et al., 2017. A combinatorial screen of the CLOUD uncovers a synergy targeting the androgen receptor. *Nat Chem Biol* 13(7): 771–8, Doi: 10.1038/nchembio.2382.
- [13] Giagnoni, G., Casiraghi, L., Senini, R., Revel, L., Parolaro, D., Sala, M., et al., 1983. Loperamide: evidence of interaction with mu and delta opioid receptors. *Life Sciences* 33 Suppl 1: 315–8, Doi: 10.1016/0024-3205(83)90506-4.
- [14] Groer, C.E., Tidgewell, K., Moyer, R.A., Harding, W.W., Rothman, R.B., Prinzano, T.E., et al., 2007. An opioid agonist that does not induce mu-opioid receptor--arrestin interactions or receptor internalization. *Molecular Pharmacology* 71(2): 549–57, Doi: 10.1124/mol.106.028258.
- [15] Xu, H., Partilla, J.S., Wang, X., Rutherford, J.M., Tidgewell, K., Prinzano, T.E., et al., 2007. A comparison of noninternalizing (herkinorin) and internalizing (DAMGO) mu-opioid agonists on cellular markers related to opioid tolerance and dependence. *Synapse (New York, N.Y.)* 61(3): 166–75, Doi: 10.1002/syn.20356.
- [16] Kuo, T., Kraakman, M.J., Damle, M., Gill, R., Lazar, M.A., Accili, D., 2019. Identification of *C2CD4A* as a human diabetes susceptibility gene with a role in β cell insulin secretion. *Proceedings of the National Academy of Sciences* 116(40): 20033 LP – 20042, Doi: 10.1073/pnas.1904311116.
- [17] Gilon, P., Chae, H.-Y., Rutter, G.A., Ravier, M.A., 2014. Calcium signaling in pancreatic β -cells in health and in Type 2 diabetes. *Cell Calcium* 56(5): 340–61, Doi: 10.1016/j.ceca.2014.09.001.
- [18] Gandasi, N.R., Yin, P., Riz, M., Chibalina, M. V., Cortese, G., Lund, P.-E., et al., 2017. Ca^{2+} channel clustering with insulin-containing granules is disturbed in type 2 diabetes. *The Journal of Clinical Investigation* 127(6): 2353–64, Doi: 10.1172/JCI88491.
- [19] Ozcan, L., Wong, C.C.L., Li, G., Xu, T., Pajvani, U., Park, S.K.R., et al., 2012. Calcium signaling through CaMKII regulates hepatic glucose production in fasting and obesity. *Cell Metabolism* 15(5): 739–51, Doi: 10.1016/j.cmet.2012.03.002.
- [20] Barg, S., 2003. Mechanisms of exocytosis in insulin-secreting B-cells and glucagon-secreting A-cells. *Pharmacol Toxicol* 92(1): 3–13, Doi: 10.1034/j.1600-0773.2003.920102.x.
- [21] Bensellam, M., Jonas, J.C., Laybutt, D.R., 2018. Mechanisms of beta-cell dedifferentiation in diabetes: recent findings and future research directions. *J Endocrinol* 236(2): R109-r143, Doi: 10.1530/joe-17-0516.
- [22] Weiss, M., Steiner, D.F., Philipson, L.H., 2000. Insulin Biosynthesis, Secretion,

- Structure, and Structure-Activity Relationships. In: Feingold, K.R., Anawalt, B., Boyce, A., Chrousos, G., de Herder, W.W., Dungan, K. et al., editors. South Dartmouth (MA).
- [23] Leibiger, I.B., Leibiger, B., Berggren, P.O., 2008. Insulin signaling in the pancreatic beta-cell. *Annu Rev Nutr* 28: 233–51, Doi: 10.1146/annurev.nutr.28.061807.155530.
- [24] Leibiger, B., Moede, T., Muhandiramlage, T.P., Kaiser, D., Vaca Sanchez, P., Leibiger, I.B., et al., 2012. Glucagon regulates its own synthesis by autocrine signaling. *Proc Natl Acad Sci U S A* 109(51): 20925–30, Doi: 10.1073/pnas.1212870110.
- [25] Ohkuma, S., Poole, B., 1978. Fluorescence probe measurement of the intralysosomal pH in living cells and the perturbation of pH by various agents. *Proc Natl Acad Sci U S A* 75(7): 3327–31.
- [26] Rajpal, G., Schuiki, I., Liu, M., Volchuk, A., Arvan, P., 2012. Action of protein disulfide isomerase on proinsulin exit from endoplasmic reticulum of pancreatic β -cells. *The Journal of Biological Chemistry* 287(1): 43–7, Doi: 10.1074/jbc.C111.279927.
- [27] Ouyang, W., Liao, W., Luo, C.T., Yin, N., Huse, M., Kim, M. V., et al., 2012. Novel Foxo1-dependent transcriptional programs control T(reg) cell function. *Nature* 491(7425): 554–9, Doi: 10.1038/nature11581.
- [28] Kalvisa, A., Siersbæk, M.S., Præstholm, S.M., Christensen, L.J.L., Nielsen, R., Stohr, O., et al., 2018. Insulin signaling and reduced glucocorticoid receptor activity attenuate postprandial gene expression in liver. *PLOS Biology* 16(12): e2006249.
- [29] Tuch, B.E., Szymanska, B., Yao, M., Tabiin, M.T., Gross, D.J., Holman, S., et al., 2003. Function of a genetically modified human liver cell line that stores, processes and secretes insulin. *Gene Therapy* 10(6): 490–503, Doi: 10.1038/sj.gt.3301911.
- [30] Orci, L., Ravazzola, M., Amherdt, M., Yanaihara, C., Yanaihara, N., Halban, P., et al., 1984. Insulin, not C-peptide (proinsulin), is present in crinophagic bodies of the pancreatic B-cell. *The Journal of Cell Biology* 98(1): 222–8, Doi: 10.1083/jcb.98.1.222.
- [31] Marsh, B.J., Soden, C., Alarcón, C., Wicksteed, B.L., Yaekura, K., Costin, A.J., et al., 2007. Regulated autophagy controls hormone content in secretory-deficient pancreatic endocrine beta-cells. *Molecular Endocrinology (Baltimore, Md.)* 21(9): 2255–69, Doi: 10.1210/me.2007-0077.
- [32] Jung, H.S., Chung, K.W., Won Kim, J., Kim, J., Komatsu, M., Tanaka, K., et al., 2008. Loss of autophagy diminishes pancreatic beta cell mass and function with resultant hyperglycemia. *Cell Metabolism* 8(4): 318–24, Doi: 10.1016/j.cmet.2008.08.013.
- [33] Fielenbach, N., Antebi, A., 2008. C. elegans dauer formation and the molecular basis of plasticity. *Genes & Development* 22(16): 2149–65, Doi: 10.1101/gad.1701508.
- [34] Fajardo, R.J., Karim, L., Calley, V.I., Bouxsein, M.L., 2014. A Review of Rodent Models of Type 2 Diabetic Skeletal Fragility. *Journal of Bone and Mineral Research* 29(5): 1025–40, Doi: <https://doi.org/10.1002/jbmr.2210>.

- [35] Spijker, H.S., Song, H., Ellenbroek, J.H., Roefs, M.M., Engelse, M.A., Bos, E., et al., 2015. Loss of β -Cell Identity Occurs in Type 2 Diabetes and Is Associated With Islet Amyloid Deposits. *Diabetes* 64(8): 2928, Doi: 10.2337/db14-1752.
- [36] White, M.G., Marshall, H.L., Rigby, R., Huang, G.C., Amer, A., Booth, T., et al., 2013. Expression of Mesenchymal and α -Cell Phenotypic Markers in Islet β -Cells in Recently Diagnosed Diabetes. *Diabetes Care* 36(11): 3818, Doi: 10.2337/dc13-0705.
- [37] Sun, J., Ni, Q., Xie, J., Xu, M., Zhang, J., Kuang, J., et al., 2018. β -Cell Dedifferentiation in Patients With T2D With Adequate Glucose Control and Nondiabetic Chronic Pancreatitis. *The Journal of Clinical Endocrinology & Metabolism* 104(1): 83–94, Doi: 10.1210/jc.2018-00968.
- [38] Marselli, L., Suleiman, M., Masini, M., Campani, D., Bugliani, M., Syed, F., et al., 2014. Are we overestimating the loss of beta cells in type 2 diabetes? *Diabetologia* 57(2): 362–5, Doi: 10.1007/s00125-013-3098-3.
- [39] Lu, T.T.-H., Heyne, S., Dror, E., Casas, E., Leonhardt, L., Boenke, T., et al., 2018. The Polycomb-Dependent Epigenome Controls β Cell Dysfunction, Dedifferentiation, and Diabetes. *Cell Metabolism* 27(6): 1294-1308.e7, Doi: 10.1016/j.cmet.2018.04.013.
- [40] Fred, R.G., Bang-Berthelsen, C.H., Mandrup-Poulsen, T., Grunnet, L.G., Welsh, N., 2010. High Glucose Suppresses Human Islet Insulin Biosynthesis by Inducing miR-133a Leading to Decreased Polypyrimidine Tract Binding Protein-Expression. *PLoS One* 5(5): e10843, Doi: 10.1371/journal.pone.0010843.
- [41] Kim, J.W., You, Y.H., Jung, S., Suh-Kim, H., Lee, I.K., Cho, J.H., et al., 2013. miRNA-30a-5p-mediated silencing of Beta2/NeuroD expression is an important initial event of glucotoxicity-induced beta cell dysfunction in rodent models. *Diabetologia* 56(4): 847–55, Doi: 10.1007/s00125-012-2812-x.
- [42] Xu, G., Chen, J., Jing, G., Shalev, A., 2013. Thioredoxin-interacting protein regulates insulin transcription through microRNA-204. *Nature Medicine* 19(9): 1141–6, Doi: 10.1038/nm.3287.
- [43] Sebastiani, G., Po, A., Miele, E., Ventriglia, G., Ceccarelli, E., Bugliani, M., et al., 2015. MicroRNA-124a is hyperexpressed in type 2 diabetic human pancreatic islets and negatively regulates insulin secretion. *Acta Diabetologica* 52(3): 523–30, Doi: 10.1007/s00592-014-0675-y.
- [44] Marquina-Sanchez, B., Fortelny, N., Farlik, M., Vieira, A., Collombat, P., Bock, C., et al., 2020. Single-cell RNA-seq with spike-in cells enables accurate quantification of cell-specific drug effects in pancreatic islets. *Genome Biology* 21(1): 106, Doi: 10.1186/s13059-020-02006-2.
- [45] Idevall-Hagren, O., Tengholm, A., 2020. Metabolic regulation of calcium signaling in beta cells. *Seminars in Cell & Developmental Biology* 103: 20–30, Doi:

- <https://doi.org/10.1016/j.semcdb.2020.01.008>.
- [46] Li, S., Hao, B., Lu, Y., Yu, P., Lee, H.C., Yue, J., 2012. Intracellular alkalization induces cytosolic Ca²⁺ increases by inhibiting sarco/endoplasmic reticulum Ca²⁺-ATPase (SERCA). *PLoS One* 7(2): e31905, Doi: 10.1371/journal.pone.0031905.
- [47] Orci, L., Ravazzola, M., Storch, M.J., Anderson, R.G., Vassalli, J.D., Perrelet, A., 1987. Proteolytic maturation of insulin is a post-Golgi event which occurs in acidifying clathrin-coated secretory vesicles. *Cell* 49(6): 865–8.
- [48] Sun-Wada, G.H., Toyomura, T., Murata, Y., Yamamoto, A., Futai, M., Wada, Y., 2006. The $\alpha 3$ isoform of V-ATPase regulates insulin secretion from pancreatic beta-cells. *J Cell Sci* 119(Pt 21): 4531–40, Doi: 10.1242/jcs.03234.
- [49] Dechant, R., Binda, M., Lee, S.S., Pelet, S., Winderickx, J., Peter, M., 2010. Cytosolic pH is a second messenger for glucose and regulates the PKA pathway through V-ATPase. *Embo J* 29(15): 2515–26, Doi: 10.1038/emboj.2010.138.
- [50] Liu, I.M., Chi, T.C., Chen, Y.C., Lu, F.H., Cheng, J.T., 1999. Activation of opioid mu-receptor by loperamide to lower plasma glucose in streptozotocin-induced diabetic rats. *Neuroscience Letters* 265(3): 183–6, Doi: 10.1016/s0304-3940(99)00226-8.
- [51] Cheng, J.T., Liu, I.M., Chi, T.C., Tzeng, T.F., 2001. Increase of opioid mu-receptor gene expression in streptozotocin-induced diabetic rats. *Hormone and Metabolic Research = Hormon- Und Stoffwechselforschung = Hormones et Metabolisme* 33(8): 467–71, Doi: 10.1055/s-2001-16939.
- [52] Tzeng, T.F., Liu, I.M., Lai, T.Y., Tsai, C.C., Chang, W.C., Cheng, J.T., 2003. Loperamide increases glucose utilization in streptozotocin-induced diabetic rats. *Clinical and Experimental Pharmacology & Physiology* 30(10): 734–8, Doi: 10.1046/j.1440-1681.2003.03903.x.
- [53] Tzeng, T.-F., Lo, C.-Y., Cheng, J.-T., Liu, I.-M., 2007. Activation of mu-opioid receptors improves insulin sensitivity in obese Zucker rats. *Life Sciences* 80(16): 1508–16, Doi: 10.1016/j.lfs.2007.01.016.
- [54] Kim, D., Pertea, G., Trapnell, C., Pimentel, H., Kelley, R., Salzberg, S.L., 2013. TopHat2: accurate alignment of transcriptomes in the presence of insertions, deletions and gene fusions. *Genome Biology* 14(4): R36, Doi: 10.1186/gb-2013-14-4-r36.
- [55] Wang, L., Wang, S., Li, W., 2012. RSeQC: quality control of RNA-seq experiments. *Bioinformatics (Oxford, England)* 28(16): 2184–5, Doi: 10.1093/bioinformatics/bts356.
- [56] Kent, W.J., Sugnet, C.W., Furey, T.S., Roskin, K.M., Pringle, T.H., Zahler, A.M., et al., 2002. The human genome browser at UCSC. *Genome Research* 12(6): 996–1006, Doi: 10.1101/gr.229102.
- [57] Subramanian, A., Tamayo, P., Mootha, V.K., Mukherjee, S., Ebert, B.L., Gillette, M.A., et al., 2005. Gene set enrichment analysis: a knowledge-based approach for

- interpreting genome-wide expression profiles. *Proceedings of the National Academy of Sciences of the United States of America* 102(43): 15545–50, Doi: 10.1073/pnas.0506580102.
- [58] Kubicek, S., Gilbert, J.C., Fomina-Yadlin, D., Gitlin, A.D., Yuan, Y., Wagner, F.F., et al., 2012. Chromatin-targeting small molecules cause class-specific transcriptional changes in pancreatic endocrine cells. *Proc Natl Acad Sci U S A* 109(14): 5364–9, Doi: 10.1073/pnas.1201079109.
- [59] Xin, Y., Kim, J., Ni, M., Wei, Y., Okamoto, H., Lee, J., et al., 2016. Use of the Fluidigm C1 platform for RNA sequencing of single mouse pancreatic islet cells. *Proc Natl Acad Sci U S A* 113(12): 3293–8, Doi: 10.1073/pnas.1602306113.
- [60] Fomina-Yadlin, D., Kubicek, S., Walpita, D., Dancik, V., Hecksher-Sorensen, J., Bittker, J.A., et al., 2010. Small-molecule inducers of insulin expression in pancreatic alpha-cells. *Proc Natl Acad Sci U S A* 107(34): 15099–104, Doi: 10.1073/pnas.1010018107.
- [61] Li, J., Casteels, T., Huber, K.V.M., Lardeau, C.-H., Klughammer, J., Farlik, M., et al., 2017. Artemisinin Target GABAA Receptor Signaling and Impair α Cell Identity. *Cell* 168(1–2), Doi: 10.1016/j.cell.2016.11.010.

2.2 SMNDC1 links chromatin remodeling and splicing to regulate pancreatic hormone expression

Pancreatic alpha and beta cells share strong cellular plasticity and key transcription factor expressions due to their common Ngn3-expressing developmental progenitor. However, insulin transcription is restricted to beta cells, as well as the expressions of the insulin promoter-binding transcription factors: Pdx1 and MafA. Multiple studies have now shown that forced overexpression of Ngn3, Pdx1 and MafA is sufficient to induce insulin transcription in secondary endocrine organs. In order to elucidate the epigenetic factors repressing insulin, Pdx1 and MafA expression in alpha cells, we performed an RNA interference screen targeting over 300 proteins with chromatin binding domains. We identified the splicing factor, Survival Motor Neuron Domain Containing 1 (Smndc1), to potently repress insulin mRNA levels in alpha cells. Upon Smndc1 knockdown, we observed a strong and sustained upregulation of insulin, Pdx1 and MafA mRNA levels. Characterization of Smndc1 revealed it directly binds and splices chromatin remodeler Atrx's mRNA, thus maintaining its protein levels. Loss of either Smndc1 or Atrx triggers a robust stabilization of Pdx1 mRNA, with subsequent induction of insulin transcription. Importantly, loss of SMNDC1 in pancreatic human islets results in a functional amelioration of glucose responsiveness and increased insulin secretion.

SMNDC1 links chromatin remodeling and splicing to regulate pancreatic hormone expression

Tamara Casteels¹, Simon Bajew^{2,3}, Jiří Reiniš¹, Michael Schuster¹, André Müller¹, Bridget K. Wagner⁴, Christoph Bock¹, and Stefan Kubicek^{1,5}

¹CeMM Research Center for Molecular Medicine of the Austrian Academy of Sciences, Lazarettgasse 14, 1090 Vienna, Austria

²Centre for Genomic Regulation (CRG), The Barcelona Institute of Science and Technology, Carrer del Dr. Aiguader 88, 08003 Barcelona, Spain

³Universitat Pompeu Fabra, Carrer del Dr. Aiguader 88, 08003 Barcelona, Spain

⁴Broad Institute, 415 Main Street, Cambridge, Massachusetts 02142, USA

⁵Correspondence to: Stefan Kubicek, skubicek@cemm.oeaw.ac.at.

Keywords

Insulin transcription, pancreatic islets, RNAi screen, SMNDC1, chromatin remodelers, splicing, alpha cells, beta cells

Abstract

Insulin expression is restricted to the pancreatic beta cells, which are physically or functionally depleted in diabetes. Identifying targetable pathways repressing insulin in non-beta cells, particularly in the developmentally related glucagon-secreting alpha cells, is an important aim of regenerative medicine. Here, we performed an RNA interference screen in the murine alpha cell line, alphaTC1, to identify silencers of insulin expression. We discovered that knockdown of the splicing factor SmnDC1 (Survival Motor Neuron Domain Containing 1) triggered a global repression of alpha cell gene-expression programs in favor of increased beta cell markers. Mechanistically, SmnDC1 knockdown upregulated the key beta cell transcription factor Pdx1, by modulating the activities of the BAF and Atrx families of chromatin remodeling complexes. SMNDC1's repressive role was conserved in human pancreatic islets, its loss triggering enhanced insulin secretion and PDX1 expression. Our study identifies SmnDC1 as a key factor connecting splicing and chromatin remodeling to the control of insulin expression in human and mouse islet cells.

Introduction

Pancreatic islet alpha and beta cells tightly maintain glucose homeostasis via the controlled release of their respective hormones, glucagon and insulin. Loss of beta cells causes the deregulation of this tight hormone balance, resulting in hyperglycemia and diabetes (Campbell and Newgard, 2021). Replenishment of functional beta cell mass or generation of alternative insulin sources therefore constitutes an important therapeutic goal. Due to their physical and developmental proximity, alpha cells represent a promising target for reprogramming (Collombat et al., 2003; Gradwohl et al., 2000; Gromada et al., 2018). Bivalent epigenetic marks on genomic loci of important beta cell transcription factors PDX1 and MAFA in alpha cells suggest they are primed for cellular conversion (Bramswig et al., 2013). This inherent plasticity can be exploited for transdifferentiation to beta cells with loss or gain of one transcription factor, Arx, Pax4 or Pdx1 (Chakravarthy et al., 2017; Collombat et al., 2009; Courtney et al., 2013; Furuyama et al., 2019; Yang et al., 2011). Pdx1 is arguably the most defining beta cell transcription factor. Its expression instigates islet development and is required for the initial generation of beta cell mass (Jonsson et al., 1994; Servitja and Ferrer, 2004; Stoffers et al., 1997). It then maintains mature beta cell identity by repressively binding to the loci of alpha cell specific genes (Gao et al., 2014). Along with MafA, Pdx1 is also responsible for driving insulin transcription through direct binding to the insulin promoter (Docherty et al., 2005; Matsuoka et al., 2003; Ohlsson et al., 1993). The critical roles of PDX1 and MAFA in insulin regulation are further highlighted in their sufficient capacity to initiate insulin expression in human alpha and PPY cells (Furuyama et al., 2019), and in even more distant non-islet cell types when in combination with the endocrine progenitor marker NGN3 (Ariyachet et al., 2016; Banga et al., 2012; Chen et al., 2014; Hickey et al., 2013; Luo et al., 2014; Yamada et al., 2015; Zhou et al., 2008).

While transcription factors are the drivers of cell identity changes, they are not easily therapeutically targetable, in contrast to the chromatin pathways that control their expression. Several chromatin factors have been identified to play key roles in maintaining pancreatic islet cell identity, including DNA methylation (Chakravarthy et al., 2017; Dhawan et al., 2011) and the BAF chromatin remodeling complex (McKenna et al., 2015; Spaeth et al., 2019). To systematically identify chromatin proteins repressing insulin transcription, we performed an RNA interference screen in murine alpha cells. We identified Survival Motor Neuron Domain Containing 1 (Smndc1) knockdown to induce a strong upregulation of insulin expression. Smndc1, also known as SPF30 and SMNrp, is an arginine-methylation binding Tudor domain protein involved in the assembly of the mature spliceosome complex (Meister et al., 2001;

Rappsilber et al., 2001). Our results uncover a regulatory circuit of *Smn1* controlling key transcription factors via modulation of chromatin regulation, gene expression and splicing, both in murine alpha cells and in primary human islets.

Results

RNAi screen identifies *Smn1* as repressor of insulin expression in alpha cells

With the overarching aim of identifying silencers of insulin expression, we designed an RNAi library with an epigenetic focus, specifically targeting genes with chromatin-binding domains. The final library targeted 358 genes, with an average of 5 short hairpins per gene. We treated the murine alpha cell line, aTC1, with this final library for 7 days, after which we quantified insulin mRNA levels using Nanostring technology. Strong knockdown of *Smn1* induced a reproducible 3-4-fold increase in insulin mRNA counts (Figure 1A). To gain a more global understanding of gene expression changes upon *Smn1* knockdown, we performed RNAseq and validated our initial observations of increased insulin mRNA (Figure 1B). Globally, *Smn1* knockdown caused upregulation of beta cell genes and downregulation of alpha cell genes in gene set enrichment analysis for genes differentially expressed between aTC1 and murine beta cell lines Min6 or bTC3 cells (Figures 1C and S1A). This shift towards a more beta cell character was also evident from the upregulation of the key beta cell transcription factors *Pdx1* and *MafA*. Prolonged knockdown revealed a sustained increase in insulin, *Pdx1* and *MafA* mRNAs, with an insulin peak at day 5 post-transduction (Figure 1D). At the protein level, intracellular insulin expression was increased from negligible to a concentration of 0.9 ng/mL (Figure 1E). While robustly detectable, this concentration is significantly lower compared to insulin levels in the Min6 beta cell line (Figure S1B). We further analyzed global proteome changes in aTC1 following *Smn1* knockdown and observed a good correlation to transcription changes (Figure S1C). When analyzing at the single cell level, we observe that insulin induction is not homogenous, and rather restricted to approximately 15% of the cell population (Figures 1F and S1D). Also *Smn1* levels appeared heterogenous post-knockdown (Figure 1F), suggesting that a specifically robust threshold of *Smn1* depletion is needed to achieve insulin expression. The need for particularly strong *Smn1* knockdown equally explains the lack of insulin induction with hairpins 96-98 that result in inefficient *Smn1* knock-down in the original screen (Figure 1A). In line with this observation, complete knock out of *Smn1* using CRISPR-Cas9 technology yielded insulin induction comparable to the best shRNAs, thereby also substantiating their on-target activity (Figure S1E). However, due to *Smn1*'s pan-essentiality (Blomen et al., 2015; Dempster et al., 2019), cell viability was severely compromised following one week of full knockout, making clonal selection

impossible, and restricting subsequent experiments to acute shRNA-mediated knockdowns. In summary, these results suggest that strong downregulation of *Smndc1* in murine alpha cells results in stimulation of insulin expression at both the mRNA and protein levels.

SMNDC1 knockdown in human pancreatic islets increases beta-cell markers and insulin secretion

We next sought to verify whether the effects of *Smndc1* knockdown were conserved in human islets. Based on initial testing in HEK293T cells, we identified two promising human SMNDC1-targeting shRNAs (#1 and #3) (Figures S2A and S2B). Lentiviral transduction of intact human islets can be challenging, however, with low levels of viral particles successfully penetrating the inner core of cells (Barbu et al., 2006). Dissociation of the islets into a single cell monolayer can improve efficiency (Walpita et al., 2012), but maintenance of the 3D architecture and cell-cell contacts is preferable for proper functional studies on insulin secretion. We therefore utilized an eGFP-containing shRNA plasmid to facilitate visualization of transduction efficiency. We also included a 3 minute trypsinization step prior to transduction in order to increase accessibility to the core, while keeping the islet structure intact (Jimenez-Moreno et al., 2015). Impressively, we were able to successfully transduce ~60% of cells in this manner, both alpha and beta cells (Figures 2A, 2B and S2C). RT-qPCR analysis on the bulk cells showed successful knockdown of SMNDC1 (Figure 2C). What's more, glucose-stimulated insulin secretion (GSIS) assays revealed that SMNDC1 knockdown not only increased insulin mRNA levels (Figure 2C), but also islet glucose responsiveness, resulting in increased insulin secretion in high glucose conditions (Figure 2D). Glucagon secretion, on the other hand, was largely unaffected (Figure S2D). We repeated these experiments with islets from 3 additional donors, employing both shRNA #1 and #3 (or only #1 in the case of Donor 5). The results we observed were consistent with the initial experiments, including an increase in insulin protein levels upon SMNDC1 knockdown (Figures 2E, 2F, 2G and S2E). We then sorted the successfully transduced GFP positive fractions and conducted transcriptome analyses by RNA-seq. Globally, we observed an increase in almost all the important beta cell genes, with a particularly strong upregulation of MAFA (Figures 2H and S2F). Most importantly, we could also detect a robust increase in PDX1 mRNA levels (Figures 2H and S2F). Also insulin mRNA was consistently upregulated except in islets from donor 3 that exhibited exceptionally high basal insulin levels (Figure S2G). *ABCC8* and *KCNJ11*, two voltage-gated channels at the cell surface with central roles in insulin secretion, were also upregulated upon SMNDC1 knockdown, correlating with the increases in GSIS (Figure 2H). These data reveal that the SMNDC1 knockdown-induced shift towards a more beta cell character is conserved in human islets, with important increases in PDX1 and MAFA mRNA levels (Figure 2H). This further

caused a positive effect on islet function, characterized by increased glucose responsiveness and insulin secretion (Figures 2D, 2E, 2G and S2E).

Smndc1 interacts with proteins involved in splicing and chromatin remodeling

In order to understand Smndc1's function and protein interactions in pancreatic islet cells, we performed immunoprecipitation coupled to mass spectrometry (IP-MS) in both alpha and beta cell lines (Figures 3A, S3A and S3B). In line with its published role as a spliceosome constituent (Talbot et al., 1998), a third of Smndc1's interactome consisted of proteins involved in RNA splicing (Figures 3B, 3C and SFig 3C). Proteins associated with mRNA processing, transport, stabilization and translation also constituted a large part, with 60% of Smndc1's interactors classified as RNA binding proteins (Figures 3B, 3C, S3D and S3E). Less expectedly, a strong enrichment for subunits of the BAF chromatin remodeling complex was also noted (Figures 3B, 3C, S3F and S3G). Particularly the core complex members were strongly enriched in both alpha and beta cells, including the catalytic ATPase Smarca4/Brg1 and the complex unifying scaffolds Smarcc1/BAF155 and Smarcc2/BAF170, along with the important DNA binding subunit Smarce1/BAF57 (Alfert et al., 2019; Wang et al., 1998). In contrast, the enrichment of the Arid subunits appears cell-type specific with Arid1a being enriched in beta cells and Arid1b specifically pulled-down in alpha cells. To assess which of these interactions were direct and which were mediated by co-purifying RNAs, we treated the alpha cell lysate with RNase A and repeated the IP-MS experiment. We found that RNA hydrolysis depleted over half of the Smndc1 interactors (Figure 3D). Strikingly, almost all the protein interactors involved in RNA splicing, translation, stability and localization dropped out, suggesting an mRNA-mediated interaction with Smndc1 (Figures 3E, S3C, S3D and S3E). Remarkably though, BAF complex interaction was unaffected, hinting at a more direct interaction with Smndc1 (Figures 3E and S3F). The BAF complex, specifically the ATPase subunit Smarca2, has previously been associated with splicing factor binding and regulation of alternative splicing (Allemand et al., 2016; Batsché et al., 2006; Patrick et al., 2015), but no direct protein interactor bridging the two pathways has been described. The resilient non-RNA mediated interaction between Smndc1, Smarca4, Smarcc1, Smarcc2 and Smarce1 could be that link.

Smarca4 itself has already been linked to the regulation of insulin expression in beta cells. The BAF complex, specifically the Smarca4 subunit, has been found indispensable in the recruitment of Pdx1 to enhancer and promoter regions of critical beta cell genes such as *Ins2*, *MafA* and *Slc2a2* (McKenna et al., 2015; Spaeth et al., 2019). In order to understand whether this function was conserved in alpha cells and how it related to Smndc1, we concomitantly knocked down Smndc1 and Smarca4. Strikingly, loss of Smarca4 significantly lowered the

increase in insulin expression observed upon Smndc1 knockdown (Figure S4A). Smarca4 has also been found to be bound to the Pdx1 promoter in beta cells (McKenna et al., 2015). Smarca4 ChIP-qPCR experiments in the alpha cell line revealed that Smndc1 knockdown significantly enhanced the presence of Smarca4 at the Pdx1 promoter (Figure S4B). This recruitment appears specific, as no changes were observed at the MafA promoter (Figure S4B). Pdx1 is known to further bind to its own promoter and enhancer regions, regulating a positive feedback loop (Wang et al., 2018b), which could explain the increases in Pdx1 mRNA we observe upon Smndc1 knockdown (Figure 1D).

Smndc1 loss did not greatly affect the protein levels of its interactors, with the exception of two proteins: G3bp2 and Atrx, both found to be significantly decreased (Figure 3F). G3bp2 is chiefly cytoplasmic, whereas Atrx has a nuclear localization more in line with the majority of Smndc1's interactors. Similar to Smarca4, Atrx is a chromatin remodeler with a DNA-dependent ATPase domain of the SWI/SNF-like superfamily of proteins. Moreover, Atrx's interaction with Smndc1 is unaffected by RNase treatment (Figure S3E). This suggests the two proteins are part of a common complex and might regulate similar genes. Due to Atrx's principal presence at sites of heterochromatin and its apparently repressive roles at transcription start sites (Bérubé et al., 2000; Sadic et al., 2015), it could be hypothesized that this regulation involves chromatin silencing of important beta cell genes upstream of insulin. Overall, the proteomics experiments confirmed Smndc1's interactions with the splicing machinery, uncovered a novel interaction with the BAF complex, which seems important in Smndc1's repression of Pdx1 and insulin, as well as an interesting link to gene silencing via Atrx.

Smndc1 regulates Atrx protein levels via alternative splicing

Due to Smndc1's substantial interaction with splicing factors and RNA binding proteins, we reanalyzed our RNAseq datasets for the emergence of alternatively spliced transcripts. We set a threshold for the change in isoform levels (change in *percentage spliced in* or dPSI) of at least 15% to qualify for significantly occurring differentially spliced events (DiffAS). Strikingly, Smndc1 knockdown appeared to stimulate a general retention of introns and skipping of alternatively spliced cassette exons (Figures 4A and 4B). In total, Smndc1 knockdown caused skipping of 805 exons and retention of 392 introns, whereas only 72 exons were more included and 36 introns were more efficiently spliced upon knockdown. We further validated these findings for 20 transcripts by RT-PCR (Figure S5A). Recent observations correlating increases in Smndc1 gene expression with reduced intron retention (Thomas et al., 2020) corroborate our results and together confirm Smndc1's global role in splicing regulation. Stratifying the differential splicing events into their predicted impacts on genes'

ORFs uncovered an expected discrepancy between exons and introns. Intron retention resulted in widespread disruption (DISR) rather than preservation (PROT) of coding sequences, whereas the opposite was true for exon skipping, with a minority of events mapping to non-coding RNAs, 3' and 5' UTRs (Figure 4C). As an example, the *Smndc1* knockdown-induced skipping of *Pax6*'s exon 5a represents a change predicted to not cause a frameshift or nonsense mediated decay (NMD) (Figures 4B and S5B). This is confirmed by our RNAseq and whole cell proteomics datasets, in which no significant changes to *Pax6* levels are observed post-*Smndc1* knockdown (Figure S5C). Interestingly, it was recently discovered that this *Pax6*-5a isoform is significantly enriched in alpha cells and required for *Pax6* binding and transcriptional activation of alpha cell targets genes, such as glucagon and *MafB* (Singer et al., 2019). What's more, inclusion of exon 5a appears to rely on the long non-coding RNA (lncRNA) *Paupar*, whose levels are significantly decreased upon *Smndc1* loss (Figure S5C). Thus, the global depletion in alpha cell genes we observe upon *Smndc1* knockdown (Figures 1C and S1A) could be a consequence of decreased *Pax6* exon 5a inclusion and *Pax6* binding. However, the observed increases in glucagon and insulin protein (Figures 1E and S1C), not noted in strictly *Paupar*-deficient cells (Singer et al., 2019), suggest there is more to the phenotype. As a second example, two retained introns appearing in *Atrx*'s transcripts are predicted to trigger NMD upon intron inclusion (Figures 4B, 4D and S5D), based on the presence of premature stop codons at least 50 nucleotides upstream of the exon–exon junction within the retained intron (Nagy and Maquat, 1998). We observe these retained introns in 15% of sequenced *Atrx* transcripts, which likely underestimates intron retention, given the frequent nuclear and NMD-mediated cytoplasmic degradation of transcripts that retain introns, which is also consistent with the overall reduced *Atrx* expression we observe at both the protein and transcript levels (Figures S1C, 4E, S5E and S5F). Both of *Atrx*'s retained introns are located prior or within its SNF2 domain and would potentially generate truncated protein isoforms lacking ATPase activity and consequent chromatin remodeling ability, even without considering the decrease in mRNA and protein levels predicted to be triggered by NMD (Figures 4D, S5D and S5G). These splicing changes coupled with the significant decrease in both *Atrx*'s total mRNA and protein levels, effectively support a role for *Smndc1* in the regulation of *Atrx* activity. Globally, the events with disruptive effect on ORFs were enriched in genes involved in RNA processing and chromatin modifications (Figure S5H), which are likely to have consequential effects on gene expression. This is in contrast to the events with preserved ORFs, which are mostly enriched for cytoskeletal transport genes (Figure S5I).

In human samples, splicing changes induced by *SMNDC1* knock down correlated remarkably well in islets from donors 3 and 4 (Figures S6A and S6B). In order to distinguish between low

and high confidence events, we focused solely on the ones with a dPSI of at least 10 induced by both of the SMNDC1 shRNAs in the same direction (retention or skipping) ($dPSI > |10|$ and $shRNA = 2$). In islets from donor 5 we observed very few significant splicing changes, therefore we did not further analyze these data. The correlation between the two hairpins in both donors was very strong, suggesting robust on-target effects (Figures 4F and S6C). In total, 471 exons were skipped and 865 introns were spliced out, whereas 825 exons were included and 349 introns were retained between the two donors (Figures 4G and S6D). Intronic splicing changes once again correlated with increased ORF disruption. The global landscape of intron retention and exon skipping observed in murine cells (Figure 4A), however, appeared reversed in human islets, favoring instead intron splicing and exon inclusion (Figure 4H). This is perfectly exemplified by the three highly correlative spliced ATRX introns and two included PAX6 exons in Donor 4 post-SMNDC1 knockdown (HsaINT0015708, HsaINT0015709, HsaINT0015713, HsaEX6001410 and HsaEX6001411) (Figures 4F and S6E). Overall, the 1702 SMNDC1 differentially spliced genes had a similar enrichment profile to the murine genes (Figure S6F). The affected genes were mostly involved in chromatin organization and RNA binding, processing and localization. Importantly, we could observe a significant decrease in ATRX protein levels upon SMNDC1 knockdown in a 6th donor (Figure S7A). Combined with the appearance of ATRX splice isoforms in SMNDC1 deficient human islets (Figure 4F), this confirms that ATRX targeting by SMNDC1 is conserved.

Loss of *Smndc1* and *Atrx* both trigger a global increase in chromatin accessibility and beta cell genes

Smndc1 knockdown caused differential splicing of a large number of additional splicing factors (e.g. *Srsf1*, *Srsf4* and *Rbm5*), most likely propagating its downstream splicing effects. This observation is consistent with previously published cross-regulatory splicing networks that uncovered complex relationships between RNA-binding proteins and exons or introns that they co-regulate (Brooks et al., 2015; Lareau and Brenner, 2015; Papasaikas et al., 2015; Rösel-Hillgärtner et al., 2013; Saha et al., 2017; Saltzman et al., 2011). To isolate the RNAs specifically bound and affected by *Smndc1*, we performed native RNA immunoprecipitation assays followed by RNA-seq in the alpha cell line (Figure 5A). An enrichment in the RNAs of genes involved in chromatin organization and silencing was immediately noticeable (Figures 5A and 5B), further substantiating *Smndc1*'s role in regulating gene expression. Particularly noticeable was the strong interaction with *Atrx* and *Smarca4* mRNAs, as well as *Atrx*'s published interactor macroH2A1 (Ratnakumar et al., 2012). Globally comparing all the genes whose RNAs are significantly bound by *Smndc1*, and upon *Smndc1* loss alternatively spliced and decreased on both total mRNA and final protein levels, yielded only 5 genes (Figure S8A). Out of this list, one single gene was also physically bound by *Smndc1* in IP-MS: *Atrx*. To

discern whether this direct physical proximity with *Smndc1* also phenotypically connects *Atrx* to insulin repression, we knocked down *Atrx* in the alpha cell line (Figures 5C, S5D and S8B). Importantly, loss of *Atrx* on its own was sufficient to induce a significant increase in insulin, *Pdx1* and *MafA* mRNA levels, supporting a contributing role in *Smndc1*'s phenotype (Figure 5C).

To further probe this relationship between *Atrx* and *Smndc1*, we performed ATAC-seq on aTC1 cells transduced with *Smndc1* and *Atrx* shRNAs. Strikingly, loss of either *Atrx* or *Smndc1* triggered a global increase in chromatin accessibility (Figures 5D, 5E and S9A), in line with *Atrx*'s published links to heterochromatin maintenance (Bérubé et al., 2000; Dyer et al., 2017; Sadic et al., 2015). What's more, approximately 50% of the upregulated peaks were shared between the two knockdowns (Figure 5E), supporting the hypothesis that the two proteins are part of a common complex and regulate similar genes. This notion is further strengthened by the lack of discordant peaks between the two knockdowns (Figure S9B), and the maintained correlation when accessibility was compared at the gene-level (Figures 5F and S9C). A large proportion of the upregulated peaks are located at or 10kb prior to genes' transcriptional start sites (TSS) (Figures S9C and S9D), suggesting both knockdowns would influence gene transcription. In effect, when analyzing the 869 genes whose accessibility was increased upon both *Smndc1* and *Atrx* knockdowns, we observe an enrichment for genes involved in transcription, RNA binding and chromatin organization (Figures 5D and 5G). We also observe an enrichment for genes involved in endocrine pancreas development (GO: 0031018), mainly driven by the genes *Nkx6-1*, *Nkx2-2*, *Pax6* and *NeuroD1* (Figures 5D and S10A-D). Interestingly, an enrichment for genes required for stem cell maintenance is also present (Figures 5G and S11A-C). Consistently, when we reanalyzed our RNAseq dataset we found a notable enrichment for totipotency genes (Figure S11D), suggesting an overall increase in cell plasticity upon decrease in either *Smndc1* or *Atrx*.

Stabilization of *Pdx1* mRNA is upstream of *Smndc1* knockdown's increase in insulin transcription

The lack of differential accessibility observed at the *Pdx1* locus upon *Smndc1* or *Atrx* knockdown suggests that factors downstream of transcription might also contribute to the regulation of *Pdx1* mRNA levels. Based on our data, we know (1) *Smndc1* mainly interacts with RNA binding proteins (Figures 2A-C) (2) there is a global enrichment in the accessibility of genes with RNA binding properties upon both *Smndc1* and *Atrx* knockdowns (Figure 5D) and (3) we detect increased BAF complex binding at the *Pdx1* promoter (Figure S4B). Therefore, we could hypothesize that *Smndc1* and *Atrx* knockdowns might trigger differential recruitment of RNA binding proteins to the *Pdx1* locus, including factors involved in mRNA

stabilization and presentation to the translation machinery (Glisovic et al., 2008). We therefore tested whether Pdx1 mRNA stability was affected by Smn1c1 or Atrx. We found that their loss induced a drastic increase in Pdx1 mRNA half-life from less than 1 hour to more than 4 hours, stabilizing the transcript to levels beyond those observed in beta cells (Figure 6A). This effect appeared to be quite Pdx1-specific, as only subtle or non-existent shifts in MafB and MafA mRNA stability were observed (Figure S12A). In fact, loss of Pdx1 completely abolished Smn1c1 knockdown's increase in Ins2 mRNA levels, underlining its essential position in the phenotype (Figure 6B). Smn1c1 knockdown's reliance and evident effects on Pdx1 expression and stability coupled with Pdx1's key role in insulin transcription, prompted us to look at insulin promoter activity. We used an indirect approach, by which we co-transfected alpha cells with Smn1c1 hairpins and an mCherry expression cassette driven by the rat insulin promoter (RIP), which importantly preserves the Pdx1, MafA and NeuroD1 binding sites (Figure 6C). The presence of mCherry signal therefore directly correlates to RIP activation and upregulation of insulin transcription (Figure S13A). Loss of Smn1c1 triggered a positive shift in mCherry expression in a quarter of the cells, relative to empty vector (Figures 6D and S13B). Hence, the increase in Ins2 mRNA observed following Smn1c1 knockdown can be directly attributed to an increase in insulin transcription downstream of the insulin promoter. Sorting out and sequencing the upper and lower quadrants of mCherry-expressing cells firstly revealed differences in the levels of both Smn1c1 and Ins2 in the two populations (Figure 6E). As previously hypothesized, cells that showed stronger insulin induction exhibited also more pronounced Smn1c1 depletion (Figure S13A). Secondly, the RIP-mCherry positive cells showed a significant upregulation in certain genes required for beta-cell function (i.e. Ins1, Slc2a2, Ryr2 and Iapp) not seen in the unsorted population (Figure S13C). Some of these correspond to Pdx1 target genes, substantiating an enrichment in Pdx1 downstream effectors (Figures 6E and 6F). Lastly, the strong overlap in differentially spliced events and the enrichment for the previously observed Atrx and Pax6-5a splice isoforms in the RIP-mCherry-positive population suggest these events are truly Smn1c1-driven and persist in the insulin-positive fraction (Figures S13D and S13E). Summed up, these results propose a mechanism by which Smn1c1 knockdown, via a direct binding to Atrx mRNA, triggers a mis-splicing and decrease of Atrx levels, promoting a global opening of chromatin including increased BAF complex occupancy at the Pdx1 promoter with subsequent Pdx1 mRNA stabilization, overall resulting in increased insulin transcription.

Discussion

Pancreatic beta cells represent the sole source of insulin in the human body. Expression and secretion of insulin is essential for the maintenance of normoglycemia and survival. Hence, there is a drive to generate novel insulin cell sources. To do this, we require a specific understanding of how insulin expression is regulated in beta cells, and how it is silenced in others. Due to the close developmental link between alpha and beta cells, evident via their common Ngn3⁺ progenitor and shared expression of multiple transcription factors, alpha cells represent an excellent candidate for studying the epigenetic mechanisms underlying insulin repression. By targeting over 300 chromatin-associated factors in alphaTC1 cells, we identified Smndc1 as a regulator of insulin silencing in murine alpha cells. We further linked Smndc1 and its function to the chromatin remodellers Smarca4 and Atrx. Atrx is associated with heterochromatin and gene silencing (Bérubé et al., 2000; Goldberg et al., 2010; Sadic et al., 2015; Sarma et al., 2014), while loss of function mutations in alpha cells have been linked to pancreatic neuroendocrine tumour development (Chan et al., 2018; Jiao et al., 2011). Atrx has not, however, been previously associated with the regulation of insulin expression. It is tempting to speculate the Atrx-dependent control of hormone expression in alpha cells might also contribute to tumor formation following Atrx mutation. We found that Smndc1 directly regulates Atrx levels via splicing and that Atrx loss results in upregulation of the key beta cell identity genes *Ins2*, *Pdx1* and *MafA*, as well as increased *Pdx1* mRNA stability. Smarca4 is a core member of the BAF complex, which is a key regulator of gene expression, both via transcriptional activation and repression, with critical roles in lineage specification and cell fate determination (Alfert et al., 2019). In beta cells its presence has been positively linked to insulin, *Pdx1* and *MafA* expression (McKenna et al., 2015). An important part of this function is mediated via binding to the *Pdx1* promoter. What we have identified is that BAF complex binding to the *Pdx1* locus is impeded in alpha cells, in an Smndc1-mediated manner. Together, these results brought us to the conclusion that Smndc1 helps maintain an alpha cell phenotype by limiting insulin transcription, through silencing and destabilization of *Pdx1* mRNA.

Beta cell development and identity are specified by consistent *Pdx1* expression from embryonic to mature cells. *Pdx1* deficiency leads to pancreatic agenesis in both mice and humans, underlining its universal requirement for pancreatic development (Jonsson et al., 1994; Stoffers et al., 1997). Mature beta cell function is equally compromised upon *Pdx1* loss, which triggers forms of mature onset diabetes of the young and type 2 diabetes (Servitja and Ferrer, 2004). This is likely due to decreased expression of *Pdx1* regulated genes *Nr5a2*, *Iapp*, *Slc2a2* and insulin (*Ins1/Ins2*), all important for beta cell development and function (Servitja

and Ferrer, 2004). In line with increased Pdx1 activity, all of these genes are significantly increased in the RIP-mCherry positive dataset. For activation of insulin transcription, Pdx1 cooperates with MafA and NeuroD1, all of which have binding sites on the insulin promoter (Docherty et al., 2005). NeuroD1 is already highly expressed in alpha cells, while Smndc1 knockdown drives the increase in MafA and Pdx1. In turn, MafA and MafB, upregulated in our RIP-mCherry positive cells, further activate Pdx1 expression by binding to its enhancer (Vanhoose et al., 2008). Hence, the increased beta cell character observed upon Smndc1 knockdown is likely triggered by a positive feedback loop between Pdx1 targets and Pdx1 itself.

Pax6, on the other hand, is important for the expression of both alpha and beta cell key genes. Pax6 directly controls the transcription of alpha cell target genes: glucagon, MafB, NeuroD1 and Maf by binding to their promoters in alpha cells (Gosmain et al., 2010). Yet, it is equally important for the maintenance of beta cell identity through direct binding and transcriptional activation of Nkx6-1, MafA and Pdx1 and repression of non-beta cell programs in beta cells (Gosmain et al., 2012; Swisa et al., 2017). It's been hypothesized that this differential binding in alpha and beta cells is due to the presence of different Pax6 isoforms in the two cells, such as the alpha-cell specific Pax6-5a isoform (Singer et al., 2019). Loss of Pax6-5a triggers a transcriptional and functional impairment of alpha cell character through reduced expression and binding of Pax6 to alpha-cell target genes and decreased glucagon secretion. The decrease in Pax6-5a upon Smndc1 knockdown, along with the increased chromatin accessibility and cell plasticity, might therefore flip Pax6 activity in a beta cell direction and contribute to the increases in Pdx1 mRNA stability we observe. Interestingly, Nkx2.2 is significantly downregulated upon Smndc1 knockdown (Figure S8C). No studies have focused on the role of Nkx2.2 in alpha cells, however knockdown in bulk human islets revealed a striking global upregulation of genes (Domínguez Gutiérrez et al., 2016). This suggests Nkx2.2 has a globally repressive nature and, based on this and our own results, could also have a role in the repression of beta cell genes in alpha cells.

Gene expression is heavily reliant on mRNA transcription, processing, stability and ultimate translation. Smndc1's interactome is enriched for proteins involved in mRNA metabolism (Figures 3 and S3). It interacts with Pabpc1, Eif4e and Eif4g, whose mRNA occupancy correlates positively with stability and consequent translational efficiency (Rissland et al., 2017). The spliceosome complex, in turn, communicates the location of exon-exon junctions and premature stop codons to the translation machinery, dictating NMD activation (Moore and Proudfoot, 2009). In fact, approximately 20% of alternatively spliced genes in humans and mice are predicted to yield premature stop codons and trigger NMD (Baek and Green, 2005).

NMD itself is spearheaded by phosphorylation of another SmnDC1 interactor, the RNA helicase UPF1. All 4 Hu proteins: Elavl1, Elavl2, Elavl3 and Elavl4 are equally bound by SmnDC1. Interestingly, Elavl4, also known as HuD, has been linked to insulin mRNA destabilization (Lee et al., 2012). Hence, it is possible that loss of SmnDC1 might redirect the localization and binding of some of these proteins, affecting downstream mRNA stabilizations, namely in Pdx1, and altering global gene expression as we see with the alpha cell transcriptome's shift to a more beta cell character.

Comparisons of our human islet splicing results to our murine data displayed a poor correlation. In general, alternative splice isoforms are not conserved between humans and mice (Modrek and Lee, 2003; Yeo et al., 2005). This is also evident in our dataset, in which less than 20% of the alternatively spliced genes are shared between human and mouse (Figure S6G). Of those, only 2 shared similar events with the same consequent disrupted ontogeny (ALKBH3 and SZRD1). Due to the vastly co-transcriptional nature of mRNA splicing, it stands to reason that alternatively spliced genes should largely correlate with actively transcribed ones. It is important to recognize that due to the co-sequencing of alpha and beta cells in the bulk human islets, it is likely that the overall SMNDC1-mediated alternative splicing profile does not accurately reflect cell-specific regulation by SMNDC1. Differential splice isoforms induced by SMNDC1 knockdown were also much more abundant in Donor 4 (Figures 4F and S6C), with the 40 year age discrepancy between the donors a possible confounding factor (Wang et al., 2018a). Thus, also considering the previously mentioned lack of conservation between human and mouse splice isoforms, direct and specific comparisons between our murine and human splicing datasets can't be confidently conducted.

Importantly, though, we found SmnDC1 knockdown to have a positive effect on bulk human islets, increasing the expression of beta cell specific transcription factors and enhancing insulin secretion (Figure 2). Since we know that we are successfully transducing both alpha and beta cells through co-staining of glucagon and insulin with the GFP vector (Figure S2C), it is presently not possible to confirm whether this is a solely alpha-cell driven phenotype. Major advances have been made in the field of single cell RNAseq (scRNAseq), specifically in droplet-based methods which allow for sequencing of thousands of cells per experiment (Hwang et al., 2018). However, this comes with decreased depth, as previous human islet scRNAseq experiments from our lab on the 10X Chromium platform could not detect SMNDC1 expression (Marquina-Sanchez et al., 2020), which would complicate knockdown efficiency segregation. More sensitive methods such as Smartseq2 show robust SmnDC1 expression in all islet cell types but typically only allow studying fewer cells, making it challenging and expensive to ensure sufficient amounts of alpha and beta cells are sequenced (Ziegenhain et

al., 2017). Hence, to ensure maximum yield and sequencing depth, we focused on bulk human islets and could observe a correlation with the effects in murine alpha cells. Future experiments could focus on whole body effects of *Smndc1* loss, particularly in beta-cell depleted streptozotocin mice. *Smndc1*'s essentiality, ubiquitous expression and robust loss necessary to stimulate insulin expression could, however, pose challenges for *in vivo* testing. One would require a potent, conditional, alpha cell-specific knockdown. While challenging, previous experiments suggest this could be feasible, with knockdown efficiencies of up to 90% achieved depending on the shRNAs (Kleinhammer et al., 2011).

Alternatively, the generation and identification of small molecules targeting *Smndc1* could provide a pulsed and reversible inhibition for facilitated *in vitro* and *in vivo* work. None exist so far, but several inhibitors for other Tudor domain proteins have recently been discovered (Arrowsmith and Schapira, 2019). Work in beta cell stem cell differentiation has benefited from small molecules to improve efficiency of reprogramming (Velazco-Cruz et al., 2020) and might benefit from *Smndc1* inhibition, with its upregulation of *Pdx1* and insulin expression.

The fact that no patients with functional mutations in *SMNDC1* have been identified, nor have any mouse models been generated (<http://www.informatics.jax.org/>), suggest its loss is linked to embryonic lethality. This is unsurprising given its observed essentiality in mature cells. *Smndc1* does however have an extensively more studied paralog, *SMN1* (Survival Motor Neuron 1). They both contain a Tudor domain that recognizes and binds symmetrically dimethylated arginines, in which they share 50% sequence homology (Tripsianes et al., 2011). Loss of function mutations in *SMN1* trigger the severe neuromuscular disorder Spinal Muscular Atrophy (SMA). Studies in SMA murine models and patients revealed they both display fasting hypoglycemia, which has been linked to an islet phenotype of increased glucagon-positive cell mass at the expense of insulin-positive cells (Bowerman et al., 2012; Butchbach et al., 2010). We did not identify a direct protein interaction between *SMNDC1* and *SMN1*, nor any effect on *SMN1* protein or mRNA expression upon *Smndc1* knockdown. Hence, *Smndc1* and *Smn1* appear functionally diverse, with even potentially antagonistic roles on insulin expression. Future studies will need to address the interplay between these two closely related proteins that both affect islet function.

In summary, we identified *Smndc1* as a key new player in the regulation of insulin and *Pdx1* repression in alpha cells. We showed that in murine alpha cells, *Smndc1* prevents the recruitment of the BAF complex to the *Pdx1* promoter and further destabilizes *Pdx1* mRNA. We further confirmed that insulin transcription is turned on upon *Smndc1* knockdown, through activation of a co-transduced rat insulin promoter, and that this is dependent upon the

presence of Pdx1. Lastly, we could demonstrate that loss of SMNDC1 functionally improves bulk human islets by increasing their glucose responsiveness and upregulating genes necessary for insulin secretion and beta cell identity, specifically PDX1.

Materials and Methods

Reagents

Antibodies used were directed against Insulin (Agilent Dako IR00261-2), Smndc1 (Novus Biologicals NBP1-47302 for IP-MS, RIP and western blots; Abcam ab89131 for western blot; Thermo Fisher Scientific PA5-31148 for immunofluorescence), Brg1 (Abcam ab110641), Smarcc1 (Cell Signaling Technology 11956S), Atrx (Atlas Antibodies HPA001906 for western blot; Santa Cruz Biotechnology sc-55584 for immunofluorescence), alpha tubulin (Abcam ab7291), glucagon (Abcam ab92517) and rabbit IgG control (Abcam ab37415). All fluorescently-labelled secondary antibodies were purchased from Thermo Fisher Scientific. HRP-labelled secondary antibodies were bought from Jackson ImmunoResearch. Actinomycin D (BML-GR300-0005) was acquired from Enzo Life Sciences. Smndc1 shRNA #95 (TRCN0000123795) bacterial stock and all primers and oligos were ordered from Sigma.

Cell Culture

The murine alphaTC1 and bTC3 cell lines were obtained from ATCC. The cells were grown in low-glucose DMEM medium (Biowest L0066) supplemented with 10% FBS, 50 U/ml penicillin and 50 µg/ml streptomycin. The Lenti-X™ 293T cell line was purchased from Takara Bio (632180). Cell were grown in high-glucose DMEM medium (Sigma D5796) supplemented with 10% FBS, 1mM sodium pyruvate, 50 U/ml penicillin and 50 µg/ml streptomycin.

Human Islets

	Gender	Age (years)	BMI	HbA1c	Source (via IIDP)
1	Male	32	28.5	5.2	<i>University of Wisconsin</i>
2	Female	33	30.4	4.9	<i>The Scharp-Lacy Research Institute</i>
3	Male	24	23.9	5.0	<i>University of Pennsylvania</i>
4	Male	64	25.5	-	<i>The Scharp-Lacy Research Institute</i>
5	Male	42	37.3	5.6	<i>The Scharp-Lacy Research Institute</i>
6	Male	46	28.1	5.0	<i>The Scharp-Lacy Research Institute</i>

Human islets were obtained through the Integrated Islet Distribution Program (IIDP; NIH Grant # 2UC4DK098085) from approved brain-dead organ donors (JDRF awards 31-2012-783 and 1-RSC-2014-100-I-X). All studies were approved by the Ethics Committee of the Medical University of Vienna (EK-Nr. 1228/2015). No material or information for this study was procured from living individuals.

Human islets were cultured in CMRL medium (Thermo Fisher Scientific 11530037) supplemented with 10% FBS, 1X GlutaMAX™ Supplement (Thermo Fisher Scientific 35050038), 50 U/mL penicillin, and 50 µg/mL streptomycin. Dissociation into single cells for sorting and immunofluorescence was performed using Accutase® solution (Sigma A6964) at 37°C for 20 min, followed by neutralization with CMRL medium.

Gene Knockdowns and Knockouts

All shRNA oligos used in this study were ordered from Sigma based on the TRC shRNA library (<https://portals.broadinstitute.org/gpp/public/>) and subcloned into pLKO.1 (Addgene plasmid #10878)(Moffat et al., 2006) or pLKO.3G (Addgene plasmid #14748) vectors. shRNAs used: Smn dc1 (TRCN0000123795), Smarca4 (TRCN0000071386), Atrx (TRCN0000081911), Pdx1 (TRCN0000086029), ATRX (TRCN0000013592), SMNDC1 #1 (TRCN0000377256), SMNDC1 #2 (TRCN0000001138), SMNDC1 #3 (TRCN0000349546) and SMNDC1 #4 (TRCN0000318422). The Smn dc1-targeting all-in-one Cas9/gRNA vector was also purchased from Sigma (gRNA: GAGCTTGCGAGCGTCTCCGA**AAGG**). Lentiviral production in Lenti-X™ 293T cells was done using Lipofectamine™ 3000 (Thermo Fisher Scientific L3000008) with the second-generation packaging plasmids psPAX2 (Addgene plasmid #12260) and pMD2.G (Addgene plasmid #12259). Cells were transduced with filtered viral supernatant and 8µg/mL Polybrene® (Santa Cruz Biotechnology sc-134220) 50h post-transfection. 48h selection with 2µg/mL puromycin was included for pLKO.1 or gRNA-transduced cells. For pLKO.3G-transduced human islets, islets were dissociated to single cells on Day 5 and sorted for GFP signal on a SH800S Cell Sorter (Sony) with a 100µm chip. Only the top 25% of GFP positive cells from each population was sorted to ensure robust shRNA expression.

pCLX-RIP-mCherry (Addgene plasmid #114310) was co-transfected along with Smn dc1 shRNA into Lenti-X™ 293T cells. 5 days post-transduction, which included a 48h selection with 2µg/mL puromycin, cells were sorted in sorting buffer (PBS, 2% FBS, 4mM EDTA) for mCherry expression on the SH800S Cell Sorter (Sony) with a 100µm chip. Sorted cells were pelleted and RNA extracted using the RNeasy Mini kit (Qiagen).

NanoString Analysis

Hybridized mRNA levels were measured using the NanoString nCounter Analysis System, according to the manufacturer's instructions.

RNA Sequencing Library Preparation

Murine alphaTC1 cells

RNA from three independent biological replicates (unsorted murine alphaTC1) or four independent biological replicates (sorted empty vector, RIP-mCherry positive and negative alphaTC1) was isolated using the RNeasy Mini kit (QIAGEN 74106). Total RNA was quantified using the Qubit 2.0 Fluorometric Quantitation system (Thermo Fisher Scientific) and the RNA integrity number was determined using the Experion Automated Electrophoresis System (Bio-Rad). RNAseq libraries were prepared using the TruSeq Stranded mRNA LT sample preparation kit (Illumina) using Sciclone and Zephyr liquid-handling workstations (PerkinElmer) for pre- and post-PCR steps, respectively. Library concentrations were quantified using the Qubit 2.0 Fluorometric Quantitation system (Life Technologies), with size distribution assessed on the Experion Automated Electrophoresis System (Bio-Rad). Individual samples were diluted and pooled into next-generation sequencing (NGS) libraries in equimolar amounts. 75-bp paired-end sequencing was performed on HiSeq 3000/4000 instruments (Illumina).

Human islets

For the preparation of NGS libraries from low-input samples we followed the Smart-seq2 protocol (Picelli et al., 2014). The subsequent library preparation from the amplified cDNA was performed using the Nextera XT DNA library prep kit (Illumina). Library concentrations were quantified with the Qubit 2.0 Fluorometric Quantitation system (Life Technologies) and the size distribution was assessed using the Experion Automated Electrophoresis System (Bio-Rad). For sequencing, samples were diluted and pooled into NGS libraries in equimolar amounts. 75-bp paired-end sequencing was performed on a HiSeq 3000/4000 instrument (Illumina).

RNA Sequencing Transcriptome Analysis

Raw data acquisition (HiSeq Control Software, HCS, HD 3.4.0.38) and base calling (Real-Time Analysis Software, RTA, 2.7.7) was performed on-instruments, while the subsequent raw data processing off the instruments involved two custom programs based on Picard tools (2.19.2) (<https://github.com/epigen/picard/>, <https://broadinstitute.github.io/picard/>). In a first step, base calls were converted into lane-specific, multiplexed, unaligned BAM files suitable for long-term archival (IlluminaBasecallsToMultiplexSam, 2.19.2-CeMM). In a second step,

archive BAM files were demultiplexed into sample-specific, unaligned BAM files (IlluminaSamDemux, 2.19.2-CeMM).

NGS reads were mapped to the Genome Reference Consortium GRCh38 (human islets) or GRCm38 (alphaTC1 cells) assembly via “Spliced Transcripts Alignment to a Reference” (STAR) (Dobin et al., 2013) utilising the “basic” Ensembl transcript annotation from version e100 (April 2020) as reference transcriptome. Since the hg38/mm10 assembly flavour of the UCSC Genome Browser was preferred for downstream data processing with Bioconductor packages for entirely technical reasons, Ensembl transcript annotation had to be adjusted to UCSC Genome Browser sequence region names. STAR was run with options recommended by the ENCODE project. Aligned NGS reads overlapping Ensembl transcript features were counted with the Bioconductor (3.11) GenomicAlignments (1.24.0) package via the summarizeOverlaps function in Union mode, considering that the Illumina TruSeq stranded mRNA protocol leads to sequencing of the second strand so that all reads needed inverting before counting and that Smart-seq2 does not yield strand-specific data. Transcript-level counts were aggregated to gene-level counts and the Bioconductor DESeq2 (1.28.1) package (<https://bioconductor.org/packages/release/bioc/html/DESeq2.html>) was used to test for differential expression based on a model using the negative binomial distribution.

Biologically meaningful results were extracted from the model, log₂-fold values were shrunk with the CRAN ashr (2.2.-47) package (Stephens, 2017), while two-tailed p-values obtained from Wald testing were adjusted with the Bioconductor Independent Hypothesis Weighting (IHW, 1.16.0) package (Ignatiadis et al., 2016). Downstream data interpretation and visualization was performed using Python plotting package matplotlib (2.2.3; Python 3.7.2).

Gene Ontology and Gene Set Enrichment Analysis

Gene Ontology (GO) annotations were identified using GO Enrichment Analysis (Mi et al., 2019). They are stated in each figure with their corresponding number in brackets. TRRUST transcription factor enrichments were found using ENRICH (Xie et al., 2021). For Gene Set Enrichment Analysis (GSEA), genes whose differential expression with DESeq2 post-Smndc1 knockdown had an adjusted p-value of ≤ 0.05 were ranked according to log₂(Fold Change). The ranked GSEA was performed using GenePattern’s “GSEAPreranked” module (<https://cloud.genepattern.org/>) using our in house or published (Lawlor et al., 2017) murine alpha and beta cell gene sets.

RT-qPCR

RNA was isolated using the RNeasy Mini kit (Qiagen 74106). The amount of RNA per sample was quantified using a NanoDrop 1000 Spectrophotometer (Thermo Fisher Scientific), ensuring a 260/280 ratio ≥ 2 . Normalized RNA amounts were reverse transcribed using the LunaScript[®] RT SuperMix Kit (NEB E3010). Quantitative real-time PCR was performed using Luna[®] Universal qPCR Master Mix (NEB M3003) on a LightCycler[®] 480 real-time PCR system (Roche). Data were normalized to the housekeeping gene GAPDH and relative expression was quantified using the comparative $2^{-\Delta\Delta CT}$ method. All RT-qPCR experiments detailed in this study are representative of 3 biological replicates and 2 technical replicates. All primers used can be found in Table S3.

Co-Immunoprecipitation and Western Blotting

Murine alphaTC1 and betaTC3 cells were lysed in plate for 20mins on ice in freshly prepared IP lysis buffer: 50mM HEPES pH 8.0, 150mM NaCl, 5mM EDTA, 0.5% NP-40, 50mM NaF, 1.5mM Na₃VO₄, 1.0mM PMSF, and protease inhibitor cocktail (Roche). The resultant suspension was centrifuged at 14,000g for 30mins at 4°C. Supernatant protein concentrations were measured using the Pierce[™] BCA Protein Assay Kit (Thermo Fisher Scientific 23225). If treating with RNase A, lysates were then incubated with 200µg/mL RNase A for 20mins rotating at room temperature. 150µl Dynabeads[™] Protein G (Thermo Fisher Scientific 10003D) were washed with 2 x 1mL IP lysis buffer prior to 10mins rotating incubation at room temperature with 11µg Smndc1 antibody or no antibody control. Bead-antibody complexes were washed with 2 x 1mL IP lysis buffer and incubated with 2mg of whole cell lysate for 4 hours rotating at 4°C. Some supernatant was retained post-IP for western blot analysis. Beads were washed with 3 x 1mL IP lysis buffer followed by 2 x 1mL IP wash buffer: 50 mM HEPES pH 8.0, 150 mM NaCl, and 5 mM EDTA to remove NP-40. If lysates were RNase-treated, 200µg/mL RNase A was added to the first three IP lysis buffer washes. Bound proteins were eluted with 150µl 2% SDS elution buffer: 50 mM HEPES, pH 8.0, 150 mM NaCl, 5 mM EDTA, and 2% SDS in a 20-minute rotating room temperature incubation. 15µl were removed for western blot analysis and the remaining samples were frozen at -20°C until further processing.

For western blot analysis, inputs, supernatants and eluates were loaded onto an SDS–polyacrylamide gel and then transferred by electrophoresis to a nitrocellulose membrane (GE Healthcare Life Science). All the blots were incubated with corresponding primary antibodies diluted 1:1000 in 5% milk at 4 °C overnight and in HRP-labeled secondary antibodies diluted 1:20000 for 1h at RT. The signals were detected using Clarity ECL Western Blotting Substrate (Bio-Rad) on a ChemiDoc MP Imaging System (Bio-Rad).

LC-MS/MS Analysis of Smndc1 Co-IP Samples

Sample Preparation

IP eluates were prepared for LC-MS/MS analysis using a modified Filter Assisted Sample Preparation (FASP) procedure (Wiśniewski et al., 2009). Samples were heated to 99°C for 5 min. FASP was performed using a 30 kDa molecular weight cutoff filter (VIVACON 500; Sartorius Stedim Biotech GmbH). 50µL of each cleared protein extract was mixed with 200µL of freshly prepared 8M urea in 100mM Tris-HCl (pH 8.5) (UA-solution) in the filter unit and centrifuged at 14,000g for 15 min at 20°C to remove SDS. Any residual SDS was washed out by a second washing step with 200µL of UA. The proteins were alkylated with 100µL of 50mM iodoacetamide in the dark for 30 min at RT. Afterward, three washing steps with 100µL of UA solution were performed, followed by three washing steps with 100µL of 50mM TEAB buffer (Sigma-Aldrich). Proteins were digested with 1.25µg trypsin overnight at 37°C. Peptides were recovered using 40µL of 50mM TEAB buffer followed by 50µL of 0.5M NaCl (Sigma-Aldrich). Peptides were desalted using C18 solid phase extraction spin columns (The Nest Group), organic solvent removed in a vacuum concentrator at 45°C and reconstituted in 5% formic acid and stored at -80°C until LC-MS/MS analysis.

LC-MS/MS

Liquid chromatography mass spectrometry of SMNDC1 precipitated samples was performed on a Q Exactive™ Hybrid Quadrupole-Orbitrap (ThermoFisher Scientific, Waltham, MA) coupled to a Dionex U3000 RSLC nano system (Thermo Fisher Scientific, San Jose, CA) via nanoflex source interface. Tryptic peptides were loaded onto a trap column (Acclaim™ PepMap™ 100 C18, 3µm, 5 × 0.3 mm, Thermo Fisher Scientific) at a flow rate of 10µL/min using 0.1% TFA as loading buffer. After loading, the trap column was switched in-line with a 40 cm, 75µm inner diameter analytical column (packed in-house with ReproSil-Pur 120 C18-AQ, 3µm, Dr. Maisch). Mobile-phase A consisted of 0.4% formic acid in water and mobile-phase B of 0.4% formic acid in a mix of 90% acetonitrile and 10% water. The flow rate was set to 230nL/min and a 90 min gradient used (4 to 24% solvent B within 82 min, 24 to 36% solvent B within 8 min and, 36 to 100% solvent B within 1 min, 100% solvent B for 6 min before re-equilibrating at 4% solvent B for 18 min). For the MS/MS experiment, the Q Exactive™ MS was operated in a top 10 data-dependent acquisition mode with a MS¹ scan range of 375 to 1,650 m/z at a resolution of 70,000 (at 200 m/z). Automatic gain control (AGC) was set to a target of 3×10E6 and a maximum injection time of 55ms. MS²-scans were acquired at a resolution of 15,000 (at 200 m/z) with AGC settings of 1×10E5 and a maximum injection time of 110 ms. Precursor isolation width was set to 1.6 Da and the HCD normalized collision energy to 30%. The threshold for selecting precursor ions for MS² was set to 1.8×10E4. Dynamic exclusion for selected ions was 90 sec. A single lock mass at m/z 445.120024 was

employed (Olsen et al). All samples were analysed in duplicates, back-to-back replicates. XCalibur version 4.1.31.9 and Tune 2.9.2926 were used to operate the instrument.

LC-MS/MS Analysis of Smndc1 Knockdown Whole Cell Proteomics

Sample Preparation

Each washed cell pellet was lysed separately in 40 μ L of freshly prepared lysis buffer containing 50mM HEPES (pH 8.0), 2% SDS, 0.1M DTT, 1mM PMSF and protease inhibitor cocktail (Sigma-Aldrich). Samples rested at RT for 20 minutes before heating to 99°C for 5 min. After cooling down to RT, DNA was sheared by sonication using a Covaris S2 high performance ultrasonicator. Cell debris was removed by centrifugation at 20,000g for 15 min at 20°C. Supernatant was transferred to fresh Eppendorf tubes and protein concentration determined using the BCA protein assay kit (Thermo Fisher Scientific). A total of 200 μ g protein per sample was processed for LC-MS/MS analysis using an adapted Single-pot solid-phase-enhanced sample preparation (SP3) methodology (Hughes et al., 2019). In short, equal volumes (125 μ L/ 6250 μ g) of two different kind of paramagnetic carboxylate modified particles (SpeedBeads 45152105050250 and 65152105050250, GE Healthcare) were mixed, washed three times with 250 μ L water and reconstituted to a final concentration of 50 μ g/ μ L with LC-MS grade water (LiChrosolv, MERCK). SDS-containing samples from the immunoprecipitation step were reduced with a final concentration of 50mM DTT and incubated at 60°C for 1 hour. After cooling down to room temperature, reduced cysteins were alkylated with iodoacetamide at a final concentration of 55mM for 30 min in the dark. For tryptic digestion, 40 μ g of mixed beads were added to reduced and alkylated samples, vortexed gently and incubated for 5 minutes at room temperature. The formed particles-protein complexes were precipitated by addition of acetonitrile to a final concentration of 70% [V/V], mixed briefly before incubating for 18 minutes at room temperature. Particles were then immobilized using a magnetic rack (DynaMag™-2 Magnet, Thermo Fisher Scientific) and supernatant discarded. SDS was removed by washing two times with 200 μ L 70% ethanol and one time with 180 μ L 100% acetonitrile. After removal of organic solvent, particles were resuspended in 100 μ L of 50mM NH₄HCO₃ and samples digested by incubating with 1 μ g of Trypsin overnight at 37°C. Peptides were cleaned up by acidifying the samples to a final concentration of 1% TFA prior to immobilizing the beads on the magnetic rack to perform solid phase extraction of the recovered supernatant using C18 SPE columns (SUM SS18V, NEST group, USA) according to the manufacturer. Peptides were eluted using two times 50 μ L 90% Acetonitrile, 0.4% formic acid, dried in a vacuum concentrator before reconstitution in 40 μ L of 0.1% TFA (Suprapur, MERCK).

LC-MS/MS

Label-free 1D-shotgun LC-MS/MS analysis of whole cell extracts was performed on an Orbitrap Fusion Lumos mass spectrometer (ThermoFisher Scientific) coupled to a Dionex Ultimate 3000RSLC nano system (ThermoFisher Scientific) via nanoflex source interface. Approximately 1 µg of total peptide was loaded onto a trap column (Pepmap 100, 5 µm, 5 × 0.3mm, ThermoFisher Scientific) at a flow rate of 10 µL/min using 0.1% TFA as loading buffer. After loading, the trap column was switched in-line with a 50cm, 100 µm inner diameter analytical column (packed in-house with ReproSil-Pur 120 C18-AQ, 2.4 µm, Dr. Maisch) at 50°C. Mobile-phase A consisted of 0.4% formic acid in water and mobile-phase B of 0.4% formic acid in a mix of 90% acetonitrile and 10% water. The flow rate was set to 300 nL/min and a 210 min gradient used (4 to 7% solvent B within 1 min, 7 to 24% solvent B within 190 min, 24 to 36% solvent B within 8 min, 36 to 100% solvent B within 1 min and, 100% solvent B for 10 min before equilibrating at 4% solvent B for 18 min). MS acquisition consisted of an untargeted Data Dependent Acquisition (DDA). Full MS scans were acquired with a mass range of 375 – 1650 m/z in the Orbitrap at a resolution of 120,000 (at 200 m/z of 200). Automatic gain control (AGC) was set to a target value of 4 × 10⁵ and a maximum injection time of 50 msec. Precursor ions for MS₂ analysis were selected using a TopN dependant scan approach with a cycle time of 3 sec. MS₂ spectra were acquired in the linear ion trap (IT) using rapid scan speed and a quadrupole isolation window of 1.6 Da. Higher energy collision induced dissociation (HCD) was applied with a normalized collision energy (NCE) of 30%. AGC target was set to 1 × 10⁴ and a maximum injection time of 25 msec. Peptide monoisotopic precursor selection (MIPS) was enabled including peptide charge states of 2-6 with an intensity threshold for precursor selection set to 5 × 10³ and a dynamic exclusion for selected ions set to 90 sec. A single lock mass at m/z 445.120024 was employed (Olsen et al., 2005). XCalibur version 4.3.73.11 and Tune 3.3.2782.28 were used to operate the instrument.

MS Data Analysis

Acquired raw data files were processed using the Proteome Discoverer 2.4.1.15 platform, utilising the database search engine Sequest HT. Percolator V3.0 was used to remove false positives with a false discovery rate (FDR) of 1% on PSM, peptide and protein level under strict conditions. Searches were performed with full tryptic digestion against the mouse SwissProt database v2017.10.25 (25,097 sequences plus 298 appended known contaminants) with up to two miscleavage sites. Oxidation (+15.9949 Da) of methionine, deamidation (+0.9840 Da) of arginine and glutamine as well as phosphorylation (+79.9663 Da) of serine, threonine or tyrosine was set as variable modification, whilst carbamidomethylation (+57.0214 Da) of cysteine residues was set as fixed modifications. Data

was searched with mass tolerances of ± 10 ppm and 0.6 Da on the precursor and fragment ions, respectively. Results were filtered to include peptide spectrum matches (PSMs) with Sequest HT cross-correlation factor (Xcorr) scores of ≥ 0.9 and high peptide confidence. For calculation of protein areas, Minora Feature Detector node and Precursor Ions Quantifier node, both integrated in Thermo Proteome Discoverer were used. Automated chromatographic alignment and feature linking mapping were enabled with total peptide amount used for normalization between individual runs. Protein abundances were calculated using sum intensities of respective peptide features including only unique peptide groups. Protein ratios were generated using the non-nested approach and p-values calculation was performed applying t-test and Benjamini-Hochberg correction. Identification of significant interactors and fold changes for Smndc1 IP-MS results was done through Resource for Evaluation of Protein Interaction Networks (REPRINT) using SAINT scoring (<https://reprint-apms.org/>)(Mellacheruvu et al., 2013).

Glucose Stimulated Insulin Secretion Assay

Intact human islets were incubated in low glucose (0.3 g/L glucose) KRB buffer for one hour followed by high glucose (3 g/L glucose) KRB buffer for another hour. Supernatants after both the low and high glucose challenges were collected to measure insulin content using a Human Insulin ELISA kit (Alpco 80-INSHU-E01.1). Supernatant volumes were normalized to total protein or RNA. All results are representative of 2 technical replicates.

Intracellular Insulin Protein Measurements

Whole cell extracts were generated by lysing cells in Triton lysis buffer containing 150 mM sodium chloride, 1mM EDTA, 1.0% Triton X-100 and 50 mM Tris, pH 7.4 supplemented with Protease Inhibitor Cocktail (Roche) and total protein levels quantified using a Pierce™ BCA Protein Assay Kit (Thermo Fisher Scientific 23225) to facilitate normalization of replicates to total protein. Intracellular insulin levels were then measured using an Ultrasensitive Mouse Insulin ELISA kit (Alpco 80-INSMSU-E01).

Immunofluorescence

Cells were fixed in 3.7% formaldehyde for ten minutes at room temperature, permeabilized with 0.2% Triton X-100 in PBS (PBST) for 30 minutes and blocked with PBST supplemented with 5% goat serum, 5% donkey serum and 1% BSA for 1 hour. Incubation with primary antibodies, diluted in blocking buffer, was done overnight at 4°C. After 3 x 5-minute PBST washes, cells were incubated at room temperature for 1 hour with fluorescently-labeled secondary antibodies, diluted 1:500 in PBST, and 5µg/mL Hoechst 33342. Cells were washed with PBST for 3 x 5 minutes and stored at 4°C in the dark until analysis.

Images were taken using an automated microscope (Perkin Elmer Operetta) using a 20X objective. Images were exposed for 50ms in the Hoechst channel and 200ms in Alexa Fluor 488 and 546 channels. Images were analyzed using the Harmony software. Nuclei were identified by Harmony Method C and cytoplasm was defined based on the nuclei (Harmony Method C). For higher resolution images (Figure 1E), cells were imaged with a 63X objective on an LSM700 laser scanning confocal microscope (Carl Zeiss Optics).

Splicing Analysis

Alternative splicing was quantified using VAST-TOOLS v2.5.1 (Irimia et al., 2014; Tapial et al., 2017) and the following species databases: *M. musculus* (species code mm10/Mm2, based on GRCm38.p5 Ensembl v88; vastdb.mm2.23.06.20) and *H. sapiens* (species code hg38/Hs2, based on GRCh38.p10 Ensembl v88; vastdb.hs2.23.06.20). Briefly, VAST-TOOLS fragments reads into 50nt read groups of which one random sub-read is used for quantification to avoid counting bias. 50nt reads are then aligned to a reference genome and mapped to splice junction database. Alternative splicing events were called differential if a given event was supported by at least LOW read threshold (—noVLOW), had non-overlapping PSI distribution between two sample groups (—min_range 5) and minimum absolute dPSI of 10 or 15 —min_dPSI 10/15, as specified in text). For more details on methods, read threshold and commands, refer to VAST-TOOLS page (<https://github.com/vastgroup/vast-tools>).

For the PCR validations, primers were ordered as suggested on vastdb.crg.eu. 200ng of cDNA was amplified for 30 cycles using OneTaq[®] Quick-Load 2X Master Mix (NEB M0486).

RNA Immunoprecipitation

Protocol was adapted from a previous publication (Rissland et al., 2017). Briefly, cells were washed twice with ice cold PBS and incubated for 10 minutes on ice in 2mL Lysis Buffer A: 100mM KCl, 0.1mM EDTA, 20mM Hepes pH 7.5, 0.4% NP-40, 10% glycerol and freshly added 20U/mL RNase inhibitor (Takara Bio 2313A), 1mM DTT and protease inhibitor cocktail (Roche). After centrifugation, cleared lysates were incubated with Smndc1 or IgG control antibodies for 1 hour rotating at 4°C. Following 3 washes with Lysis Buffer A, Dynabeads[™] Protein G (Thermo Fisher Scientific) were added to the lysate-antibody mixture for an additional 1 hour rotating at 4°C. For 5 x 10⁶ cells: 100µl beads and 5µg antibody was used. Beads were washed 3 times with Lysis Buffer A, resuspended in 1mL TRIzol[™] reagent (Thermo Fisher Scientific 15596026) and RNA extracted according to the manufacturer's guidelines. RNA was eluted in 50µl RNase-free water and cleaned up using the RNeasy Mini kit (Qiagen). Experiments are representative of three biological replicates.

ATAC-seq

Protocol was performed on three individual biological replicates according to a previous publication (Schick et al., 2019). Reads were aligned to the mm10 genome with bowtie2. Peaks were called using macs2, uniquely mapped read counts were obtained for consensus peaks using samtools and bedtools. Consensus region annotation was performed with Homer, and Urope using Ensembl regulatory build (version GRCm38) and GENCODE annotation (vM25). A Snakemake workflow developed at CeMM was used for these tasks, available at https://github.com/sreichl/atacseq_pipeline.

Differential expression analysis was carried out with DESeq2 on raw count data. Here, differing FRiP (fraction of reads in pairs) values across replicates were adjusted for by specifying FRiP as a covariate in the design formula. Differential regions were defined as having an adjusted p-value <0.1. All peaks were assigned to their closest gene based on genomic distance. Representative fold changes were obtained for each gene by calculating the maximum absolute log₂(fold change) value across all peaks assigned to a gene. Gene Ontology (GO) enrichment analysis (Mi et al., 2019) was performed at the gene level, discarding genes with discordant peaks, i.e. genes with peaks with both negative and positive log₂(fold change) values.

For each sample, genome browser tracks in bigWig format were generated using deepTools bamCoverage tool (Ramírez et al., 2016) from BAM files merged with samtools. Coverage heatmaps around TSS sites were generated with deepTools plotHeatmap tool for all ENSEMBL transcripts of genes with significant peaks. Browser tracks were visualized using Integrative Genomics Viewer (IGV) browser.

ChIP-qPCR

Cells were fixed and chromatin isolated as previously described (Schick et al., 2019). Chromatin was sheared in sonication buffer: 50mM Tris-HCl pH 8.0, 10mM EDTA, 1% SDS, 1x protease inhibitor cocktail, on a Bioruptor[®] Pico (Diagenode) in 2 rounds of 10 minutes on ice followed by 10 cycles (30s ON/30s OFF). After centrifugation, the supernatant was diluted 1:10 in dilution buffer: 20mM Tris-HCl pH 8.0, 1mM EDTA, 167mM NaCl, 1% Triton X-100, 0.01% SDS, 1x protease inhibitor cocktail to reduce the final SDS concentration. Antibody and bead incubations, washes and decrosslinking were performed as previously described (Schick et al., 2019). DNA was extracted using the QIAquick PCR Purification kit (Qiagen) and RT-qPCR was performed using Luna[®] Universal qPCR Master Mix (NEB M3003) on a LightCycler[®] 480 (Roche). The PCR primers used corresponded to MafB site1, Pdx1 Area I, MafA R3 and

Albumin's distal TAAT-containing region as previously published (McKenna et al., 2015). Experiments are representative of three independently isolated chromatin preparations.

mRNA Stability Measurements

Cells were cultured with 50µg/mL Actinomycin D (Enzo Life Sciences) for the specified time intervals, pelleted and RNA extracted using the RNeasy Mini kit (Qiagen). RT-qPCR results were normalized to the housekeeping gene GAPDH and relative expression to time point zero was quantified using the comparative $2^{-\Delta\Delta CT}$ method. Results are representative of three biological replicates and two technical replicates.

Statistical Analysis

Data is presented as mean \pm SD or SEM, except for RT-qPCR results presented as \pm fold change range. The number of independent experiments is indicated. Unless otherwise specified, three independent biological replicates were performed per experiment. Statistical comparisons, independent of sequencing or proteomics data, were performed using paired or unpaired two-tailed Student's t tests and results are indicated in the individual figures (*ns* = $p > 0.05$; * $p \leq 0.05$; ** $p \leq 0.01$; *** $p \leq 0.001$; **** $p \leq 0.0001$).

Acknowledgements

We thank CeMM's Biomedical Sequencing Facility and Proteomics and Metabolomics Facility for their generation and processing of our RNA sequencing and proteomics data. We are also grateful to Stuart L. Schreiber for his assistance in the initial RNA interference screen and to Juan Valcárcel for his splicing expertise. This work was supported by JDRF grants 3-SRA-2015-20-Q-R and 17-2011-258. Research in the Kubicek lab is supported by the Austrian Federal Ministry for Digital and Economic Affairs and the National Foundation for Research, Technology, and Development, the Austrian Science Fund (FWF) F4701 and the European Research Council (ERC) under the European Union's Horizon 2020 research and innovation program (ERC-CoG-772437).

Author Contributions

T.C. and S.K. planned the study and designed the experiments; T.C. performed the experiments; T.C., J.R., M.S., A.M. and S.B. analyzed the data; T.C. and S.K. wrote the manuscript with input from all coauthors; C.B., B.K.W., and S.K. supervised the work.

Conflict of Interest

The authors declare no conflict of interest.

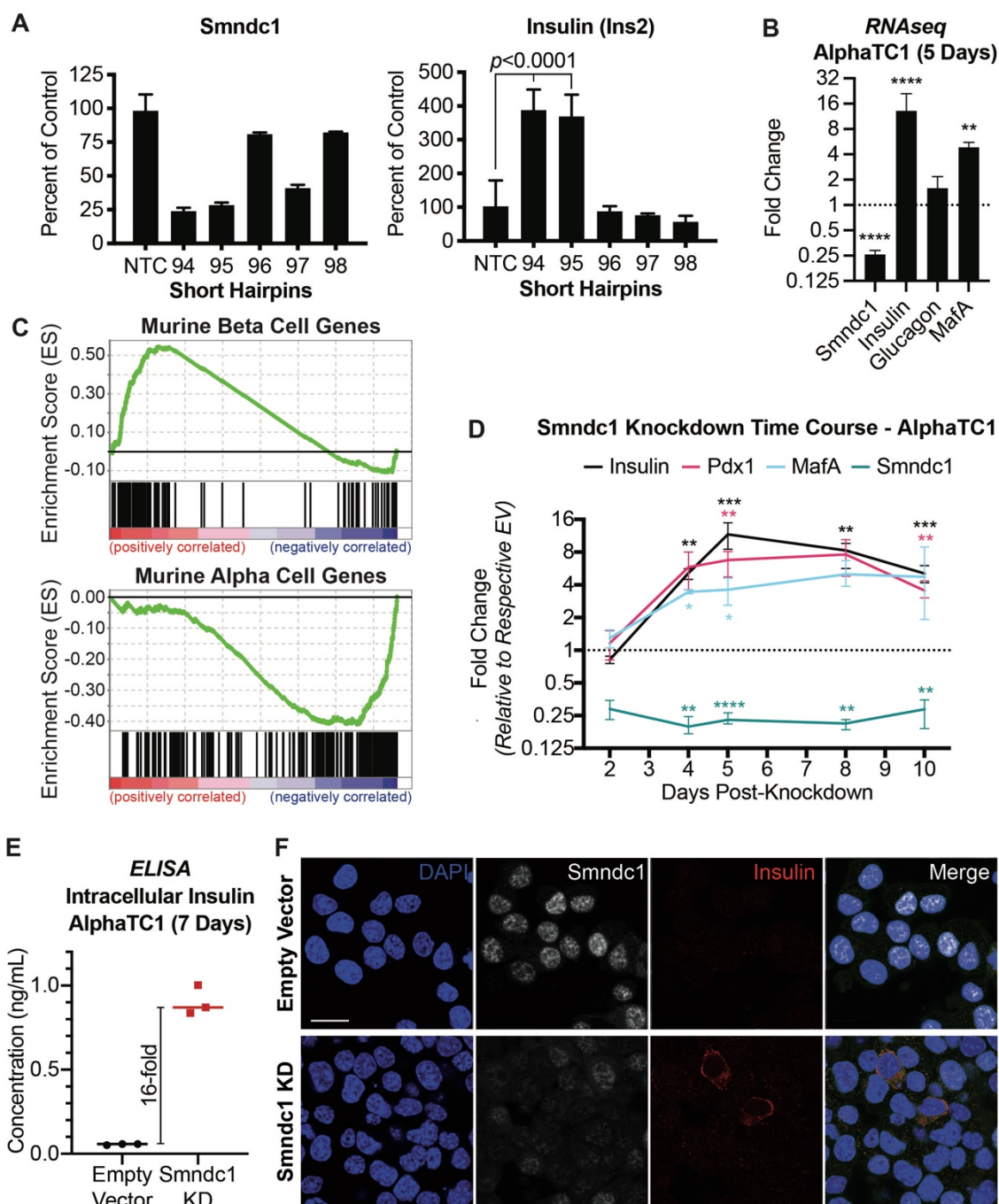


Figure 1 SmnDC1 knockdown triggers an upregulation of insulin mRNA and protein in murine alphaTC1 cells

(A) Bar graph representations of the SmnDC1-targeting hairpins, highlighting the significant SmnDC1 knockdown and consequent insulin upregulation in hairpins #94 and #95. (B) RNAseq results after 5-day SmnDC1 knockdown (hairpin #95) in 3 biological replicates of murine alphaTC1 cells, represented as fold change relative to empty vector control. (C) Gene set enrichment analysis (GSEA) for genes significantly differentially expressed post-SmnDC1 knockdown. The ranked list was compared to the top 1000 most significantly differentially

expressed genes between alphaTC1 and Min6 cells from in house datasets (Table S2). **(D)** RT-qPCR of *Smndc1* knockdown time course, testing mRNA levels of Insulin (black), *Pdx1* (magenta), *MafA* (light blue) and *Smndc1* (teal). **(E)** Insulin protein levels in whole cell lysates of murine alphaTC1 cells 7 days post-*Smndc1* knockdown vs. empty vector control. Measured by ELISA. **(F)** Immunofluorescence panel of murine alphaTC1 cells 5 days after transduction with *Smndc1* shRNA or empty vector control. White = *Smndc1*, red = insulin and blue = DAPI. Scale bar = 10 μ m.

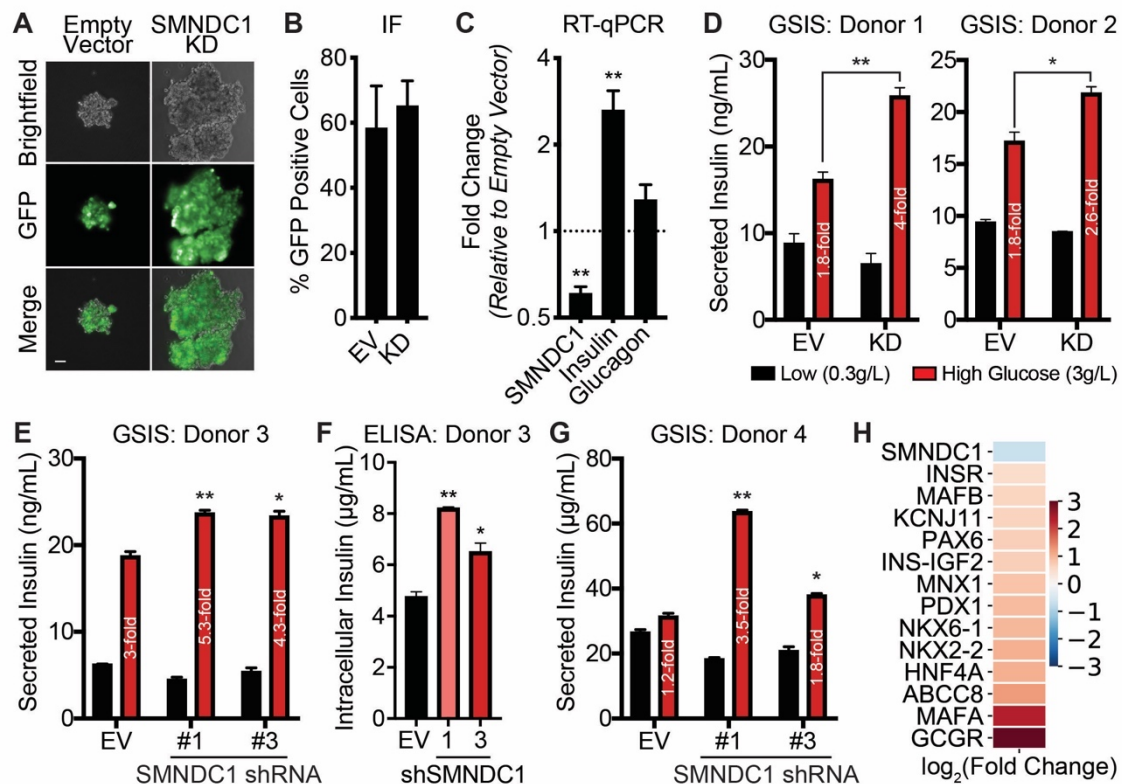
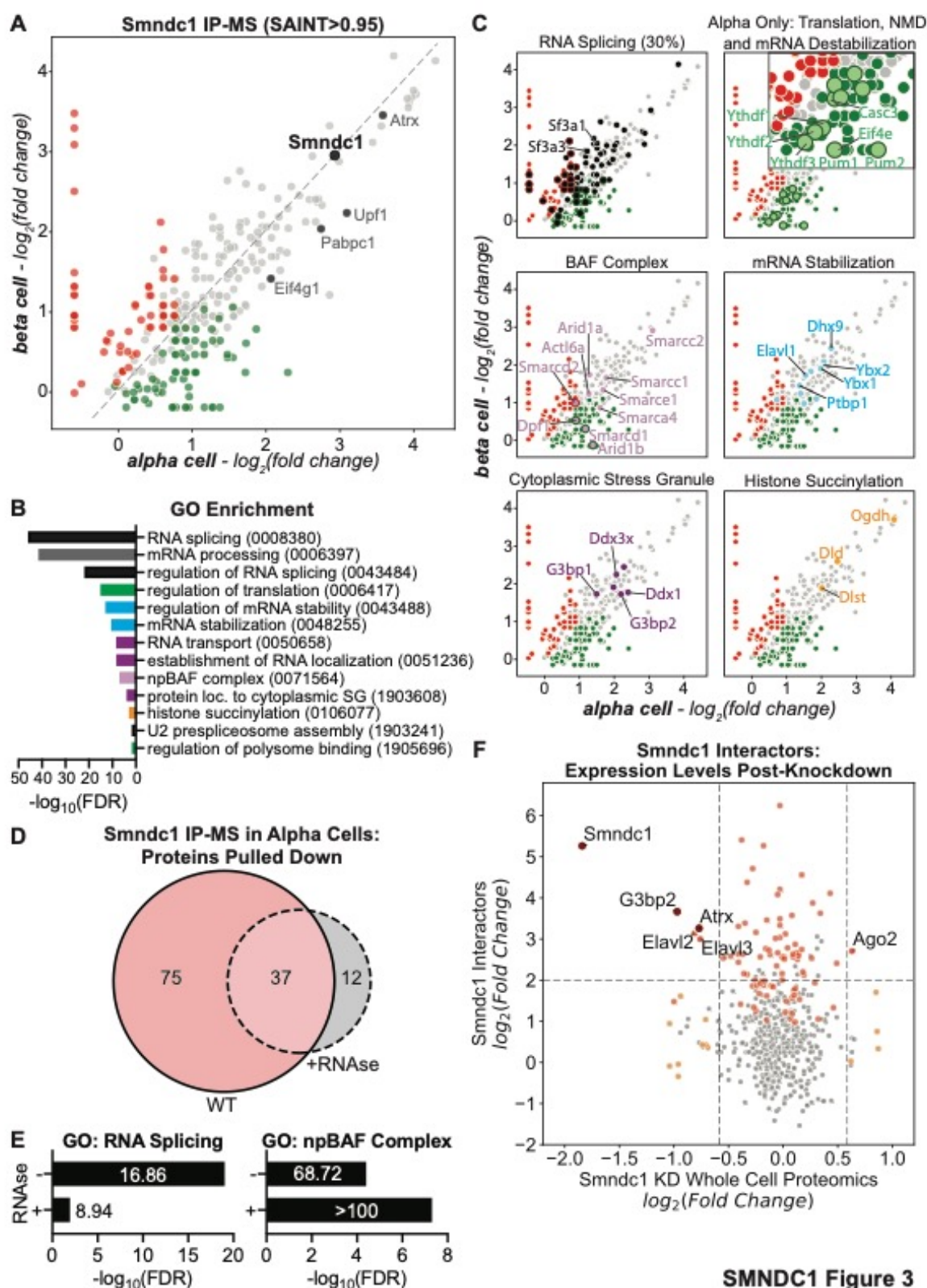


Figure 2 Insulin secretion is enhanced in human islets with decreased SMNDC1 expression

(A) Live imaging of intact human islets 4 days after transduction with GFP co-expressing pLKO.1 shRNA vector. Scale bar = 10 μ m. **(B)** Quantification of GFP⁺ cell number after dissociating the islets into single cell monolayers. **(C)** RT-qPCR on the unsorted bulk human islets from donors 1 and 2, 5 days post transduction with SMNDC1 shRNA #3 relative to empty vector. N=2. **(D)** ELISA on supernatants of unsorted, transduced, human islets from donors 1 and 2 post-glucose stimulated insulin secretion (GSIS) assay. EV = empty vector; KD = + SMNDC1 shRNA #3. **(E)** ELISA GSIS results from donor 3. **(F)** ELISA on whole cell lysate of unsorted, transduced, human islets from donor 3. **(G)** ELISA GSIS results from donor 4. **(H)** Heatmap of RNAseq results from bulk, sorted human islets from donors 3,4 and 5, 5 days post-transduction. All represented genes have a significant adjusted p-value of ≤ 0.05 .



SMNDC1 Figure 3

Figure 3 SMNDC1 protein interactome reveals enrichment for chromatin remodelers

(A) Endogenous Smndc1 immunoprecipitation coupled to mass spectrometry (IP-MS) results from the average of 2 replicates of murine alphaTC1 vs. betaTC3 cells. Only significant interactors, quantified as having a SAINT score greater than 0.95, are mapped. Smndc1 is

highlighted along with genes involved in mRNA processing and NMD (Eif4g1, Pabpc1, Upf1). **(B)** Gene ontology (GO) enrichment for Smn1's interactors shared by both murine alpha and beta cell lines. **(C)** Separate scatter plots of IP-MS results highlighting the enriched subclasses of proteins. **(D)** Number of proteins significantly differentially enriched by Smn1 antibody +/- RNase A treatment. **(E)** Bar graphs highlighting depleted enrichment for proteins with RNA splicing gene ontology post-RNase A treatment, and contrasting increase in fold enrichment for npBAF complex members. **(F)** Smn1 IP-MS vs. Smn1 knockdown whole cell proteomics results. Red colors represent proteins significantly pulled down in IP-MS (SAINT > 0.95). Orange depicts proteins whose expression was significantly altered upon Smn1 knockdown. Dark red are the proteins significant to both datasets. Dashed lines highlight proteins with a strong Smn1 interaction (≥ 4 -fold over IgG control), or at least 1.5-fold differential expression post-Smn1 knockdown relative to empty vector control.

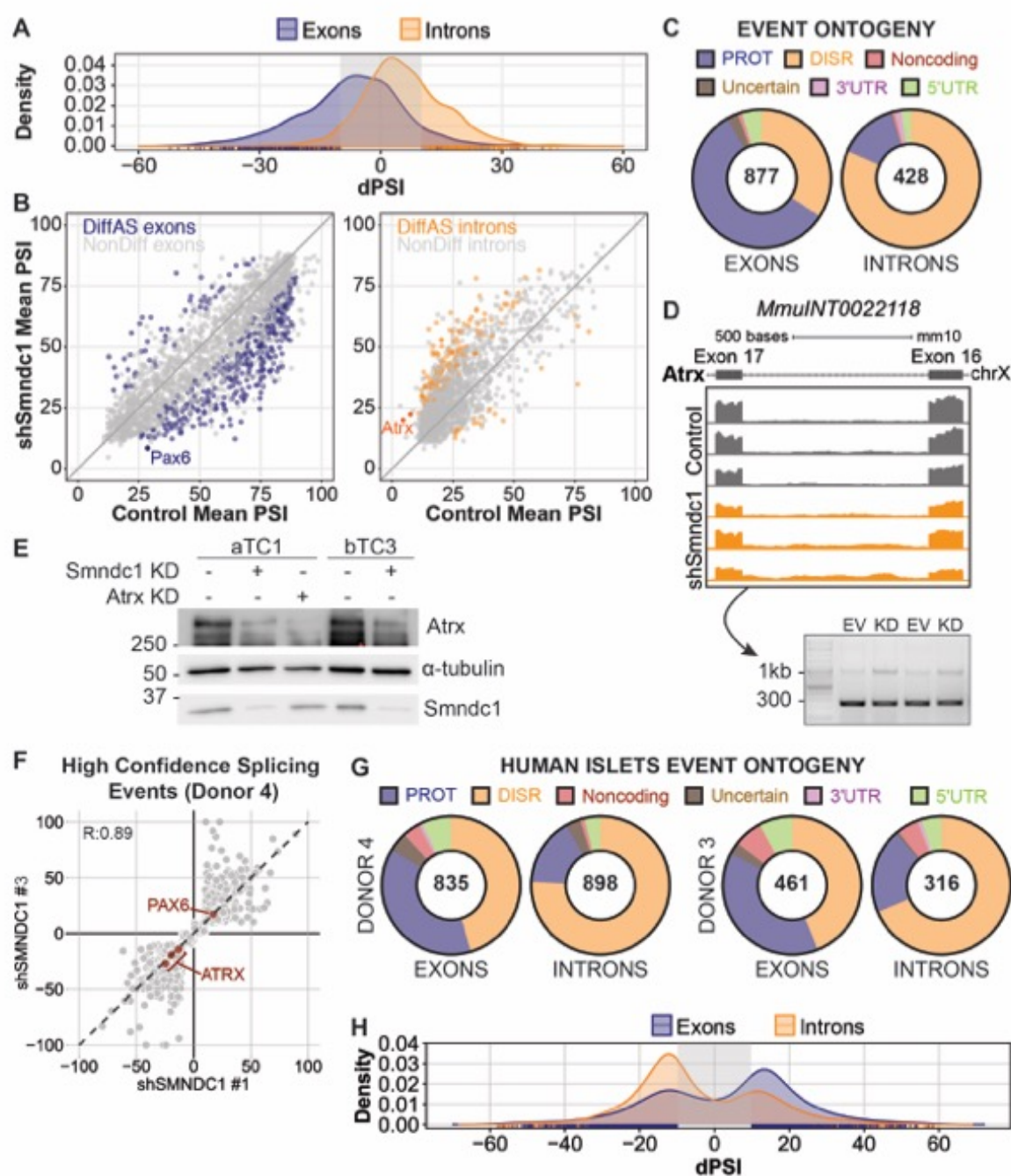


Figure 4 Widespread emergence of alternative splice isoforms upon Smndc1 knockdown include a disrupted Atrx coding sequence

(A) Distribution plot of alternatively spliced events affecting introns and exons in murine alphaTC1 cells treated with Smndc1 shRNA. Plot highlights a positive shift in the percentage spliced in (dPSI) of introns, correlating with increased intron retention relative to empty vector, and a negative shift for exons, signifying increased exon skipping. (B) Scatter plot representation of panel (A), divided into exons and introns and highlighting the significantly enriched splice isoforms (dPSI \geq |15|). Abcc8 and Atrx are shown as examples of exon skipping and intron retention, respectively. (C) Proportion of the total 1305 alternatively spliced

events corresponding to their different predicted ontogeny. PROT: preserved coding sequence; DISR: disrupted coding sequence. **(D)** Genome browser tracks of event MmuINT0022118, relating to a retained intron between exons 16 and 17 of Atrx. Arrow points to PCR validating increase in intron retention upon Smndc1 knockdown. EV = empty vector; KD = Smndc1 knockdown. **(E)** Western blot of 5-day Smndc1 or Atrx knockdowns in alphaTC1 or betaTC3 cells, highlighting the loss of Atrx protein upon Smndc1 knockdown in both cell lines. **(F)** Scatter plot of all high confidence splicing events in donor 4. High confidence events are found in both hairpins, in the same direction with a dPSI \geq |10|. Three ATRX skipped introns and 2 overlapping PAX6 included exons are highlighted. **(G)** Predicted ontogeny of the differentially spliced events in human islets from Donors 3 and 4 post-SMNDC1 knockdown. **(H)** Distribution plot of alternatively spliced high confidence events affecting introns and exons in both human islet donors treated with both Smndc1 shRNAs. Shaded area represents the non-significant events with dPSI $<$ |10|.

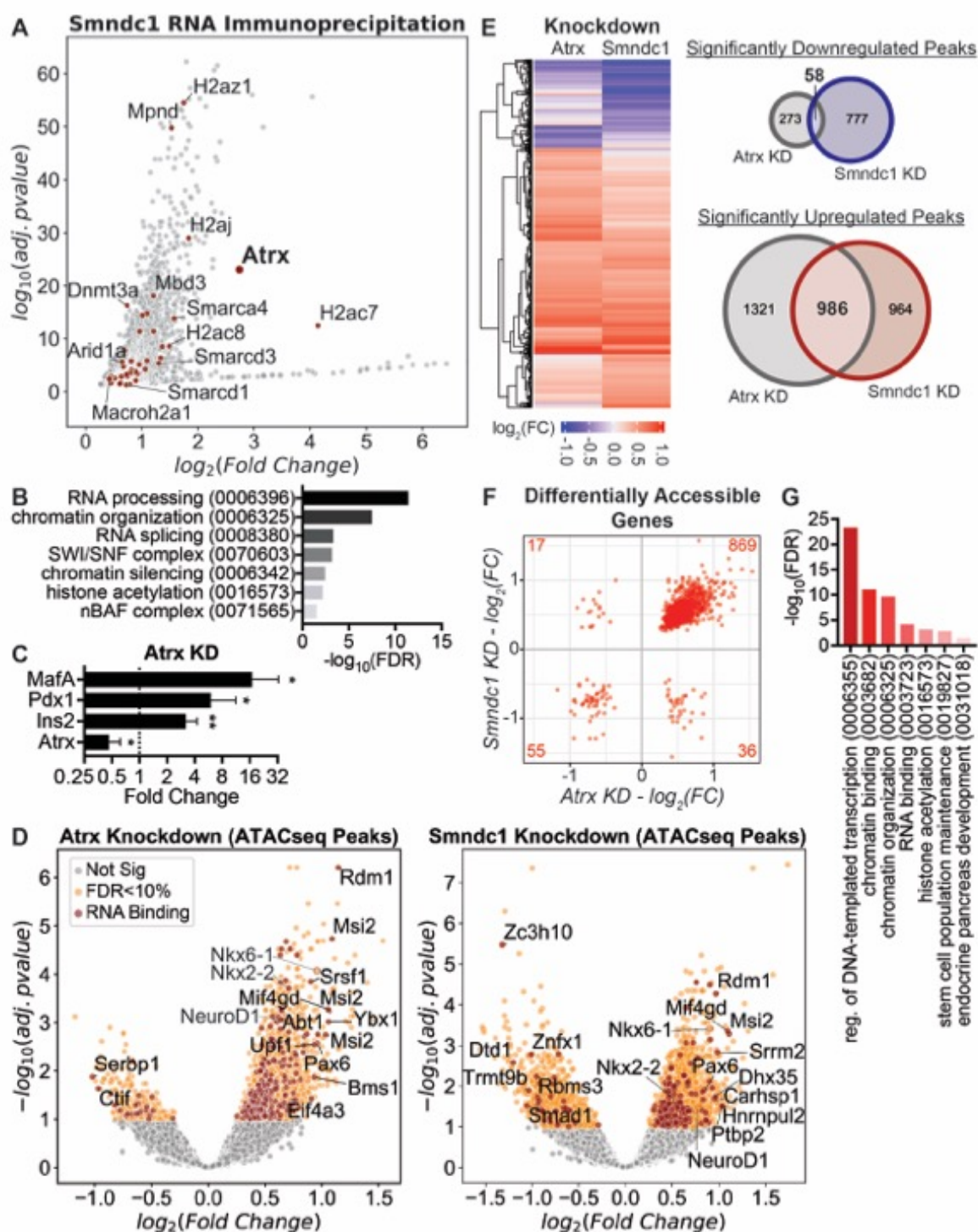


Figure 5 Loss of Smndc1 and Atrx both trigger a global increase in chromatin accessibility and beta cell genes

(A) Significantly enriched genes from Smndc1 RNA immunoprecipitation in murine alphaTC1 cells. In red: genes involved in chromatin silencing and remodeling. (B) GO enrichment for genes plotted in panel (A). (C) RT-qPCR results of 5-day Atrx knockdown in alphaTC1 cells. (D) Volcano plots of differentially accessible peaks from ATAC-seq results. Left: alphaTC1 cells 5 days post-transduction with Atrx shRNA, relative to empty vector control. Right:

alphaTC1 cells 5 days post-Smndc1 knockdown, relative to empty vector control. Gray dots = adjusted p-value ≥ 0.1 ; orange dots = adjusted p-value < 0.1 ; dark red dots = adjusted p-value < 0.1 and categorized as RNA binding (GO:0003723). **(E)** Heat map of significantly differentially accessible peaks in either Atrx or Smndc1 knockdown alphaTC1 cells relative to empty vector. On the right: Venn diagrams comparing upregulated or downregulated peaks in both knockdowns, highlighting the strong overlap and bias towards upregulation. **(F)** Correlation between common significantly differentially accessible genes in both knockdowns. In genes with multiple peaks, the strongest peak was chosen to represent the fold change, while genes with discordant peaks were disregarded. **(G)** Gene ontology enrichment for the genes with significantly increased accessibility in both knockdowns.

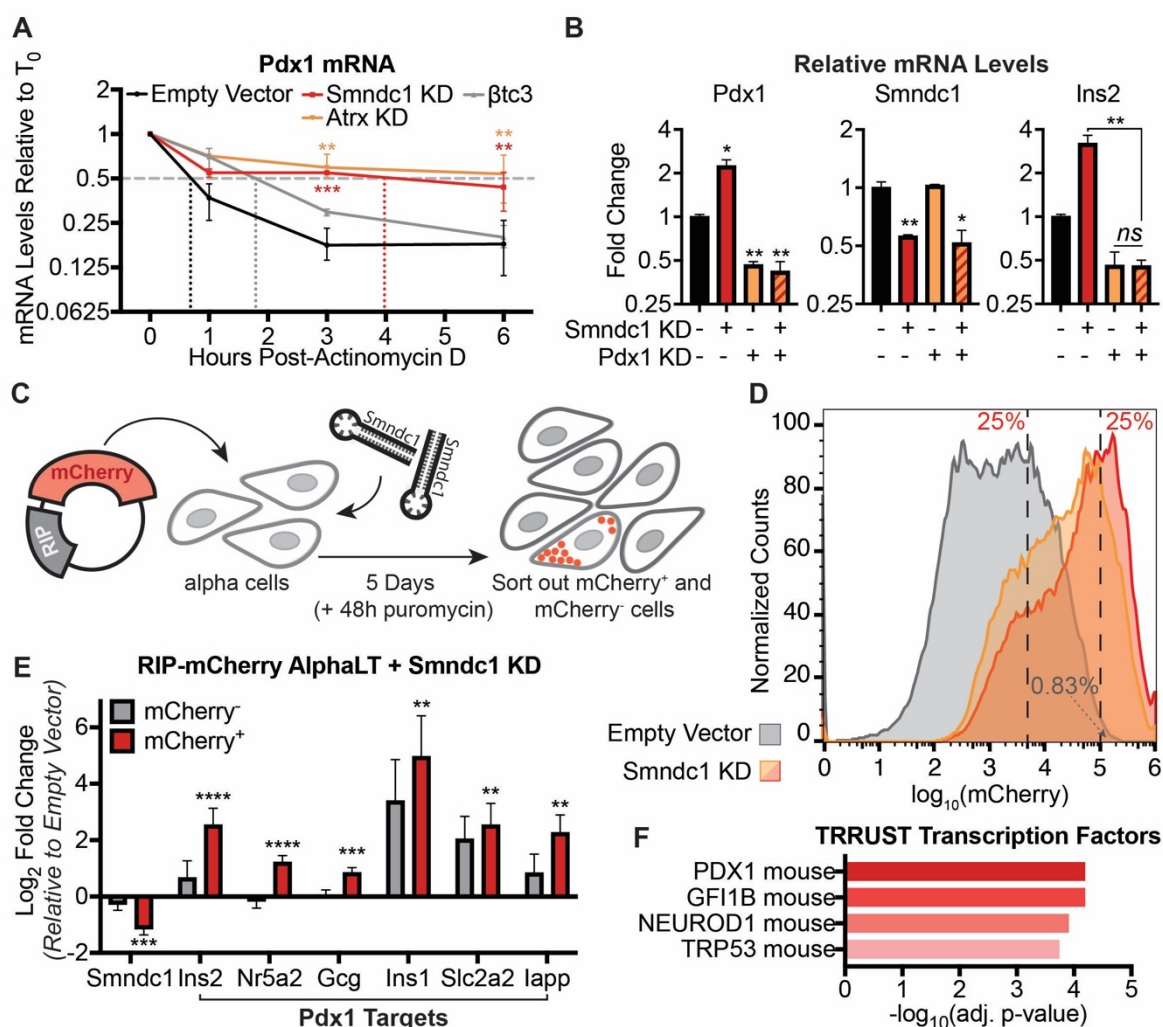


Figure 6 Smndc1 knockdown stabilizes Pdx1 mRNA and upregulates insulin transcription

(A) RT-qPCR results for remaining Pdx1 mRNA levels following specified intervals of actinomycin D treatment in alphaTC1 cells transduced with empty vector (black), Smndc1 shRNA (red) or Atrx shRNA (orange), and β TC3 cells (grey). N=3. (B) RT-qPCR results of 5-day Pdx1 knockdown (or empty vector) followed by 5-day Smndc1 knockdown (or empty vector) in alphaTC1 cells. Rightmost panel highlights inability of Smndc1 knockdown to upregulate Ins2 mRNA levels when Pdx1 is lost. (C) Schematic representation of Smndc1 shRNA and RIP-mCherry co-transduction experiment. (D) RIP-mCherry expressing alphaTC1 FACS results after 5 days of Smndc1 knockdown or empty vector control co-expression. A representative 2 of the Smndc1 knockdown biological replicates are shown out of the final 4 to avoid graph overcrowding. (E) RNAseq results of the sorted RIP-mCherry high vs. low expressing cells relative to empty vector control. (F) Enrichment of the significantly upregulated genes in RIP-mCherry⁺ cells for murine transcription factor targets (Han et al., 2018).

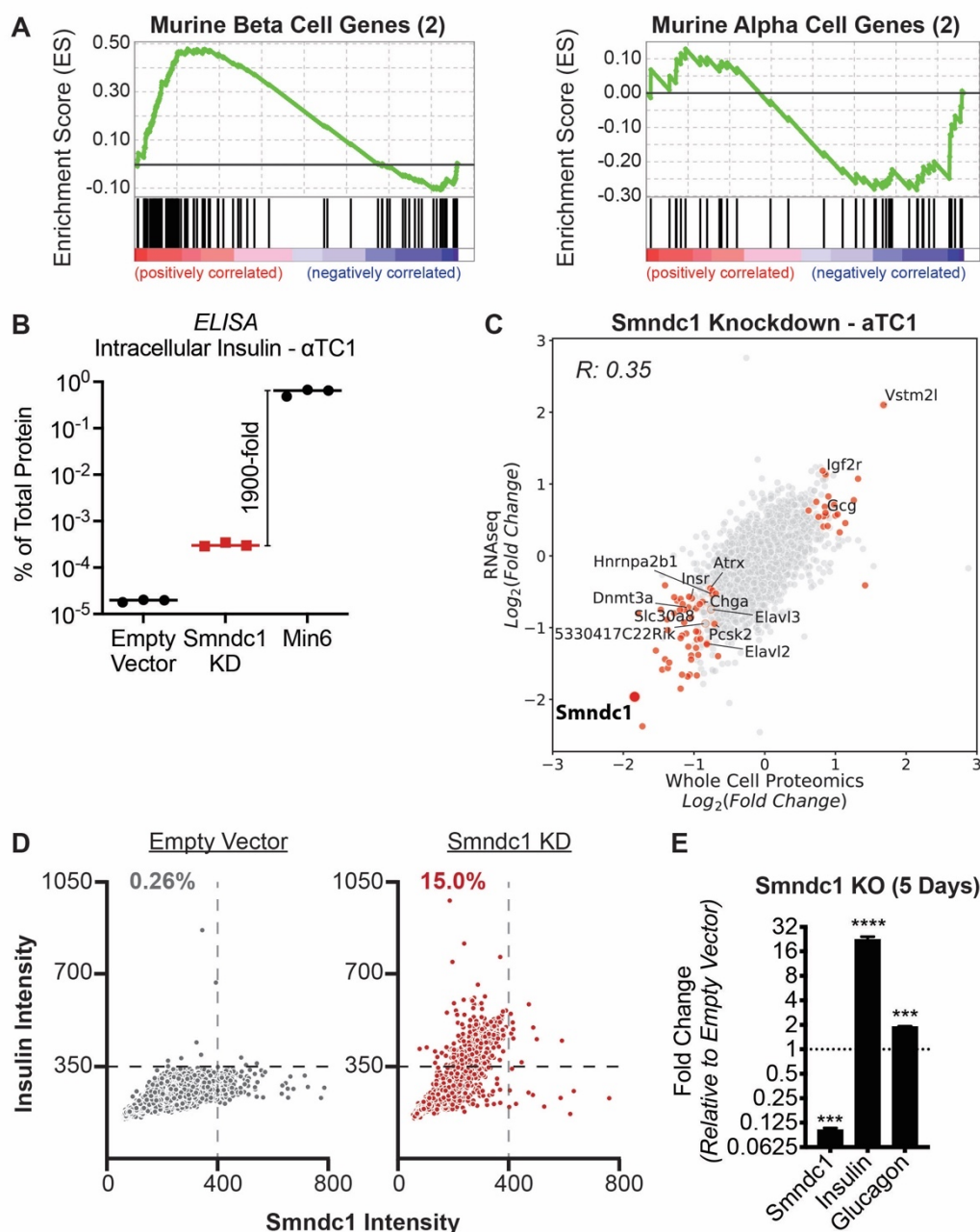


Figure S1. SmnDC1 knockdown upregulates insulin protein in a subset of alpha cells (Related to Figure 1)

(A) GSEA for genes significantly differentially expressed post-SmnDC1 knockdown. The ranked list was compared to the top 1000 most significantly differentially expressed genes between alphaTC1 and bTC3 in a published dataset (Lawlor et al., 2017). Trend towards enrichment of beta cells genes and depletion of alpha cell-specific genes is apparent. **(B)** Insulin protein levels in whole cell lysates of murine alphaTC1 cells 7 days post-SmnDC1 knockdown vs. empty vector control or wild-type Min6 cells. ELISA results represented as percent of insulin protein relative to whole cell lysate total protein amount. **(C)** Correlation of RNAseq and whole cell proteomics results post-SmnDC1 knockdown in murine alphaTC1 cells.

Red dots signify genes/proteins significantly altered in both RNAseq and whole cell proteomics datasets (i.e. adjusted p -value ≤ 0.05). **(D)** Quantification of SmnDC1 knockdown immunofluorescence results. Vertical and horizontal dashed lines represent threshold for strong SmnDC1 or insulin signal, respectively. Percentages correlate to top left quadrant, i.e. cells with weak SmnDC1 and strong insulin expression. **(E)** RT-qPCR results of SmnDC1, insulin and glucagon mRNA levels 5 days after transduction of an SmnDC1 gRNA.

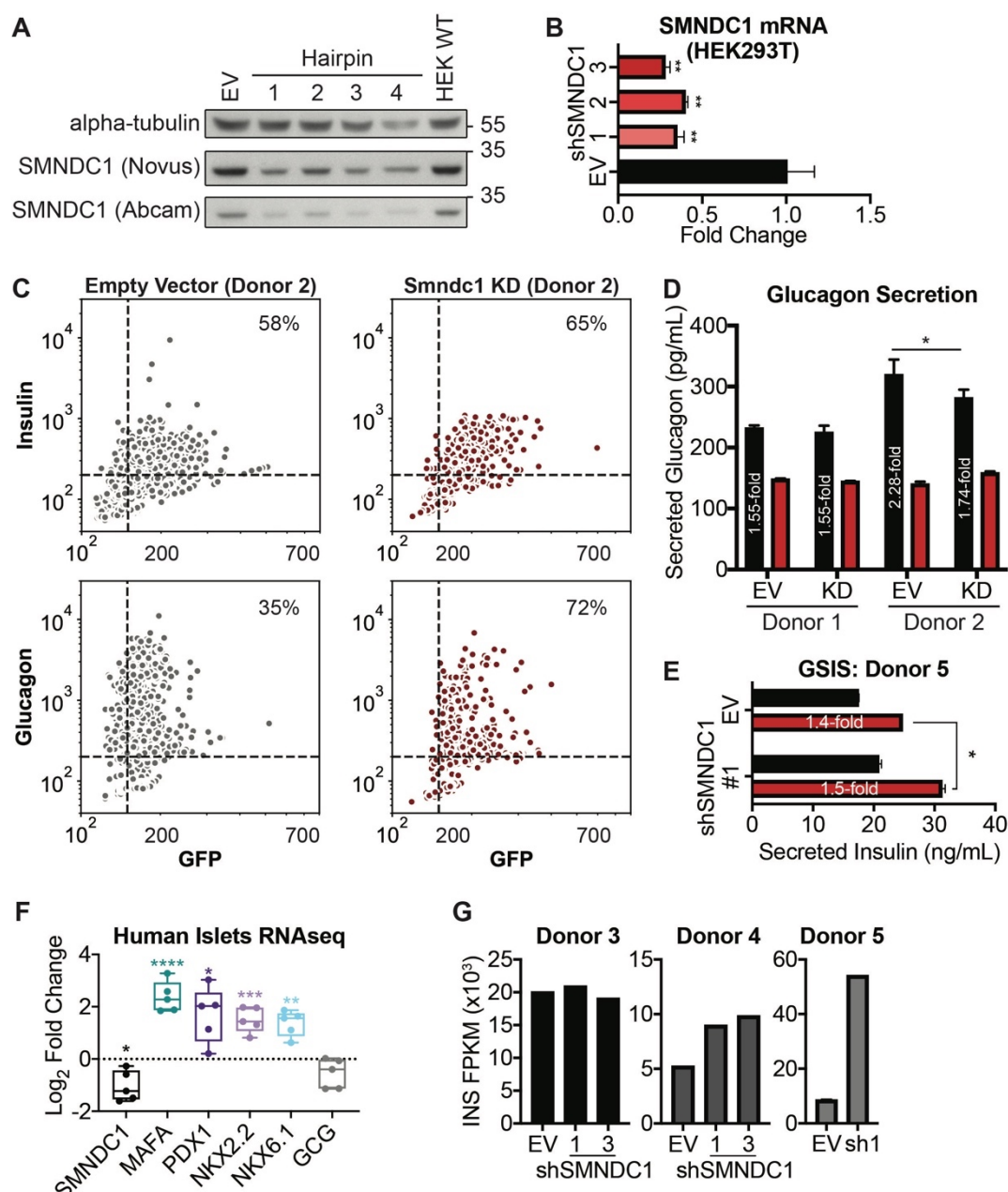


Figure S2. SMNDC1 knockdown effects on transcriptome and insulin secretion of human islets (Related to Figure 2)

(A) Western blot for SMNDC1 protein expression in HEK293T cells, 5 days post transduction with specified SMNDC1 shRNAs, empty vector and non-transfected controls. Antibody brands

are listed in brackets. **(B)** RT-qPCR results of SMNDC1 knockdown in HEK293T cells. **(C)** Immunofluorescence quantification of donor 2 dissociated human islets 5 days post-SMNDC1 knockdown, stained for insulin, glucagon and GFP (vector). Panels highlight successful transduction of both alpha and beta cells. Percentages correlate to number of insulin or glucagon positive cells within the GFP positive population. **(D)** ELISA results of glucagon protein levels in human islet supernatants pre- and post-glucose stimulation. No significant change is observed between empty vector control and SMNDC1 knockdown (shRNA #3) in Donor 1, with a slight decrease in glucagon secretion observed in Donor 2 upon SMNDC1 knockdown. **(E)** ELISA on whole cell lysate of unsorted, transduced, human islets from donor 5 post-GSIS. **(F)** RNAseq results from bulk, sorted human islets from donors 3,4 and 5, 5 days post-SMNDC1 knockdown. Individual points represent individual donors and hairpins. **(G)** RNAseq results of INS mRNA FPKMs in individual donors treated with specified SMNDC1 shRNAs.

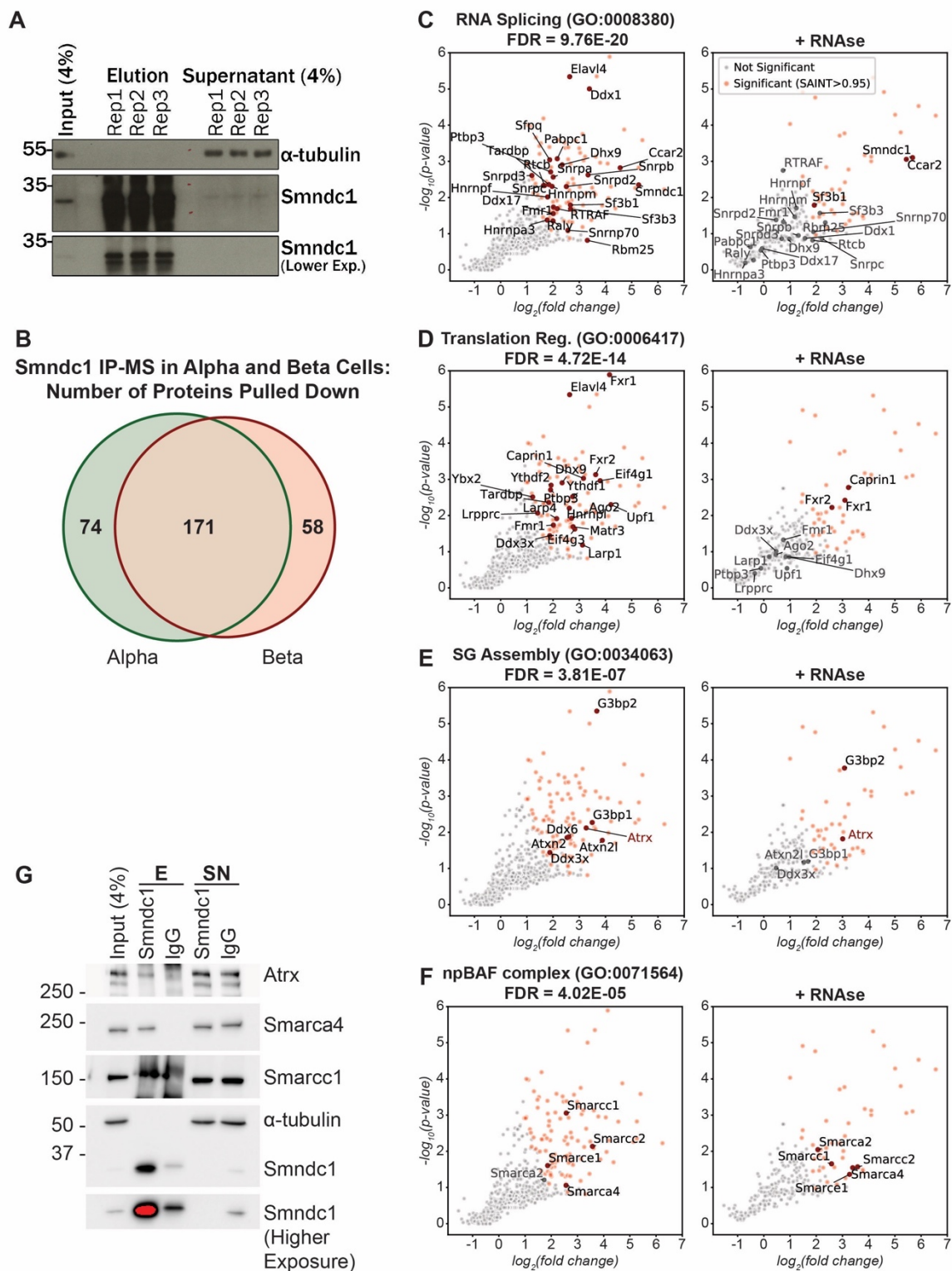
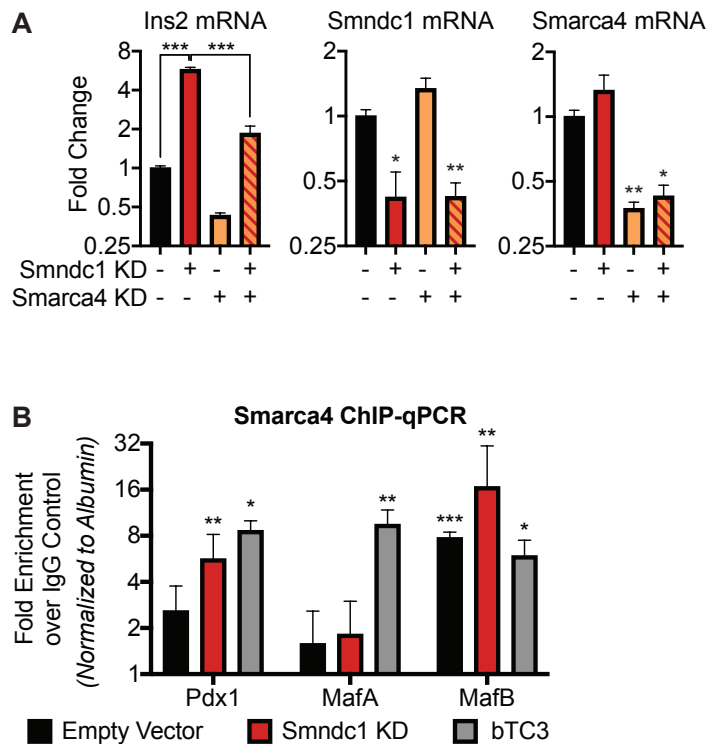


Figure S3. Majority of SMNDC1's protein interactions are RNA-dependent, with the exception of the BAF complex and Atrx (Related to Figure 3)

(A) Western blot of Smndc1 antibody co-immunopurification in murine alphaTC1 cells. Successful pulldown of Smndc1 protein and absence of alpha-tubulin in eluates and Smndc1 in supernatants confirms efficacy. **(B)** Venn diagram of common SMNDC1 interactions in murine alphaTC1 and bTC3 cells. **(C)-(F)** SMNDC1 protein interactome +/- RNase A treatment

in murine alphaTC1 cells. Light red dots represent significant interactors (SAINT ≥ 0.95). Dark red dots represent proteins with a significant SAINT score associated with the titled GO enrichment term. The grey dots represent the non-significant interactors. **(G)** Western blot of Smndc1 antibody co-immunoprecipitation in murine alphaTC1 cells. Pulldowns of Atrx, Smarca4 and Smarcc1 exclusively by the Smndc1 antibody and not by the IgG control confirm IP-MS interaction results.



SMNDC1 SFig. 4

Figure S4. The BAF complex, particularly Smarca4, is necessary for the observed increases in Pdx1 and Ins2 mRNA post-Smndc1 knockdown (Related to Figure 3)

(A) RT-qPCR results of 5-day Smarca4 knockdown (or empty vector) followed by 5-day Smndc1 knockdown (or empty vector) in alphaTC1 cells. **(B)** Smarca4 ChIP-qPCR for Pdx1, MafA and MafB loci in alphaTC1 cells transduced with empty vector or Smndc1 shRNA for 5 days, and murine bTC3 cells. Significance corresponds to the fold enrichment of the Smarca4 antibody vs. the IgG control in 3 independent biological replicates.

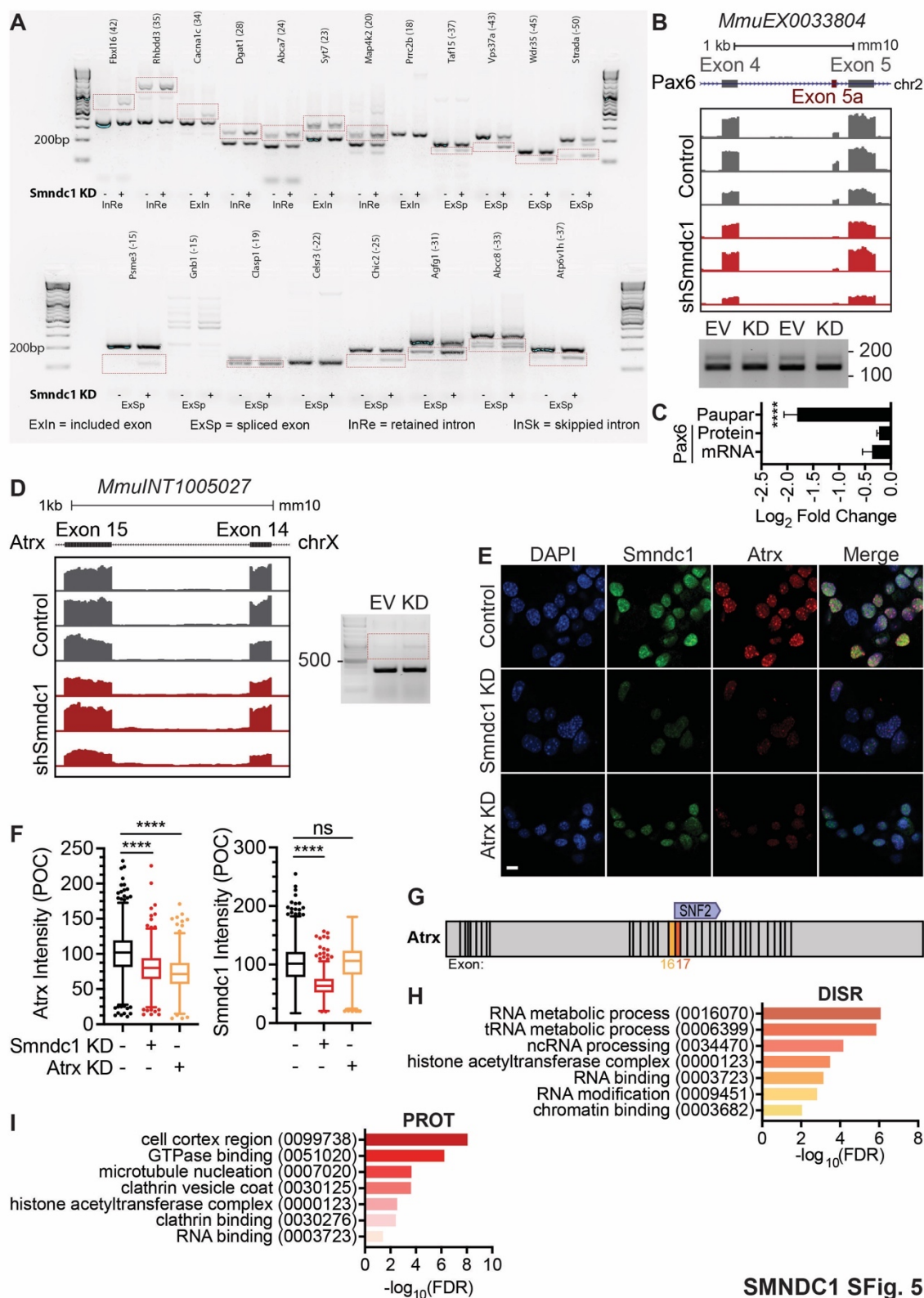


Figure S5. PCR validations of alternatively spliced events post-Smndc1 knockdown (Related to Figure 4)

(A) PCR validations of 20 different alternatively spliced events post-Smndc1 knockdown. Red dashed lines illustrate the alternative splice isoforms. Negative dPSIs (written in brackets by the gene names) relate to skipped exons or spliced introns and positive dPSIs to retained

introns or included exons. **(B)** Genome browser tracks for event MmuEX0033804, correlating to the skipping of Pax6's exon 5a. RT-PCR validation below. Upper bands represent the Pax6-5a isoform, for which there is a clear depletion with Smn dc1 knockdown. **(C)** RNAseq and whole cell proteomics results highlighting no significant change in Pax6 mRNA or protein levels upon Smn dc1 knockdown but a significant decrease of Paupar lncRNA. **(D)** Genome browser tracks for event MmuINT1005027, relating to retention of the intron between exons 14 and 15 of Atrx. Empty vector control treatment in gray; Smn dc1 shRNA transduced replicates in red. RT-PCR validation on the right. Dashed red lines highlight the splice isoform, enriched in Smn dc1 knockdown cells. **(E)** Representative immunofluorescence panel of alphaTC1 cells 5 days post-transduction with Smn dc1 or Atrx shRNAs. Scale bar = 10µm. **(F)** Immunofluorescence quantification of alphaTC1 cells 5 days post-transduction with Smn dc1 or Atrx shRNAs, stained with Atrx and Smn dc1 antibodies. Atrx and Smn dc1 relative intensities are listed as percentage of control (POC). Highlights loss of Atrx protein upon Smn dc1 knockdown, with no effect on Smn dc1 protein upon Atrx loss. N=3. **(G)** Schematic of Atrx locus, with the length and positions of its 35 exons relative to the location of its SNF2 domain-coding region. **(H)** GO enrichment for alternatively spliced genes with events predicted to disrupt the coding sequence (DISR). **(I)** GO enrichment for alternatively spliced genes with events predicted to preserve the ORF (PROT).

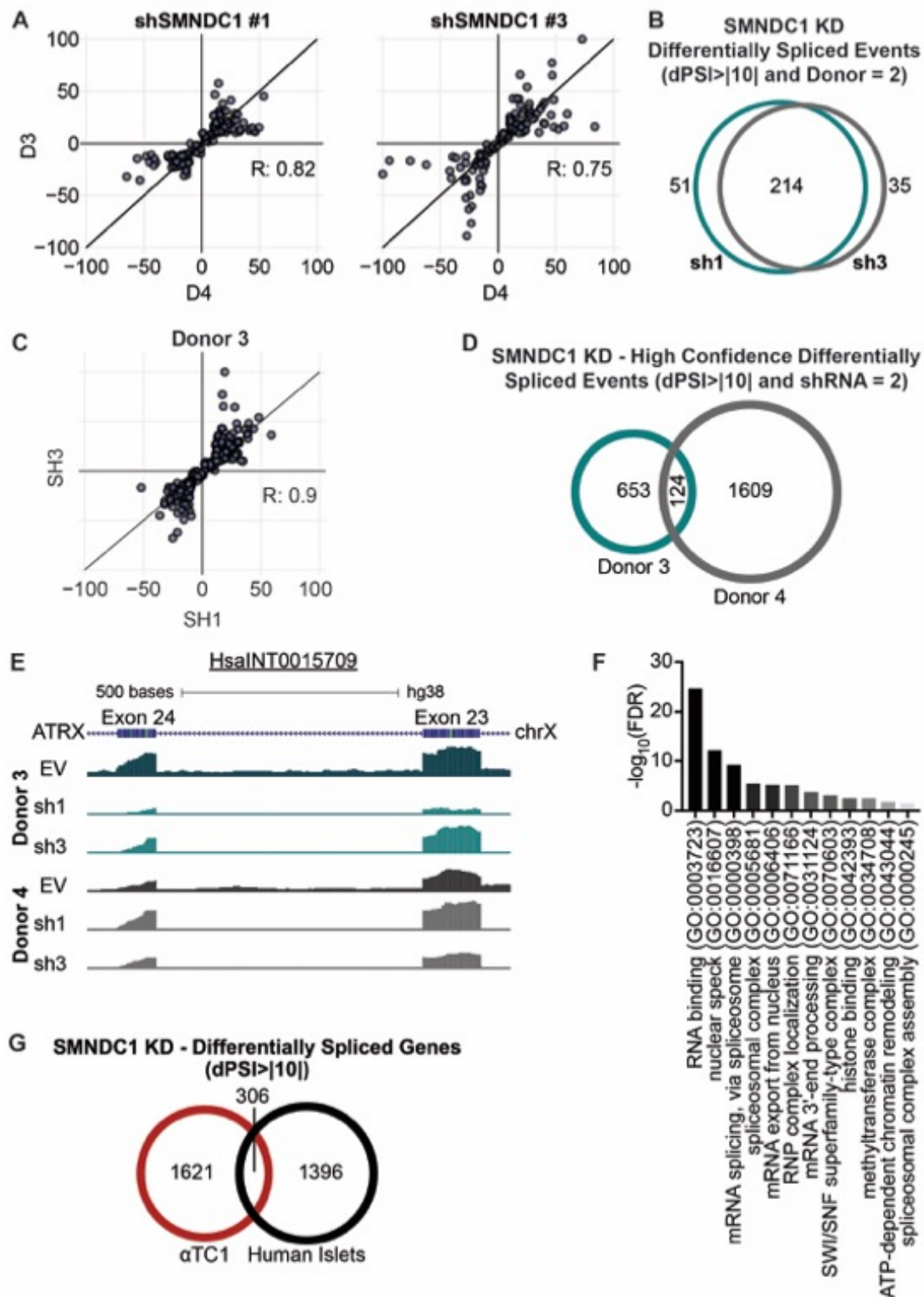


Figure S6. Alternative splicing changes post-SMNDC1 knockdown in human islets (Related to Figure 4)

(A) Scatter plots correlating alternative splicing events in Donors 3 and 4 triggered by SMNDC1 shRNA #1 or #3. **(B)** Venn diagram of correlation between alternatively spliced events triggered by SMNDC1 shRNAs #1 and #3 in both donors. **(C)** Scatter plot of high

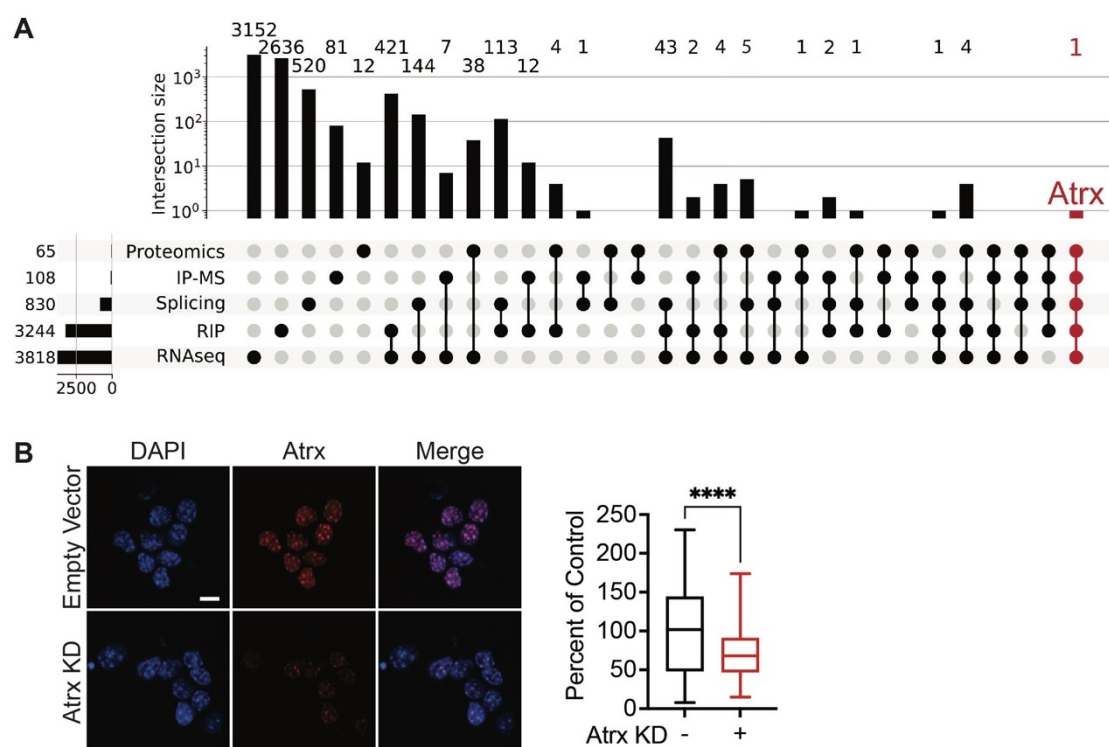
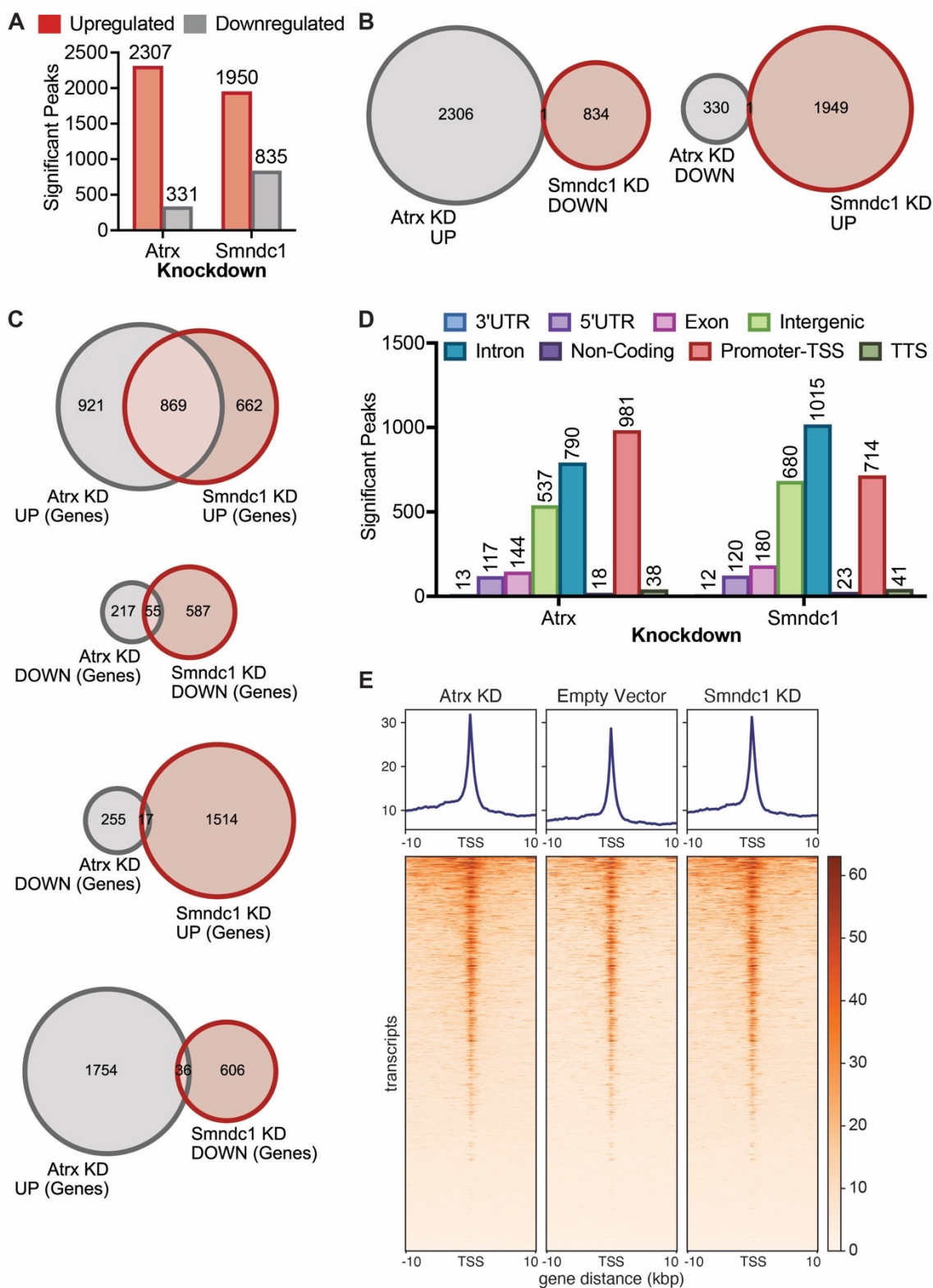


Figure S8. A strong connection exists between Atrx and Smndc1 (Related to Figure 5)

(A) Upset plot of common genes significantly enriched (adjusted p-value ≤ 0.05) in our RIP, RNAseq, whole cell proteomics, IP-MS protein interactome and splice isoform datasets post-Smndc1 knockdown. In red: Atrx revealed as the only shared gene between all 5 datasets. Bar graph bottom left = number of significant genes identified in each dataset. Top bar graph = number of genes shared by the different datasets. **(B)** Immunofluorescence panel of alphaTC1 cells 5 days post-Atrx shRNA transduction, with quantification on the right. Scale bar = 10 μ m.



commonly and discordantly regulated accessibility between *Smndc1* and *Atrx* knockdowns, at the gene level. **(D)** HOMER annotation of significant peaks, highlighting that most differentially accessible peaks are located within introns or TSS. **(E)** Heat map showing the spatial relationship between all sequenced transcripts of genes with significant peaks and TSS. Increased peaks at or prior to TSS observed with both knockdowns.

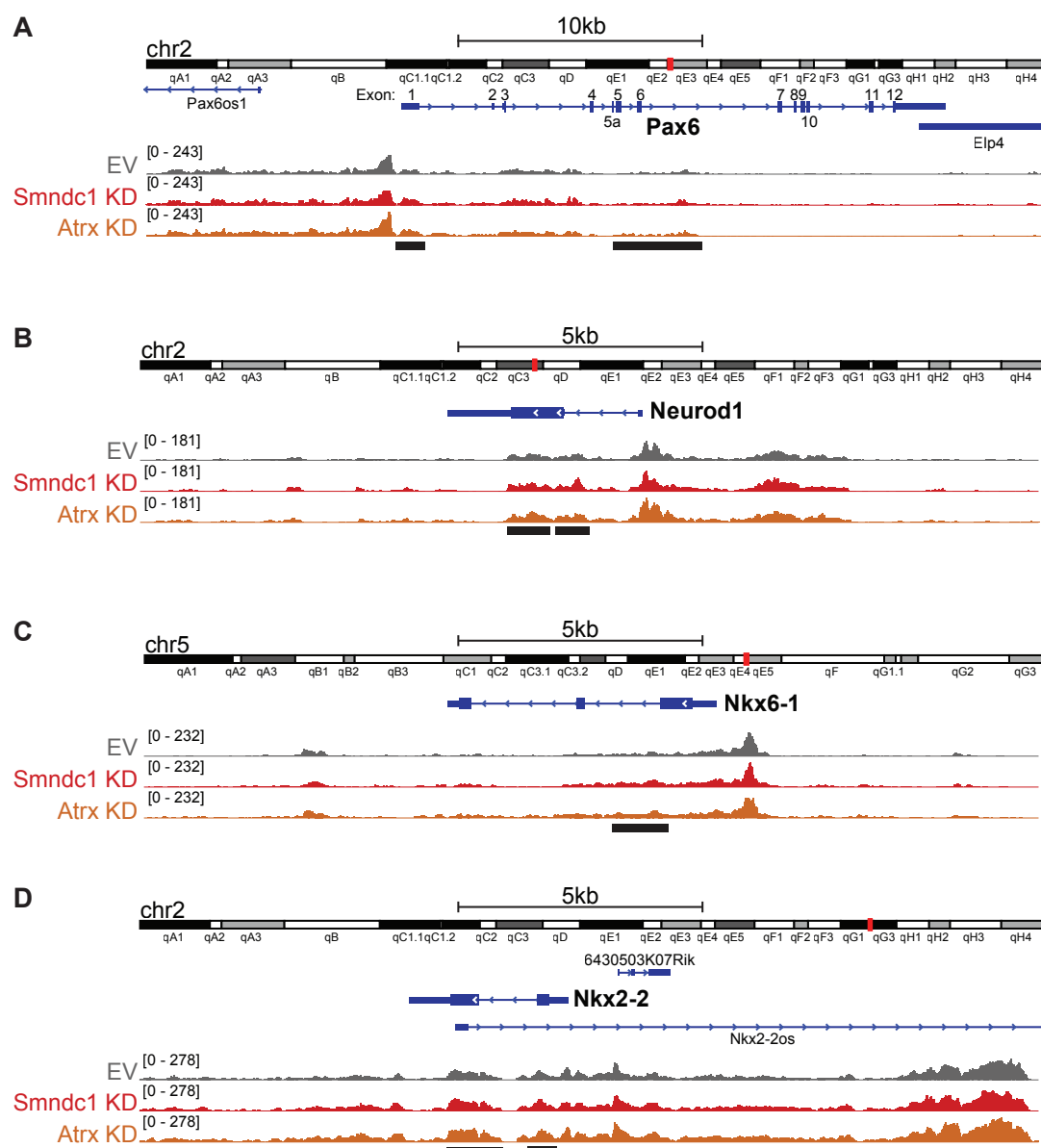


Figure S10. Increased accessibility at key islet transcription factors upon *Atrx* and *Smndc1* knockdown (Related to Figure 5)

Genome browser tracks for **(A)** *Pax6*, **(B)** *NeuroD1*, **(C)** *Nkx6-1* and **(D)** *Nkx2-2*. Black bars at the bottom represent significantly differentially accessible peaks in both *Smndc1* and *Atrx* knockdown alphaTC1 cells.

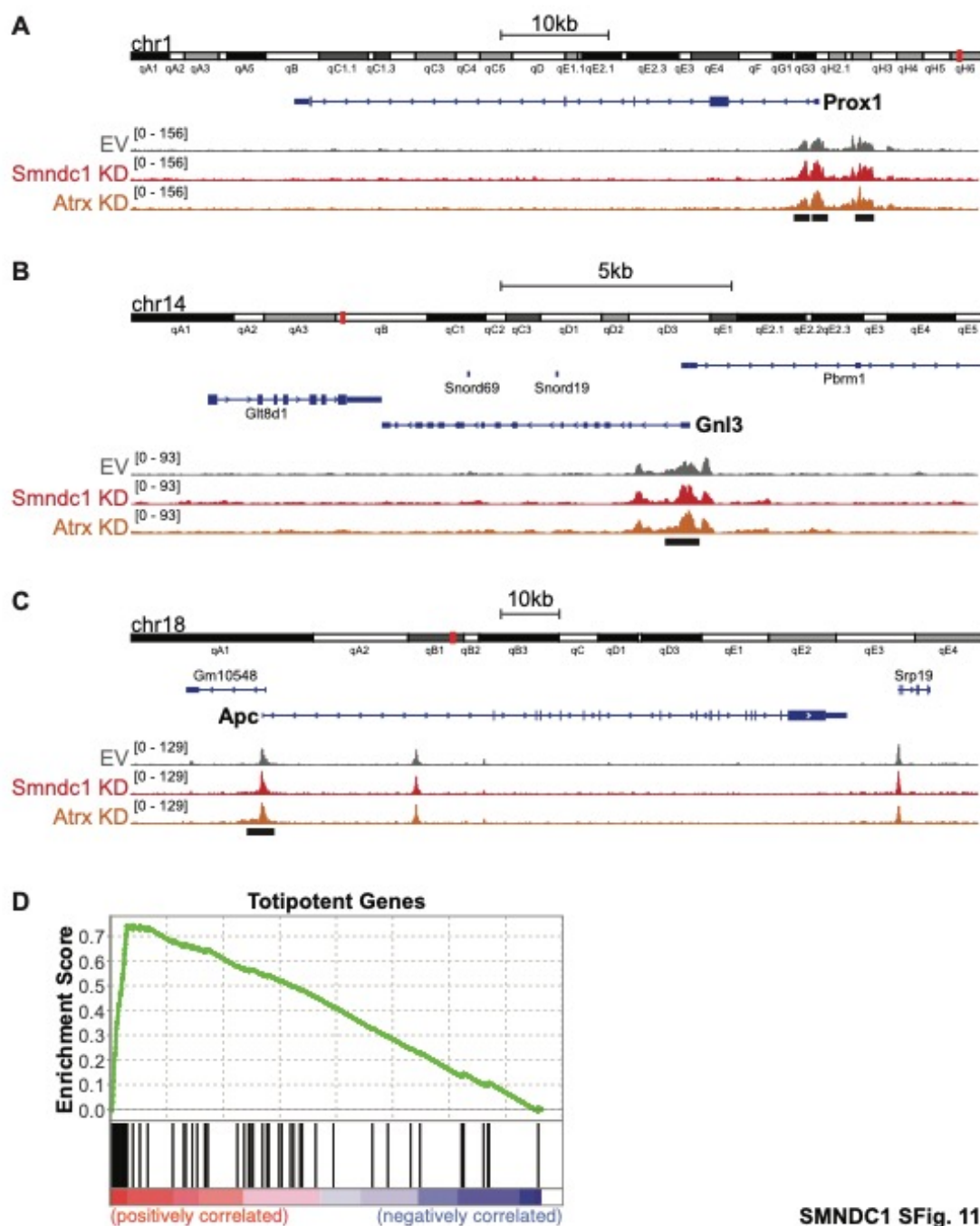


Figure S11. Loss of Smndc1 triggers an increase in plasticity genes (Related to Figure 5)

Genome browser tracks for **(A)** Prox1, **(B)** Gnl3 and **(C)** Apc. Black bars at the bottom represent significantly differentially accessible peaks in both Smndc1 and Atrx knockdown alphaTC1 cells. **(D)** GSEA for genes significantly differentially expressed post-Smndc1 knockdown. The ranked list was compared to 266 totipotency genes (Shen et al., 2021).

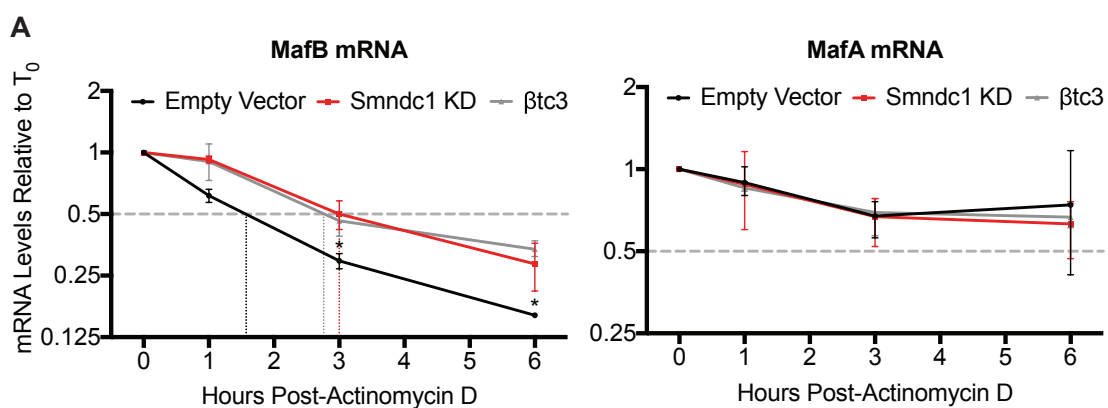
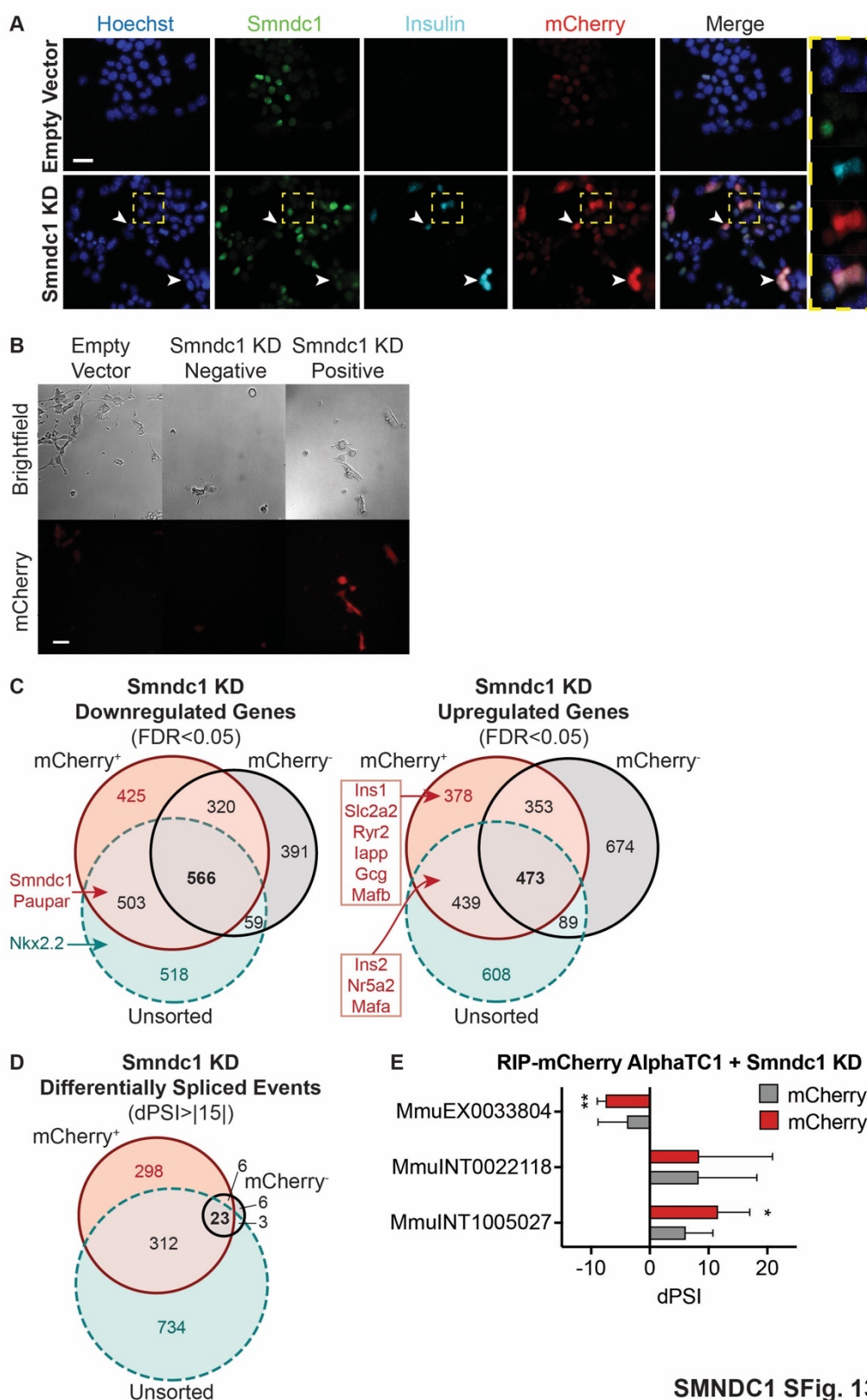


Figure S12. Increased mRNA stability upon SmnDC1 knockdown is restricted to Pdx1 (Related to Figure 6)

(A) RT-qPCR results for remaining MafB and MafA mRNA levels following specified intervals of actinomycin D treatment in alphaTC1 cells transduced with empty vector (black), SmnDC1 shRNA (red) and bTC3 cells (grey).



SMNDC1 SFig. 13

Figure S13. Co-transduced RIP-mCherry signal correlates with insulin mRNA and protein levels (Related to Figure 6)

(A) Immunofluorescence panel of unsorted and non-selected murine alphaTC1 cells 8 days after they were co-transduced with SmnDC1 shRNA (or empty vector control) and RIP-

mCherry. Dashed yellow boxes highlight colocalization of RIP-mCherry signal (red) with insulin (light blue), mutually exclusive from cells with detectable Smn dc1 signal (green). Scale bar = 20 μ m. **(B)** Live imaging of selected murine alphaTC1 cells 5 days after they were co-transduced with Smn dc1 shRNA (or empty vector control) and RIP-mCherry, sorted for RIP-mCherry expression (bottom 25% = negative vs. top 25% = positive). Scale bar = 20 μ m. **(C)** Venn diagram of significantly differentially expressed genes in RIP-mCherry negative, RIP-mCherry positive and original non-cotransduced RNAseq datasets post-Smn dc1 knockdown. Several genes of interest are highlighted. Nkx2.2 downregulation in RIP-mCherry positive cells had a *p*-value of 0.062 (Table S1). Ins2 and MafA mRNA are significantly upregulated in both RIP-mCherry positive and unsorted populations. **(D)** Venn diagram of differentially spliced events ($dPSI > |15|$) in RIP-mCherry negative, RIP-mCherry positive and original non-cotransduced RNAseq datasets post-Smn dc1 knockdown. **(E)** Differentially retained introns of Atrx and exon 5a of Pax6 post-Smn dc1 knockdown and their abundance in RIP-mCherry positive and negative sorted cells. Enrichment for events Mmu1005027 and MmuEX0033804 present in RIP-mCherry positive alphaTC1 cells.

References

- Alfert, A., Moreno, N., and Kerl, K. (2019). The BAF complex in development and disease. *Epigenetics Chromatin* 12, 19.
- Allemand, E., Myers, M.P., Garcia-Bernardo, J., Harel-Bellan, A., Krainer, A.R., and Muchardt, C. (2016). A Broad Set of Chromatin Factors Influences Splicing. *PLOS Genet.* 12, e1006318.
- Ariyachet, C., Tovaglieri, A., Xiang, G., Lu, J., Shah, M.S., Richmond, C.A., Verbeke, C., Melton, D.A., Stanger, B.Z., Mooney, D., et al. (2016). Reprogrammed Stomach Tissue as a Renewable Source of Functional β Cells for Blood Glucose Regulation. *Cell Stem Cell* 18, 410–421.
- Arrowsmith, C.H., and Schapira, M. (2019). Targeting non-bromodomain chromatin readers. *Nat. Struct. Mol. Biol.* 26, 863–869.
- Baek, D., and Green, P. (2005). Sequence conservation, relative isoform frequencies, and nonsense-mediated decay in evolutionarily conserved alternative splicing. *Proc. Natl. Acad. Sci. U. S. A.* 102, 12813–12818.
- Banga, A., Akinci, E., Greder, L. V, Dutton, J.R., and Slack, J.M.W. (2012). In vivo reprogramming of Sox9⁺ cells in the liver to insulin-secreting ducts. *Proc. Natl. Acad. Sci.* 109, 15336 LP – 15341.
- Barbu, A.R., Bodin, B., Welsh, M., Jansson, L., and Welsh, N. (2006). A perfusion protocol for highly efficient transduction of intact pancreatic islets of Langerhans. *Diabetologia* 49, 2388–2391.
- Batsché, E., Yaniv, M., and Muchardt, C. (2006). The human SWI/SNF subunit Brm is a regulator of alternative splicing. *Nat. Struct. Mol. Biol.* 13, 22–29.
- Bérubé, N.G., Smeenk, C.A., and Picketts, D.J. (2000). Cell cycle-dependent phosphorylation of the ATRX protein correlates with changes in nuclear matrix and chromatin association. *Hum. Mol. Genet.* 9, 539–547.
- Blomen, V.A., Majek, P., Jae, L.T., Bigenzahn, J.W., Nieuwenhuis, J., Staring, J., Sacco, R., van Diemen, F.R., Olk, N., Stukalov, A., et al. (2015). Gene essentiality and synthetic lethality in haploid human cells. *Science* (80-.). 350, 1092–1096.
- Bowerman, M., Swoboda, K.J., Michalski, J.P., Wang, G.S., Reeks, C., Beauvais, A., Murphy, K., Woulfe, J., Screatton, R.A., Scott, F.W., et al. (2012). Glucose metabolism and pancreatic defects in spinal muscular atrophy. *Ann Neurol* 72, 256–268.
- Bramswig, N.C., Everett, L.J., Schug, J., Dorrell, C., Liu, C., Luo, Y., Streeter, P.R., Najj, A., Grompe, M., and Kaestner, K.H. (2013). Epigenomic plasticity enables human pancreatic α to β cell reprogramming. *J. Clin. Invest.* 123, 1275–1284.
- Brooks, A.N., Duff, M.O., May, G., Yang, L., Bolisetty, M., Landolin, J., Wan, K., Sandler, J., Booth, B.W., Celniker, S.E., et al. (2015). Regulation of alternative splicing in *Drosophila* by

56 RNA binding proteins. *Genome Res.* 25, 1771–1780.

Butchbach, M.E.R., Rose Jr, F.F., Rhoades, S., Marston, J., McCrone, J.T., Sinnott, R., and Lorson, C.L. (2010). Effect of diet on the survival and phenotype of a mouse model for spinal muscular atrophy. *Biochem. Biophys. Res. Commun.* 391, 835–840.

Campbell, J.E., and Newgard, C.B. (2021). Mechanisms controlling pancreatic islet cell function in insulin secretion. *Nat. Rev. Mol. Cell Biol.* 22, 142–158.

Chakravarthy, H., Gu, X., Enge, M., Dai, X., Wang, Y., Damond, N., Downie, C., Liu, K., Wang, J., Xing, Y., et al. (2017). Converting Adult Pancreatic Islet α Cells into β Cells by Targeting Both *Dnmt1* and *Arx*. *Cell Metab.* 25, 622–634.

Chan, C.S., Laddha, S. V, Lewis, P.W., Koletsky, M.S., Robzyk, K., Da Silva, E., Torres, P.J., Untch, B.R., Li, J., Bose, P., et al. (2018). *ATRX*, *DAXX* or *MEN1* mutant pancreatic neuroendocrine tumors are a distinct alpha-cell signature subgroup. *Nat. Commun.* 9, 4158.

Chen, Y.-J., Finkbeiner, S.R., Weinblatt, D., Emmett, M.J., Tameire, F., Yousefi, M., Yang, C., Maehr, R., Zhou, Q., Shemer, R., et al. (2014). De novo formation of insulin-producing “neo- β cell islets” from intestinal crypts. *Cell Rep.* 6, 1046–1058.

Collombat, P., Mansouri, A., Hecksher-Sorensen, J., Serup, P., Krull, J., Gradwohl, G., and Gruss, P. (2003). Opposing actions of *Arx* and *Pax4* in endocrine pancreas development. *Genes Dev* 17, 2591–2603.

Collombat, P., Xu, X., Ravassard, P., Sosa-Pineda, B., Dussaud, S., Billestrup, N., Madsen, O.D., Serup, P., Heimberg, H., and Mansouri, A. (2009). The ectopic expression of *Pax4* in the mouse pancreas converts progenitor cells into alpha and subsequently beta cells. *Cell* 138, 449–462.

Courtney, M., Gjernes, E., Druelle, N., Ravaud, C., Vieira, A., Ben-Othman, N., Pfeifer, A., Avolio, F., Leuckx, G., Lacas-Gervais, S., et al. (2013). The inactivation of *Arx* in pancreatic alpha-cells triggers their neogenesis and conversion into functional beta-like cells. *PLoS Genet* 9, e1003934.

Dempster, J.M., Rossen, J., Kazachkova, M., Pan, J., Kugener, G., Root, D.E., and Tsherniak, A. (2019). Extracting Biological Insights from the Project Achilles Genome-Scale CRISPR Screens in Cancer Cell Lines. *BioRxiv* 720243.

Dhawan, S., Georgia, S., Tschen, S.I., Fan, G., and Bhushan, A. (2011). Pancreatic beta cell identity is maintained by DNA methylation-mediated repression of *Arx*. *Dev Cell* 20, 419–429.

Dobin, A., Davis, C.A., Schlesinger, F., Drenkow, J., Zaleski, C., Jha, S., Batut, P., Chaisson, M., and Gingeras, T.R. (2013). STAR: ultrafast universal RNA-seq aligner. *Bioinformatics* 29, 15–21.

Docherty, H.M., Hay, C.W., Ferguson, L.A., Barrow, J., Durward, E., and Docherty, K. (2005). Relative contribution of *PDX-1*, *MafA* and *E47/beta2* to the regulation of the human insulin promoter. *Biochem. J.* 389, 813–820.

- Dyer, M.A., Qadeer, Z.A., Valle-Garcia, D., and Bernstein, E. (2017). ATRX and DAXX: Mechanisms and Mutations. *Cold Spring Harb. Perspect. Med.* 7.
- Furuyama, K., Chera, S., van Gorp, L., Oropeza, D., Ghila, L., Damond, N., Vethe, H., Paulo, J.A., Joosten, A.M., Berney, T., et al. (2019). Diabetes relief in mice by glucose-sensing insulin-secreting human α -cells. *Nature* 567, 43–48.
- Gao, T., McKenna, B., Li, C., Reichert, M., Nguyen, J., Singh, T., Yang, C., Pannikar, A., Doliba, N., Zhang, T., et al. (2014). Pdx1 maintains β cell identity and function by repressing an α cell program. *Cell Metab.* 19, 259–271.
- Glisovic, T., Bachorik, J.L., Yong, J., and Dreyfuss, G. (2008). RNA-binding proteins and post-transcriptional gene regulation. *FEBS Lett.* 582, 1977–1986.
- Goldberg, A.D., Banaszynski, L.A., Noh, K.-M., Lewis, P.W., Elsaesser, S.J., Stadler, S., Dewell, S., Law, M., Guo, X., Li, X., et al. (2010). Distinct factors control histone variant H3.3 localization at specific genomic regions. *Cell* 140, 678–691.
- Gosmain, Y., Marthinet, E., Cheyssac, C., Guérardel, A., Mamin, A., Katz, L.S., Bouzakri, K., and Philippe, J. (2010). Pax6 controls the expression of critical genes involved in pancreatic α cell differentiation and function. *J. Biol. Chem.* 285, 33381–33393.
- Gosmain, Y., Katz, L.S., Masson, M.H., Cheyssac, C., Poisson, C., and Philippe, J. (2012). Pax6 is crucial for β -cell function, insulin biosynthesis, and glucose-induced insulin secretion. *Mol. Endocrinol.* 26, 696–709.
- Gradwohl, G., Dierich, A., LeMeur, M., and Guillemot, F. (2000). neurogenin3 is required for the development of the four endocrine cell lineages of the pancreas. *Proc Natl Acad Sci U S A* 97, 1607–1611.
- Gromada, J., Chabosseau, P., and Rutter, G.A. (2018). The α -cell in diabetes mellitus. *Nat. Rev. Endocrinol.* 14, 694–704.
- Han, H., Cho, J.-W., Lee, S.S., Yun, A., Kim, H., Bae, D., Yang, S., Kim, C.Y., Lee, M., Kim, E., et al. (2018). TRRUST v2: an expanded reference database of human and mouse transcriptional regulatory interactions. *Nucleic Acids Res.* 46, D380–D386.
- Hickey, R.D., Galivo, F., Schug, J., Brehm, M.A., Haft, A., Wang, Y., Benedetti, E., Gu, G., Magnuson, M.A., Shultz, L.D., et al. (2013). Generation of islet-like cells from mouse gall bladder by direct ex vivo reprogramming. *Stem Cell Res.* 11, 503–515.
- Hughes, C.S., Moggridge, S., Müller, T., Sorensen, P.H., Morin, G.B., and Krijgsveld, J. (2019). Single-pot, solid-phase-enhanced sample preparation for proteomics experiments. *Nat. Protoc.* 14, 68–85.
- Hwang, B., Lee, J.H., and Bang, D. (2018). Single-cell RNA sequencing technologies and bioinformatics pipelines. *Exp. Mol. Med.* 50, 1–14.
- Ignatiadis, N., Klaus, B., Zaugg, J.B., and Huber, W. (2016). Data-driven hypothesis weighting increases detection power in genome-scale multiple testing. *Nat. Methods* 13, 577–580.

- Irimia, M., Weatheritt, R.J., Ellis, J.D., Parikshak, N.N., Gonatopoulos-Pournatzis, T., Babor, M., Quesnel-Vallières, M., Tapial, J., Raj, B., O'Hanlon, D., et al. (2014). A highly conserved program of neuronal microexons is misregulated in autistic brains. *Cell* 159, 1511–1523.
- Jiao, Y., Shi, C., Edil, B.H., de Wilde, R.F., Klimstra, D.S., Maitra, A., Schulick, R.D., Tang, L.H., Wolfgang, C.L., Choti, M.A., et al. (2011). DAXX/ATRX, MEN1, and mTOR pathway genes are frequently altered in pancreatic neuroendocrine tumors. *Science* 331, 1199–1203.
- Jimenez-Moreno, C.M., Herrera-Gomez, I. de G., Lopez-Noriega, L., Lorenzo, P.I., Cobo-Vuilleumier, N., Fuente-Martin, E., Mellado-Gil, J.M., Parnaud, G., Bosco, D., Gauthier, B.R., et al. (2015). A Simple High Efficiency Intra-Islet Transduction Protocol Using Lentiviral Vectors. *Curr. Gene Ther.* 15, 436–446.
- Jonsson, J., Carlsson, L., Edlund, T., and Edlund, H. (1994). Insulin-promoter-factor 1 is required for pancreas development in mice. *Nature* 371, 606–609.
- Kleinhammer, A., Wurst, W., and Kühn, R. (2011). Constitutive and conditional RNAi transgenesis in mice. *Methods* 53, 430–436.
- Lareau, L.F., and Brenner, S.E. (2015). Regulation of splicing factors by alternative splicing and NMD is conserved between kingdoms yet evolutionarily flexible. *Mol. Biol. Evol.* 32, 1072–1079.
- Lawlor, N., Youn, A., Kursawe, R., Ucar, D., and Stitzel, M.L. (2017). Alpha TC1 and Beta-TC-6 genomic profiling uncovers both shared and distinct transcriptional regulatory features with their primary islet counterparts. *Sci. Rep.* 7, 11959.
- Lee, E.K., Kim, W., Tominaga, K., Martindale, J.L., Yang, X., Subaran, S.S., Carlson, O.D., Mercken, E.M., Kulkarni, R.N., Akamatsu, W., et al. (2012). RNA-binding protein HuD controls insulin translation. *Mol. Cell* 45, 826–835.
- Luo, H., Chen, R., Yang, R., Liu, Y., Chen, Y., Shu, Y., and Chen, H. (2014). Reprogramming of Mice Primary Hepatocytes into Insulin-Producing Cells by Transfection with Multicistronic Vectors. *J. Diabetes Res.* 2014, 716163.
- Marquina-Sanchez, B., Fortelny, N., Farlik, M., Vieira, A., Collombat, P., Bock, C., and Kubicek, S. (2020). Single-cell RNA-seq with spike-in cells enables accurate quantification of cell-specific drug effects in pancreatic islets. *Genome Biol.* 21, 106.
- Matsuoka, T., Zhao, L., Artner, I., Jarrett, H.W., Friedman, D., Means, A., and Stein, R. (2003). Members of the large Maf transcription family regulate insulin gene transcription in islet beta cells. *Mol. Cell. Biol.* 23, 6049–6062.
- McKenna, B., Guo, M., Reynolds, A., Hara, M., and Stein, R. (2015). Dynamic Recruitment of Functionally Distinct Swi/Snf Chromatin Remodeling Complexes Modulates Pdx1 Activity in Islet β Cells. *Cell Rep.* 10, 2032–2042.
- Meister, G., Hannus, S., Plottner, O., Baars, T., Hartmann, E., Fakan, S., Laggerbauer, B., Fischer, U., Plöttner, O., Baars, T., et al. (2001). SMNrp is an essential pre-mRNA splicing

- factor required for the formation of the mature spliceosome. *EMBO J.* 20, 2304–2314.
- Mellacheruvu, D., Wright, Z., Couzens, A.L., Lambert, J.-P., St-Denis, N.A., Li, T., Miteva, Y. V, Hauri, S., Sardi, M.E., Low, T.Y., et al. (2013). The CRAPome: a contaminant repository for affinity purification–mass spectrometry data. *Nat. Methods* 10, 730–736.
- Mi, H., Muruganujan, A., Ebert, D., Huang, X., and Thomas, P.D. (2019). PANTHER version 14: more genomes, a new PANTHER GO-slim and improvements in enrichment analysis tools. *Nucleic Acids Res.* 47, D419–D426.
- Modrek, B., and Lee, C.J. (2003). Alternative splicing in the human, mouse and rat genomes is associated with an increased frequency of exon creation and/or loss. *Nat. Genet.* 34, 177–180.
- Moffat, J., Grueneberg, D.A., Yang, X., Kim, S.Y., Kloepper, A.M., Hinkle, G., Piqani, B., Eisenhaure, T.M., Luo, B., Grenier, J.K., et al. (2006). A lentiviral RNAi library for human and mouse genes applied to an arrayed viral high-content screen. *Cell* 124, 1283–1298.
- Moore, M.J., and Proudfoot, N.J. (2009). Pre-mRNA Processing Reaches Back to Transcription and Ahead to Translation. *Cell* 136, 688–700.
- Nagy, E., and Maquat, L.E. (1998). A rule for termination-codon position within intron-containing genes: when nonsense affects RNA abundance. *Trends Biochem. Sci.* 23, 198–199.
- Ohlsson, H., Karlsson, K., and Edlund, T. (1993). IPF1, a homeodomain-containing transactivator of the insulin gene. *EMBO J.* 12, 4251–4259.
- Olsen, J. V, de Godoy, L.M.F., Li, G., Macek, B., Mortensen, P., Pesch, R., Makarov, A., Lange, O., Horning, S., and Mann, M. (2005). Parts per million mass accuracy on an Orbitrap mass spectrometer via lock mass injection into a C-trap. *Mol. Cell. Proteomics* 4, 2010–2021.
- Papasaikas, P., Rao, A., Huggins, P., Valcarcel, J., and Lopez, A.J. (2015). Reconstruction of composite regulator-target splicing networks from high-throughput transcriptome data. *BMC Genomics* 16, S7.
- Patrick, K.L., Ryan, C.J., Xu, J., Lipp, J.J., Nissen, K.E., Roguev, A., Shales, M., Krogan, N.J., and Guthrie, C. (2015). Genetic Interaction Mapping Reveals a Role for the SWI/SNF Nucleosome Remodeler in Spliceosome Activation in Fission Yeast. *PLOS Genet.* 11, e1005074.
- Picelli, S., Faridani, O.R., Björklund, A.K., Winberg, G., Sagasser, S., and Sandberg, R. (2014). Full-length RNA-seq from single cells using Smart-seq2. *Nat. Protoc.* 9, 171–181.
- Ramírez, F., Ryan, D.P., Grüning, B., Bhardwaj, V., Kilpert, F., Richter, A.S., Heyne, S., Dündar, F., and Manke, T. (2016). deepTools2: a next generation web server for deep-sequencing data analysis. *Nucleic Acids Res.* 44, W160–W165.
- Rappilber, J., Ajuh, P., Lamond, A.I., and Mann, M. (2001). SPF30 Is an Essential Human Splicing Factor Required for Assembly of the U4/U5/U6 Tri-small Nuclear Ribonucleoprotein

into the Spliceosome*. *J. Biol. Chem.* 276, 31142–31150.

Ratnakumar, K., Duarte, L.F., LeRoy, G., Hasson, D., Smeets, D., Vardabasso, C., Bönisch, C., Zeng, T., Xiang, B., Zhang, D.Y., et al. (2012). ATRX-mediated chromatin association of histone variant macroH2A1 regulates α -globin expression. *Genes Dev.* 26, 433–438.

Rissland, O.S., Subtelny, A.O., Wang, M., Lugowski, A., Nicholson, B., Laver, J.D., Sidhu, S.S., Smibert, C.A., Lipshitz, H.D., and Bartel, D.P. (2017). The influence of microRNAs and poly(A) tail length on endogenous mRNA–protein complexes. *Genome Biol.* 18, 211.

Rösel-Hillgärtner, T.D., Hung, L.-H., Khrameeva, E., Le Querrec, P., Gelfand, M.S., and Bindereif, A. (2013). A novel intra-U1 snRNP cross-regulation mechanism: alternative splicing switch links U1C and U1-70K expression. *PLoS Genet.* 9, e1003856.

Sadic, D., Schmidt, K., Groh, S., Kondofersky, I., Ellwart, J., Fuchs, C., Theis, F.J., and Schotta, G. (2015). Atrx promotes heterochromatin formation at retrotransposons. *EMBO Rep.* 16, 836–850.

Saha, A., Kim, Y., Gewirtz, A.D.H., Jo, B., Gao, C., McDowell, I.C., Engelhardt, B.E., and Battle, A. (2017). Co-expression networks reveal the tissue-specific regulation of transcription and splicing. *Genome Res.* 27, 1843–1858.

Saltzman, A.L., Pan, Q., and Blencowe, B.J. (2011). Regulation of alternative splicing by the core spliceosomal machinery. *Genes Dev.* 25, 373–384.

Sarma, K., Cifuentes-Rojas, C., Ergun, A., Del Rosario, A., Jeon, Y., White, F., Sadreyev, R., and Lee, J.T. (2014). ATRX directs binding of PRC2 to Xist RNA and Polycomb targets. *Cell* 159, 869–883.

Schick, S., Rendeiro, A.F., Runggatscher, K., Ringler, A., Boidol, B., Hinkel, M., Májek, P., Vulliard, L., Penz, T., Parapatics, K., et al. (2019). Systematic characterization of BAF mutations provides insights into intracomplex synthetic lethality in human cancers. *Nat. Genet.* 51, 1399–1410.

Servitja, J.M., and Ferrer, J. (2004). Transcriptional networks controlling pancreatic development and beta cell function. *Diabetologia* 47, 597–613.

Shen, H., Yang, M., Li, S., Zhang, J., Peng, B., Wang, C., Chang, Z., Ong, J., and Du, P. (2021). Mouse totipotent stem cells captured and maintained through spliceosomal repression. *Cell* 184, 2843-2859.e20.

Singer, R.A., Arnes, L., Cui, Y., Wang, J., Gao, Y., Guney, M.A., Burnum-Johnson, K.E., Rabadan, R., Ansong, C., Orr, G., et al. (2019). The Long Noncoding RNA Paupar Modulates PAX6 Regulatory Activities to Promote Alpha Cell Development and Function. *Cell Metab.* 30, 1091-1106.e8.

Spaeth, J.M., Liu, J.-H., Peters, D., Guo, M., Osipovich, A.B., Mohammadi, F., Roy, N., Bhushan, A., Magnuson, M.A., Hebrok, M., et al. (2019). The Pdx1-Bound Swi/Snf Chromatin Remodeling Complex Regulates Pancreatic Progenitor Cell Proliferation and Mature Islet β -

Cell Function. *Diabetes* 68, 1806 LP – 1818.

Stephens, M. (2017). False discovery rates: a new deal. *Biostatistics* 18, 275–294.

Stoffers, D.A., Zinkin, N.T., Stanojevic, V., Clarke, W.L., and Habener, J.F. (1997). Pancreatic agenesis attributable to a single nucleotide deletion in the human IPF1 gene coding sequence. *Nat. Genet.* 15, 106–110.

Swisa, A., Avrahami, D., Eden, N., Zhang, J., Feleke, E., Dahan, T., Cohen-Tayar, Y., Stolovich-Rain, M., Kaestner, K.H., Glaser, B., et al. (2017). PAX6 maintains β cell identity by repressing genes of alternative islet cell types. *J. Clin. Invest.* 127, 230–243.

Talbot, K., Miguel-Aliaga, I., Mohaghegh, P., Ponting, C.P., and Davies, K.E. (1998). Characterization of a gene encoding survival motor neuron (SMN)-related protein, a constituent of the spliceosome complex. *Hum. Mol. Genet.* 7, 2149–2156.

Tapial, J., Ha, K.C.H., Sterne-Weiler, T., Gohr, A., Braunschweig, U., Hermoso-Pulido, A., Quesnel-Vallières, M., Permanyer, J., Sodaei, R., Marquez, Y., et al. (2017). An atlas of alternative splicing profiles and functional associations reveals new regulatory programs and genes that simultaneously express multiple major isoforms. *Genome Res.* 27, 1759–1768.

Thomas, J.D., Polaski, J.T., Feng, Q., De Neef, E.J., Hoppe, E.R., McSharry, M. V, Pangallo, J., Gabel, A.M., Belleville, A.E., Watson, J., et al. (2020). RNA isoform screens uncover the essentiality and tumor-suppressor activity of ultraconserved poison exons. *Nat. Genet.* 52, 84–94.

Tripsianes, K., Madl, T., Machyna, M., Fessas, D., Englbrecht, C., Fischer, U., Neugebauer, K.M., and Sattler, M. (2011). Structural basis for dimethylarginine recognition by the Tudor domains of human SMN and SPF30 proteins. *Nat Struct Mol Biol* 18, 1414–1420.

Vanhoose, A.M., Samaras, S., Artner, I., Henderson, E., Hang, Y., and Stein, R. (2008). MafA and MafB regulate Pdx1 transcription through the Area II control region in pancreatic beta cells. *J. Biol. Chem.* 283, 22612–22619.

Velazco-Cruz, L., Goedegebuure, M.M., and Millman, J.R. (2020). Advances Toward Engineering Functionally Mature Human Pluripotent Stem Cell-Derived β Cells . *Front. Bioeng. Biotechnol.* 8, 786.

Walpita, D., Hasaka, T., Spoonamore, J., Vetere, A., Takane, K.K., Fomina-Yadlin, D., Fiaschi-Taesch, N., Shamji, A., Clemons, P.A., Stewart, A.F., et al. (2012). A human islet cell culture system for high-throughput screening. *J Biomol Screen* 17, 509–518.

Wang, K., Wu, D., Zhang, H., Das, A., Basu, M., Malin, J., Cao, K., and Hannenhalli, S. (2018a). Comprehensive map of age-associated splicing changes across human tissues and their contributions to age-associated diseases. *Sci. Rep.* 8, 10929.

Wang, W., Chi, T., Xue, Y., Zhou, S., Kuo, A., and Crabtree, G.R. (1998). Architectural DNA binding by a high-mobility-group/kinesin-like subunit in mammalian SWI/SNF-related complexes. *Proc. Natl. Acad. Sci.* 95, 492 LP – 498.

Wang, X., Sterr, M., Burtscher, I., Chen, S., Hieronimus, A., Machicao, F., Staiger, H., Häring, H.-U., Lederer, G., Meitinger, T., et al. (2018b). Genome-wide analysis of PDX1 target genes in human pancreatic progenitors. *Mol. Metab.* 9, 57–68.

Wiśniewski, J.R., Zougman, A., Nagaraj, N., and Mann, M. (2009). Universal sample preparation method for proteome analysis. *Nat. Methods* 6, 359–362.

Xie, Z., Bailey, A., Kuleshov, M. V, Clarke, D.J.B., Evangelista, J.E., Jenkins, S.L., Lachmann, A., Wojciechowicz, M.L., Kropiwnicki, E., Jagodnik, K.M., et al. (2021). Gene Set Knowledge Discovery with Enrichr. *Curr. Protoc.* 1, e90.

Yamada, T., Cavelti-Weder, C., Caballero, F., Lysy, P.A., Guo, L., Sharma, A., Li, W., Zhou, Q., Bonner-Weir, S., and Weir, G.C. (2015). Reprogramming Mouse Cells With a Pancreatic Duct Phenotype to Insulin-Producing β -Like Cells. *Endocrinology* 156, 2029–2038.

Yang, Y.P., Thorel, F., Boyer, D.F., Herrera, P.L., and Wright, C. V (2011). Context-specific alpha- to-beta-cell reprogramming by forced Pdx1 expression. *Genes Dev* 25, 1680–1685.

Yeo, G.W., Van Nostrand, E., Holste, D., Poggio, T., and Burge, C.B. (2005). Identification and analysis of alternative splicing events conserved in human and mouse. *Proc. Natl. Acad. Sci. U. S. A.* 102, 2850 LP – 2855.

Zhou, Q., Brown, J., Kanarek, A., Rajagopal, J., and Melton, D.A. (2008). In vivo reprogramming of adult pancreatic exocrine cells to beta-cells. *Nature* 455, 627–632.

Ziegenhain, C., Vieth, B., Parekh, S., Reinius, B., Guillaumet-Adkins, A., Smets, M., Leonhardt, H., Heyn, H., Hellmann, I., and Enard, W. (2017). Comparative Analysis of Single-Cell RNA Sequencing Methods. *Mol. Cell* 65, 631-643.e4.

3. DISCUSSION

3.1 General Discussion

Insulin expression in pancreatic beta cells is regulated at multiple stages at both the mRNA and protein level. Firstly, the transcription factor, RNA binding protein and methylation landscape surrounding the insulin locus and other key beta cell gene loci is critical in determining the transcription, stability, transport, splicing and consequent translation of their mRNAs. For instance, insulin transcription can be enhanced upon glucose exposure, with increased Pdx1 and Ptbp1 binding (Magro & Solimena, 2013; Wang *et al*, 2016a). However, a second level of regulation exists post-transcriptionally. Keeping with the glucose exposure example, if levels remain elevated and uncontrolled, ER stress triggers the active degradation of insulin mRNA in an IRE1a-dependent manner (Lipson *et al*, 2008).

These different regulatory layers of insulin expression are highlighted in the results from our two papers detailed in Sections 2.1 and 2.2. While we observe an increase in insulin protein levels both after loperamide treatment and Smnbc1 knockdown, only Smnbc1 knockdown yields an increase in insulin mRNA levels. Loperamide's activities are strictly downstream, positively stimulating insulin protein biosynthesis, from processing to secretion. As previously mentioned, ER stress can have a highly detrimental effect on insulin expression and overall beta cell survival. Furthermore, loss of the ER surface calcium ATPase, Serca2, and consequent ER calcium depletion has been shown to aggravate ER stress and promote beta cell apoptosis (Cardozo *et al*, 2005). Loperamide leads to a robust, reproducible and conserved increase in Serca2 mRNA and protein. What's more, it also regulates the expression of multiple other ER proteins and yields an increase in proinsulin export from the ER, highlighted by increased proinsulin near the cellular periphery, as well as increased processing into mature insulin. The increases in insulin protein levels post-loperamide are dramatic and most likely a result of altered pH and calcium. These results reiterate the importance of ER function for overall beta cell identity and function.

In fact, recent studies suggest ER stress also contributes to the demise of beta cells in autoimmune T1D, and that alleviation of that stress can prevent disease progression (Engin *et al*, 2013; Morita *et al*, 2017; Lee *et al*, 2020). This is because beta cell death in T1D is not exclusively a consequence of direct CD8 T cell-mediated killing, but also beta cell-intrinsic, following proinflammatory cytokine-induced oxidative and ER stress (Atkinson *et al*, 2011; Burrack *et al*, 2017). Genetic deletion or small molecule inhibition of IRE1a hyperactivation and introduction of chemical chaperones could all prevent terminal UPR activation and rescue

functional beta cell numbers. In fact, it's been noted that up to 50% of beta cells survive the initial destructive autoimmune attack characteristic of T1D onset, yet are functionally incompetent and incapable of promoting euglycemia (Akirav *et al*, 2008; Krogvold *et al*, 2015). This suggests there is a window early within disease onset, mostly likely coinciding with the so-called "honeymoon period", within which removal of ER stress through UPR protein modulation or alleviation of hyperglycemia can trigger remission in both humans and mice (Engin *et al*, 2013; Krogvold *et al*, 2015; Morita *et al*, 2017; Tang *et al*, 2019; Lee *et al*, 2020). Hence, it is tempting to postulate that loperamide treatment, through increased beta cell identity and functionality, on top of rescued ER calcium levels and proinsulin biosynthesis, could equally rescue functionality in the surviving T1D beta cells.

This is even more plausible when compared to loperamide's positive effects in diabetic human islets and murine models. Patients with T2D experience decreased insulin expression and secretion, as well as increased bihormonal cell populations (Marchetti *et al*, 2020), characteristics all rescued upon loperamide treatment in our *in vitro* experiments. Other small molecules have also been shown to modulate ER stress and ameliorate function in T2D islets. Metformin, GLP-1 and Rapamycin, for instance, have all been associated with increased insulin secretion, number of insulin granules, and expression of genes involved in beta cell identity and function (Bugliani *et al*, 2019; Lupi *et al*, 2008; Marchetti *et al*, 2004; Masini *et al*, 2009). Specifically, all three ameliorated autophagy, a process both protective against ER stress and impaired in T2D beta cells. Ultrastructural studies of beta cells treated with loperamide reveal a striking increase in autophagosomes plus expression of autophagy-related genes. Rapamycin and metformin both inhibit mTORC1, a known autophagy inhibitor, whose sustained hyperactivation is observed in diabetic beta cells and contributes to their functional demise (Ardestani *et al*, 2018). Interestingly, FoxO1 has also been found to inhibit mTORC1 activity in multiple tissues (Chen *et al*, 2010; Lin *et al*, 2014; Southgate *et al*, 2007). Our results suggest loperamide increases active nuclear FoxO1 levels. Therefore, further experiments could elucidate whether loperamide equally modulates autophagy and beta cell survival and function through suppression of mTOR, and whether loperamide synergizes with metformin and rapamycin.

In effect, the direct target of loperamide in beta cells remains undefined. We have ruled out loperamide's canonical receptor, mu-opioid, due to its very low expression in beta cells and the inability of its antagonist, naltrexone, to counteract loperamide's insulin increase. Moreover, early studies on opioid users revealed increased hyperglycemia due to detrimental effects to their glucose recognition and insulin secretion (Giugliano, 1984). Loperamide, on the other hand, lowered blood glucose levels in diabetic db/db mice, with no effect on wild-

type mice, and increased insulin expression and secretion in diabetic human pancreatic islets, reinforcing a non-opioid mode of action. Interestingly, loperamide has also been proposed to bind the calcium sensor calmodulin in an opioid-independent manner (Zavec *et al*, 1982; Daly & Harper, 2000). CaMKII phosphorylation and activation, as observed upon loperamide treatment, requires direct binding by Ca²⁺-bound calmodulin (Clapham, 2007). Furthermore, chemical inhibition of calmodulin-CaMKII binding limited loperamide's increase of insulin protein and FoxO1 nuclear localization. Hence, loperamide's mechanism of action appears to rely on the activation of CaMKII. However, whether loperamide's ability to bind calmodulin is important for this activation, or whether it is secondary to loperamide's increase in intracellular calcium levels, is yet to be determined. More recently, loperamide was linked to the protein menin (Yue *et al*, 2016), a protein shown to stabilize FoxO1 levels in beta cells by preventing its ubiquitination and phosphorylation by AKT (Jiang *et al*, 2019). Our preliminary results could not identify a direct interaction between FoxO1 and menin in the Min6 cell line, however we did observe a decrease in total phosphorylated AKT levels upon loperamide treatment (Figure 7).

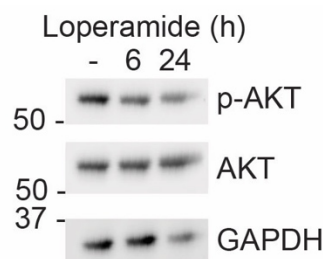


Figure 7. Loperamide treatment leads to rapid decrease in phosphorylated AKT levels in Min6 cells.

Follow-up experiments in menin-null cells could distinguish its role, if any, in loperamide's phenotype, and whether a direct interaction between the two exists and is necessary. In fact, identifying a direct molecular target for loperamide in beta cells, using either thermal shift or affinity based chemical proteomics, could pave the way for the identification of more potent analogs, increased beta cell specificity and further information on FoxO1 activation. Analogues could also help solve structure-activity relationships, providing critical knowledge on what part of loperamide is necessary for the insulin phenotype.

Contrastingly, in our second study, we used direct genetic perturbation as opposed to small molecules, which has both advantages and limitations. While small molecules represent a therapeutically superior option, with their ease of delivery and rapid bioavailability, they also suffer from binding promiscuity, leading to off-target effects (Lehár *et al*, 2008). This can of course also be a plus, as highlighted by our repurposing of loperamide from its original, gut-

specific anti-diarrheal activity to a previously unknown islet-specific, FoxO1-driven inhibition of diabetic beta cell dedifferentiation. However, as previously mentioned, the identification of a specific molecular target can be challenging. The use of RNA interference to knockdown genes of interest is much more controlled and specific. Furthermore, our use of multiple short hairpins, in both murine cell lines and human islets, diminishes specificity reservations. Consequently, through shRNA silencing, we identified *Smndc1* to regulate insulin expression in alpha cells upstream of transcription, through decreased *Pdx1* mRNA stability and global silencing of chromatin. We also successfully mapped out *Smndc1*'s direct protein interactors, namely the chromatin remodelers *Atrx* and *Smarca4*. *Atrx* is known to help deposit H3K9me3 and H3K27me3 marks on chromatin and to maintain chromatin in a heterochromatic state (Dyer *et al*, 2017). Previous studies have shown that alpha cells possess bivalent histone marks on important beta cell transcription factors, such as *Pdx1* and *MafA* (Bramswig *et al*, 2013). Elucidating whether *Atrx* is involved in the maintenance of these repressive marks in alpha cells could be key to resolving *Smndc1*'s mechanism of action, since *Smndc1* directly regulates *Atrx* protein levels through binding and splicing of its mRNA. Interestingly, *Smndc1* is also involved in the splicing of known functional beta cell genes, namely *Pax6* and *Abcc8*.

The transcription factor *Pax6* is necessary for both insulin and glucagon transcription as detailed in Section 1.1.2 and Figure 3. It was recently found that binding of *Pax6* to the glucagon promoter, and other important alpha cell genes, requires a specific splice isoform (Singer *et al*, 2019). This isoform includes an additional exon between exons 5 and 6, termed exon 5a. Interestingly, *Smndc1* is necessary for the complete inclusion of this exon, as loss of *Smndc1* correlates with a significant loss of *Pax6* exon 5a. In beta cells, *Pax6* is involved in upregulation of insulin and *MafA* transcription (Swisa *et al*, 2017a), both observed in alpha cells upon *Smndc1* loss. Hence, whether this switch in *Pax6* isoforms, from alpha to beta-cell specific, helps propagate *Smndc1* knockdown's shift in cell identity could be an important next question to address.

Abcc8, encoding the Sur1 protein, forms part of the ATP-sensitive potassium channel found on the surface of both alpha and beta cells. In alpha cells, it is responsible for alpha-cell intrinsic glucose sensing and glucagon secretion regulation (Rorsman *et al*, 2008). Interestingly, no haploinsufficiency is observed upon loss of one Sur1 allele, while complete deletion of Sur1 results in mice with maintained normoglycemia, unless stressed (Seghers *et al*, 2000). In fact, loss or gain of function mutations in *ABCC8* can result in congenital hyperinsulinism, a recessive genetic disorder in which patients suffer from uncontrolled insulin secretion and hypoglycemia, or neonatal diabetes, respectively (Ortiz & Bryan, 2015). *Smndc1*

knockdown induces skipping of *Abcc8*'s 31st exon, a change unlikely to affect translation of the final protein due to preservation of the coding sequence (Figure 8).

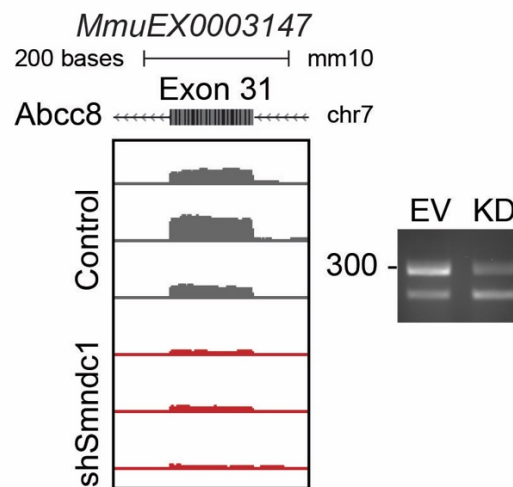


Figure 8. Genome browser tracks for event MmuEX0003147, correlating to the skipping of Abcc8's 31st exon in murine alpha cell line alphaTC1. A 33% decrease in the number of transcripts harboring this exon is observed upon Smndc1 knockdown (shSmndc1). PCR validation on the right. Lower bands represent the splice isoform with the skipped exon, for which there is a clear enrichment with Smndc1 knockdown.

Notably, exon 31 forms part of *Abcc8*'s second transmembrane domain, mutations in which can affect ATP affinity and hydrolysis (Ortiz & Bryan, 2015). Questions of whether this mutant form of *Abcc8* phenocopies relevant aspects of *Smndc1* knockdown's phenotype, specifically the increase in insulin secretion we observe in human islets, or whether it inhibits glucagon secretion and helps drive the loss of alpha cell character, could be key to the overall molecular mechanism and understanding of alpha cell identity maintenance.

3.2 Conclusion and Future Prospects

In conclusion, by using alpha or dedifferentiated beta cells as starting materials and genetic or chemical perturbations, we could analyze and characterize novel pathways and targets regulating insulin expression at the transcriptional or post-translational stage. Referring to our aims in Section 1.4, we successfully identified a protein regulating insulin repression in alpha cells, *Smndc1*, and a small molecule inhibitor of beta cell dedifferentiation, loperamide (Figure 9).

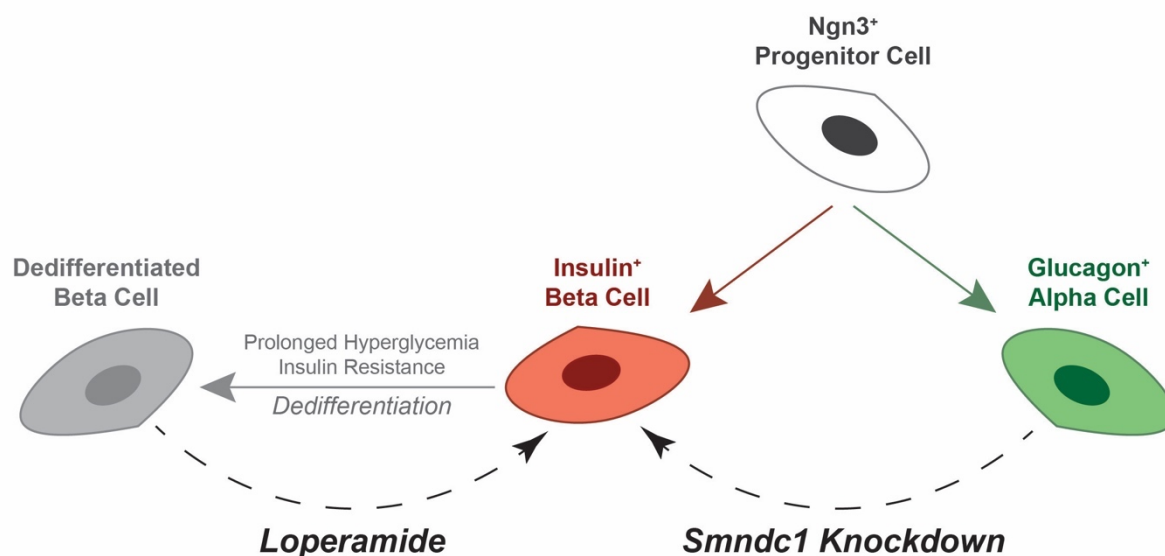


Figure 9. Summary of thesis work findings.

The work detailed in the first part of this thesis drives home the main point that increased insulin transcription is not the only step necessary to yield a functional beta cell. Proper intracellular and intragranular calcium and pH control, promoted autophagy and proinsulin folding, as well as persistent nuclear FoxO1 expression are all necessary to rescue insulin secretion in failing beta cells. In the second part of the thesis, alpha cell repression of insulin transcription was found to involve multiple regulatory steps and proteins. Specifically, sustained SmnDC1 and Atrx expressions coupled to restricted BAF complex promoter binding maintained impaired *Pdx1* mRNA stability, low *MafA* expression and a *Pax6* alpha cell specific splice isoform. Future experiments involving overexpression of the SmnDC1 knockdown induced *Abcc8* splice isoform, ChIPs for Atrx deposited H3K27me3 and H3K9me3 marks, and development of SmnDC1 small molecule inhibitors for simplified acute and in vivo treatments could aid in further understanding alpha cell identify preservation. Identification of loperamide's direct protein interactor in beta cells, on the other hand, could provide new molecular targets for FoxO1 protein regulation.

4. MATERIALS AND METHODS

Corresponding materials and methods are described in detail within the published or submitted manuscripts in Sections 2.1 and 2.2.

5. REFERENCES

- Ackermann AM, Wang Z, Schug J, Najj A & Kaestner KH (2016) Integration of ATAC-seq and RNA-seq identifies human alpha cell and beta cell signature genes. *Mol Metab* 5: 233–244
- Aguayo-Mazzucato C & Bonner-Weir S (2018) Pancreatic β Cell Regeneration as a Possible Therapy for Diabetes. *Cell Metab* 27: 57–67 doi:10.1016/j.cmet.2017.08.007 [PREPRINT]
- Ahlgren U, Jonsson J, Jonsson L, Simu K & Edlund H (1998) β -Cell-specific inactivation of the mouse *Pdx1* gene results in loss of the β -cell phenotype and maturity onset diabetes. *Genes Dev* 12: 1763–1768
- Akirav E, Kushner JA & Herold KC (2008) β -Cell Mass and Type 1 Diabetes: Going, Going, Gone? *Diabetes* 57: 2883–2888 doi:10.2337/db07-1817 [PREPRINT]
- Al-Hasani K, Pfeifer A, Courtney M, Ben-Othman N, Gjernes E, Vieira A, Druelle N, Avolio F, Ravassard P, Leuckx G, *et al* (2013) Adult duct-lining cells can reprogram into β -like cells able to counter repeated cycles of toxin-induced diabetes. *Dev Cell* 26: 86–100
- Allen HL, Flanagan SE, Shaw-Smith C, De Franco E, Akerman I, Caswell R, Consortium IPA, Ferrer J, Hattersley AT & Ellard S (2011) GATA6 haploinsufficiency causes pancreatic agenesis in humans. *Nat Genet* 44: 20–22
- Andersen FG, Heller RS, Petersen HV, Jensen J, Madsen OD & Serup P (1999) Pax6 and Cdx2/3 form a functional complex on the rat glucagon gene promoter G1-element. *FEBS Lett* 445: 306–310
- Apelqvist A, Ahlgren U & Edlund H (1997) Sonic hedgehog directs specialised mesoderm differentiation in the intestine and pancreas. *Curr Biol* 7: 801–804
- Arda HE, Li L, Tsai J, Torre EA, Rosli Y, Peiris H, Spitale RC, Dai C, Gu X, Qu K, *et al* (2016) Age-Dependent Pancreatic Gene Regulation Reveals Mechanisms Governing Human β Cell Function. *Cell Metab* 23: 909–920
- Ardestani A, Lypse B, Kido Y, Leibowitz G & Maedler K (2018) mTORC1 Signaling: A Double-Edged Sword in Diabetic β Cells. *Cell Metab* 27: 314–331 doi:10.1016/j.cmet.2017.11.004 [PREPRINT]
- Ariyachet C, Tovaglieri A, Xiang G, Lu J, Shah MS, Richmond CA, Verbeke C, Melton DA, Stanger BZ, Mooney D, *et al* (2016) Reprogrammed Stomach Tissue as a Renewable Source of Functional β Cells for Blood Glucose Regulation. *Cell Stem Cell* 18: 410–421
- Arrojo e Drigo R, Ali Y, Diez J, Srinivasan DK, Berggren P-O & Boehm BO (2015) New insights into the architecture of the islet of Langerhans: a focused cross-species assessment. *Diabetologia* 58: 2218–2228
- Artner I, Bianchi B, Raum JC, Guo M, Kaneko T, Cordes S, Sieweke M & Stein R (2007) MafB

- is required for islet beta cell maturation. *Proc Natl Acad Sci U S A* 104: 3853–3858
- Artner I, Hang Y, Mazur M, Yamamoto T, Guo M, Lindner J, Magnuson MA & Stein R (2010) MafA and MafB regulate genes critical to beta-cells in a unique temporal manner. *Diabetes* 59: 2530–2539
- Artner I, Le Lay J, Hang Y, Elghazi L, Schisler JC, Henderson E, Sosa-Pineda B & Stein R (2006) MafB: an activator of the glucagon gene expressed in developing islet alpha- and beta-cells. *Diabetes* 55: 297–304
- Atkinson MA, Bluestone JA, Eisenbarth GS, Hebrok M, Herold KC, Accili D, Pietropaolo M, Arvan PR, Von Herrath M, Markel DS, *et al* (2011) How does type 1 diabetes develop? The notion of homicide or β -cell suicide revisited. *Diabetes* 60: 1370–1379 doi:10.2337/db10-1797 [PREPRINT]
- Avrahami D, Wang YJ, Schug J, Feleke E, Gao L, Liu C, Consortium H, Najj A, Glaser B & Kaestner KH (2020) Single-cell transcriptomics of human islet ontogeny defines the molecular basis of β -cell dedifferentiation in T2D. *Mol Metab* 42: 101057
- Azzarelli R, Hurley C, Sznurkowska MK, Rulands S, Hardwick L, Gamper I, Ali F, McCracken L, Hindley C, McDuff F, *et al* (2017) Multi-site Neurogenin3 Phosphorylation Controls Pancreatic Endocrine Differentiation. *Dev Cell* 41: 274-286.e5
- Babaya N, Nakayama M, Moriyama H, Gianani R, Still T, Miao D, Yu L, Hutton JC & Eisenbarth GS (2006) A new model of insulin-deficient diabetes: male NOD mice with a single copy of *Ins1* and no *Ins2*. *Diabetologia* 49: 1222–1228
- Bader E, Migliorini A, Gegg M, Moruzzi N, Gerdes J, Roscioni SS, Bakhti M, Brandl E, Irmeler M, Beckers J, *et al* (2016) Identification of proliferative and mature β -cells in the islets of Langerhans. *Nat* 2016 5357612 535: 430–434
- Balcazar N, Sathyamurthy A, Elghazi L, Gould A, Weiss A, Shiojima I, Walsh K & Bernal-Mizrachi E (2009) mTORC1 Activation Regulates β -Cell Mass and Proliferation by Modulation of Cyclin D2 Synthesis and Stability. *J Biol Chem* 284: 7832
- Banga A, Akinci E, Greder L V, Dutton JR & Slack JMW (2012) In vivo reprogramming of Sox9⁺ cells in the liver to insulin-secreting ducts. *Proc Natl Acad Sci* 109: 15336 LP – 15341
- Banting FG, Best CH, Collip JB, Campbell WR & Fletcher AA (1922) Pancreatic Extracts in the Treatment of Diabetes Mellitus. *Can Med Assoc J* 12: 141–146
- Bastidas-Ponce A, Scheibner K, Lickert H & Bakhti M (2017) Cellular and molecular mechanisms coordinating pancreas development. *Development* 144: 2873–2888
- Bechard ME, Bankaitis ED, Hipkens SB, Ustione A, Piston DW, Yang Y-P, Magnuson MA & Wright CVE (2016) Precommitment low-level Neurog3 expression defines a long-lived mitotic endocrine-biased progenitor pool that drives production of endocrine-committed cells. *Genes Dev*

- Ben-Othman N, Vieira A, Courtney M, Record F, Gjernes E, Avolio F, Hadzic B, Druelle N, Napolitano T, Navarro-Sanz S, *et al* (2017) Long-Term GABA Administration Induces Alpha Cell-Mediated Beta-like Cell Neogenesis. *Cell* 168: 73-85.e11
- Bock T, Pakkenberg B & Buschard K (2003) Increased Islet Volume but Unchanged Islet Number in ob/ob Mice. *Diabetes* 52: 1716–1722
- Bonner Weir S, Trent DF & Weir GC (1983) Partial pancreatectomy in the rat and subsequent defect in glucose-induced insulin release. *J Clin Invest* 71: 1544–1553
- Boughton CK & Hovorka R (2021) New closed-loop insulin systems. *Diabetologia* 64: 1007–1015 doi:10.1007/s00125-021-05391-w [PREPRINT]
- Bramswig NC, Everett LJ, Schug J, Dorrell C, Liu C, Luo Y, Streeter PR, Najj A, Grompe M & Kaestner KH (2013) Epigenomic plasticity enables human pancreatic α to β cell reprogramming. *J Clin Invest* 123: 1275–1284
- Brennan K, Huangfu D & Melton D (2007) All β Cells Contribute Equally to Islet Growth and Maintenance. *PLoS Biol* 5: 1520–1529
- Bugliani M, Mossuto S, Grano F, Suleiman M, Marselli L, Boggi U, De Simone P, Eizirik DL, Cnop M, Marchetti P, *et al* (2019) Modulation of autophagy influences the function and survival of human pancreatic beta cells under endoplasmic reticulum stress conditions and in type 2 diabetes. *Front Endocrinol (Lausanne)* 10: 52
- Burrack AL, Martinov T & Fife BT (2017) T cell-mediated beta cell destruction: Autoimmunity and alloimmunity in the context of type 1 diabetes. *Front Endocrinol (Lausanne)* 8: 343 doi:10.3389/fendo.2017.00343 [PREPRINT]
- Butler AE, Janson J, Bonner-Weir S, Ritzel R, Rizza RA & Butler PC (2003) β -Cell Deficit and Increased β -Cell Apoptosis in Humans With Type 2 Diabetes. *Diabetes* 52: 102 LP – 110
- Campbell JE & Newgard CB (2021) Mechanisms controlling pancreatic islet cell function in insulin secretion. *Nat Rev Mol Cell Biol* 22: 142–158
- Cardozo AK, Ortis F, Storling J, Feng YH, Rasschaert J, Tonnesen M, Van Eylen F, Mandrup-Poulsen T, Herchuelz A & Eizirik DL (2005) Cytokines downregulate the sarcoendoplasmic reticulum pump Ca^{2+} ATPase 2b and deplete endoplasmic reticulum Ca^{2+} , leading to induction of endoplasmic reticulum stress in pancreatic β -cells. *Diabetes* 54: 452–461
- Van de Casteele M, Leuckx G, Baeyens L, Cai Y, Yuchi Y, Coppens V, De Groef S, Eriksson M, Svensson C, Ahlgren U, *et al* (2013) Neurogenin 3+ cells contribute to β -cell neogenesis and proliferation in injured adult mouse pancreas. *Cell Death Dis* 4: e523–e523
- Casteels T, Zhang Y, Frogne T, Sturtzel C, Lardeau C-H, Sen I, Liu X, Hong S, Pauler FM, Penz T, *et al* (2021) An inhibitor-mediated beta cell dedifferentiation model reveals distinct roles for FoxO1 in glucagon repression and insulin maturation. *Mol Metab*:

101329

- Chakravarthy H, Gu X, Enge M, Dai X, Wang Y, Damond N, Downie C, Liu K, Wang J, Xing Y, *et al* (2017) Converting Adult Pancreatic Islet α Cells into β Cells by Targeting Both Dnmt1 and Arx. *Cell Metab* 25: 622–634
- Chen CC, Jeon SM, Bhaskar PT, Nogueira V, Sundararajan D, Tonic I, Park Y & Hay N (2010) FoxOs Inhibit mTORC1 and Activate Akt by Inducing the Expression of Sestrin3 and Rictor. *Dev Cell* 18: 592–604
- Chen H, Gu X, Liu Y, Wang J, Wirt SE, Bottino R, Schorle H, Sage J & Kim SK (2011) PDGF signalling controls age-dependent proliferation in pancreatic β -cells. *Nat* 2011 4787369 478: 349–355
- Chen H, Gu X, Su I, Bottino R, Contreras JL, Tarakhovsky A & Kim SK (2009) Polycomb protein Ezh2 regulates pancreatic β -cell Ink4a/Arf expression and regeneration in diabetes mellitus. *Genes Dev* 23: 975–985
- Chen Y-C, Taylor AJ & Verchere CB (2018) Islet prohormone processing in health and disease. *Diabetes Obes Metab* 20 Suppl 2: 64–76
- Chen Y-J, Finkbeiner SR, Weinblatt D, Emmett MJ, Tameire F, Yousefi M, Yang C, Maehr R, Zhou Q, Shemer R, *et al* (2014) De novo formation of insulin-producing ‘neo- β cell islets’ from intestinal crypts. *Cell Rep* 6: 1046–1058
- Chen Y-S, Gleaton J, Yang Y, Dhayalan B, Phillips NB, Liu Y, Broadwater L, Jarosinski MA, Chatterjee D, Lawrence MC, *et al* (2021) Insertion of a synthetic switch into insulin provides metabolite-dependent regulation of hormone–receptor activation. *Proc Natl Acad Sci* 118: e2103518118
- Cheng C-W, Villani V, Buono R, Wei M, Kumar S, Yilmaz OH, Cohen P, Sneddon JB, Perin L & Longo VD (2017) Fasting-Mimicking Diet Promotes Ngn3-Driven β -Cell Regeneration to Reverse Diabetes. *Cell* 168: 775-788.e12
- Chera S, Baronnier D, Ghila L, Cigliola V, Jensen JN, Gu G, Furuyama K, Thorel F, Gribble FM, Reimann F, *et al* (2014) Diabetes recovery by age-dependent conversion of pancreatic delta-cells into insulin producers. *Nature* 514: 503–507
- Chung CH, Hao E, Piran R, Keinan E & Levine F (2010) Pancreatic β -cell neogenesis by direct conversion from mature α -cells. *Stem Cells* 28: 1630–1638
- Cinti F, Bouchi R, Kim-Muller JY, Ohmura Y, Sandoval PR, Masini M, Marselli L, Suleiman M, Ratner LE, Marchetti P, *et al* (2016) Evidence of β -Cell Dedifferentiation in Human Type 2 Diabetes. *J Clin Endocrinol Metab* 101: 1044–1054
- Clapham DE (2007) Calcium Signaling. *Cell* 131: 1047–1058 doi:10.1016/j.cell.2007.11.028 [PREPRINT]
- Collombat P, Hecksher-Sorensen J, Krull J, Berger J, Riedel D, Herrera PL, Serup P & Mansouri A (2007) Embryonic endocrine pancreas and mature beta cells acquire alpha

- and PP cell phenotypes upon Arx misexpression. *J Clin Invest* 117: 961–970
- Collombat P, Mansouri A, Hecksher-Sorensen J, Serup P, Krull J, Gradwohl G & Gruss P (2003) Opposing actions of Arx and Pax4 in endocrine pancreas development. *Genes Dev* 17: 2591–2603
- Collombat P, Xu X, Ravassard P, Sosa-Pineda B, Dussaud S, Billestrup N, Madsen OD, Serup P, Heimberg H & Mansouri A (2009) The ectopic expression of Pax4 in the mouse pancreas converts progenitor cells into alpha and subsequently beta cells. *Cell* 138: 449–462
- Conrad E, Dai C, Spaeth J, Guo M, Cyphert HA, Scoville D, Carroll J, Yu W-M, Goodrich L V, Harlan DM, *et al* (2016) The MAFB transcription factor impacts islet α -cell function in rodents and represents a unique signature of primate islet β -cells. *Am J Physiol Endocrinol Metab* 310: E91–E102
- Courtney M, Gjernes E, Druelle N, Ravaud C, Vieira A, Ben-Othman N, Pfeifer A, Avolio F, Leuckx G, Lacas-Gervais S, *et al* (2013) The inactivation of Arx in pancreatic alpha-cells triggers their neogenesis and conversion into functional beta-like cells. *PLoS Genet* 9: e1003934
- Cox AR, Lam CJ, Rankin MM, King KA, Chen P, Martinez R, Li C & Kushner JA (2016) Extreme obesity induces massive beta cell expansion in mice through self-renewal and does not alter the beta cell lineage. *Diabetol* 2016 596 59: 1231–1241
- Cyphert HA, Walker EM, Hang Y, Dhawan S, Haliyur R, Bonatakis L, Avrahami D, Brissova M, Kaestner KH, Bhushan A, *et al* (2019) Examining How the MAFB Transcription Factor Affects Islet β -Cell Function Postnatally. *Diabetes* 68: 337 LP – 348
- Dai C, Brissova M, Hang Y, Thompson C, Poffenberger G, Shostak A, Chen Z, Stein R & Powers AC (2012) Islet-enriched gene expression and glucose-induced insulin secretion in human and mouse islets. *Diabetologia* 55: 707–718
- Daly JW & Harper J (2000) Loperamide: Novel effects on capacitative calcium influx. *Cell Mol Life Sci* 57: 149–157 doi:10.1007/s000180050504 [PREPRINT]
- Daneman D (2006) Type 1 diabetes. *Lancet* 367: 847–858
- Dassaye R, Naidoo S & Cerf ME (2016) Transcription factor regulation of pancreatic organogenesis, differentiation and maturation. *Islets* 8: 13–34 doi:10.1080/19382014.2015.1075687 [PREPRINT]
- Davegårdh C, García-Calzón S, Bacos K & Ling C (2018) DNA methylation in the pathogenesis of type 2 diabetes in humans. *Mol Metab* 14: 12–25
- Decker K, Goldman DC, Grasch CL & Sussel L (2006) Gata6 is an important regulator of mouse pancreas development. *Dev Biol* 298: 415–429
- Desgraz R & Herrera PL (2009) Pancreatic neurogenin 3-expressing cells are unipotent islet precursors. *Development* 136: 3567–3574

- Dhawan S, Dirice E, Kulkarni RN & Bhushan A (2016) Inhibition of TGF- β Signaling Promotes Human Pancreatic β -Cell Replication. *Diabetes* 65: 1208–1218
- Dhawan S, Georgia S, Tschen SI, Fan G & Bhushan A (2011) Pancreatic beta cell identity is maintained by DNA methylation-mediated repression of Arx. *Dev Cell* 20: 419–429
- Dhawan S, Tschen S-I & Bhushan A (2009) Bmi-1 regulates the Ink4a/Arf locus to control pancreatic β -cell proliferation. *Genes Dev* 23: 906
- Dhawan S, Tschen S-I, Zeng C, Guo T, Hebrok M, Matveyenko A & Bhushan A (2015) DNA methylation directs functional maturation of pancreatic β cells. *J Clin Invest* 125: 2851–2860
- Dirice E, Walpita D, Vetere A, Meier BC, Kahraman S, Hu J, Dančik V, Burns SM, Gilbert TJ, Olson DE, *et al* (2016) Inhibition of DYRK1A Stimulates Human β -Cell Proliferation. *Diabetes* 65: 1660
- Dor Y, Brown J, Martinez OI & Melton DA (2004) Adult pancreatic β -cells are formed by self-duplication rather than stem-cell differentiation. *Nature* 429: 41–46
- Dorrell C, Schug J, Canaday PS, Russ HA, Tarlow BD, Grompe MT, Horton T, Hebrok M, Streeter PR, Kaestner KH, *et al* (2016) Human islets contain four distinct subtypes of β cells. *Nat Commun* 2016 71 7: 1–9
- Dumonteil E, Laser B, Constant I & Philippe J (1998) Differential Regulation of the Glucagon and Insulin I Gene Promoters by the Basic Helix-Loop-Helix Transcription Factors E47 and BETA2 *. *J Biol Chem* 273: 19945–19954
- Dyer MA, Qadeer ZA, Valle-Garcia D & Bernstein E (2017) ATRX and DAXX: Mechanisms and Mutations. *Cold Spring Harb Perspect Med* 7
- Engin F, Yermalovich A, Ngyuen T, Hummasti S, Fu W, Eizirik DL, Mathis D & Hotamisligil GS (2013) Restoration of the unfolded protein response in pancreatic β cells protects mice against type 1 diabetes. *Sci Transl Med* 5: 211ra156-211ra156
- Esni F, Ghosh B, Biankin A V, Lin JW, Albert MA, Yu X, MacDonald RJ, Civin CI, Real FX, Pack MA, *et al* (2004) Notch inhibits Ptf1 function and acinar cell differentiation in developing mouse and zebrafish pancreas. *Development* 131: 4213–4224
- Esni F, Täljedal IB, Perl AK, Cremer H, Christofori G & Semb H (1999) Neural cell adhesion molecule (N-CAM) is required for cell type segregation and normal ultrastructure in pancreatic islets. *J Cell Biol* 144: 325–337
- Fred RG, Bang-Berthelsen CH, Mandrup-Poulsen T, Grunnet LG & Welsh N (2010) High Glucose Suppresses Human Islet Insulin Biosynthesis by Inducing miR-133a Leading to Decreased Polypyrimidine Tract Binding Protein-Expression. *PLoS One* 5: e10843
- Fujitani Y (2017) Transcriptional regulation of pancreas development and β -cell function [Review]. *Endocr J* 64: 477–486
- Fujitani Y, Fujitani S, Boyer DF, Gannon M, Kawaguchi Y, Ray M, Shiota M, Stein RW,

- Magnuson MA & Wright CVE (2006) Targeted deletion of a cis-regulatory region reveals differential gene dosage requirements for Pdx1 in foregut organ differentiation and pancreas formation. *Genes Dev* 20: 253–266
- Furuyama K, Chera S, van Gurp L, Oropeza D, Ghila L, Damond N, Vethe H, Paulo JA, Joosten AM, Berney T, *et al* (2019) Diabetes relief in mice by glucose-sensing insulin-secreting human α -cells. *Nature* 567: 43–48
- Fusco J, Xiao X, Prasad K, Sheng Q, Chen C, Ming Y-C & Gittes G (2017) GLP-1/Exendin-4 induces β -cell proliferation via the epidermal growth factor receptor. *Sci Reports* 2017 7: 1–6
- Gao T, McKenna B, Li C, Reichert M, Nguyen J, Singh T, Yang C, Pannikar A, Doliba N, Zhang T, *et al* (2014) Pdx1 maintains β cell identity and function by repressing an α cell program. *Cell Metab* 19: 259–271
- Gelling RW, Du XQ, Dichmann DS, Rømer J, Huang H, Cui L, Obici S, Tang B, Holst JJ, Fledelius C, *et al* (2003) Lower blood glucose, hyperglucagonemia, and pancreatic α cell hyperplasia in glucagon receptor knockout mice. *Proc Natl Acad Sci U S A* 100: 1438–1443
- Georgia S & Bhushan A (2004) β cell replication is the primary mechanism for maintaining postnatal β cell mass. *J Clin Invest* 114: 963–968
- Ghosh R, Colon-Negron K & Papa FR (2019) Endoplasmic reticulum stress, degeneration of pancreatic islet β -cells, and therapeutic modulation of the unfolded protein response in diabetes. *Mol Metab* 27: S60–S68
- Giugliano D (1984) Morphine, opioid peptides, and pancreatic islet function. *Diabetes Care* 7: 92–98 doi:10.2337/diacare.7.1.92 [PREPRINT]
- Gomez DL, O'Driscoll M, Sheets TP, Hruban RH, Oberholzer J, McGarrigle JJ & Shambloott MJ (2015) Neurogenin 3 Expressing Cells in the Human Exocrine Pancreas Have the Capacity for Endocrine Cell Fate. *PLoS One* 10: e0133862
- Gosmain Y, Avril I, Mamin A & Philippe J (2007) Pax-6 and c-Maf functionally interact with the alpha-cell-specific DNA element G1 in vivo to promote glucagon gene expression. *J Biol Chem* 282: 35024–35034
- Gosmain Y, Cheyssac C, Heddad Masson M, Dibner C & Philippe J (2011) Glucagon gene expression in the endocrine pancreas: the role of the transcription factor Pax6 in α -cell differentiation, glucagon biosynthesis and secretion. *Diabetes Obes Metab* 13 Suppl 1: 31–38
- Gosmain Y, Katz LS, Masson MH, Cheyssac C, Poisson C & Philippe J (2012) Pax6 is crucial for β -cell function, insulin biosynthesis, and glucose-induced insulin secretion. *Mol Endocrinol* 26: 696–709
- Gradwohl G, Dierich A, LeMeur M & Guillemot F (2000) neurogenin3 is required for the

- development of the four endocrine cell lineages of the pancreas. *Proc Natl Acad Sci U S A* 97: 1607–1611
- Gu C, Stein GH, Pan N, Goebbels S, Hörnberg H, Nave K-A, Herrera P, White P, Kaestner KH, Sussel L, *et al* (2010) Pancreatic β Cells Require NeuroD to Achieve and Maintain Functional Maturity. *Cell Metab* 11: 298–310
- Gu G, Dubauskaite J & Melton DA (2002) Direct evidence for the pancreatic lineage: NGN3+ cells are islet progenitors and are distinct from duct progenitors. *Development* 129: 2447–2457
- Del Guerra S, Lupi R, Marselli L, Masini M, Bugliani M, Sbrana S, Torri S, Pollera M, Boggi U, Mosca F, *et al* (2005) Functional and molecular defects of pancreatic islets in human type 2 diabetes. *Diabetes* 54: 727–735
- Guo S, Dai C, Guo M, Taylor B, Harmon JS, Sander M, Robertson RP, Powers AC & Stein R (2013) Inactivation of specific beta cell transcription factors in type 2 diabetes. *J Clin Invest* 123: 3305–3316
- Gurdon JB (1962) The Developmental Capacity of Nuclei taken from Intestinal Epithelium Cells of Feeding Tadpoles. *Development* 10: 622–640
- Gutiérrez GD, Bender AS, Cirulli V, Mastracci TL, Kelly SM, Tsirigos A, Kaestner KH & Sussel L (2017) Pancreatic β cell identity requires continual repression of non- β cell programs. *J Clin Invest* 127: 244–259
- Hang Y & Stein R (2011) MafA and MafB activity in pancreatic β cells. *Trends Endocrinol Metab* 22: 364–373
- Hang Y, Yamamoto T, Benninger RKP, Brissova M, Guo M, Bush W, Piston DW, Powers AC, Magnuson M, Thurmond DC, *et al* (2014) The MafA Transcription Factor Becomes Essential to Islet β -Cells Soon After Birth. *Diabetes* 63: 1994 LP – 2005
- Hay CW & Docherty K (2006) Comparative Analysis of Insulin Gene Promoters. *Diabetes* 55: 3201 LP – 3213
- He KH, Juhl K, Karadimos M, El Khattabi I, Fitzpatrick C, Bonner-Weir S & Sharma A (2014) Differentiation of pancreatic endocrine progenitors reversibly blocked by premature induction of MafA. *Dev Biol* 385: 2–12
- Hebrok M, Kim SK & Melton DA (1998) Notochord repression of endodermal Sonic hedgehog permits pancreas development. *Genes Dev* 12: 1705–1713
- Heit JJ, Apelqvist AA, Gu X, Winslow MM, Neilson JR, Crabtree GR & Kim SK (2006) Calcineurin/NFAT signalling regulates pancreatic beta-cell growth and function. *Nature* 443: 345–349
- Heller RS, Jenny M, Collombat P, Mansouri A, Tomasetto C, Madsen OD, Mellitzer G, Gradwohl G & Serup P (2005) Genetic determinants of pancreatic epsilon-cell development. *Dev Biol* 286: 217–224

- Hickey RD, Galivo F, Schug J, Brehm MA, Haft A, Wang Y, Benedetti E, Gu G, Magnuson MA, Shultz LD, *et al* (2013) Generation of islet-like cells from mouse gall bladder by direct ex vivo reprogramming. *Stem Cell Res* 11: 503–515
- Holland AM, Hale MA, Kagami H, Hammer RE & MacDonald RJ (2002) Experimental control of pancreatic development and maintenance. *Proc Natl Acad Sci* 99: 12236 LP – 12241
- Horikawa Y & Enya M (2019) Genetic Dissection and Clinical Features of MODY6 (NEUROD1-MODY). *Curr Diab Rep* 19: 12
- Hussain MA & Habener JF (1999) Glucagon Gene Transcription Activation Mediated by Synergistic Interactions of pax-6 and cdx-2 with the p300 Co-activator *. *J Biol Chem* 274: 28950–28957
- Iacovazzo D, Flanagan SE, Walker E, Quezado R, de Sousa Barros FA, Caswell R, Johnson MB, Wakeling M, Brändle M, Guo M, *et al* (2018) &em>MAFA missense mutation causes familial insulinomatosis and diabetes mellitus. *Proc Natl Acad Sci* 115: 1027 LP – 1032
- Ilonen J, Lempainen J & Veijola R (2019) The heterogeneous pathogenesis of type 1 diabetes mellitus. *Nat Rev Endocrinol* 15: 635–650
- Iype T, Francis J, Garmey JC, Schisler JC, Nesher R, Weir GC, Becker TC, Newgard CB, Griffen SC & Mirmira RG (2005) Mechanism of insulin gene regulation by the pancreatic transcription factor Pdx-1: application of pre-mRNA analysis and chromatin immunoprecipitation to assess formation of functional transcriptional complexes. *J Biol Chem* 280: 16798–16807
- Jennings RE, Berry AA, Kirkwood-Wilson R, Roberts NA, Hearn T, Salisbury RJ, Blaylock J, Piper Hanley K & Hanley NA (2013) Development of the Human Pancreas From Foregut to Endocrine Commitment. *Diabetes* 62: 3514 LP – 3522
- De Jesus DF, Zhang Z, Kahraman S, Brown NK, Chen M, Hu J, Gupta MK, He C & Kulkarni RN (2019) m(6)A mRNA Methylation Regulates Human β -Cell Biology in Physiological States and in Type 2 Diabetes. *Nat Metab* 1: 765–774
- Jiang Z, Xing B, Feng Z, Ma J, Ma X & Hua X (2019) Menin Upregulates FOXO1 Protein Stability by Repressing Skp2-Mediated Degradation in β Cells. *Pancreas* 48: 267–274
- Johansson KA, Dursun U, Jordan N, Gu G, Beermann F, Gradwohl G & Grapin-Botton A (2007) Temporal Control of Neurogenin3 Activity in Pancreas Progenitors Reveals Competence Windows for the Generation of Different Endocrine Cell Types. *Dev Cell* 12: 457–465
- Johnston NR, Mitchell RK, Haythorne E, Pessoa MP, Semplici F, Ferrer J, Piemonti L, Marchetti P, Bugliani M, Bosco D, *et al* (2016) Beta Cell Hubs Dictate Pancreatic Islet Responses to Glucose. *Cell Metab* 24: 389–401
- Jonsson J, Carlsson L, Edlund T & Edlund H (1994) Insulin-promoter-factor 1 is required for

- pancreas development in mice. *Nature* 371: 606–609
- Jørgensen MC, Ahnfelt-Rønne J, Hald J, Madsen OD, Serup P & Hecksher-Sørensen J (2007) An Illustrated Review of Early Pancreas Development in the Mouse. *Endocr Rev* 28: 685–705
- Kataoka K, Han S, Shioda S, Hirai M, Nishizawa M & Handa H (2002) MafA is a glucose-regulated and pancreatic beta-cell-specific transcriptional activator for the insulin gene. *J Biol Chem* 277: 49903–49910
- Katoh MC, Jung Y, Ugboma CM, Shimbo M, Kuno A, Basha WA, Kudo T, Oishi H & Takahashi S (2018) MafB Is Critical for Glucagon Production and Secretion in Mouse Pancreatic α Cells In Vivo. *Mol Cell Biol* 38
- Katsarou A, Gudbjörnsdóttir S, Rawshani A, Dabelea D, Bonifacio E, Anderson BJ, Jacobsen LM, Schatz DA & Lernmark Å (2017) Type 1 diabetes mellitus. *Nat Rev Dis Prim* 3: 17016
- Kawamori D, Kaneto H, Nakatani Y, Matsuoka T, Matsuhisa M, Hori M & Yamasaki Y (2006) The Forkhead Transcription Factor Foxo1 Bridges the JNK Pathway and the Transcription Factor PDX-1 through Its Intracellular Translocation *. *J Biol Chem* 281: 1091–1098
- Kim-Muller JY, Kim YJR, Fan J, Zhao S, Banks AS, Prentki M & Accili D (2016) FoxO1 Deacetylation Decreases Fatty Acid Oxidation in β -Cells and Sustains Insulin Secretion in Diabetes *. *J Biol Chem* 291: 10162–10172
- Kim SK & Melton DA (1998) Pancreas development is promoted by cyclopamine, a Hedgehog signaling inhibitor. *Proc Natl Acad Sci* 95: 13036 LP – 13041
- Kitamura T & Ido Kitamura Y (2007) Role of FoxO Proteins in Pancreatic β Cells. *Endocr J* 54: 507–515
- Kitamura YI, Kitamura T, Kruse J-P, Raum JC, Stein R, Gu W & Accili D (2005) FoxO1 protects against pancreatic beta cell failure through NeuroD and MafA induction. *Cell Metab* 2: 153–163
- Knoch K-P, Bergert H, Borgonovo B, Saeger H-D, Altkrüger A, Verkade P & Solimena M (2004) Polypyrimidine tract-binding protein promotes insulin secretory granule biogenesis. *Nat Cell Biol* 6: 207–214
- Krapp A, Knöfler M, Ledermann B, Bürki K, Berney C, Zoerkler N, Hagenbüchle O & Wellauer PK (1998) The bHLH protein PTF1-p48 is essential for the formation of the exocrine and the correct spatial organization of the endocrine pancreas. *Genes Dev* 12: 3752–3763
- Krätzner R, Fröhlich F, Lepler K, Schröder M, Röher K, Dickel C, Tzvetkov M V, Quentin T, Oetjen E & Knepel W (2008) A Peroxisome Proliferator-Activated Receptor γ -Retinoid X Receptor Heterodimer Physically Interacts with the Transcriptional Activator PAX6 to Inhibit Glucagon Gene Transcription. *Mol Pharmacol* 73: 509 LP – 517
- Krentz NAJ, van Hoof D, Li Z, Watanabe A, Tang M, Nian C, German MS & Lynn FC (2017)

- Phosphorylation of NEUROG3 Links Endocrine Differentiation to the Cell Cycle in Pancreatic Progenitors. *Dev Cell* 41: 129-142.e6
- Krishnamurthy J, Ramsey MR, Ligon KL, Torrice C, Koh A, Bonner-Weir S & Sharpless NE (2006) p16 INK4a induces an age-dependent decline in islet regenerative potential. *Nat* 2006 4437110 443: 453–457
- Krogvold L, Skog O, Sundström G, Edwin B, Buanes T, Hanssen KF, Ludvigsson J, Grabherr M, Korsgren O & Dahl-Jørgensen K (2015) Function of isolated pancreatic islets from patients at onset of type 1 diabetes: Insulin secretion can be restored after some days in a nondiabetogenic environment in vitro results from the divid study. *Diabetes* 64: 2506–2512
- Kubicek S, Gilbert JC, Fomina-Yadlin D, Gitlin AD, Yuan Y, Wagner FF, Holson EB, Luo T, Lewis TA, Taylor B, *et al* (2012) Chromatin-targeting small molecules cause class-specific transcriptional changes in pancreatic endocrine cells. *Proc Natl Acad Sci U S A* 109: 5364–5369
- Kulkarni SD, Muralidharan B, Panda AC, Bakthavachalu B, Vindu A & Seshadri V (2011) Glucose-stimulated Translation Regulation of Insulin by the 5' UTR-binding Proteins*. *J Biol Chem* 286: 14146–14156
- Kuroda A, Rauch TA, Todorov I, Ku HT, Al-Abdullah IH, Kandeel F, Mullen Y, Pfeifer GP & Ferreri K (2009) Insulin Gene Expression Is Regulated by DNA Methylation. *PLoS One* 4: e6953
- Lakshminpathi J, Alvarez-Perez JC, Rosselot C, Casinelli GP, Stamateris RE, Rausell-Palamos F, O'Donnell CP, Vasavada RC, Scott DK, Alonso LC, *et al* (2016) PKC ζ Is Essential for Pancreatic β -Cell Replication During Insulin Resistance by Regulating mTOR and Cyclin-D2. *Diabetes* 65: 1283–1296
- Larsen HL & Grapin-Botton A (2017) The molecular and morphogenetic basis of pancreas organogenesis. *Semin Cell Dev Biol* 66: 51–68
- Lee EK & Gorospe M (2010) Minireview: Posttranscriptional Regulation of the Insulin and Insulin-Like Growth Factor Systems. *Endocrinology* 151: 1403–1408
- Lee EK, Kim W, Tominaga K, Martindale JL, Yang X, Subaran SS, Carlson OD, Mercken EM, Kulkarni RN, Akamatsu W, *et al* (2012) RNA-binding protein HuD controls insulin translation. *Mol Cell* 45: 826–835
- Lee H, Lee Y-S, Harenda Q, Pietrzak S, Oktay HZ, Schreiber S, Liao Y, Sonthalia S, Ciecko AE, Chen Y-G, *et al* (2020) Beta Cell Dedifferentiation Induced by IRE1 α Deletion Prevents Type 1 Diabetes. *Cell Metab* 31: 822-836.e5
- Lee S, Zhang J, Saravanakumar S, Flisher MF, Grimm DR, Meulen T van der & Huising MO (2021) Virgin β -Cells at the Neogenic Niche Proliferate Normally and Mature Slowly. *Diabetes* 70: 1070–1083

- Lehár J, Stockwell BR, Giaever G & Nislow C (2008) Combination chemical genetics. *Nat Chem Biol* 4: 674–681 doi:10.1038/nchembio.120 [PREPRINT]
- Li F, Wan M, Zhang B, Peng Y, Zhou Y, Pi C, Xu X, Ye L & Zheng* XZ and L (2018a) Bivalent Histone Modifications and Development. *Curr Stem Cell Res Ther* 13: 83–90 doi:http://dx.doi.org/10.2174/1574888X12666170123144743 [PREPRINT]
- Li J, Casteels T, Huber KVM, Lardeau C-H, Klughammer J, Farlik M, Sdelci S, Májek P, Pauler FM, Penz T, *et al* (2017) Artemisinin Target GABAA Receptor Signaling and Impair α Cell Identity. *Cell* 168
- Li S-W, Koya V, Li Y, Donelan W, Lin P, Reeves WH & Yang L-J (2010) Pancreatic duodenal homeobox 1 protein is a novel β -cell-specific autoantigen for type I diabetes. *Lab Invest* 90: 31–39
- Li W, Nakanishi M, Zumsteg A, Shear M, Wright C, Melton DA & Zhou Q (2014) In vivo reprogramming of pancreatic acinar cells to three islet endocrine subtypes. *Elife* 3: e01846
- Li Y, Cao X, Li L-X, Brubaker PL, Edlund H & Drucker DJ (2005) β -Cell β -Cell Pdx1 Expression Is Essential for the Glucoregulatory, Proliferative, and Cytoprotective Actions of Glucagon-Like Peptide-1. *Diabetes* 54: 482 LP – 491
- Li Z, Zhou M, Cai Z, Liu H, Zhong W, Hao Q, Cheng D, Hu X, Hou J, Xu P, *et al* (2018b) RNA-binding protein DDX1 is responsible for fatty acid-mediated repression of insulin translation. *Nucleic Acids Res* 46: 12052–12066
- Lin A, Yao J, Zhuang L, Wang D, Han J, Lam EW-F & Gan B (2014) The FoxO-BNIP3 axis exerts a unique regulation of mTORC1 and cell survival under energy stress. *Oncogene* 33: 3183–3194
- Lin J-C, Yan Y-T, Hsieh W-K, Peng P-J, Su C-H & Tarn W-Y (2013) RBM4 promotes pancreas cell differentiation and insulin expression. *Mol Cell Biol* 33: 319–327
- Lipson KL, Ghosh R & Urano F (2008) The role of IRE1 α in the degradation of insulin mRNA in pancreatic beta-cells. *PLoS One* 3: e1648
- Lu J, Liu K-C, Schulz N, Karampelias C, Charbord J, Hilding A, Rautio L, Bertolino P, Östenson C-G, Brismar K, *et al* (2016) IGFBP 1 increases β -cell regeneration by promoting α - to β -cell transdifferentiation. *EMBO J* 35: 2026–2044
- Luo H, Chen R, Yang R, Liu Y, Chen Y, Shu Y & Chen H (2014) Reprogramming of Mice Primary Hepatocytes into Insulin-Producing Cells by Transfection with Multicistronic Vectors. *J Diabetes Res* 2014: 716163
- Lupi R, Del Guerra S, Mancarella R, Novelli M, Valgimigli L, Pedulli GF, Paolini M, Soleti A, Filippini F, Mosca F, *et al* (2007) Insulin secretion defects of human type 2 diabetic islets are corrected in vitro by a new reactive oxygen species scavenger. *Diabetes Metab* 33: 340–345

- Lupi R, Mancarella R, Del Guerra S, Bugliani M, Del Prato S, Boggi U, Mosca F, Filipponi F & Marchetti P (2008) Effects of exendin-4 on islets from type 2 diabetes patients. *Diabetes, Obes Metab* 10: 515–519
- Magro MG & Solimena M (2013) Regulation of β -cell function by RNA-binding proteins. *Mol Metab* 2: 348–355
- Mannerstedt K, Mishra NK, Engholm E, Lundh M, Madsen CS, Pedersen PJ, Le-Huu P, Pedersen SL, Buch-Månson N, Borgström B, *et al* (2021) An Aldehyde Responsive, Cleavable Linker for Glucose Responsive Insulins. *Chem - A Eur J* 27: 3166–3176
- Marchetti P, Del Guerra S, Marselli L, Lupi R, Masini M, Pollera M, Bugliani M, Boggi U, Vistoli F, Mosca F, *et al* (2004) Pancreatic islets from type 2 diabetic patients have functional defects and increased apoptosis that are ameliorated by metformin. *J Clin Endocrinol Metab* 89: 5535–5541
- Marchetti P, Suleiman M, De Luca C, Baronti W, Bosi E, Tesi M & Marselli L (2020) A direct look at the dysfunction and pathology of the β cells in human type 2 diabetes. *Semin Cell Dev Biol* 103: 83–93 doi:10.1016/j.semcd.2020.04.005 [PREPRINT]
- Masini M, Bugliani M, Lupi R, Del Guerra S, Boggi U, Filipponi F, Marselli L, Masiello P & Marchetti P (2009) Autophagy in human type 2 diabetes pancreatic beta cells. *Diabetologia* 52: 1083–1086
- Mastracci TL, Anderson KR, Papizan JB & Sussel L (2013) Regulation of Neurod1 Contributes to the Lineage Potential of Neurogenin3+ Endocrine Precursor Cells in the Pancreas. *PLOS Genet* 9: e1003278
- Matsuoka T, Artner I, Henderson E, Means A, Sander M & Stein R (2004) The MafA transcription factor appears to be responsible for tissue-specific expression of insulin. *Proc Natl Acad Sci U S A* 101: 2930 LP – 2933
- Matsuoka TA, Kawashima S, Miyatsuka T, Sasaki S, Shimo N, Katakami N, Kawamori D, Takebe S, Herrera PL, Kaneto H, *et al* (2017) Mafa Enables Pdx1 to Effectively Convert Pancreatic Islet Progenitors and Committed Islet alpha-Cells Into beta-Cells In Vivo. *Diabetes* 66: 1293–1300
- McDonald TJ & Ellard S (2013) Maturity onset diabetes of the young: identification and diagnosis. *Ann Clin Biochem* 50: 403–415
- McKenna B, Guo M, Reynolds A, Hara M & Stein R (2015) Dynamic Recruitment of Functionally Distinct Swi/Snf Chromatin Remodeling Complexes Modulates Pdx1 Activity in Islet β Cells. *Cell Rep* 10: 2032–2042
- Meier JJ, Butler AE, Saisho Y, Monchamp T, Galasso R, Bhushan A, Rizza RA & Butler PC (2008) β -Cell Replication Is the Primary Mechanism Subservicing the Postnatal Expansion of β -Cell Mass in Humans. *Diabetes* 57: 1584–1594
- Melloul D, Marshak S & Cerasi E (2002) Regulation of insulin gene transcription. *Diabetologia*

- 45: 309–326
- van der Meulen T, Mawla AM, DiGruccio MR, Adams MW, Nies V, Dölleman S, Liu S, Ackermann AM, Cáceres E, Hunter AE, *et al* (2017) Virgin Beta Cells Persist throughout Life at a Neogenic Niche within Pancreatic Islets. *Cell Metab* 25: 911-926.e6
- Meyerovich K, Ortis F, Allagnat F & Cardozo AK (2016) Endoplasmic reticulum stress and the unfolded protein response in pancreatic islet inflammation. *J Mol Endocrinol* 57: R1–R17
- Miettinen PJ, Huotari M, Koivisto T, Ustinov J, Palgi J, Rasilainen S, Lehtonen E, Keski-Oja J & Otonkoski T (2000) Impaired migration and delayed differentiation of pancreatic islet cells in mice lacking EGF-receptors. *Development* 127: 2617–2627
- Miyatsuka T, Kosaka Y, Kim H & German MS (2011) Neurogenin3 inhibits proliferation in endocrine progenitors by inducing Cdkn1a. *Proc Natl Acad Sci* 108: 185 LP – 190
- Miyazaki S, Tashiro F & Miyazaki JI (2016) Transgenic expression of a single transcription factor Pdx1 induces transdifferentiation of pancreatic acinar cells to endocrine cells in adult mice. *PLoS One* 11: e0161190
- Moede T, Leibiger IB & Berggren P-O (2020) Alpha cell regulation of beta cell function. *Diabetologia* 63: 2064–2075
- Moin ASM & Butler AE (2019) Alterations in Beta Cell Identity in Type 1 and Type 2 Diabetes. *Curr Diab Rep* 19: 83
- Morita S, Villalta SA, Feldman HC, Register AC, Rosenthal W, Hoffmann-Petersen IT, Mehdizadeh M, Ghosh R, Wang L, Colon-Negron K, *et al* (2017) Targeting ABL-IRE1 α Signaling Spares ER-Stressed Pancreatic β Cells to Reverse Autoimmune Diabetes. *Cell Metab* 25: 883-897.e8
- Nasteska D, Fine NHF, Ashford FB, Cuzzo F, Vilorio K, Smith G, Dahir A, Dawson PWJ, Lai Y-C, Bastidas-Ponce A, *et al* (2021) PDX1LOW MAFALOW β -cells contribute to islet function and insulin release. *Nat Commun* 2021 121 12: 1–19
- Naya FJ, Huang HP, Qiu Y, Mutoh H, DeMayo FJ, Leiter AB & Tsai MJ (1997) Diabetes, defective pancreatic morphogenesis, and abnormal enteroendocrine differentiation in BETA2/neuroD-deficient mice. *Genes Dev* 11: 2323–2334
- Neiman D, Moss J, Hecht M, Magenheimer J, Piyanzin S, Shapiro AMJ, de Koning EJP, Razin A, Cedar H, Shemer R, *et al* (2017) Islet cells share promoter hypomethylation independently of expression, but exhibit cell-type-specific methylation in enhancers. *Proc Natl Acad Sci* 114: 13525 LP – 13530
- Ni Q, Gu Y, Xie Y, Yin Q, Zhang H, Nie A, Li W, Wang Y, Ning G, Wang W, *et al* (2017) Raptor regulates functional maturation of murine beta cells. *Nat Commun* 8: 15755
- Nir T, Melton DA & Dor Y (2007) Recovery from diabetes in mice by β cell regeneration. *J Clin Invest* 117: 2553–2561
- Nishimura W, Bonner-Weir S & Sharma A (2009) Expression of MafA in pancreatic progenitors

- is detrimental for pancreatic development. *Dev Biol* 333: 108–120
- Nishimura W, Kondo T, Salameh T, El Khattabi I, Dodge R, Bonner-Weir S & Sharma A (2006) A switch from MafB to MafA expression accompanies differentiation to pancreatic beta-cells. *Dev Biol* 293: 526–539
- Noso S, Kataoka K, Kawabata Y, Babaya N, Hiromine Y, Yamaji K, Fujisawa T, Aramata S, Kudo T, Takahashi S, *et al* (2010) Insulin transactivator MafA regulates intrathymic expression of insulin and affects susceptibility to type 1 diabetes. *Diabetes* 59: 2579–2587
- Nostro MC, Sarangi F, Yang C, Holland A, Elefanty AG, Stanley EG, Greiner DL & Keller G (2015) Efficient Generation of NKX6-1+ Pancreatic Progenitors from Multiple Human Pluripotent Stem Cell Lines. *Stem Cell Reports* 4: 591–604
- Ortiz D & Bryan J (2015) Neonatal diabetes and congenital hyperinsulinism caused by mutations in ABCC8/SUR1 are associated with altered and opposite affinities for ATP and ADP. *Front Endocrinol (Lausanne)* 6: 48
- Pagliuca FW & Melton DA (2013) How to make a functional beta-cell. *Development* 140: 2472–2483
- Pagliuca FW, Millman JR, Gurtler M, Segel M, Van Dervort A, Ryu JH, Peterson QP, Greiner D & Melton DA (2014) Generation of functional human pancreatic beta cells in vitro. *Cell* 159: 428–439
- Pan FC, Brissova M, Powers AC, Pfaff S & Wright CVE (2015) Inactivating the permanent neonatal diabetes gene Mnx1 switches insulin-producing β -cells to a δ -like fate and reveals a facultative proliferative capacity in aged β -cells. *Development* 142: 3637–3648
- Pan FC & Wright C (2011) Pancreas organogenesis: from bud to plexus to gland. *Dev Dyn an Off Publ Am Assoc Anat* 240: 530–565
- Papizan JB, Singer RA, Tschen S-I, Dhawan S, Friel JM, Hipkens SB, Magnuson MA, Bhushan A & Sussel L (2011) Nkx2.2 repressor complex regulates islet β -cell specification and prevents β -to- α -cell reprogramming. *Genes Dev* 25: 2291–2305
- Parent A V., Faleo G, Chavez J, Saxton M, Berrios DI, Kerper NR, Tang Q & Hebrok M (2021) Selective deletion of human leukocyte antigens protects stem cell-derived islets from immune rejection. *Cell Rep* 36: 109538
- Parker JC, Andrews KM, Allen MR, Stock JL & McNeish JD (2002) Glycemic control in mice with targeted disruption of the glucagon receptor gene. *Biochem Biophys Res Commun* 290: 839–843
- Parsons JA, Clarkbrelje T & Sorenson RL (1992) Adaptation of islets of langerhans to pregnancy: Increased islet cell proliferation and insulin secretion correlates with the onset of placental lactogen secretion. *Endocrinology* 130: 1459–1466
- Poitout V, Olson LK & Robertson RP (1996) Chronic exposure of betaTC-6 cells to

- supraphysiologic concentrations of glucose decreases binding of the RIPE3b1 insulin gene transcription activator. *J Clin Invest* 97: 1041–1046
- Prado CL, Pugh-Bernard AE, Elghazi L, Sosa-Pineda B & Sussel L (2004) Ghrelin cells replace insulin-producing β cells in two mouse models of pancreas development. *Proc Natl Acad Sci U S A* 101: 2924 LP – 2929
- Prasad-Reddy L & Isaacs D (2015) A clinical review of GLP-1 receptor agonists: Efficacy and safety in diabetes and beyond. *Drugs Context* 4
- Ramzy A, Asadi A & Kieffer TJ (2020) Revisiting Proinsulin Processing: Evidence That Human β -Cells Process Proinsulin With Prohormone Convertase (PC) 1/3 but Not PC2. *Diabetes* 69: 1451 LP – 1462
- Rane SG, Dubus P, Mettus R V., Galbreath EJ, Boden G, Reddy EP & Barbacid M (1999) Loss of Cdk4 expression causes insulin-deficient diabetes and Cdk4 activation results in β -islet cell hyperplasia. *Nat Genet* 1999 22: 44–52
- Razavi R, Najafabadi HS, Abdullah S, Smukler S, Arntfield M & Kooy D van der (2015) Diabetes Enhances the Proliferation of Adult Pancreatic Multipotent Progenitor Cells and Biases Their Differentiation to More β -Cell Production. *Diabetes* 64: 1311–1323
- Redondo MJ, Jeffrey J, Fain PR, Eisenbarth GS & Orban T (2008) Concordance for Islet Autoimmunity among Monozygotic Twins. *N Engl J Med* 359: 2849–2850
- Regué L, Zhao L, Ji F, Wang H, Avruch J & Dai N (2021) RNA m6A reader IMP2/IGF2BP2 promotes pancreatic β -cell proliferation and insulin secretion by enhancing PDX1 expression. *Mol Metab* 48: 101209
- Rezania A, Bruin JE, Arora P, Rubin A, Batushansky I, Asadi A, O'Dwyer S, Quiskamp N, Mojibian M, Albrecht T, *et al* (2014) Reversal of diabetes with insulin-producing cells derived in vitro from human pluripotent stem cells. *Nat Biotechnol* 32: 1121–1133
- Ritz-Laser B, Estreicher A, Klages N, Saule S & Philippe J (1999) Pax-6 and Cdx-2/3 Interact to Activate Glucagon Gene Expression on the G₁ Control Element *. *J Biol Chem* 274: 4124–4132
- Robertson RP (2004) Chronic Oxidative Stress as a Central Mechanism for Glucose Toxicity in Pancreatic Islet Beta Cells in Diabetes *. *J Biol Chem* 279: 42351–42354
- Robertson RP, Harmon J, Tran PO, Tanaka Y & Takahashi H (2003) Glucose Toxicity in β -Cells: Type 2 Diabetes, Good Radicals Gone Bad, and the Glutathione Connection. *Diabetes* 52: 581 LP – 587
- Roep BO, Thomaidou S, van Tienhoven R & Zaldumbide A (2021) Type 1 diabetes mellitus as a disease of the β -cell (do not blame the immune system?). *Nat Rev Endocrinol* 17: 150–161
- Romer AI, Singer RA, Sui L, Egli D & Sussel L (2019) Murine Perinatal β -Cell Proliferation and the Differentiation of Human Stem Cell-Derived Insulin-Expressing Cells Require

- NEUROD1. *Diabetes* 68: 2259–2271
- Rorsman P, Berggren PO, Bokvist K, Ericson H, Möhler H, Östenson CG & Smith PA (1989) Glucose-inhibition of glucagon secretion involves activation of GABAA-receptor chloride channels. *Nature* 341: 233–236
- Rorsman P, Salehi SA, Abdulkader F, Braun M & MacDonald PE (2008) KATP-channels and glucose-regulated glucagon secretion. *Trends Endocrinol Metab* 19: 277–284 doi:10.1016/j.tem.2008.07.003 [PREPRINT]
- Russell R, Carnese PP, Hennings TG, Walker EM, Russ HA, Liu JS, Giacometti S, Stein R & Hebrok M (2020) Loss of the transcription factor MAFB limits β -cell derivation from human PSCs. *Nat Commun* 11: 2742
- Sachdeva MM & Stoffers DA (2009) Minireview: Meeting the Demand for Insulin: Molecular Mechanisms of Adaptive Postnatal β -Cell Mass Expansion. *Mol Endocrinol* 23: 747–758
- Salem V, Silva LD, Suba K, Georgiadou E, Gharavy SNM, Akhtar N, Martin-Alonso A, Gaboriau DCA, Rothery SM, Stylianides T, *et al* (2019) Leader β -cells coordinate Ca²⁺ dynamics across pancreatic islets in vivo. *Nat Metab* 2019 16 1: 615–629
- Sander M, Neubüser A, Kalamaras J, Ee HC, Martin GR & German MS (1997) Genetic analysis reveals that PAX6 is required for normal transcription of pancreatic hormone genes and islet development. *Genes Dev* 11: 1662–1673
- Sander M, Sussel L, Connors J, Scheel D, Kalamaras J, Dela Cruz F, Schwitzgebel V, Hayes-Jordan A & German M (2000) Homeobox gene Nkx6.1 lies downstream of Nkx2.2 in the major pathway of beta-cell formation in the pancreas. *Development* 127: 5533–5540
- Schaffer AE, Freude KK, Nelson SB & Sander M (2010) Nkx6 transcription factors and Ptf1a function as antagonistic lineage determinants in multipotent pancreatic progenitors. *Dev Cell* 18: 1022–1029
- Schwitzgebel VM, Scheel DW, Connors JR, Kalamaras J, Lee JE, Anderson DJ, Sussel L, Johnson JD & German MS (2000) Expression of neurogenin3 reveals an islet cell precursor population in the pancreas. *Development* 127: 3533–3542
- Scoville DW, Cyphert HA, Liao L, Xu J, Reynolds A, Guo S & Stein R (2015) MLL3 and MLL4 Methyltransferases Bind to the MAFA and MAFB Transcription Factors to Regulate Islet β -Cell Function. *Diabetes* 64: 3772 LP – 3783
- Seaberg RM, Smukler SR, Kieffer TJ, Enikolopov G, Asghar Z, Wheeler MB, Korbitt G & Van Der Kooy D (2004) Clonal identification of multipotent precursors from adult mouse pancreas that generate neural and pancreatic lineages. *Nat Biotechnol* 22: 1115–1124
- Seghers V, Nakazaki M, DeMayo F, Aguilar-Bryan L & Bryan J (2000) Sur1 knockout mice. A model for K(ATP) channel-independent regulation of insulin secretion. *J Biol Chem* 275: 9270–9277
- Sellick GS, Barker KT, Stolte-Dijkstra I, Fleischmann C, Coleman RJ, Garrett C, Gloy AL,

- Edghill EL, Hattersley AT, Wellauer PK, *et al* (2004) Mutations in PTF1A cause pancreatic and cerebellar agenesis. *Nat Genet* 36: 1301–1305
- Seymour PA, Shih HP, Patel NA, Freude KK, Xie R, Lim CJ & Sander M (2012) A Sox9/Fgf feed-forward loop maintains pancreatic organ identity. *Development* 139: 3363–3372
- Sharon N, Chawla R, Mueller J, Vanderhooft J, Whitehorn LJ, Rosenthal B, Gürtler M, Estanboulieh RR, Shvartsman D, Gifford DK, *et al* (2019) A Peninsular Structure Coordinates Asynchronous Differentiation with Morphogenesis to Generate Pancreatic Islets. *Cell* 176: 790-804.e13
- Shaw-Smith C, De Franco E, Lango Allen H, Battle M, Flanagan SE, Borowiec M, Taplin CE, van Alfen-van der Velden J, Cruz-Rojo J, Perez de Nanclares G, *et al* (2014) GATA4 mutations are a cause of neonatal and childhood-onset diabetes. *Diabetes* 63: 2888–2894
- Shen W, Taylor B, Jin Q, Nguyen-Tran V, Meeusen S, Zhang Y-Q, Kamireddy A, Swafford A, Powers AF, Walker J, *et al* (2015) Inhibition of DYRK1A and GSK3B induces human β -cell proliferation. *Nat Commun* 6
- Shih HP, Kopp JL, Sandhu M, Dubois CL, Seymour PA, Grapin-Botton A & Sander M (2012) A Notch-dependent molecular circuitry initiates pancreatic endocrine and ductal cell differentiation. *Development* 139: 2488–2499
- Shrestha S, Saunders DC, Walker JT, Camunas-Soler J, Dai X-Q, Haliyur R, Aramandla R, Poffenberger G, Prasad N, Bottino R, *et al* (2021) Combinatorial transcription factor profiles predict mature and functional human islet α and β cells. *bioRxiv*: 2021.02.23.432522
- Sinagoga KL, Stone WJ, Schiesser J V, Schweitzer JI, Sampson L, Zheng Y & Wells JM (2017) Distinct roles for the mTOR pathway in postnatal morphogenesis, maturation and function of pancreatic islets. *Development* 144: 2402–2414
- Singer RA, Arnes L, Cui Y, Wang J, Gao Y, Guney MA, Burnum-Johnson KE, Rabadan R, Ansong C, Orr G, *et al* (2019) The Long Noncoding RNA Paupar Modulates PAX6 Regulatory Activities to Promote Alpha Cell Development and Function. *Cell Metab* 30: 1091-1106.e8
- Smukler SR, Arntfield ME, Razavi R, Bikopoulos G, Karpowicz P, Seaberg R, Dai F, Lee S, Ahrens R, Fraser PE, *et al* (2011) The Adult Mouse and Human Pancreas Contain Rare Multipotent Stem Cells that Express Insulin. *Cell Stem Cell* 8: 281–293
- Song Z, Fusco J, Zimmerman R, Fischbach S, Chen C, Ricks DM, Prasad K, Shiota C, Xiao X & Gittes GK (2016) Epidermal Growth Factor Receptor Signaling Regulates β 2 Cell Proliferation in Adult Mice *. *J Biol Chem* 291: 22630–22637
- Sørensen H, Winzell MS, Brand CL, Fosgerau K, Gelling RW, Nishimura E & Ahren B (2006) Glucagon receptor knockout mice display increased insulin sensitivity and impaired β -

- cell function. *Diabetes* 55: 3463–3469
- Sosa-Pineda B, Chowdhury K, Torres M, Oliver G & Gruss P (1997) The Pax4 gene is essential for differentiation of insulin-producing beta cells in the mammalian pancreas. *Nature* 386: 399–402
- Southgate RJ, Neill B, Prelovsek O, El-Osta A, Kamei Y, Miura S, Ezaki O, McLoughlin TJ, Zhang W, Unterman TG, *et al* (2007) FOXO1 regulates the expression of 4E-BP1 and inhibits mTOR signaling in mammalian skeletal muscle. *J Biol Chem* 282: 21176–21186
- Spaeth JM, Liu J-H, Peters D, Guo M, Osipovich AB, Mohammadi F, Roy N, Bhushan A, Magnuson MA, Hebrok M, *et al* (2019) The Pdx1-Bound Swi/Snf Chromatin Remodeling Complex Regulates Pancreatic Progenitor Cell Proliferation and Mature Islet β -Cell Function. *Diabetes* 68: 1806 LP – 1818
- Spijker HS, Ravelli RBG, Mommaas-Kienhuis AM, van Apeldoorn AA, Engelse MA, Zaldumbide A, Bonner-Weir S, Rabelink TJ, Hoeben RC, Clevers H, *et al* (2013) Conversion of mature human β -cells into glucagon-producing α -cells. *Diabetes* 62: 2471–2480
- Spijker HS, Song H, Ellenbroek JH, Roefs MM, Engelse MA, Bos E, Koster AJ, Rabelink TJ, Hansen BC, Clark A, *et al* (2015) Loss of β -Cell Identity Occurs in Type 2 Diabetes and Is Associated With Islet Amyloid Deposits. *Diabetes* 64: 2928
- St-Onge L, Sosa-Pineda B, Chowdhury K, Mansouri A & Gruss P (1997) Pax6 is required for differentiation of glucagon-producing alpha-cells in mouse pancreas. *Nature* 387: 406–409
- Staffers DA, Ferrer J, Clarke WL & Habener JF (1997) Early-onset type-II diabetes mellitus (MODY4) linked to IPF1. *Nat Genet* 17: 138–139
- Stoffers D (2000) Insulinotropic glucagon-like peptide 1 agonists stimulate expression of homeodomain protein IDX-1 and increase islet size in mouse pancreas. *Diabetes* 49: 741–748
- Stoffers DA, Zinkin NT, Stanojevic V, Clarke WL & Habener JF (1997) Pancreatic agenesis attributable to a single nucleotide deletion in the human IPF1 gene coding sequence. *Nat Genet* 15: 106–110
- Suckale J & Solimena M (2010) The insulin secretory granule as a signaling hub. *Trends Endocrinol Metab* 21: 599–609
- Sun J, Cui J, He Q, Chen Z, Arvan P & Liu M (2015) Proinsulin misfolding and endoplasmic reticulum stress during the development and progression of diabetes. *Mol Aspects Med* 42: 105–118
- Sun T & Han X (2020) Death versus dedifferentiation: The molecular bases of beta cell mass reduction in type 2 diabetes. *Semin Cell Dev Biol* 103: 76–82
- Svendsen B, Larsen O, Gabe MBN, Christiansen CB, Rosenkilde MM, Drucker DJ & Holst JJ

- (2018) Insulin Secretion Depends on Intra-islet Glucagon Signaling. *Cell Rep* 25: 1127-1134.e2
- Swisa A, Avrahami D, Eden N, Zhang J, Feleke E, Dahan T, Cohen-Tayar Y, Stolovich-Rain M, Kaestner KH, Glaser B, *et al* (2017a) PAX6 maintains β cell identity by repressing genes of alternative islet cell types. *J Clin Invest* 127: 230–243
- Swisa A, Glaser B & Dor Y (2017b) Metabolic Stress and Compromised Identity of Pancreatic Beta Cells. *Front Genet* 8: 21 (<https://www.frontiersin.org/article/10.3389/fgene.2017.00021>) [PREPRINT]
- Szabat M, Lynn FC, Hoffman BG, Kieffer TJ, Allan DW & Johnson JD (2012) Maintenance of β -Cell Maturity and Plasticity in the Adult Pancreas. *Diabetes* 61: 1365–1371
- Takahashi K & Yamanaka S (2006) Induction of Pluripotent Stem Cells from Mouse Embryonic and Adult Fibroblast Cultures by Defined Factors. *Cell* 126: 663–676
- Talchai C, Xuan S, Lin H V, Sussel L & Accili D (2012) Pancreatic β cell dedifferentiation as a mechanism of diabetic β cell failure. *Cell* 150: 1223–1234
- Tang R, Zhong T, Wu C, Zhou Z & Li X (2019) The Remission Phase in Type 1 Diabetes: Role of Hyperglycemia Rectification in Immune Modulation. *Front Endocrinol (Lausanne)* 10: 824 doi:10.3389/fendo.2019.00824 [PREPRINT]
- Tang X, Uhl S, Zhang T, Xue D, Li B, Vandana JJ, Acklin JA, Bonnycastle LL, Narisu N, Erdos MR, *et al* (2021) SARS-CoV-2 infection induces beta cell transdifferentiation. *Cell Metab*
- Teta M, Long SY, Wartschow LM, Rankin MM & Kushner JA (2005) Very Slow Turnover of β -Cells in Aged Adult Mice. *Diabetes* 54: 2557–2567
- Teta M, Rankin MM, Long SY, Stein GM & Kushner JA (2007) Growth and Regeneration of Adult β Cells Does Not Involve Specialized Progenitors. *Dev Cell* 12: 817–826
- Thompson PJ, Shah A, Ntranos V, Van Gool F, Atkinson M & Bhushan A (2019) Targeted Elimination of Senescent Beta Cells Prevents Type 1 Diabetes. *Cell Metab* 29: 1045-1060.e10
- Thorel F, Nepote V, Avril I, Kohno K, Desgraz R, Chera S & Herrera PL (2010) Conversion of adult pancreatic alpha-cells to beta-cells after extreme beta-cell loss. *Nature* 464: 1149–1154
- Tschen S, Zeng C, Field L, Dhawan S, Bhushan A & Georgia S (2017) Cyclin D2 is sufficient to drive β cell self-renewal and regeneration. <https://doi.org/10.1080/1538410120171319999> 16: 2183–2191
- Tuomilehto J (2013) The Emerging Global Epidemic of Type 1 Diabetes. *Curr Diab Rep* 13: 795–804
- Vanhoose AM, Samaras S, Artner I, Henderson E, Hang Y & Stein R (2008) MafA and MafB regulate Pdx1 transcription through the Area II control region in pancreatic beta cells. *J Biol Chem* 283: 22612–22619

- Vegas AJ, Veisoh O, Gürtler M, Millman JR, Pagliuca FW, Bader AR, Doloff JC, Li J, Chen M, Olejnik K, *et al* (2016) Long-term glycemic control using polymer-encapsulated human stem cell-derived beta cells in immune-competent mice. *Nat Med* 2015 223 22: 306–311
- Velazco-Cruz L, Goedegebuure MM & Millman JR (2020) Advances Toward Engineering Functionally Mature Human Pluripotent Stem Cell-Derived β Cells . *Front Bioeng Biotechnol* 8: 786 (<https://www.frontiersin.org/article/10.3389/fbioe.2020.00786>) [PREPRINT]
- Wang D, Wang J, Bai L, Pan H, Feng H, Clevers H & Zeng YA (2020a) Long-Term Expansion of Pancreatic Islet Organoids from Resident Procr+ Progenitors. *Cell* 180: 1198-1211.e19
- Wang H, Brun T, Kataoka K, Sharma AJ & Wollheim CB (2007) MAFA controls genes implicated in insulin biosynthesis and secretion. *Diabetologia* 50: 348–358
- Wang P, Alvarez-Perez J-C, Felsenfeld DP, Liu H, Sivendran S, Bender A, Kumar A, Sanchez R, Scott DK, Garcia-Ocaña A, *et al* (2015) A high-throughput chemical screen reveals that harmine-mediated inhibition of DYRK1A increases human pancreatic beta cell replication. *Nat Med* 2015 214 21: 383–388
- Wang S, Jensen JN, Seymour PA, Hsu W, Dor Y, Sander M, Magnuson MA, Serup P & Gu G (2009) Sustained β -Neurog3 expression in hormone-expressing islet cells is required for endocrine maturation and function. *Proc Natl Acad Sci* 106: 9715 LP – 9720
- Wang W, Shi Q, Guo T, Yang Z, Jia Z, Chen P & Zhou C (2016a) PDX1 and ISL1 differentially coordinate with epigenetic modifications to regulate insulin gene expression in varied glucose concentrations. *Mol Cell Endocrinol* 428: 38–48
- Wang Y, Sun J, Lin Z, Zhang W, Wang S, Wang W, Wang Q & Ning G (2020b) β -mRNA Methylation Controls Functional Maturation in Neonatal Murine β -Cells. *Diabetes* 69: 1708 LP – 1722
- Wang YJ, Golson ML, Schug J, Traum D, Liu C, Vivek K, Dorrell C, Naji A, Powers AC, Chang K-M, *et al* (2016b) Single-Cell Mass Cytometry Analysis of the Human Endocrine Pancreas. *Cell Metab* 24: 616–626
- Wang YJ, Schug J, Won K-J, Liu C, Naji A, Avrahami D, Golson ML & Kaestner KH (2016c) Single-Cell Transcriptomics of the Human Endocrine Pancreas. *Diabetes* 65: 3028–3038
- Watada H, Mirmira RG, Leung J & German MS (2000) Transcriptional and Translational Regulation of β -Cell Differentiation Factor Nkx6.1*. *J Biol Chem* 275: 34224–34230
- Wen JH, Chen YY, Song SJ, Ding J, Gao Y, Hu QK, Feng RP, Liu YZ, Ren GC, Zhang CY, *et al* (2009) Paired box 6 (PAX6) regulates glucose metabolism via proinsulin processing mediated by prohormone convertase 1/3 (PC1/3). *Diabetologia* 52: 504–513
- White MG, Marshall HL, Rigby R, Huang GC, Amer A, Booth T, White S & Shaw JAM (2013) Expression of Mesenchymal and α -Cell Phenotypic Markers in Islet β -Cells in Recently

- Diagnosed Diabetes. *Diabetes Care* 36: 3818
- Wideman RD, Yu ILY, Webber TD, Verchere CB, Johnson JD, Cheung AT & Kieffer TJ (2006) Improving function and survival of pancreatic islets by endogenous production of glucagon-like peptide 1 (GLP-1). *Proc Natl Acad Sci U S A* 103: 13468–13473
- Wilcox CL, Terry NA, Walp ER, Lee RA & May CL (2013) Pancreatic α -Cell Specific Deletion of Mouse Arx Leads to α -Cell Identity Loss. *PLoS One* 8
- Wills QF, Boothe T, Asadi A, Ao Z, Warnock GL, Kieffer TJ & Johnson JD (2016) Statistical approaches and software for clustering islet cell functional heterogeneity. <http://dx.doi.org/10.1080/1938201420161150664> 8: 48–56
- Wilson ME, Scheel D & German MS (2003) Gene expression cascades in pancreatic development. *Mech Dev* 120: 65–80
- Xiao X, Chen Z, Shiota C, Prasad K, Guo P, El-Gohary Y, Paredes J, Welsh C, Wiersch J & Gittes GK (2013) No evidence for β cell neogenesis in murine adult pancreas. *J Clin Invest* 123: 2207–2217
- Xiao X, Guo P, Shiota C, Zhang T, Coudriet GM, Fischbach S, Prasad K, Fusco J, Ramachandran S, Witkowski P, *et al* (2018) Endogenous Reprogramming of Alpha Cells into Beta Cells, Induced by Viral Gene Therapy, Reverses Autoimmune Diabetes. *Cell Stem Cell* 22: 78-90.e4
- Xie J, Sayed NM El, Qi C, Zhao X, Moore CE & Herbert TP (2014) Exendin-4 stimulates islet cell replication via the IGF1 receptor activation of mTORC1/S6K1. *J Mol Endocrinol* 53: 105–115
- Xu X, D'Hoker J, Stangé G, Bonn e S, De Leu N, Xiao X, Van De Casteele M, Mellitzer G, Ling Z, Pipeleers D, *et al* (2008) β 2; Cells Can Be Generated from Endogenous Progenitors in Injured Adult Mouse Pancreas. *Cell* 132: 197–207
- Xuan S, Borok MJ, Decker KJ, Battle MA, Duncan SA, Hale MA, Macdonald RJ & Sussel L (2012) Pancreas-specific deletion of mouse Gata4 and Gata6 causes pancreatic agenesis. *J Clin Invest* 122: 3516–3528
- Xuan S & Sussel L (2016) GATA4 and GATA6 regulate pancreatic endoderm identity through inhibition of hedgehog signaling. *Development* 143: 780–786
- Yamada T, Cavelti-Weder C, Caballero F, Lysy PA, Guo L, Sharma A, Li W, Zhou Q, Bonner-Weir S & Weir GC (2015) Reprogramming Mouse Cells With a Pancreatic Duct Phenotype to Insulin-Producing β -Like Cells. *Endocrinology* 156: 2029–2038
- Yang YP, Thorel F, Boyer DF, Herrera PL & Wright C V (2011) Context-specific alpha- to-beta-cell reprogramming by forced Pdx1 expression. *Genes Dev* 25: 1680–1685
- Ye L, Robertson MA, Hesselton D, Stainier DYR & Anderson RM (2015) Glucagon is essential for alpha cell transdifferentiation and beta cell neogenesis. *Development* 142: 1407–1417
- Ye L, Robertson MA, Mastracci TL & Anderson RM (2016) An insulin signaling feedback loop

- regulates pancreas progenitor cell differentiation during islet development and regeneration. *Dev Biol* 409: 354–369
- Yi Q, Min G, Suming H & Roland S (2002) Insulin Gene Transcription Is Mediated by Interactions between the p300 Coactivator and PDX-1, BETA2, and E47. *Mol Cell Biol* 22: 412–420
- Yuan Y, Hartland K, Boskovic Z, Wang Y, Walpita D, Lysy PA, Zhong C, Young DW, Kim YK, Tolliday NJ, *et al* (2013) A small-molecule inducer of PDX1 expression identified by high-throughput screening. *Chem Biol* 20: 1513–1522
- Yue L, Du J, Ye F, Chen Z, Li L, Lian F, Zhang B, Zhang Y, Jiang H, Chen K, *et al* (2016) Identification of novel small-molecule inhibitors targeting menin-MLL interaction, repurposing the antidiarrheal loperamide. *Org Biomol Chem* 14: 8503–8519
- Zavec JH, Jackson TE, Limp GL & Yellin TO (1982) Relationship between anti-diarrheal activity and binding to calmodulin. *Eur J Pharmacol* 78: 375–377
- Zhang C, Moriguchi T, Kajihara M, Esaki R, Harada A, Shimohata H, Oishi H, Hamada M, Morito N, Hasegawa K, *et al* (2005) MafA is a key regulator of glucose-stimulated insulin secretion. *Mol Cell Biol* 25: 4969–4976
- Zhang J, McKenna LB, Bogue CW & Kaestner KH (2014) The diabetes gene Hhex maintains δ -cell differentiation and islet function. *Genes Dev* 28: 829–834
- Zhao H, Huang X, Liu Z, Pu W, Lv Z, He L, Li Y, Zhou Q, Lui KO & Zhou B (2021) Pre-existing beta cells but not progenitors contribute to new beta cells in the adult pancreas. *Nat Metab* 2021 33 3: 352–365
- Zhou Q, Brown J, Kanarek A, Rajagopal J & Melton DA (2008) In vivo reprogramming of adult pancreatic exocrine cells to beta-cells. *Nature* 455: 627–632
- Zinger A & Leibowitz G (2014) Islet transplantation in type 1 diabetes: hype, hope and reality - a clinician's perspective. *Diabetes Metab Res Rev* 30: 83–87

6. CURRICULUM VITAE

Nationalities: Belgian & Israeli
 Mobile: +43.676.5871997
 E-mail: casteels.tamara@gmail.com

Address: Berggasse 37/47
 1090 Vienna, Austria
www.linkedin.com/in/tcasteels

Professional Profile

A molecular biologist with a strong interest in understanding and manipulating cell plasticity. I have a strong background in stem cell culture, screening and epigenetic techniques. Currently, I am focused on uncovering epigenetic factors involved in insulin repression, with the aim of transdifferentiating mature pancreatic alpha cells to insulin-secreting beta-like cells.

Education and Relevant Professional Experience

October 2014 – Present: PhD in Molecular Biology Vienna, AT
 CeMM Research Centre for Molecular Medicine of the Austrian Academy of Sciences

Supervisor: Dr. Stefan Kubicek

Aim of doctoral thesis: identify epigenetic factors involved in the regulation of insulin expression and the maintenance of beta cell identity.

- Validated novel modulators of insulin expression from chemical and genetic screens
- Characterized their mechanisms of action (affinity proteomics, CRISPR knockout clones, splicing analysis, ChIP-seq, ATAC-seq, RIP-seq, immunofluorescence analysis etc.)

2013–2014: MRes in Stem Cells and Developmental Biology London, UK
 University College London (Distinction)

Supervisor: Dr. Francesco Saverio Tedesco

- Directed the differentiation of genetically-corrected induced pluripotent stem cells from Duchenne muscular dystrophy patients into mesoangioblasts
- Characterized the resulting cells and transplanted them into *mdx* mice to study engraftment potential

July – August 2012: Summer internship London, UK
 Laboratory of Stem Cell Differentiation - Institute of Reproductive and Developmental Biology

Supervisor: Dr. Wei Cui

- Cultured human embryonic stem cells
- Performed general molecular biology experiments (western blots, cloning, qPCR, etc.)

2010–2013: BSc in Biochemistry London, UK
 Imperial College London (2:1 Honours)

Final year dissertation supervisor: Dr. Cristina Lo Celso

- Designed, cloned and transfected an inducible, constitutively active form of β -catenin
- Cultured haematopoietic stem cells
- Performed time-lapse microscopy and analysed cell movements using ImageJ

2008-2010: Bilingual International Baccalaureate Diploma Brussels, BE
 International School of Brussels

Specialised Laboratory Techniques

- Cell Culture
 - o *Human embryonic stem cells*
 - o *Haematopoietic stem cells*
 - o *Induced pluripotent stem cells*
 - o *Donor-derived human pancreatic islets*
- Differentiation of iPS cells to mesoangioblasts
- Epigenetic analysis techniques: RNAseq, ChIPseq, SLAMseq, ATACseq, RIPseq

- Cell/tissue staining (inc. immunofluorescence, histological stainings, confocal microscopy)
- Use of cryostat for preparation of tissue sections (muscle and pancreatic islets)
- Generation of clonal cells lines (CRISPR knockout and base editing)
- Intramuscular/intraperitoneal injections into preclinical mouse models
- Explantation and dehydration of muscle samples
- Data visualisation with Seaborn and Spotfire
- Basic data analysis with Python
- Image analysis with ImageJ and CellProfiler

Additional Skills/Achievements

Courses:

2018: Data manipulation and visualisation with Python (Physalia)

2014: UK Home Office personal license holder (animal testing and research)

Scientific Meetings:

Oral presentations

2016: 52nd EASD Annual Meeting, European Association for the Study of Diabetes

Title: “High Throughput Screens Identify Key Factors in Alpha to Beta Cell Transdifferentiation”

Poster presentations

2019: Cold Spring Harbor 84th Symposium: RNA Control & Regulation

2017: Gordon Research Conference on Pancreatic Diseases

2016: The Islet Study Group meeting 2016

2015: ENDO 2015, The Endocrine Society’s 97th Annual Meeting & Expo

2015: 15th Annual Rachmiel Levine Diabetes and Obesity Symposium

2014: ISSCR 12th annual meeting in Vancouver, Canada

Awards:

2019: Won the 15th YSA PhD Symposium Poster Award in Endocrinology and Metabolism

2015: Won the Helmsley Charitable Trust Abstract Award in Type 1 Diabetes

2010: Won the International School of Brussels “Steve Leiser Prize for Biology”

Leadership/Mentoring/Management:

2017: PhD Student Representative

2016: Supervised two summer students in the lab on their respective projects

Languages:

English (fluent); Hebrew (mother tongue); French (fluent); German (conversational; B1)

Publications

1. **Casteels T**, Bajew S, Reiniš J, Schuster M, Müller A, Wagner BK, Bock C & Kubicek S. SMNDC1 links chromatin remodeling and splicing to regulate pancreatic hormone expression (*submitted*)
2. **Casteels T**, Zhang Y, Frogne T, Sturtzel C, Lardeau C-H, Sen I, Liu X, Hong S, Pauler FM, Penz T, *et al* (2021) An inhibitor-mediated beta cell dedifferentiation model reveals distinct roles for FoxO1 in glucagon repression and insulin maturation. *Molecular Metabolism* doi: 10.1016/j.molmet.2021.101329
3. Li J, **Casteels T**, Huber KVM, Lardeau C-H, Klughammer J, Farlik M, Sdelci S, Májek P, Pauler FM, Penz T, *et al* (2017) Artemisinins Target GABAA Receptor Signaling and Impair α Cell Identity. *Cell* 168 doi: 10.1016/j.cell.2016.11.010